Insights from Mathematical Modeling on the Natural History, Dynamics, and Control of Dengue

Quirine Astrid ten Bosch

Publication Date

24-03-2017

INSIGHTS FROM MATHEMATICAL MODELING ON THE NATURAL HISTORY, DYNAMICS, AND CONTROL OF DENGUE

A Dissertation

Submitted to the Graduate School

of the University of Notre Dame

in Partial Fulfillment of the Requirements

for the Degree of

Doctor of Philosophy

by

Quirine Astrid ten Bosch

_____

T. Alex Perkins, Director

Graduate Program in Biological Sciences

Notre Dame, Indiana

March 2017

INSIGHTS FROM MATHEMATICAL MODELING ON THE NATURAL HISTORY, DYNAMICS, AND CONTROL OF DENGUE

Abstract

by

Quirine Astrid ten Bosch

Dengue poses an increasing threat to about half of the world's population. In this dissertation, I present four mathematical modeling exercises aimed at improving understanding of the natural history, dynamics, and control of dengue viruses (DENV) and the mosquitoes that transmit them.

First, I present a quantitative analysis of how DENV-infected individuals across the spectrum of disease outcomes contribute to transmission. Using a suite of models, I parsed available data on viremia dynamics within humans, human infectiousness to mosquitoes, and demographic projections of the infectious reservoir. I found that individuals with inapparent or no symptoms whatsoever—i.e., 'silent' infections—are likely the primary reservoir of DENV, which casts doubts on current practices for dengue control.

Second, to examine what mechanisms govern temporal patterns characteristic of dengue epidemiology, I compared alternative models with differing assumptions about serotype-immune interactions and seasonal forcing. I found that, when assuming that

primary and secondary infections constitute the infectious reservoir, all models were capable of reproducing real-world dengue dynamics. When post-secondary infections were assumed to contribute to transmission, cross-immunity was found to be the most important factor for reproducing patterns characteristic of dengue dynamics. The competing hypothesis of cross-enhancement had limited support.

Third, I present a new modeling tool to parse data from mark-release-recapture studies. A Markov chain model fitted to data using Bayesian techniques was used to estimate the effect of a volatile vector control product on *Aedes aegypti* in an experimental hut design. I inferred concurrent product effects on unobserved processes such as mosquito repellency, which could potentially impact transmission by reducing human-mosquito contacts.

Fourth, I introduce a modeling framework to examine how different modes of action of vector control products act in symphony to effect epidemiological outcomes. I used the estimates from the experimental hut studies and additional laboratory experiments to parameterize this framework and showed that, whereas toxic effects are the most effective in reducing transmission, products that reduce human-mosquito contacts through repellency or irritancy can have a considerable impact on transmission, as well. Such spatial repellent products could augment available control tools, in particular in areas with emerging insecticide resistance.

Voor haar

CONTENTS

FIGURES

TABLES

ACKNOWLEDGMENTS

My deepest gratitude goes out to Alex Perkins, my advisor. Starting of as your first and, at that time, only graduate student was a plunge into the deep unknown. It turned out to be a warm bath. You gave me the opportunities to grow as an academic and a professional. Your hard work was sometimes terrifying, but always inspiring. (Your sharp mind equally so, especially after a fine cup of lab-brewed espresso!) Alex, I want to thank you for your trust and support. It has been an amazing ride.

I would like to thank my committee members, David Severson, Frank Collins, and Gregory Madey. You guided me through the rough patches and cheered me through the smooth ones. I am grateful for your academic and professional guidance. I truly lucked out with such a wonderful team behind me.

I want to express my gratitude to Dave Chadee. We have lost 'One of Trinidad and Tobago's greatest minds' too early. It was a great honor to work with you, a fair and passionate mentor, an inspiring voice of the vector control community across the world. Dave, you will be greatly missed.

I want to thank all my collaborators, on campus and far beyond. John Grieco and Nicole Achee, for sharing your data and knowledge and opening the doors to the fascinating world of entomology for me. Neil Lobo, for being a great mentor and a rock of support. Brajendra Singh, for guidance, perseverance, and long philosophical walks. I thank all the co-authors of the work presented in this dissertation, Hannah Clapham,

Louis Lambrechts, Benjamin Althouse, Alun Lloyd, Lance Waller, Amy Morrisson, Uriel Kitron, Gonzalo Vazquez-Prokopec, Thomas Scott, Edwin Michael, Radzi Muhammad Hassan, Fanny Castro-Llanos, Hortance Manda, Joseph Wagman, and Steven Stoddard for contributing to this work. I thank my collaborators at the Institute for Disease Modeling, in particular Phillip Eckhof, Jonathan Bloedow, Benoit Raybaud, and the rest of the team I worked with for my research assistantship. I thank my lab and office mates: Michelle Ngai, Colin Teberg, Benjamin Mayala, Diana LaTorre, Sarah Lukens, Guido Espana, Rachel Oidtman, Amir Siraj, and Karly Harrod. It would have been so much less fun without you all.

This work was partially supported by the National Institute of Allergy and Infectious Diseases of the National Institutes of Health under Award Number P01AI098670. Thank you to the Eck Institute for Global Health for supporting me for two years through the Eck fellowship. And thank you to GlaxoSmithKline, DARPA, and the Institute for Disease Modeling for financially supporting me. Thank you to the Department of Biological Sciences and the Globes Certificate in Environment and Society Program for providing a fruitful learning environment.

Thanks a lot to my family and friends for support, comfort, and revitalizing distractions. Thank you to my ‘paranimf’ Caroline Coppens for always being there for advice and protecting the ‘ademende agenda’. Thank you to my parents, Marjan en Pieter ten Bosch, for your unconditional love and support, for thirty-one years and counting. And thank you to Lysette, the co-pilot on this American adventure. I couldn’t have done it without your love, support, and eternal patience.

CHAPTER 1:

INTRODUCTION

1.1 The global burden of dengue

With a 30-fold increase in incidence over the last five decades and no signs of slowing down, dengue poses an increasing threat to about half of the world's population (1, 2). Dengue viruses (DENVs) belong to the family *Flaviviridae,* genus *Flavivirus*, and are related to other mosquito-borne viruses such as Zika, yellow fever, West Nile, and Japanese encephalitis. They circulate in four major serotypes (DENV1-4) (3, 4), and manifest a wide spectrum of clinical forms, from subclinical to classic dengue fever to the more serious forms of the disease; namely, dengue hemorrhagic fever (DHF) and dengue shock syndrome (DSS). In the absence of treatment, dengue can be highly fatal in subjects with DHF or DSS, with a case fatality rate of 15%, which may be reduced to 1% with adequate medical intervention (5). The predominant mosquito vector of dengue, *Ae. aegypti*, is an urban, day-biting container-breeding mosquito that is prevalent across the tropics and subtropics (6). *Ae. albopticus* has a wider range (6) and can be found in more rural areas, yet is believed to be a less competent vector than *Ae. aegypti* (7). In the absence of effective antiviral drugs or established vaccines, control efforts currently rely heavily on the control of the mosquito vector (8).

1.2 The transmission cycle

Dengue is transmitted through the bite of one of its mosquito vectors (predominantly *Aedes aegypti* and *Aedes albopictus*). Upon infection, the virus replicates in the human body, its viremia peaking roughly around the onset of symptoms (in the case of symptomatic infection) and reducing thereafter in response to the human immune response. The human infectiousness to the mosquito is roughly proportional to the viremia (as measured by qPCR), although factors have been found to affect the probability of infection independently, such as serological response (9), day of illness (9), virus strain (9), virus genotype (10), and clinical representation (11). This relationship will be further discussed in Chapter 2. Upon an infectious bite, the virus needs to cross the mosquito midgut and migrate to the salivary glands before onward transmission can occur. This timeframe is referred to as the extrinsic incubation period (EIP). The duration of the EIP depends, among other things, on the viral load of the blood meal (12), as well as temperature (13). Because the EIP is of similar magnitude as the mosquito's life expectancy, the potential for a mosquito to transmit DENV during its lifetime is sensitive to the local climate. This, in conjunction with the climate-driven population dynamics of the mosquito species, determines the climate-dependent suitability for dengue transmission (2).

1.3 Natural history of dengue disease

Dengue infection can result in a range of clinical outcomes, from the complete absence of perceivable symptoms or mild symptoms to dengue fever (DF) or the more severe manifestations dengue hemorrhagic fever (DHF) and dengue shock syndrome (DSS) (1). The time between infection and symptom onset (the intrinsic incubation

period (IIP)) ranges between 3 and 7 days (13). These symptoms may include fever, rash, vomiting, headaches, and severe joint pain. Severe manifestations of DENV infection typically present at a later stage of the infection, when fever diminishes. Hemorrhage and shock as a result of plasma leakage can result at this stage (4).

1.4 Diagnosis

Diagnosis of dengue is based on virological and serological methods. During the active phase of illness, definitive diagnosis is possible through RT-PCR virus detection. The peak viremia levels (typically 2-3 days after onset of fever) correlate with disease severity (14) and are predictors of the development of DHF (15). RT-PCR is relatively quick but is time-sensitive and requires expensive equipment. Approximately five days after symptom onset, viremia declines beneath detectable quantities (see Chapter 2 for a discussion on how these viral titers differ across individuals). Serological tests are commonly used instead of or in addition to virus detection. The two major markers of dengue infection, immunoglobins IgG and IgM, follow different trajectories for primary or post-primary infections, thereby providing a tool to reveal a patient's immune history (16). However, these diagnostic tools are hampered by cross-reactivity, variable sensitivity associated with the timing of specimen collection, and the need for multiple sampling time points (1).

1.5 Control

The global expansion and increasing burden of dengue present a great challenge to health agencies across the world. With the first ever dengue vaccine licensed in 2015 (17), and more candidates in different stages of the pipeline, it is hoped that more

effective control programs are on the horizon. Until then, dengue control heavily relies on the control of its mosquito vectors.

1.5.1 Vaccines

Upon official licensing in Mexico December of 2015, Dengvaxia® (CYD-TDV) became the first ever approved dengue vaccine (17). Phase-3 trials evaluating the vaccine showed vaccine efficacy (VE) against symptomatic disease of about 60% (18). This vaccine efficacy varied substantially by age, baseline serostatus, and serotype, with particularly low efficacy against DENV-2 (18). Limited efficacy in immunologically naïve individuals (pooled VE: 38.1%, 95% CI: 3.4-62.9) (18) and an elevated risk of hospitalization in 2-5 year olds (Relative Risk = 7.45, 95% CI 1.15-313.80) (18), has resulted in the exclusion of younger age groups in the initial indication (17). Other vaccine candidates are in clinical trials or under preclinical evaluation. Each of these will need to overcome safety issues associated with antibody-dependent enhancement (ADE) and cross-reactive T-cells that may contribute to adverse outcomes of vaccination in DENV-naïve individuals (17).

1.5.2 Antiviral drugs

Despite the large burden of disease associated with dengue (19) there are no antiviral drugs for the treatment or prophylaxis of DENV infection (20). Recent advances in animal and cell culture models, reverse genetics, and crystallography have granted great progress in the development of DENV-specific and non-specific inhibitors. However, none of these approaches have been shown to have beneficial clinical effects (20). As with the development of dengue vaccines, antiviral drug development is challenged by variable effects across serotypes, as well as poor pharmacokinetics, and

adverse effects (20). The recent successes in antivirals for the related hepatitis C virus however spark hope for the feasibility of a potent and safe DENV antiviral to be developed in the future (20).

1.5.3 Vector control

The conceptual premise for vector control ultimately derives from the Ross-MacDonald model, which provides a basic description of the pathogen's life cycle in the context of population-level transmission (21). Interventions that successfully reduce mosquito abundance, the survival time relative to the pathogen incubation period, or vector-host contact could potentially have large impacts on transmission. Typical control strategies include breeding site reduction to prevent adult development and insecticidal spraying to decrease the adult populations (22). The latter is largely challenged by the resting behavior of *Ae. aegypti*, which is typically found in indoor sheltered places. Unless applied indoors, the effect of such techniques is limited (22). Additionally, large-scale use of indoor residual spraying has substantial logistic limitations (22). Successes with breeding site reduction date back to the early twentieth century, when the US army achieved the elimination of *Ae. aegypti* mediated yellow fever in Havana, Cuba (23). Halfway through the last century, elimination of *Ae. aegypti* was achieved in large parts of the Caribbean and Central and South America resulting in striking reductions in yellow fever and dengue transmission (24). However, with the relaxation of control efforts, *Ae. aegypti* has reinvaded as a primary vector in the early 1970s (25). To date, primarily only the control programs in Singapore and Cuba are regarded as public health successes, yet both countries have experienced dramatic re-emergence of dengue in part as a result of decreased herd immunity (26, 27). In conjunction with the limited

effectiveness of control programs, the public health community is challenged by the expansion of the virus' global distribution. Driven by increased globalization, uncontrolled urbanization, poor waste management, emergence of insecticide resistance, and the lack of effective control efforts, the need for new, complementary control tools is ever more pertinent (28). In addition, with the recent introduction of dengue vaccines, strategies that combine vector control and vaccination have potential for more effective reduction of dengue's burden (29). Rigorous assessment of existing and novel control tools is necessary to select strategies that are best suited for this challenge.

1.5.3.1 Novel vector control tools

Given the perceived limited effectiveness of existing vector control tools, novels tool are under development. These include strategies that aim to affect the mosquito abundance, life expectancy of female mosquitoes, or refractoriness to DENV infection (30). The bacterial symbiont *Wolbachia* is one promising near-term approach. *Ae. aegypti* populations infested with the heritable *w*Mel or *w*MelPop strains display reduced DENV-transmission, while preserving fitness and thus allowing for establishment in the field. Estimates from lab studies predict that reduction of R_0 of DENV transmission of 66-75% (31). Alternative approaches to induce DENV refractoriness include genetic modification (GM) efforts. DENV-2 transmission blocking strains have been developed and tested in laboratory settings but no field trials have been conducted so far (32, 33). Other genetic engineering strategies have been developed to reduce the mosquito population. Male *Ae. aegypti* mosquitoes of the RIDL® - strain, when released in a natural population, mate with wild-type females, causing most of their offspring to die at late larval stages (34). Small field trials have confirmed the potential of this strategy, though mostly in areas

with low mosquito abundance (35, 36). Other transgenic methods under development rely on similar principles yet only affect female offspring (37, 38) or distort the sex-ratio by introducing a strain that predominantly produces male offspring (39).

Spatial repellents (SRs) constitute another new paradigm for vector control in a public-health context and will be specifically addressed in Chapters 4 and 5. SR tools consist of sub-lethal products aimed at reducing human-vector contact through either movement away from the product or interference with host detection and blood feeding. Spatial repellency is distinct from other chemical actions such as contact irritancy and toxicity. Still, many compounds exhibit a combination of modes of action. The combination and magnitude of effect depends on the concentration or dose administered. Repellency typically occurs at low vapor phase concentrations, whereas irritancy and toxicity require increasingly high levels (40). The effectiveness of SR-products has been shown in several studies, demonstrating significantly reduced *Ae. aegypti* biting rates resulting from increased mortality and disorientation, depending on the product used (41, 42). Kawada et al. showed reduced biting rates by *Anopheles* and *Culex* species resulting from metofluthrin-impregnated paper strips administered in half-open huts in Lombok, Indonesia (43). The protective effect of SRs in open or semi-closed habitats is an important feature of SRs since indoor residual spraying (IRS) and insecticide treated nets (ITNs) provide limited protection in such environments. Additionally, the sub-lethality of SRs as well as the reduced contact with IRS and ITNs may impose weaker selective pressure on the mosquito, and thereby delay the onset of resistance against active ingredients (44). The low product and distribution costs, ease of use and applicability to a variety of vectors make SRs a potentially useful addition to the current control landscape.

However, studies that demonstrate clear effects of SRs on disease transmission are scarce (45). Results of a cluster-randomized trial in China show a 77% reduction in the risk of acquiring malaria infection (tested by rapid diagnostic tests) in clusters with a coil treatment relative to control clusters (46). Similarly, reduced *Anopheles* biting rates and transmission rates were observed in a randomized placebo-controlled trial in Indonesia (47). While these studies present promising epidemiological effects of SR products on malaria, further studies are required to demonstrate significant protective efficacy against malaria, dengue, and other human infections in a diversity of settings, as well as to define optimal patterns of use and examine the potential for indirect effects such as the diversion of bites to untreated proximate households (48, 49).

To quantify the protective efficacy of SR in reducing malaria and dengue incidence, a set of field trials is ongoing. For dengue, a large-scale cluster-randomized trial (CRT) is being conducted in the city of Iquitos, Peru, measuring the effects of SR distribution on both epidemiological and entomological outcomes. While this study will be crucial for informing the adoption (or not) of SR products as a stand-alone or complementary control tool, the interpretation and generalization of such CRTs is challenged by complex, often unmeasured heterogeneities in transmission, human mobility and mosquito abundance, amongst others (50-53). In addition, the impact of spatial repellents and other vector control products (and combinations thereof) will vary between settings, for instance due to differences in insecticide resistance, species composition, and housing structures. Assessing the impact of vector control across these many scenarios is complicated, if not infeasible. Mathematical models are valuable tools for exploring the impact of vector control strategies early in the development process, and

help prioritize those products worth advancing to field trials. In Chapter 4 and 5, I introduce a set of tools to accommodate this process.

1.6 Mathematical models

Mechanistic models are powerful tools to gain insights into the complex ecological and evolutionary dynamics of infectious pathogens. Complementary to statistical or phenomenological models, mechanistic models can be used to test hypotheses on the drivers of epidemiological patterns, estimate the timing and extent of outbreaks, and guide and evaluate decision-making (54). Models of dengue transmission and control are widespread and differ substantially in the level of biological complexity they encapsulate (54). Depending on the purpose of the model, different levels of detail can be included on the human demographics, mosquito population dynamics, the natural history of DENV in a population, serotype interactions, and the effects of control efforts (54).

Models have been used to help understand the drivers of patterns typical of dengue. Dengue dynamics are typically highly seasonal with multi-annual fluctuations. In addition, the sequential, irregular replacements of serotypes are characteristic of dengue epidemiology. These dynamics are believed to be harbored by a complex interplay between environmental factors, vector ecology, and host-pathogen dynamics(55). Modeling studies have been done to elucidate the roles that cross-immunity (CI) (56-59), cross-enhancement between serotypes (60-63), and seasonal variation in the transmission rate (57, 64, 65), amongst others, play in these complex dynamics (66). The majority of these are differential-equation models (Perkins et al. 2015). Models used for answering this types of questions need to be relatively parsimonious to ensure tractability (67). A

comprehensive comparison of the main proposed model hypotheses on the drivers of observed dynamics and the challenges in finding the right level of parsimony for these models are discussed in Chapter 3.

Models intended to gain more quantitative insights such as required timing and coverage of control, or expected outbreak size, often contain increasing detail to ensure that no determining processes are overlooked (68-70). Individual-based models (IBM) are a specific group of models particularly suitable to capture great levels of detail of transmission and population dynamics. In IBMs, each individual is an autonomous agent with a certain set of properties whose actions and interactions are explicitly simulated. The emerging properties that result from these interactions can give great insights in the underlying drivers of disease dynamics, and help elucidate the role of heterogeneities in space, time, and across individuals (71). IBMs are increasingly used in vector-borne disease modeling, in particular for malaria (72) and increasingly for dengue research. Recent applications include the impact of control efforts such as vector control (73) and vaccines (74-76), and the impact of heterogeneities in projetions of vaccine impact (77).

1.7 Thesis structure and aims

In this thesis, I describe the use of mathematical models to parse data on different aspects of dengue's epidemiology. In Chapter 2, mathematical models are used to infer the proportion of overall dengue transmission that is attributable to infected individuals whose symptoms are so mild that they do not seek care and remain unreported by health surveillance systems. In Chapter 3, mathematical models are fitted to various patterns observed in dengue data to test different hypotheses on the drivers of dengue's complex dynamics. Chapter 4 and 5 address the use of mathematical models to inform the

potential impact of vector control tools, with spatial repellents as a case study. In Chapter 4, a Bayesian continuous-time Markov chain model framework is used to estimate the multifaceted effects of a spatial repellent product on mosquito behavioral and bionomic traits in an experimental hut study. In Chapter 5, a new mathematical framework using the force of infection as an outcome metric is introduced to examine the community-level impact of a spatial repellent product using data from laboratory and experimental hut settings.

1.8 References

1. World Health Organization (2012) Dengue guidelines for diagnosis, treatment, prevention and control. 2009. *WHO, Geneva, Switzerland*

2. Bhatt S*, et al* (2013) The global distribution and burden of dengue. *Nature* 496: 504-507.

3. Calisher CH*, et al* (1989) Antigenic relationships between flaviviruses as determined by cross-neutralization tests with polyclonal antisera. *J Gen Virol* 70(1): 37-43.

4. Gubler DJ, Ooi EE, Vasudevan S & Farrar J (2014) *Dengue and dengue hemorrhagic fever,* (CABI,

5. Kalayanarooj S (1999) Standardized clinical management: Evidence of reduction of dengue haemorrhagic fever case-fatality rate in thailand. *Dengue Bull* 23: 10-17.

6. Kraemer MU*, et al* (2015) The global distribution of the arbovirus vectors aedes aegypti and ae. albopictus. *Elife* 4: e08347.

7. Lambrechts L, Scott TW & Gubler DJ (2010) Consequences of the expanding global distribution of aedes albopictus for dengue virus transmission. *PLoS Negl Trop Dis* 4(5): e646.

8. Murrell S, Wu SC & Butler M (2011) Review of dengue virus and the development of a vaccine. *Biotechnol Adv* 29(2): 239-247.

9. Nguyen MN*, et al* (2013) Host and viral features of human dengue cases shape the population of infected and infectious aedes aegypti mosquitoes. *Proc Natl Acad Sci U S A* 110(22): 9072-9077.

10. Lambrechts L*, et al* (2012) Dengue-1 virus clade replacement in thailand associated with enhanced mosquito transmission. *J Virol* 86(3): 1853-1861.

11. Duong V*, et al* (2015) Asymptomatic humans transmit dengue virus to mosquitoes. *Proc Natl Acad Sci U S A* 112: 14688-14693.

12. Fontaine A, Jiolle D, Moltini-Conclois I, Lequime S & Lambrechts L (2016) Excretion of dengue virus RNA by aedes aegypti allows non-destructive monitoring of viral dissemination in individual mosquitoes. *Sci Rep* 6: 24885.

13. Chan M & Johansson MA (2012) The incubation periods of dengue viruses. *PloS One* 7(11): e50972.

14. Vaughn DW*, et al* (2000) Dengue viremia titer, antibody response pattern, and virus serotype correlate with disease severity. *J Infect Dis* 181(1): 2-9.

15. Libraty DH*, et al* (2002) Differing influences of virus burden and immune activation on disease severity in secondary dengue-3 virus infections. *J Infect Dis* 185(9): 1213-1221.

16. Peeling RW*, et al* (2010) Evaluation of diagnostic tests: Dengue. *Nature Reviews Microbiology* 8: S30-S37.

17. Vannice KS, Durbin A & Hombach J (2016) Status of vaccine research and development of vaccines for dengue. *Vaccine* 34(26): 2934-2938.

18. Hadinegoro SR*, et al* (2015) Efficacy and long-term safety of a dengue vaccine in regions of endemic disease. *N Engl J Med* 373(13): 1195-1206.

19. Stanaway JD*, et al* (2016) The global burden of dengue: An analysis from the global burden of disease study 2013. *The Lancet Infectious Diseases* 16: 712-723.

20. Kaptein SJ & Neyts J (2016) Towards antiviral therapies for treating dengue virus infections. *Current Opinion in Pharmacology* 30: 1-7.

21. Smith DL*, et al* (2012) Ross, macdonald, and a theory for the dynamics and control of mosquito-transmitted pathogens. *PLoS Pathogens* 8(4): e1002588.

22. Reiter P (2014) 25 surveillance and control of urban dengue vectors. *Dengue and Dengue Hemorrhagic Fever* : 481.

23. Strode GK (1951) Yellow fever. *Yellow Fever*

24. Monath TP (1994) Yellow fever and dengue—the interactions of virus, vector and host in the re-emergence of epidemic disease5(2): 133-145.

25. Halstead SB (2006) Dengue in the americas and southeast asia: Do they differ?. *Revista Panamericana De Salud Pública* 20(6): 407-415.

26. Egger JR, *et al* (2008) Reconstructing historical changes in the force of infection of dengue fever in singapore: Implications for surveillance and control. *Bull World Health Organ* 86(3): 187-196.

27. Armada Gessa JA & Gonzalez RF (1987) Application of environmental management principles in the programme for eradication of aedes (stegomyia) aegypti (linneus, 1762) in the republic of cuba, 1984.

28. Gubler DJ (2011) Dengue, urbanization and globalization: The unholy trinity of the 21(st) century. *Trop Med Health* 39(4 Suppl): 3-11.

29. Christofferson RC & Mores CN (2015) A role for vector control in dengue vaccine programs. *Vaccine* 33(50): 7069-7074.

30. Achee NL, *et al* (2015) A critical assessment of vector control for dengue prevention. *PLoS Negl Trop Dis* 9(5): e0003655.

31. Ferguson NM, *et al* (2015) Modeling the impact on virus transmission of wolbachia-mediated blocking of dengue virus infection of aedes aegypti. *Sci Transl Med* 7(279): 279ra37.

32. Franz AW, *et al* (2006) Engineering RNA interference-based resistance to dengue virus type 2 in genetically modified aedes aegypti. *Proc Natl Acad Sci U S A* 103(11): 4198-4203.

33. Sanchez-Vargas I, *et al* (2004) RNA interference, arthropod-borne viruses, and mosquitoes. *Virus Res* 102(1): 65-74.

34. Phuc HK, *et al* (2007) Late-acting dominant lethal genetic systems and mosquito control. *BMC Biol* 5: 11.

35. Harris AF, *et al* (2012) Successful suppression of a field mosquito population by sustained release of engineered male mosquitoes. *Nat Biotechnol* 30(9): 828-830.

36. Lacroix R, *et al* (2012) Open field release of genetically engineered sterile male aedes aegypti in malaysia. *PloS One* 7(8): e42771.

37. Alphey L, *et al* (2010) Sterile-insect methods for control of mosquito-borne diseases: An analysis. *Vector-Borne and Zoonotic Diseases* 10(3): 295-311.

38. McGraw EA & O'Neill SL (2013) Beyond insecticides: New thinking on an ancient problem. *Nature Reviews Microbiology* 11(3): 181-193.

39. Galizi R, *et al* (2014) A synthetic sex ratio distortion system for the control of the human malaria mosquito. *Nature Communications* 5

40. Grieco JP, *et al* (2007) A new classification system for the actions of IRS chemicals traditionally used for malaria control. *PLos One* 2(8): e716.

41. Rapley LP, Russell RC, Montgomery BL & Ritchie SA (2009) The effects of sustained release metofluthrin on the biting, movement, and mortality of aedes aegypti in a domestic setting. *Am J Trop Med Hyg* 81(1): 94-99.

42. Ritchie SA & Devine GJ (2013) Confusion, knock-down and kill of aedes aegypti using metofluthrin in domestic settings: A powerful tool to prevent dengue transmission. *Parasit Vectors* 6: 262-280.

43. Kawada H, Maekawa Y, Tsuda Y & Takagi M (2004) Trial of spatial repellency of metofluthrin impregnated paper strip against anopheles and culex in shelters without walls in lombok, indonesia. *J Am Mosq Control Assoc* 20(4): 434-437.

44. Achee NL, *et al* (2012) Spatial repellents: From discovery and development to evidence-based validation. *Malar J* 11(1): 164.

45. Ogoma SB, Moore SJ & Maia MF (2012) A systematic review of mosquito coils and passive emanators: Defining recommendations for spatial repellency testing methodologies. *Parasit Vectors* 5: 287.

46. Hill N, *et al* (2014) A household randomized, controlled trial of the efficacy of 0.03% transfluthrin coils alone and in combination with long-lasting insecticidal nets on the incidence of plasmodium falciparum and plasmodium vivax malaria in western yunnan province, china. *Malaria Journal* 13: 208.

47. Syafruddin D, *et al* (2014) Impact of a spatial repellent on malaria incidence in two villages in sumba, indonesia. *Am J Trop Med Hyg* 91(6): 1079-1087.

48. Maia MF, *et al* (2016) A crossover study to evaluate the diversion of malaria vectors in a community with incomplete coverage of spatial repellents in the kilombero valley, tanzania. *Parasites & Vectors* 9(1): 451.

49. Maia MF, *et al* (2013) Do topical repellents divert mosquitoes within a community?–Health equity implications of topical repellents as a mosquito bite prevention tool. *PLoS One* 8(12): e84875.

50. Liebman KA, *et al* (2014) Determinants of heterogeneous blood feeding patterns by aedes aegypti in iquitos, peru. *PLoS Neglected Tropical Diseases* 8(2): e2702.

51. LaCon G, *et al* (2014) Shifting patterns of aedes aegypti fine scale spatial clustering in iquitos, peru. *PLoS Neglected Tropical Diseases* 8(8): e3038.

52. Getis A, Morrison AC, Gray K & Scott TW (2003) Characteristics of the spatial pattern of the dengue vector, aedes aegypti, in iquitos, peru. *Am J Trop Med Hyg* 69(5): 494-505.

53. Perkins TA, *et al* (2014) Theory and data for simulating fine-scale human movement in an urban environment. *J R Soc Interface* 11(99): 10.1098/rsif.2014.0642.

54. Perkins TA*, et al* (2015) in *Dengue and Dengue Hemorrhagic Fever 2nd Edition,* eds Gubler DJ, Ooi EE, Vasudevan S & Farrar J (CABI, Oxfordshire), pp 99--114.

55. Cummings DAT*, et al* (2004) Travelling waves in the occurrence of dengue haemorrhagic fever in thailand. *Nature* 427(6972): 344-347.

56. Adams B*, et al* (2006) Cross-protective immunity can account for the alternating epidemic pattern of dengue virus serotypes circulating in bangkok. *Proc Natl Acad Sci U S A* 103(38): 14234-14239.

57. Wearing HJ & Rohani P (2006) Ecological and immunological determinants of dengue epidemics. *Proc Natl Acad Sci U S A* 103(31): 11802.

58. Nagao Y & Koelle K (2008) Decreases in dengue transmission may act to increase the incidence of dengue hemorrhagic fever. *Proc Natl Acad Sci U S A* 105(6): 2238-2243.

59. Reich NG*, et al* (2013) Interactions between serotypes of dengue highlight epidemiological impact of cross-immunity. *J R Soc Interface* 10(86): 20130414.

60. Cummings DA, Schwartz IB, Billings L, Shaw LB & Burke DS (2005) Dynamic effects of antibody-dependent enhancement on the fitness of viruses. *Proc Natl Acad Sci U S A* 102(42): 15259-15264.

61. Ferguson N, Anderson R & Gupta S (1999) The effect of antibody-dependent enhancement on the transmission dynamics and persistence of multiple-strain pathogens. *Proc Natl Acad Sci U S A* 96(2): 790.

62. Recker M*, et al* (2009) Immunological serotype interactions and their effect on the epidemiological pattern of dengue. *P Roy Soc B-Biol Sci* 276(1667): 2541.

63. Schwartz IB*, et al* (2005) Chaotic desynchronization of multistrain diseases. *Phys Rev E Stat Nonlin Soft Matter Phys* 72(6 Pt 2): 066201.

64. Aguiar M, Ballesteros S, Kooi BW & Stollenwerk N (2011) The role of seasonality and import in a minimalistic multi-strain dengue model capturing differences between primary and secondary infections: Complex dynamics and its implications for data analysis. *J Theor Biol* 289: 181-196.

65. Lourenço J & Recker M (2013) Natural, persistent oscillations in a spatial multi-strain disease system with application to dengue. *PLoS Comput Biol* 9(10): e1003308.

66. Andraud M, Hens N, Marais C & Beutels P (2012) Dynamic epidemiological models for dengue transmission: A systematic review of structural approaches. *PLoS One* 7(11): e49085.

67. Amaku M*, et al* (2014) Interpretations and pitfalls in modelling vector-transmitted infections. *Epidemiol Infect* : 1-13.

68. Magori K*, et al* (2009) Skeeter buster: A stochastic, spatially explicit modeling tool for studying aedes aegypti population replacement and population suppression strategies. *PLoS Negl Trop Dis* 3(9): e508.

69. Otero M & Solari HG (2010) Stochastic eco-epidemiological model of dengue disease transmission by aedes aegypti mosquito. *Math Biosci* 223(1): 32-46.

70. Focks DA, Daniels E, Haile DG & Keesling JE (1995) A simulation model of the epidemiology of urban dengue fever: Literature analysis, model development, preliminary validation, and samples of simulation results. *Am J Trop Med Hyg* 53(5): 489-506.

71. Auchincloss AH & Diez Roux AV (2008) A new tool for epidemiology: The usefulness of dynamic-agent models in understanding place effects on health. *Am J Epidemiol* 168(1): 1-8.

72. Arifin SN, Madey GR & Collins FH (2016) *Spatial Agent-Based Simulation Modeling in Public Health: Design, Implementation, and Applications for Malaria Epidemiology,* (John Wiley & Sons,

73. Arifin SN, Madey GR & Collins FH (2013) Examining the impact of larval source management and insecticide-treated nets using a spatial agent-based model of anopheles gambiae and a landscape generator tool. *Malaria Journal* 12(1): 1.

74. Flasche S*, et al* (2016) The long-term safety, public health impact, and cost-effectiveness of routine vaccination with a recombinant, live-attenuated dengue vaccine (dengvaxia): A model comparison study. *PLoS Medicine* 13(11): e1002181.

75. Hladish TJ*, et al* (2016) Projected impact of dengue vaccination in yucatán, mexico. *PLOS Negl Trop Dis* 10(5): e0004661.

76. Penny MA, Galactionova K, Tarantino M, Tanner M & Smith TA (2015) The public health impact of malaria vaccine RTS, S in malaria endemic africa: Country-specific predictions using 18 month follow-up phase III data and simulation models. *BMC Medicine* 13(1): 1.

77. Perkins A*, et al* (2016) Statistical and biological uncertainties associated with vaccine efficacy estimates and their implications for dengue vaccine impact projections. *bioRxiv* : 082396.

CHAPTER 2:

CONTRIBUTIONS FROM THE SILENT MAJORITY DOMINATE DENGUE VIRUS TRANSMISSION

Quirine A. ten Bosch, Hannah E. Clapham, Louis Lambrechts,

Benjamin M. Althouse, Alun L. Lloyd, Lance A. Waller, Amy C. Morrison

Uriel Kitron, Gonzalo M. Vazquez-Prokopec, Thomas W. Scott, T. Alex Perkins

2.1 Abstract

Despite estimates that each year nearly 300 million dengue virus (DENV) infections result in either no perceptible symptoms (asymptomatic) or symptoms that are sufficiently mild to go undetected by surveillance systems (1), it has been assumed that these individuals contribute little to onward transmission (2-5). Recent blood-feeding experiments with *Aedes aegypti* mosquitoes showed that people with asymptomatic and pre-symptomatic DENV infections are capable of infecting mosquitoes (6). Here, we combine those findings (6) with models of within-host viral dynamics (7) and human demographic projections to (1) quantify the net infectiousness of individuals across the spectrum of DENV infection severity and (2) estimate the fraction of transmission attributable to inapparent DENV infections. Our results show that the net infectiousness of asymptomatic individuals is relatively high at 77% (interquartile range: 16-118%) that of symptomatic individuals. Due to their numerical prominence in the infectious

reservoir, clinically inapparent infections in total could account for 73% (IQR: 71-74%) of DENV transmission. Of infections that ultimately result in symptoms, we estimate that 25% (IQR: 12-44%) of onward transmission results from mosquitoes biting individuals during the pre-symptomatic phase of their infection. Only 1.6% (IQR: 1.5-1.7%) of DENV transmission is attributable to detected apparent infections after they have presented with symptoms. These findings emphasize the need to (1) reorient current practices for outbreak response to adoption of pre-emptive strategies that account for contributions of undetected infections and (2) apply methodologies that account for undetected infections in surveillance programs, when assessing intervention impact, and when modeling mosquito-borne virus transmission.

2.2 Significance statement

Most dengue virus infections result in either no perceptible symptoms or symptoms that are so mild that they go undetected by surveillance systems. It is unclear how much these infections contribute to the overall transmission and burden of dengue. At an individual level, we show that individuals with asymptomatic infections are capable of infecting 77% as many mosquitoes as their symptomatic counterparts. At a population level, we show that 80% of infections result from individuals who display no apparent symptoms at the time of transmission. These results suggest that individuals undetected by surveillance systems may be the primary reservoir of dengue virus transmission and that policy for dengue control and prevention must be revised accordingly.

2.3 Introduction

Though often assumed benign, it is increasingly recognized that for many pathogens, inapparent infections may represent a sizeable portion of the infectious reservoir (RW.ERROR - Unable to find reference:803) and contribute substantially to transmission (10). Understanding the contribution to transmission from inapparent infections can be fundamental for inferring drivers of transmission (RW.ERROR - Unable to find reference:803), estimating the timing and scope of outbreaks (11), planning and monitoring control efforts (12), and assessing the feasibility of elimination (8, 12).

The four closely related serotypes of dengue virus (DENV1-4) are transmitted predominantly by *Aedes aegypti* mosquitoes (13). Infection with one serotype is believed to be followed by short-term, heterologous cross-immunity and life-long homologous immunity (14). Of the total 390 million annual DENV infections, an estimated 300 million do not result in symptoms severe enough for a person to seek treatment and thus go undetected by surveillance systems (1, 15). Based on observed positive correlations between DENV viremia and disease severity (2-5), it has been assumed that these individuals contribute little to onward transmission. High sero-conversion rates coinciding with few reported cases in Salvador, Brazil, however suggest that inapparent infections may contribute to silent DENV transmission (16). Recent blood-feeding experiments with *Aedes aegypti* mosquitoes showed that people with asymptomatic and pre-symptomatic DENV infections are indeed capable of infecting mosquitoes (6). Although the role of inapparent infections in DENV transmission has become more evident, what proportion of overall transmission are responsible for remains to be

determined. Our goal was to estimate the net infectiousness of DENV infected individuals with different clinical manifestations, including asymptomatic infections, and to quantify the contributions of these clinically distinct classes to overall force of infection (FoI) of DENV.

2.4 Results

2.4.1 Definitions

In our analyses, we distinguished four classes of infections (Figure 2-1). We referred to the first class as "asymptomatic" (A), which we defined as having absolutely no perceptible symptoms at any point during the infection (6). The remaining symptomatic (S) infections were divided into: inapparent symptomatic (IS), people whose symptoms are sufficiently mild to not disrupt their daily routine and thus do not prompt healthcare seeking (6, 15), and apparent symptomatic (AS) individuals, whose clinical presentation does disrupt their daily routine (the WHO definition of "at least fever and two dengue symptoms"(17) was applied as a proxy). AS individuals are detected by health surveillance systems (DAS) if they seek clinical consultation and are diagnosed as a confirmed dengue case. Others remain undetected (UAS) (Figure 2-1).

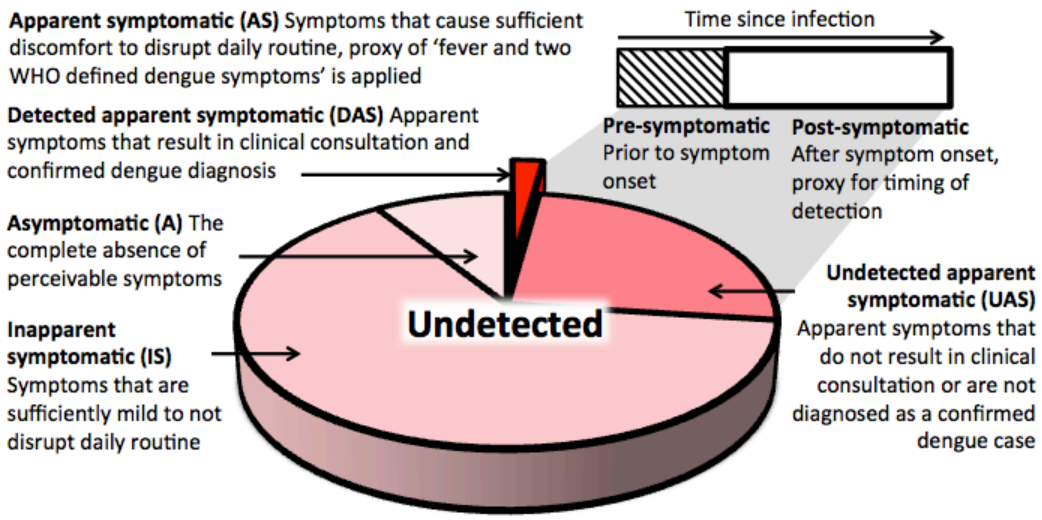

Figure 2-1: Definitions of infection classes.

2.4.2 Net infectiousness

We quantified differences in the net infectiousness to mosquitoes of individuals with A, IS, and AS infections. We modeled viral dynamics of each of these infection types by using a mechanistic model of the within-host dynamics of DENV fitted to plasma viral titers over time for patients with S infections (7). To model viremia trajectories of A infections, we multiplied viral trajectories of S infections by the ratio of random draws from normally distributed viremia levels of A and S (median ratio: 0.76, interquartile range (IQR): 0.74-0.77), as observed for natural infections in Cambodia (6). Secondary (2°) infections were parameterized to exhibit faster cell entry and accelerated clearance of viral particles than primary (1°) infections, consistent with theory for antibody dependent enhancement and increased activation of the immune system (7). This resulted in a shorter duration of detectable and potentially infectious viremia. Next, we applied logistic regression models (6) to infer mosquito-human infectiousness from human viral titers (Table S2-1). We applied different functions for A, for S before the

onset of symptoms (pre-symptomatic), and for S after symptom onset (post-symptomatic). Combining an individual viremia trajectory with functions mapping viremia onto infectiousness to mosquitoes yielded an individual-level infectiousness trajectory, the integral of which we defined as net infectiousness (Materials and methods).

The median net infectiousness to *Ae. aegypti* of asymptomatic infections was lower than that of symptomatic infections, but of similar magnitude (1°: 86%, IQR: 22-126%; 2°: 73%, IQR: 11-110%). The median net infectiousness of primary infections was greater than that of corresponding secondary infections (A: 136%, IQR: 119-256%; S: 117%, IQR: 103-139%) (Figure 2-2). Approximately one quarter of the net infectiousness of symptomatic infections occurred before symptom onset (1°: 22%, IQR: 12-34%, 2°: 28%, IQR: 12-52%). By calculating the probability that a random draw from the net infectiousness distribution of one infection class was lower than a random draw from another class, we confirmed that asymptomatic infections were more likely to be less infectious than symptomatic infections (1°: 0.55; 2°: 0.59) and secondary infections were more likely to be less infectious than primary infections (A: 0.57; S: 0.60) (Table S2-2). There was wide variability in the infectiousness of asymptomatic infections, however, with two-fold lesser or greater infectiousness compared to symptomatic infections both appearing probable (lesser, 1°: 0.37, 2°: 0.43; greater, 1°: 0.17, 2°: 0.20). Overall, primary asymptomatic infections were not significantly less infectious than secondary symptomatic infections (Wilcoxon rank sum test, $p = 0.48$).

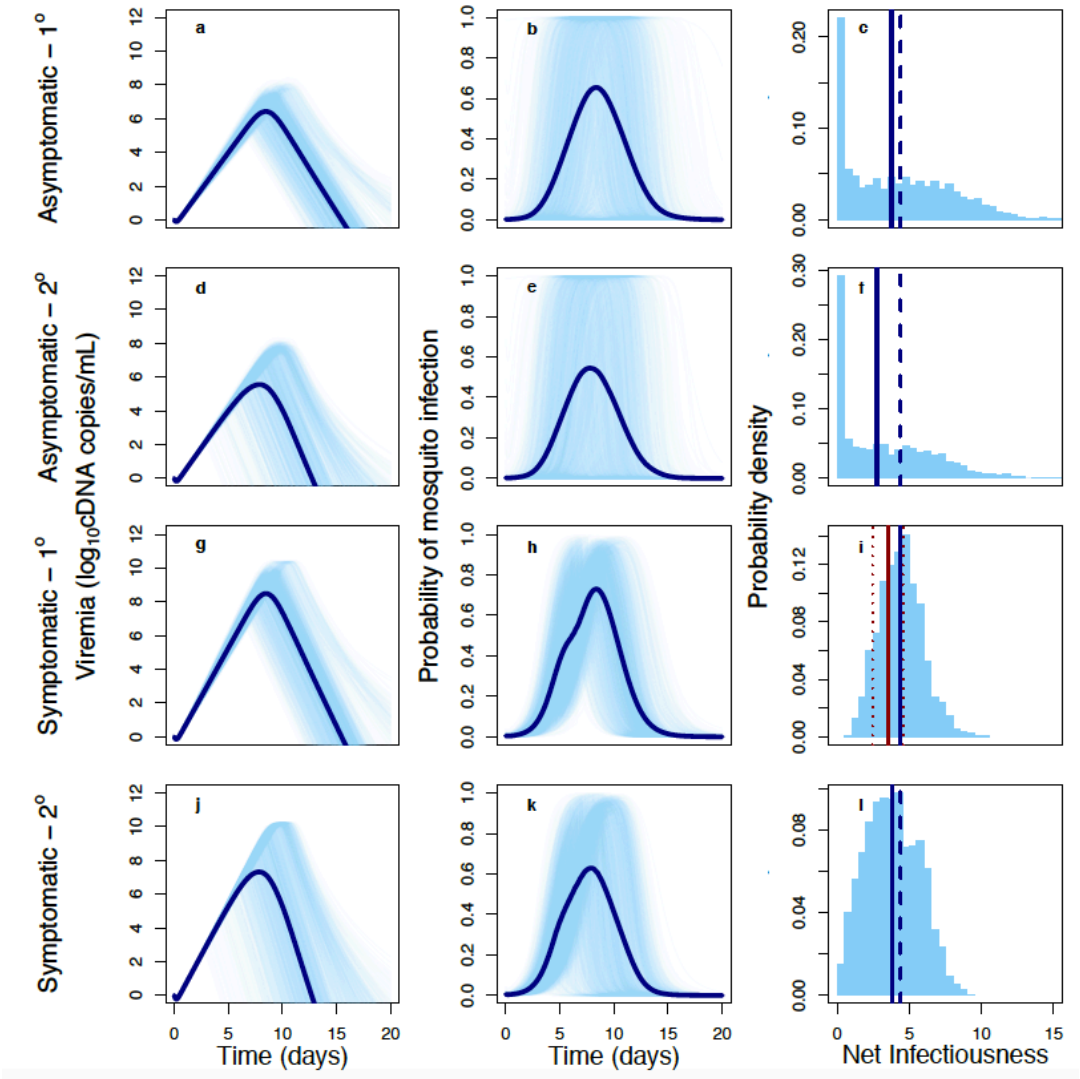

Figure 2-2: DENV viremia and infectiousness trajectories by infection class. (a,d,g,j): DENV viremia since time of infection for different infection classes and immune histories (1°: primary infection; 2°: secondary infection). Lighter lines denote 3,000 replicates and dark lines means. (b,e,h,k): Infectiousness of humans to mosquitoes over time. (c,f,i,l): Probability density of net infectiousness as defined in eq.(3) based on curves from the middle column. The solid blue line denotes the median and the dashed line denotes the median for the reference group (primary symptomatic). The solid and dashed red lines denote the mean and 95% confidence interval of the net infectiousness of primary symptomatic infections as measured empirically (18).

Relative Contributions to the Force of Infection. Next, we estimated the proportion of each infection class in a hypothetical population and derived each class' relative contribution to force of infection (FoI), the rate at which susceptible people become infected. We assumed an equal probability of being bitten by Ae. aegypti across infection classes. To quantify the proportion of people with A, IS, UAS, and DAS infections (and thus the pool of individuals who could potentially give rise to new infections among susceptibles), we performed a meta-analysis on published (A+IS):AS ratios (1° and 2°: 73%, 95% CI: 62-82%; 3° and 4°: 93%, 95% CI: 71-98%) (Figure S2-1 Figure S2-1)(15) and adopted an A:(IS+AS) ratio of 9.2% (6) and a detection rate of AS infections of 8% (95% CI: 5-15%)(19). The reality, however, is that these relationships are dynamic and can fluctuate in space and time (Figure S2-2 for a sensitivity analysis). The proportion of individuals with a given pre-exposure history (i.e., no previous DENV exposure, prior exposure to one serotype, etc.), or with temporary heterotypic immunity or permanent homotypic immunity, depends on the age distribution and the history of local transmission intensity (20). We considered scenarios for our hypothetical populations with demographic characteristics of Brazil and Thailand respectively and simulated pre-exposure history by age across values of time-averaged FoI (21) (Figure 2-3 and Figure S2-3). To estimate the contribution of each infection class to the total FoI, we formulated a relative FoI expression that accounts for the differential infectiousness and prevalence of A, IS, and AS infections with distinct pre-exposure histories (Materials and methods).

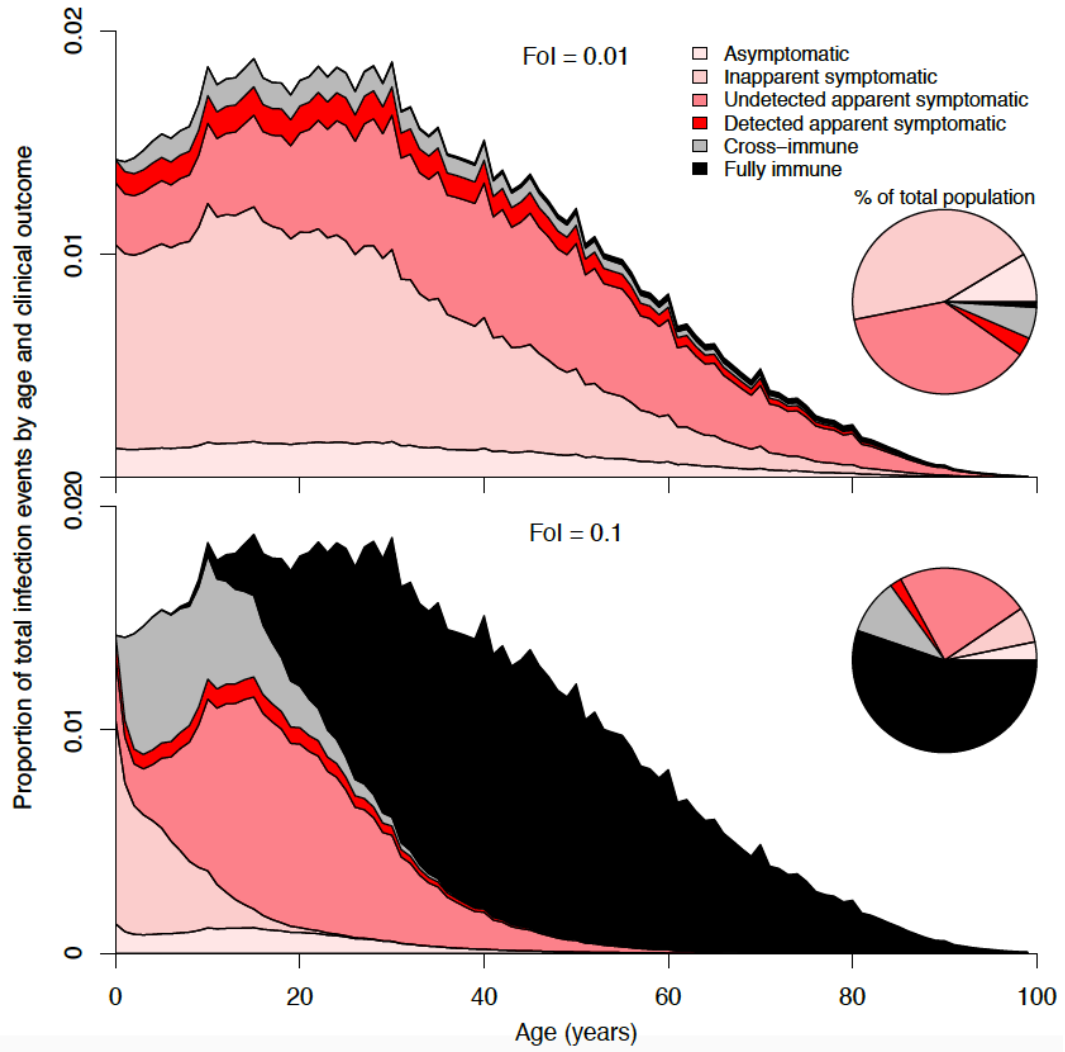

Figure 2-3: Infection class stratification by age and for FoI values of 0.01 (top) and 0.1 (bottom) for Brazil. An individuals' susceptibility to infection and clinical outcome depend on pre-exposure history. Serohistory by age is estimated using a system of ordinary differential equations with state variables denoting the proportion of the population pre-exposed to 0-4 serotypes. Transition to pre-exposure state *i* occurs at rate *i*FoI. Individuals entering a new pre-exposure state have temporary heterologous immunity (gray) to all serotypes before later becoming susceptible again to each serotype to which they do not have a history of exposure. After four infections with four different serotypes, individuals are assumed fully immune (black) to all serotypes.

Based on our metric of relative FoI, we estimated that 80% (IQR: 78-81%) of human DENV infections are attributable to individuals that do not present with apparent symptoms at the time of transmission to mosquitoes (Figure 2-4 and Figure S2-4 for Thailand). We estimated that asymptomatic and inapparent symptomatic infections could be responsible for causing 73% (IQR: 70-74%) of all human DENV infections, reflecting a near one-to-one relationship with their representation in the population. Of the remaining 27% (IQR: 26-29%) of infections, 75% (IQR: 56-88%) are attributable to bites by mosquitoes on people who eventually become symptomatic and detectable after presentation of their symptoms begins. At a detection rate of 8% (19), 1.6% (IQR: 1.5-1.7%) of total infections were estimated to result from infected individuals after they are detected by surveillance systems (1%, IQR: 0.9-1.1%; 3%, IQR: 2.8-3.3% at detection rates of 5% and 15% (19), respectively).

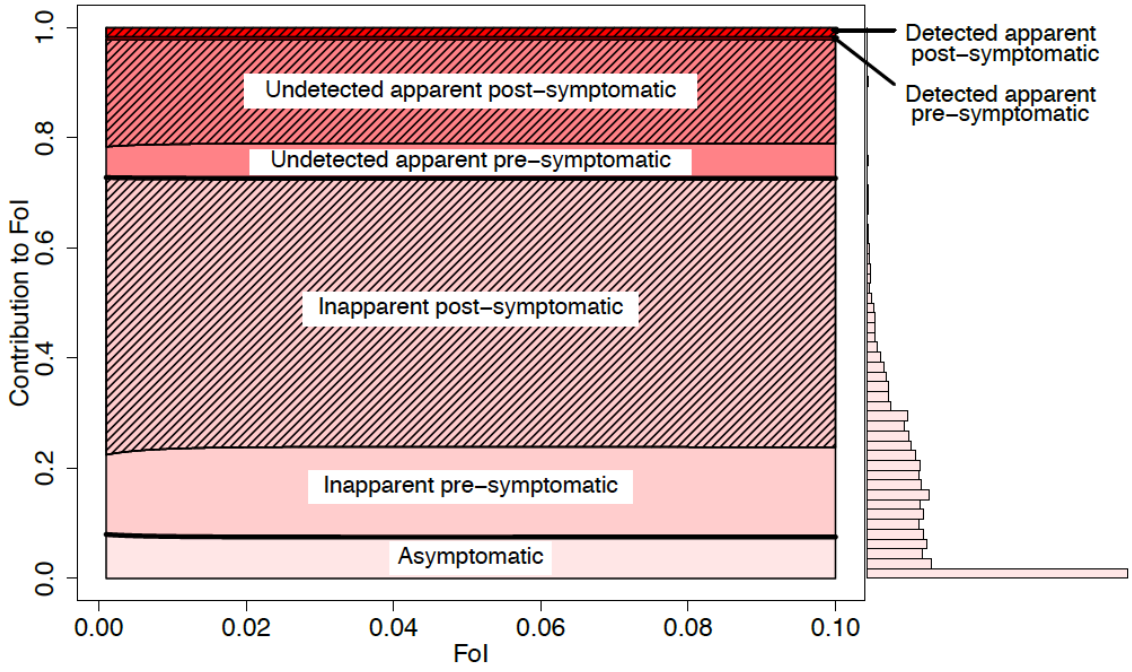

Figure 2-4: Mean contribution of each infection class to total force of infection (FoI). The contribution to the total FoI of an infection class is derived from the ratio of FoI attributable to a given class and total FoI, as in eq.(13). The respective net infectiousness is derived from the 3,000 random samples displayed in Figure 2-2. The infections are further distributed according to the estimated proportion of net infectiousness to occur before and after symptom onset (pre-symptomatic (eq.(4)) and post-symptomatic (hatched lines) (eq.(5)). The histogram shows the distribution of FoI contributions by asymptomatic infections at FoI = 0.1, accounting for parameter uncertainty.

2.4.3 Sensitivity analysis

Data on viremia and infectiousness in asymptomatic, pre-symptomatic, and post-secondary infections are sparse (6), resulting in substantial uncertainty around our estimates. We performed a variance-based sensitivity analysis (22) to identify the primary sources of uncertainty for estimating net infectiousness and the proportion of the net infectiousness occurring prior to symptom onset. Limited data on the viremia-to-infectiousness relationship of asymptomatic infections drove the wide uncertainty in estimates of their net-infectiousness whereas uncertainty and variability in time until symptom onset was responsible for the majority of uncertainty in estimates of the infectiousness prior to symptom onset (Figure S2-7).

The estimated contributions to the total force of infection (FoI) by each infection class were robust across different transmission settings (Figure 2-4) and in settings where DENV is newly emerging (Figure S2-5), but not when allowing for contributions to transmission from post-secondary infections (Figure S2-6). Under the assumption that post-secondary infectiousness and susceptibility are equivalent to secondary infections, we estimated the contribution of inapparent infections to be up to 14% (IQR: 11-14%) higher than if post-secondary infections are assumed not to contribute to transmission (Figure S2-6). This increase resulted from the relatively high proportion of IS infections among post-secondary infections, who made up a larger proportion of the infectious reservoir in more intense transmission settings. Under the assumption that IS infections are more similar in their infectiousness to A than to AS infections, the estimated contribution of inapparent infections was reduced from 73% to 69% (IQR: 33-80%), reflecting a lower bound to this assumption. The impact of accounting for the differential

viral trajectories of severe dengue cases (7) is minor due to their small numerical prominence (23), but their inclusion does increase the contribution of post-symptomatic DAS infections from 1.6% (IQR: 1.5-1.7%) to 2.6% (IQR: 2.1-3.0).

In addition, A:IS:UAS:DAS ratios vary over space and time. The contribution of inapparent (A+IS) infections across the spectrum of A:IS:AS ratios is driven by the ratio of A to IS infections, with the total contribution of A+IS infections being at least 82% of their numerical prominence in the infected population (Figure S2-2).

2.5 Discussion

Combined with other findings (7), our analysis suggests that inapparent infections, due to their numerical prominence and considerable net infectiousness, contribute appreciably to DENV transmission and its disease burden. Moreover, our finding that approximately one quarter of an individual's infectiousness occurs prior to symptom onset supports the hypothesis that a large proportion of human-to-mosquito transmission is silent (6, 16).

Substantial uncertainties, in particular in viremia and infectiousness of asymptomatic, pre-symptomatic, and post-secondary infections, underscore the need for future research on the human immune response to DENV infection and correlates of disease severity. The steep yet uncertain relationship between viral load and infectiousness in asymptomatic infections (6) results in a bimodal pattern of infectiousness in which many display very little infectiousness, whereas some are much more infectious than symptomatic individuals. Larger sample sizes could inform to what extent this is a result of individual heterogeneity or parameter uncertainty. While viral plasma titers correlate with infectiousness, other factors have been found to influence the

probability of transmission to mosquitoes independently, such as serological response (24), day of illness (24), virus strain (24), and virus genotype (25). Enhanced understanding on the differential viremia between primary and secondary infections and the mechanism underlying enhanced infection efficiency in asymptomatic and pre-symptomatic infections is pertinent yet requires more detailed immunological data on target cell populations or effector immune response to facilitate inference from mathematical models with increased immunological complexity. Decreased viremia in asymptomatic infections may result in a longer extrinsic incubation period (EIP)(26-28) and thus lower their relative contribution to transmission. However, at a given viremia level, asymptomatic infections are found to result in a higher mosquito viral load than symptomatic infections (6). The impact of lower asymptomatic viremia on the EIP may be smaller than expected based solely on viremia. Lastly, symptomatic infections may experience impaired mobility (29) or otherwise modified interactions with mosquitoes, the impacts of which on net transmission are presently not well understood. Resolving these uncertainties and identifying effective strategies for mitigating the contributions of all infections, apparent or not, to DENV transmission will require comprehensive studies that combine field work and modeling to address the coupled nature of multiple transmission heterogeneities (30).

Rates of clinical disease and detection can vary across regions due to factors such as DENV genotypes (31, 32), the clinical outcome of a previous DENV infection (31), and time since previous outbreak (33), altering the relative contributions of infection classes. Healthcare-seeking behavior and consequent reporting depends on many factors, not all of which are related to the severity of symptoms. These include socio-economic

factors, access to health care, and the perception of the quality of available care, among others (34). In addition, due to delays between symptom onset and healthcare seeking and detection, our estimates of the contribution of individuals prior to detection is almost certainly a conservative underestimate.

Our population-level projections highlight the potential contribution that silent (A+IS+UAS) and pre-symptomatic DENV carriers make to the overall transmission of dengue virus and its burden on public health, which has implications for dengue control and prevention. First, the substantial role that inapparent infections play during dengue epidemics may result in more rapid transmission and geographic spread (RW.ERROR - Unable to find reference:803) and, as a result, more wide spread transmission prior to case-driven outbreak detection and onset of control efforts (35). The considerable potential for pre-symptomatic transmission further impedes outbreak prediction from case data (36). Second, our findings raise questions about projections of the population-level impact of the recently licensed Dengvaxia® vaccine, which is thought to protect some vaccine recipients against apparent disease but not infection (37). Although spared from disease, our results suggest that these individuals could still contribute to transmission and thereby limit the indirect effects of vaccination in the event of breakthrough infections (38). Third, given the contribution of silent infections to transmission, control efforts that rely on responding to reported cases may not be effective in relatively intense transmission settings. Improving strategies with enhanced potential to prevent infections, silent or otherwise, requires a deeper understanding of the spatial and temporal scales of transmission (39). Modeling approaches that synthesize key empirical findings to estimate the contribution of inapparent infections will continue

to provide valuable insights for guiding prevention and control of dengue and other mosquito-borne viral diseases with complex interactions between within-host and between-host dynamics (40).

2.6 Materials and methods

2.6.1 Modeling individual viremia trajectories

We modeled viremia trajectories ($\log_{10}$ cDNA copies/mL of plasma) using a model (7) of virus and immune dynamics with four state variables—uninfected target cells (x), infected targets cells (y), free viral particles (v), and a clearing immune response (z)—according to

$$\begin{aligned} \frac{dx}{dt} &= A - \gamma x - \beta xv \\ \frac{dy}{dt} &= \beta xv - \delta y - \alpha xy \\ \frac{dv}{dt} &= \omega y - \kappa v \\ \frac{dz}{dt} &= \eta yz. \end{aligned} \tag{1}$$

The parameter A denotes the daily production rate of target cells, which die at rate γ and become infected proportional to the concentration of free viral particles at rate β, assuming random mixing. Infected cells die at rate δ and are cleared of infection at a rate proportional to the size of the immune response and the removal rate α. Free viral particles are produced by infected cells at rate ω and are cleared at rate κ. The immune response grows proportional to the number of infected cells at rate η. This model was fitted to individual plasma viral titers from primary and secondary apparent symptomatic (AS) infections (41) using Markov chain Monte Carlo methods (7). We used the joint

posteriors from that analysis to model viremia trajectories for primary and secondary AS infections. Inapparent symptomatic (IS) infections are assumed to have similar viremia as AS infections. To adapt this approach to model viremia trajectories of A infections, we relied on the observation by Duong et al.(42) that viremia of A infections was lower on average than that of S infections (76%, IQR: 74-77%). To account for uncertainty in this relationship, we took the ratio of 3,000 random samples from the normal distributions of symptomatic (mean: 6.27 +/- SE 0.14 $\log_{10}$ cDNA copies/mL) and asymptomatic observed viremia (mean: 4.75 +/- SE 0.39 $\log_{10}$ cDNA copies/mL)(6) and reduced the viremia trajectories of AS infections by this fraction to approximate the trajectories of A infections.

2.6.2 Infectiousness calculations

To describe the probability of infecting a mosquito given an individual's viremia (V), we used logistic regression models

$$F(V) = \frac{1}{1 + e^{-(\beta_0 + \beta_1 V)}}, \tag{2}$$

where β_0 and β_1 denote the logistic intercept and the slope coefficient for plasma viremia ($\log_{10}$ cDNA copies per mL), respectively (42). This relationship was fitted to data from DENV-infected symptomatic and asymptomatic individuals and was found to be significantly different across infection classes (asymptomatic, pre-symptomatic, and post-symptomatic) but not with respect to serotype or pre-exposure history (primary vs. post-primary infection)(6). Pre-symptomatic individuals become symptomatic after their intrinsic incubation period (IIP) is over, which is accompanied by a significantly different relationship between viremia and infectiousness (Table S2-1). Each of 3,000 samples of

symptomatic viremia trajectories had a corresponding duration of the IIP as informed by the posterior distributions derived in (7). These were paired with a realization of the regression model with coefficients randomly drawn according to their best-fit means and standard errors (Table S2-1), where the pre-symptomatic parameterization is used before the IIP concludes and the post-symptomatic parameterization is used afterwards. For the infectiousness of asymptomatic infections, the viremia-infectiousness relationship remained the same over the course of the infection. To summarize the extent of infectiousness of an individual over the entire course of their infection, we defined net infectiousness as the integral of an infectiousness curve over time

$$NI = \int F(V)\,dt. \tag{3}$$

This quantity *NI* is proportional to the expected number of mosquitoes infected by a human infection assuming that biting occurs at some constant rate over the course of the human infection. By extension, the ratio of the net infectiousness of two individuals with two different types of infections is identical to the ratio of the expected number of mosquitoes infected by people with those respective types of infections. Given that we interpret the end of the intrinsic incubation period (IIP) as the beginning of the symptomatic phase of the infection, we also used this distinction to estimate the proportion of infectiousness that occurs prior to symptom onset (PIPS)

$$PIPS = \frac{\int_0^{IIP} F(V)\,dt}{NI}, \tag{4}$$

and likewise for the proportion after symptom onset

$$PIAS = \frac{\int_{IIP}^{\infty} F(V)\,dt}{NI}. \quad (5)$$

2.6.3 Population seroprofile calculation

We calculated the proportion of the population previously exposed to 0 to 4 serotypes as a function of the population's age distribution and the time-averaged, serotype-specific force of infection (FoI) to which the population is subject. As representative examples of two DENV-endemic regions, we used national age distributions from Brazil and Thailand (see Extended Data for results for Thailand)(43). The time-averaged FoI metric (defined below) that we used was assumed to be constant with respect to virus serotype and space. Although DENV FoI is known to exhibit substantial variation with respect to these factors (21, 44), we simplified this aspect of our analysis to reflect the average across a wide geographic area or across many realizations of a complex temporal pattern of transmission.

Consistent with these assumptions and with the further assumption of FoI acting as a constant hazard, we represented the proportion pre-exposed to $i = 0\ldots 4$ serotypes at age a as $e_i(a)$. After acquiring infection at rate (4-i) x FoI, an individual has temporary heterologous immunity to all serotypes for a period of average durationσ^{-1}. The probability that an individual of age a has temporary heterologous immunity after exposure with i serotypes is represented by $r_i\,(a)$. Individuals permanently retain immunity to serotypes to which they were previously exposed; i.e. permanent temporary homologous immunity. The dynamics of these classes with respect to age follow

$$\frac{de_0}{da} = -4\,\mathrm{FoI}\,e_0$$
$$\frac{dr_i}{da}\Big|_{i=1\ldots4} = \big(4-(i-1)\big)\mathrm{FoI}\,e_{(i-1)} - \sigma r_i \qquad (6)$$
$$\frac{de_i}{da}\Big|_{i=1\ldots4} = \sigma r_i - (4-i)\,\mathrm{FoI}\,s_i.$$

Accounting for the proportion of the population in each age group $p(a)$, the population-wide proportion pre-exposed to i serotypes is

$$E_i = \sum_a \big(p(a)e_i(a)\big). \qquad (7)$$

2.6.4 Meta-analysis of (A+IS):AS ratios

The difference in the (A+IS):AS ratio between primary and secondary infections, assessed using field studies that reported pre-exposure history (15), was found to be an insignificant predictor of AS infections (likelihood ratio test, p=0.76). We extended this previous meta-analysis to include all prospective studies addressing inapparent infection rates that were in agreement with our IS definition (4, 5, 45-57) (Figure S2-1a). Post-secondary infections were associated with significantly different ratios and were assessed separately (23, 58) (Figure S2-1b). We estimated these ratios by fitting a random effects model to the logit-transformed proportions.

2.6.5 Disease outcome calculation

To calculate the proportions of infected people who have previously been exposed to zero or one serotype and who experience either an asymptomatic (A) or symptomatic (S) infection, we used E_i and our estimates of A:S ratios for a given pre-exposure history (θ_i=9.2% for primary and secondary infections, other options are assessed in Figure S2-2), resulting in

$$\begin{aligned} \Pr(\mathrm{A}) &= \sum_{i=1}^{2} E_i \theta_i \\ \Pr(\mathrm{S}) &= \sum_{i=1}^{2} E_i (1-\theta_i). \end{aligned} \tag{8}$$

Similarly, the proportion of infections to be IS or AS follows from the (A+IS):AS ratio ζ,

$$\begin{aligned} \Pr(\mathrm{A{+}IS}) &= \zeta \sum_{i=1}^{2} E_i \\ \Pr(\mathrm{AS}) &= (1-\zeta) \sum_{i=1}^{2} E_i \\ \Pr(\mathrm{IS}) &= \Pr(\mathrm{A{+}IS}) - \Pr(\mathrm{A}). \end{aligned} \tag{9}$$

2.6.6 Contribution of infection classes to total force of infection

Force of infection (FoI) is defined as the rate at which susceptible individuals become infected. Classical epidemiological theory for vector-borne diseases (VBD) posits that FoI is a function of a number of factors, including infection prevalence among hosts (X) and the infectiousness of infected hosts (59). On a per capita basis, FoI = $bmaY$ in Ross-Macdonald models of VBD transmission, where b is the probability that a susceptible host becomes infected after being bitten by an infectious vector, m is the ratio of vectors to hosts, a is the daily rate of at which a vector bites, and Y is the infection prevalence among vectors. The latter depends further on the daily vector mortality rate g, the incubation period n in the vector, human prevalence X, and the probability c that a susceptible vector becomes infected upon biting an infectious host (59).

To account for the population stratification that is necessary for our analysis, we derived a formula for the FoI that is more generalizable than the classic formula in that it allows for distinct contributions to FoI from different host groups (i.e. A, IS, UAS, and DAS infections with different pre-exposure histories). Specifically, each host group

differed in its infectiousness and its overall prevalence in the population. By separating contributions from different host groups to mosquito infectiousness and, in turn, to the FoI on susceptible hosts, we calculated the contribution of people with A infections to FoI by calculating the ratio between the FoI resulting from A infections alone and the total FoI, and similarly for IS, UAS, and DAS infections.

Differentiating between symptomatic (subscript S) and asymptomatic (subscript A) infections, we can describe FoI as

$$\begin{aligned} \mathrm{FoI}_{\mathrm{A}} &= bma\frac{ac_{\mathrm{A}}X_{\mathrm{A}}}{g+ac_{\mathrm{A}}X_{\mathrm{A}}}e^{-gn}, \\ \mathrm{FoI}_{\mathrm{S+A}} &= bma\frac{a(c_{\mathrm{A}}+\rho c_{\mathrm{S}})X_{\mathrm{A}}}{g+a(c_{\mathrm{A}}+\rho c_{\mathrm{S}})X_{\mathrm{A}}}e^{-gn}, \end{aligned} \tag{10}$$

where ρ is the prevalence of S infections relative to A. The contribution of A infections follows from dividing the quantities in (10) as

$$\frac{\mathrm{FoI}_{\mathrm{A}}}{\mathrm{FoI}_{\mathrm{S+A}}} = \left(1+\frac{\rho c_{\mathrm{S}}}{c_{\mathrm{A}}}\right)\frac{\frac{g}{a}+c_{\mathrm{A}}X_{\mathrm{A}}}{\frac{g}{a}+(c_{\mathrm{A}}+\rho c_{\mathrm{S}})X_{\mathrm{A}}}, \tag{11}$$

which demonstrates the insensitivity of our results to values of n, b, and m.

The infection probability c relates to the net infectiousness (NI) according to $NI = c/\lambda$, where λ represents the rate of recovery from infection. The prevalence X_i is proportional to the proportion of the population that has temporary heterologous immunity, R_i, according to $X_i = R_i\sigma/\lambda$. The quantity R_i is defined from eq.(6) according to $R_i = r_i(a)p(a)$. It follows that

$$cX = NI\sigma R. \tag{12}$$

Substituting eq.(12) into eq.(10) to further stratify infection classes and pre-exposure histories gives

$$\begin{aligned}
\mathrm{FoI}_{\mathrm{A}} &= bma\frac{\sum_{i=1}^{p} NI_{\mathrm{A}i}\sigma R_{\mathrm{A}i}}{\frac{g}{a}+\sum_{i=1}^{p} NI_{\mathrm{A}i}\sigma R_{\mathrm{A}i}}e^{-gn}, \\
\mathrm{FoI}_{\mathrm{A+IS+UAS+DAS}} &= bma\frac{\sum_{i=1}^{p} NI_{\mathrm{A}i}\sigma R_{\mathrm{A}i}+\sum_{i=1}^{p} NI_{\mathrm{IS}i}\sigma R_{\mathrm{IS}i}+\sum_{i=1}^{p} NI_{\mathrm{UAS}i}\sigma R_{\mathrm{UAS}i}+\sum_{i=1}^{p} NI_{\mathrm{DAS}i}\sigma R_{\mathrm{DAS}i}}{\frac{g}{a}+\sum_{i=1}^{p} NI_{\mathrm{A}i}\sigma R_{\mathrm{A}i}+\sum_{i=1}^{p} NI_{\mathrm{IS}i}\sigma R_{\mathrm{IS}i}+\sum_{i=1}^{p} NI_{\mathrm{UAS}i}\sigma R_{\mathrm{UAS}i}+\sum_{i=1}^{p} NI_{\mathrm{DAS}i}\sigma R_{\mathrm{DAS}i}}e^{-gn},
\end{aligned} \tag{13}$$

with $p = 2$ when assessing the impact of primary and secondary infections on transmission and $p = 4$ when assessing the impact of primary, secondary, and post-secondary infections on transmission.

2.6.7 Sensitivity analysis

We performed a sensitivity analysis to assess the impact of uncertainty in A:IS:AS ratios among primary and secondary infections on the absolute residual contributions of infection classes (RC_{class}) to the overall FoI (Figure S2-2); i.e. the contribution to the FoI that cannot be explained by the relative prominence of a given infection class in the population,

$$RC_{class} = \Pr(class) - \frac{\mathrm{FoI}_{class}}{\mathrm{FoI}_{total}}. \tag{14}$$

Additionally, we examined what the contribution of inapparent infections to the FoI would be under the assumption that post-secondary infections are similarly infectious as secondary infections (Figure S2-6) and using estimates from the meta-analysis presented in Figure S2-1 to estimate the proportion of post-secondary infections to be detected. This and the assumption we effectively made in the core analysis—i.e., that

post-secondary infections make no contribution to transmission—represent two different extremes and therefore provide bounds on the potential sensitivity of our results to alternative assumptions about the contributions to transmission from post-secondary infections. Similarly, we addressed uncertainty around the net infectiousness of IS infections by first assuming their net infectiousness to be similar to A infections rather than AS infections, as in the core analysis. We then examined the impact of severe AS infections by adopting fitted dengue hemorrhagic fever (DHF) viremia trajectories (7), DHF rates among S infections of 0.8% and 3% for primary and post-primary infections, respectively (23), and the assumption that all DHF cases are detected. The latter assumption provides an upper bound for the potential contribution of DAS infections given a specific detection rate.

2.6.8 Variance-based sensitivity analysis

To assess the impact of the three main sources of uncertainty in deriving two outcome variables (O) the net infectiousness and the proportion of infectiousness prior to symptoms, we performed a variance-based sensitivity analysis (22). The variance for both variables is measured under four different scenarios: 1) with all sources of uncertainty and 2-4) with all sources of uncertainty except one. The contribution to the total variance is expressed by the total-effect index

$$T_i = 1 - \frac{Var_{\mathbf{X}_{\sim i}}(O)}{Var(O)}. \quad (15)$$

Here, $\mathbf{X}$ denotes a vector of uncertain model inputs and $\sim i$ denotes that uncertainty around all inputs except i is considered. For input i we used the mean of the uncertainty distribution for the quantity of interest. The three main sources of uncertainty are

quantities describing temporal patterns of viremia, the relationship between viremia and infectiousness, and the duration of the intrinsic incubation period (IIP).

2.7 Acknowledgments

This research was funded by a grant from the US National Institutes of Health – National Institute of Allergy and Infectious Diseases (NIH/NIAID) award number P01AI098670 (to TWS). LL is supported by the French Government's Investissement d'Avenir program, Laboratoire d'Excellence Integrative Biology of Emerging Infectious Diseases (grant ANR-10-LABX-62-IBEID) and the City of Paris Emergence(s) program in Biomedical Research. BMA thanks Bill and Melinda Gates through the Global Good Fund. QAtB, BMA and TAP received support from Intellectual Ventures. ALL is supported by grant R01-AI091980 from the National Institutes of Health and by the National Science Foundation (RTG/DMS - 1246991). HEC is supported by National Institutes of Health under award no. 5R01AI102939-03.

2.8 References

1. Bhatt S*, et al* (2013) The global distribution and burden of dengue. *Nature* 496: 504-507.

2. Vaughn DW*, et al* (2000) Dengue viremia titer, antibody response pattern, and virus serotype correlate with disease severity. *J Infect Dis* 181(1): 2-9.

3. Murgue B, Roche C, Chungue E & Deparis X (2000) Prospective study of the duration and magnitude of viraemia in children hospitalised during the 1996-1997 dengue-2 outbreak in french polynesia. *J Med Virol* 60(4): 432-438.

4. Reyes M*, et al* (2010) Index cluster study of dengue virus infection in nicaragua. *Am J Trop Med Hyg* 83(3): 683-689.

5. Beckett CG*, et al* (2005) Early detection of dengue infections using cluster sampling around index cases. *Am J Trop Med Hyg* 72(6): 777-782.

6. Duong V*, et al* (2015) Asymptomatic humans transmit dengue virus to mosquitoes. *Proc Natl Acad Sci U S A* 112: 14688-14693.

7. Clapham HE, Tricou V, Van Vinh Chau N, Simmons CP & Ferguson NM (2014) Within-host viral dynamics of dengue serotype 1 infection. *J R Soc Interface* 11(96): 10.1098/rsif.2014.0094.

8. Stone W, Gonçalves BP, Bousema T & Drakeley C (2015) Assessing the infectious reservoir of falciparum malaria: Past and future. *Trends Parasitol* 31(7): 287-296.

9. Althouse BM & Scarpino SV (2015) Asymptomatic transmission and the resurgence of bordetella pertussis. *BMC Medicine* 13(1): 146.

10. Chen I*, et al* (2016) "Asymptomatic" malaria: A chronic and debilitating infection that should be treated. *PLoS Med* 13(1): e1001942.

11. Johansson MA, Vasconcelos PF & Staples JE (2014) The whole iceberg: Estimating the incidence of yellow fever virus infection from the number of severe cases. *Trans R Soc Trop Med Hyg* 108(8): 482-487.

12. Pitzer VE*, et al* (2014) Predicting the impact of vaccination on the transmission dynamics of typhoid in south asia: A mathematical modeling study. *PLoS Negl Trop Dis* 8(1): e2642.

13. Lambrechts L, Scott TW & Gubler DJ (2010) Consequences of the expanding global distribution of aedes albopictus for dengue virus transmission. *PLoS Negl Trop Dis* 4(5): e646.

14. Sabin AB (1952) Research on dengue during world war II. *Am J Trop Med Hyg* 1(1): 30-50.

15. Grange L*, et al* (2014) Epidemiological risk factors associated with high global frequency of inapparent dengue virus infections. *Frontiers in Immunology* 5

16. Teixeira MdG*, et al* (2002) Dynamics of dengue virus circulation: A silent epidemic in a complex urban area. *Tropical Medicine & International Health* 7(9): 757-762.

17. World Health Organization (2012) Dengue guidelines for diagnosis, treatment, prevention and control. 2009. *WHO, Geneva, Switzerland*

18. Nishiura H & Halstead SB (2007) Natural history of dengue virus (DENV)—1 and DENV—4 infections: Reanalysis of classic studies. *J Infect Dis* 195(7): 1007.

19. Stanaway JD*, et al* (2016) The global burden of dengue: An analysis from the global burden of disease study 2013. *The Lancet Infectious Diseases* 16: 712-723.

20. Anderson RM & May RM (1992) *Infectious diseases of humans: dynamics and control,* (Wiley Online Library,

21. Reiner RC*, et al* (2014) Time-varying, serotype-specific force of infection of dengue virus. *Proc Natl Acad Sci U S A* : 201314933.

22. Homma T & Saltelli A (1996) Importance measures in global sensitivity analysis of nonlinear models. *Reliab Eng Syst Saf* 52(1): 1-17.

23. Montoya M*, et al* (2013) Symptomatic versus inapparent outcome in repeat dengue virus infections is influenced by the time interval between infections and study year. *PLoS Negl Trop Dis* 7(8): e2357.

24. Nguyen MN*, et al* (2013) Host and viral features of human dengue cases shape the population of infected and infectious aedes aegypti mosquitoes. *Proc Natl Acad Sci U S A* 110(22): 9072-9077.

25. Lambrechts L*, et al* (2012) Dengue-1 virus clade replacement in thailand associated with enhanced mosquito transmission. *J Virol* 86(3): 1853-1861.

26. Watts DM, Burke DS, Harrison BA, Whitmire RE & Nisalak A (1987) Effect of temperature on the vector efficiency of aedes aegypti for dengue 2 virus. *Am J Trop Med Hyg* 36: 143-152.

27. Fontaine A, Jiolle D, Moltini-Conclois I, Lequime S & Lambrechts L (2016) Excretion of dengue virus RNA by aedes aegypti allows non-destructive monitoring of viral dissemination in individual mosquitoes. *Sci Rep* 6: 24885.

28. Bates M & Roca-Garcia M (1945) Laboratory studies of the saimiri-haemagog'us cycle of jungle yellow fever. *American Journal of Tropical Medicine* 25(3): 203-216.

29. Perkins TA*, et al* (2016) Calling in sick: Impacts of fever on intra-urban human mobility. *Proc Biol Sci* 283(1834): 10.1098/rspb.2016.0390.

30. Vazquez-Prokopec GM*, et al* (2016) Coupled heterogeneities and their impact on parasite transmission and control. *Trends Parasitol* 32: 356-367.

31. Katzelnick LC, Montoya M, Gresh L, Balmaseda A & Harris E (2016) Neutralizing antibody titers against dengue virus correlate with protection from symptomatic infection in a longitudinal cohort. *Proc Natl Acad Sci U S A* 113(3): 728-733.

32. Mammen M*, et al* (2014) Evaluation of dengue virus strains for human challenge studies. *Vaccine* 32(13): 1488-1494.

33. Corbett KS*, et al* (2015) Preexisting neutralizing antibody responses distinguish clinically inapparent and apparent dengue virus infections in a sri lankan pediatric cohort. *J Infect Dis* 211(4): 590-599.

34. Khun S & Manderson L (2007) Health seeking and access to care for children with suspected dengue in cambodia: An ethnographic study. *BMC Public Health* 7(1): 1.

35. Fraser C, Riley S, Anderson RM & Ferguson NM (2004) Factors that make an infectious disease outbreak controllable. *Proc Natl Acad Sci U S A* 101(16): 6146-6151.

36. Thompson RN, Gilligan CA & Cunniffe NJ (2016) Detecting presymptomatic infection is necessary to forecast major epidemics in the earliest stages of infectious disease outbreaks. *PLoS Comput Biol* 12(4): e1004836.

37. World Health Organization (2016) SAGE april 2016

38. Rodriguez-Barraquer I, Mier-y-Teran-Romero L, Burke DS & Cummings DA (2013) Challenges in the interpretation of dengue vaccine trial results. *PLoS Negl Trop Dis* 7(8): e2126.

39. Reiner RC, Stoddard ST & Scott TW (2014) Socially structured human movement shapes dengue transmission despite the diffusive effect of mosquito dispersal. *Epidemics* 6: 30-36.

40. Restif O & Graham AL (2015) Within-host dynamics of infection: From ecological insights to evolutionary predictions. *Philosophical Transactions of the Royal Society B: Biological Sciences* 370: 1675.

41. Tricou V*, et al* (2010) A randomized controlled trial of chloroquine for the treatment of dengue in vietnamese adults. *PLoS Negl Trop Dis* 4(8): e785.

42. Duong V*, et al* (2011) Clinical and virological factors influencing the performance of a NS1 antigen-capture assay and potential use as a marker of dengue disease severity. *PLoS Negl Trop Dis* 5(7): e1244.

43. Yearbook D (2010) United nations statistics division. *Statistical Dissemination Section, New York*

44. Rodriguez-Barraquer I*, et al* (2011) From re-emergence to hyperendemicity: The natural history of the dengue epidemic in brazil. *PLoS Negl Trop Dis* 5(1): e935.

45. Waterman SH*, et al* (1985) Dengue transmission in two puerto rican communities in 1982. *Am J Trop Med Hyg* 34(3): 625-632.

46. Balmaseda A*, et al* (2006) High seroprevalence of antibodies against dengue virus in a prospective study of schoolchildren in managua, nicaragua. *Trop Med Int Health* 11(6): 935-942.

47. Balmaseda A*, et al* (2010) Trends in patterns of dengue transmission over 4 years in a pediatric cohort study in nicaragua. *J Infect Dis* 201(1): 5-14.

48. Morrison AC*, et al* (2010) Epidemiology of dengue virus in iquitos, peru 1999 to 2005: Interepidemic and epidemic patterns of transmission. *PLoS Neglected Tropical Diseases* 4(5): e670.

49. Burke DS, Nisalak A, Johnson DE & Scott RM (1988) A prospective study of dengue infections in bangkok. *Am J Trop Med Hyg* 38(1): 172-180.

50. Endy TP*, et al* (2002) Epidemiology of inapparent and symptomatic acute dengue virus infection: A prospective study of primary school children in kamphaeng phet, thailand. *Am J Epidemiol* 156(1): 40-51.

51. Endy TP*, et al* (2011) Determinants of inapparent and symptomatic dengue infection in a prospective study of primary school children in kamphaeng phet, thailand. *PLoS Neglected Tropical Diseases* 5(3): e975.

52. Pengsaa K, Limkittikul K, Yoksan S, Wisetsing P & Sabchareon A (2011) Dengue antibody in thai children from maternally transferred antibody to acquired infection. *Pediatr Infect Dis J* 30(10): 897-900.

53. Yoon IK*, et al* (2012) Underrecognized mildly symptomatic viremic dengue virus infections in rural thai schools and villages. *J Infect Dis* 206(3): 389-398.

54. Mammen Jr MP*, et al* (2008) Spatial and temporal clustering of dengue virus transmission in thai villages. *PLoS Medicine* 5(11): e205.

55. Tien NTK*, et al* (2010) A prospective cohort study of dengue infection in schoolchildren in long xuyen, viet nam. *Trans R Soc Trop Med Hyg* 104(9): 592-600.

56. Chau TNB*, et al* (2009) Dengue virus infections and maternal antibody decay in a prospective birth cohort study of vietnamese infants. *J Infect Dis* 200(12): 1893-1900.

57. Porter KR*, et al* (2005) Epidemiology of dengue and dengue hemorrhagic fever in a cohort of adults living in bandung, west java, indonesia. *Am J Trop Med Hyg* 72(1): 60-66.

58. Olkowski S*, et al* (2013) Reduced risk of disease during postsecondary dengue virus infections. *J Infect Dis* 208(6): 1026-1033.

59. Smith D & McKenzie FE (2004) Statics and dynamics of malaria infection in anopheles mosquitoes. *Malaria Journal* 3(1): 13.

60. Reich NG*, et al* (2013) Interactions between serotypes of dengue highlight epidemiological impact of cross-immunity. *J R Soc Interface* 10(86): 20130414.

2.9 Supporting tables and figures

TABLE S2-1:

MODEL COEFFICIENTS FOR SUCCESSFUL HUMAN-TO-MOSQUITO TRANSMISSION

Infection class	β_0	SE	β_1	SE
Asymptomatic	-11.5	3.4	2.2	0.6
Pre-symptomatic	-5.6	0.75	1.0	0.1
Post-symptomatic	-6.6	0.39	0.9	0.05

β_0, intercept; β_1, slope coefficient for plasma viremia ($\log_{10}$ cDNA copies/mL); SE, standard error. Marginal logistic regression model based on mosquito infection status upon direct feeding(6).

TABLE S2-2:

PROBABILISTIC COMPARISON OF NET INFECTIOUSNESS UNCERTAINTY DISTRIBUTIONS

		Asymptomatic		**Symptomatic**	
		Primary	Secondary	Primary	Secondary
Asymptomatic	Primary	0.50	0.43	0.55	0.51
	Secondary	0.57	0.50	0.64	0.59
Symptomatic	Primary	0.45	0.36	0.50	0.40
	Secondary	0.49	0.41	0.60	0.50

Probability that a randomly selected value of net infectiousness from the uncertainty distribution for individuals of the type specified by the column is greater than a randomly selected value for individuals of the type specified by the row. For example, there is a 57% chance that asymptomatic primary infections have a higher net infectiousness than asymptomatic secondary infections. To provide context, we note that this probability is 0.50 for identical distributions, <0.50 when the random variable on the column is smaller than the one on the row (blue), and >0.50 when the random variable on the column is larger than the one on the row (red).

a

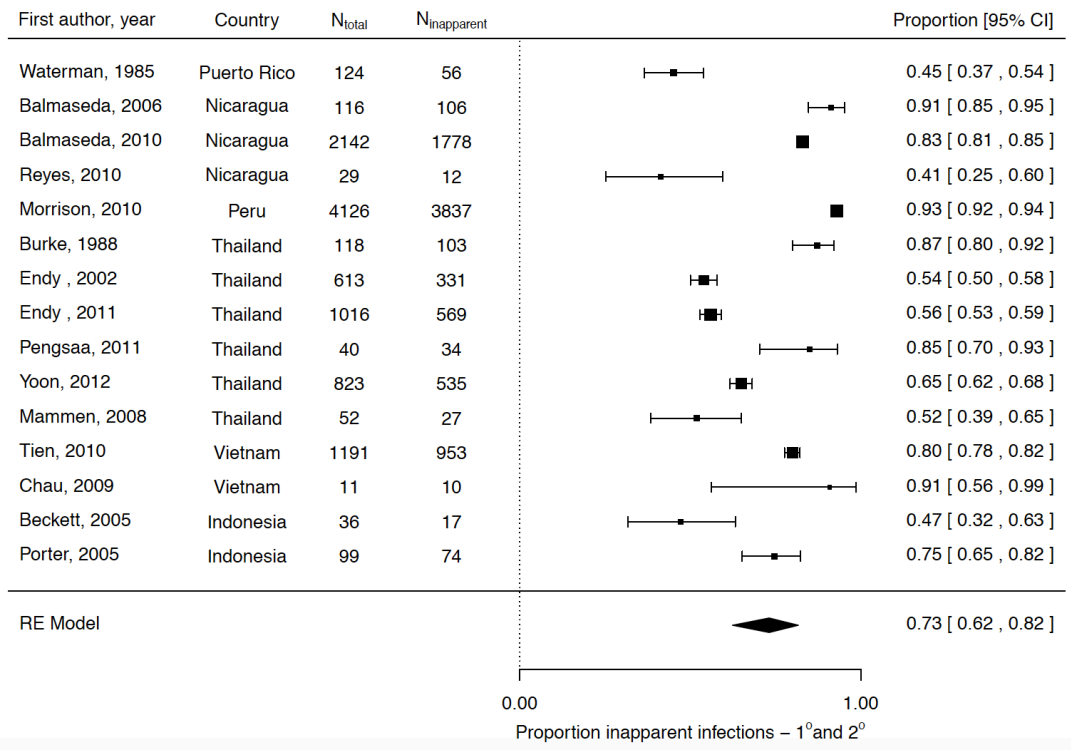

b

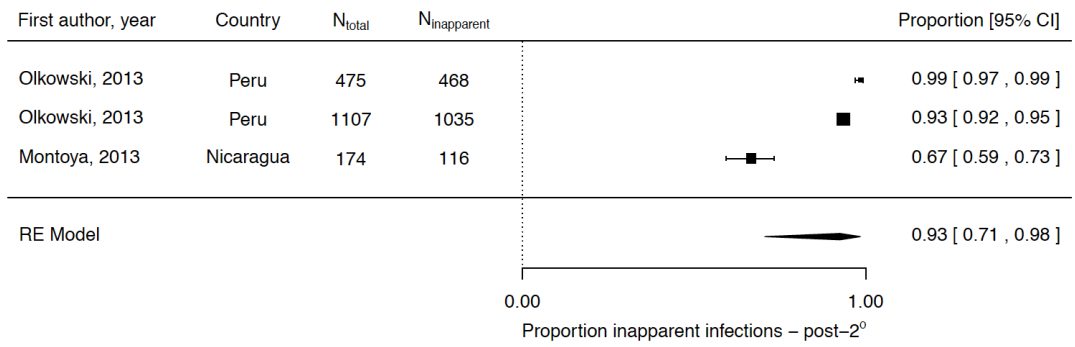

Figure S2-1: Summary estimates of the proportion of infections to be inapparent in primary or secondary infections (a) and post-secondary infections (b). Studies used were derived from a recent systematic literature review (15). The ratio between apparent and inapparent infections is not significantly different between primary and secondary infections ($p = 0.76$).

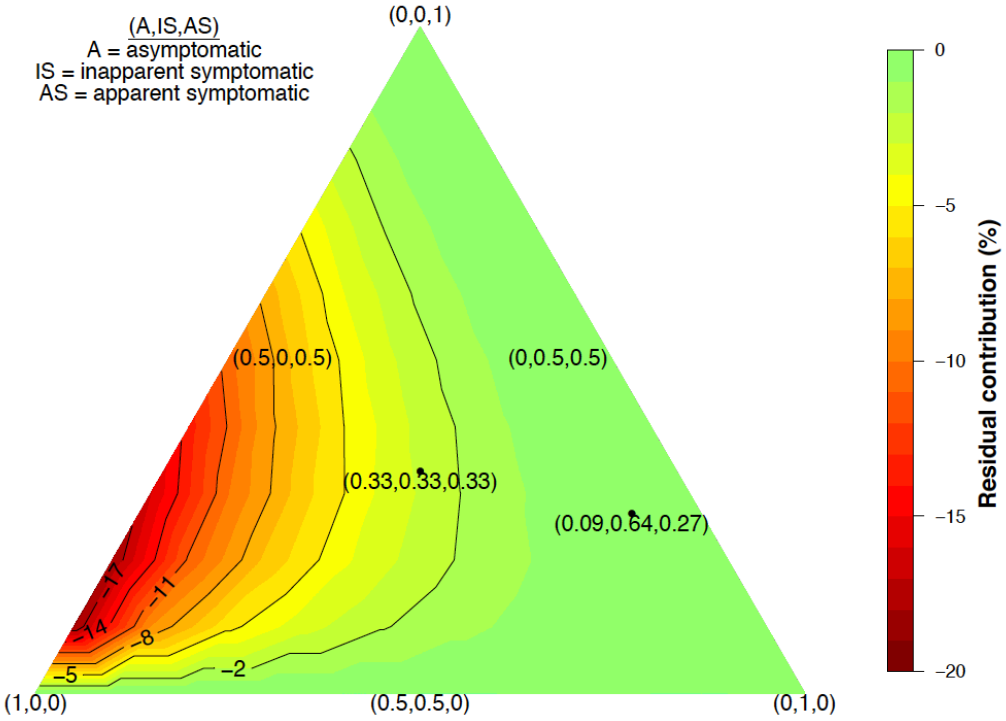

Figure S2-2: Residual contribution to the total FoI of inapparent infections (A+IS) for different A:IS:AS ratios (FoI = 0.05). Darker red colors indicate a larger absolute overestimation of the contribution to the FoI solely based on the prominence of A+IS infections in the population. The coordinates reflect the proportions per infection class with (0.09, 0.64,0.27) being the default based on Figure S2-1 and (6).

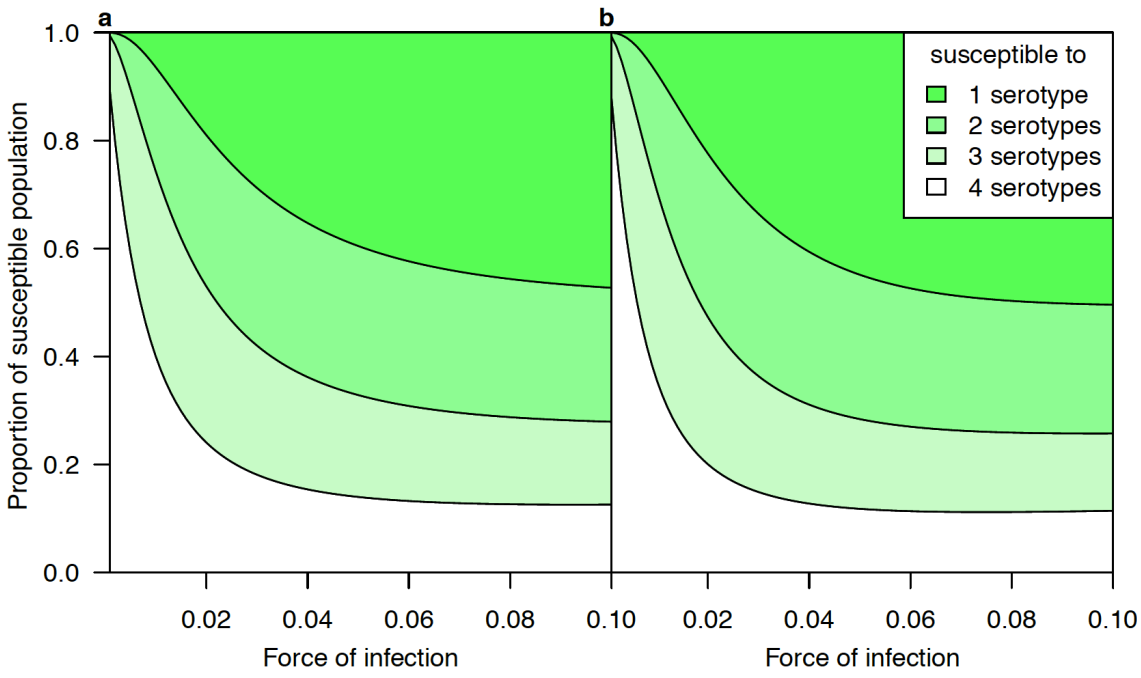

Figure S2-3: Pre-exposure profile as a function of the force of infection for (a) Brazil, (b) Thailand. The seroprevalence of the population is estimated using a system of ordinary differential equations with state variables denoting the proportion of the population pre-exposed to 0-4 serotypes. Transition to pre-exposure state i occurs at a rate (4-i)FoI. Individuals entering a new pre-exposure state retain temporary heterologous immunity to all serotypes for an average duration of 2 years (60) before becoming susceptible to heterologous serotypes.

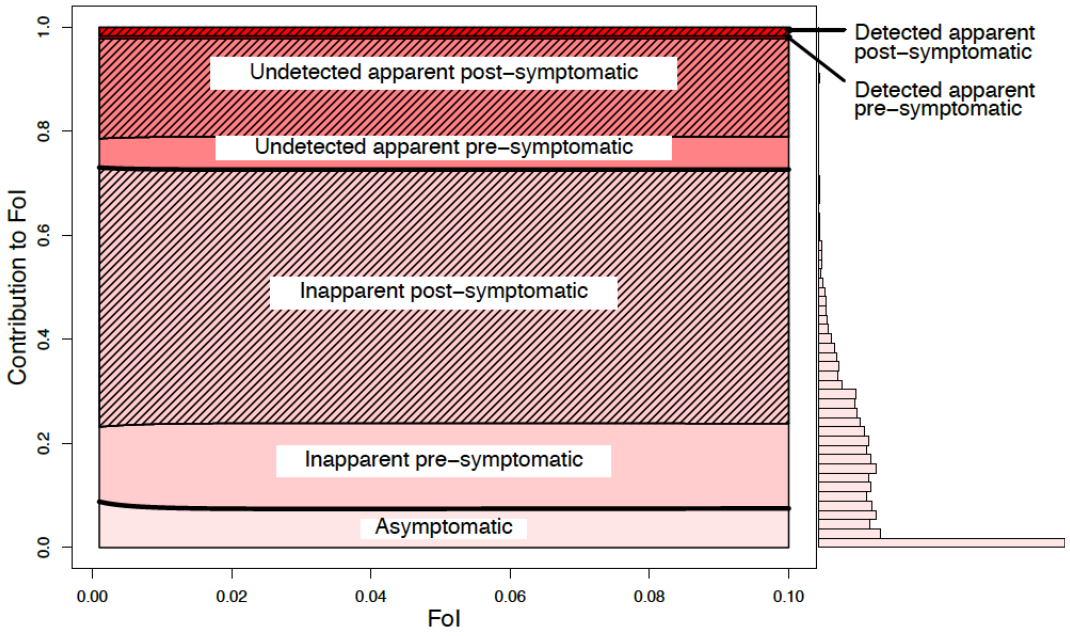

Figure S2-4: Mean contribution of infection classes to total force of infection (FoI) for Thailand. The contribution to the total FoI of a class is derived from the ratio between FoI attributable to this class and total FoI, as in eq.(13). The respective net infectiousness is derived from the 3,000 random samples displayed in Figure 2-2. The infections are further distributed according to the estimated proportion of net infectiousness to occur before and after symptom onset (pre-symptomatic (eq.(4)) and post-symptomatic (hatched lines) (eq.(5)). The histogram shows the distribution of FoI contributions by asymptomatic infections at FoI = 0.1, accounting for parameter uncertainty.

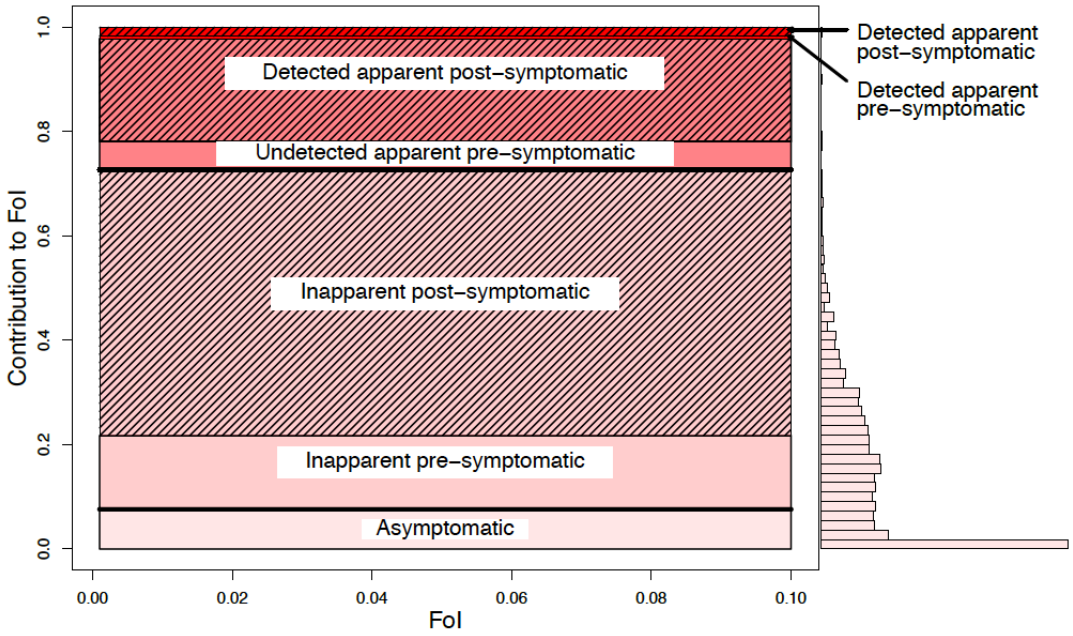

Figure S2-5: Contribution of infection classes to total FoI in an emerging setting. The contribution to the total FoI of a class is derived from the ratio between FoI attributable to this class and total FoI, as in eq.(13). The respective net infectiousness is derived from the 3,000 random samples displayed in Figure 2-2. The infections are further distributed according to the estimated proportion of net infectiousness to occur before and after symptom onset (pre-symptomatic (eq.(4)) and post-symptomatic (hatched lines) (eq.(5)). The histogram shows the distribution of FoI contributions by asymptomatic infections at FoI = 0.1, accounting for parameter uncertainty.

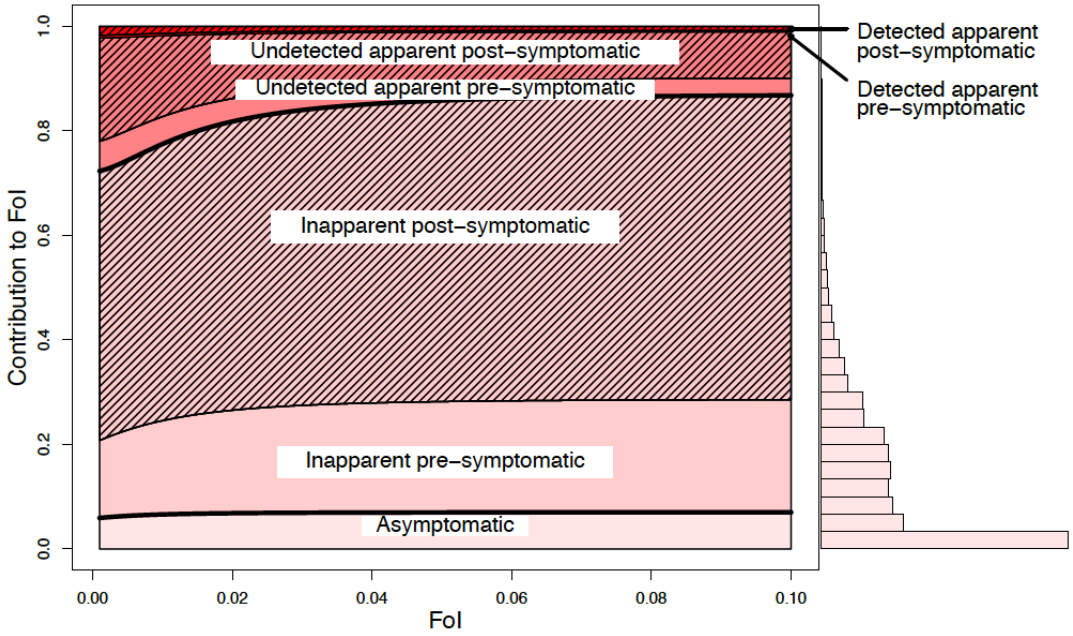

Figure S2-6: Contribution of infection classes to total FoI when accounting for the contribution of post-secondary infections to transmission. The contribution to the total FoI of a class is derived from the ratio between FoI attributable to this class and total FoI, as in eq.(13). The respective net infectiousness is derived from the 3,000 random samples displayed in Figure 2-2. The infections are further distributed according to the estimated proportion of net infectiousness to occur before and after symptom onset (pre-symptomatic (eq.(4)) and post-symptomatic (hatched lines) (eq.(5)). The histogram shows the distribution of FoI contributions by asymptomatic infections at FoI = 0.1, accounting for parameter uncertainty. Post-secondary infections are assumed to follow the same viremia trajectory as secondary infections. 93% of post-secondary infections are A or US (Figure S2-1).

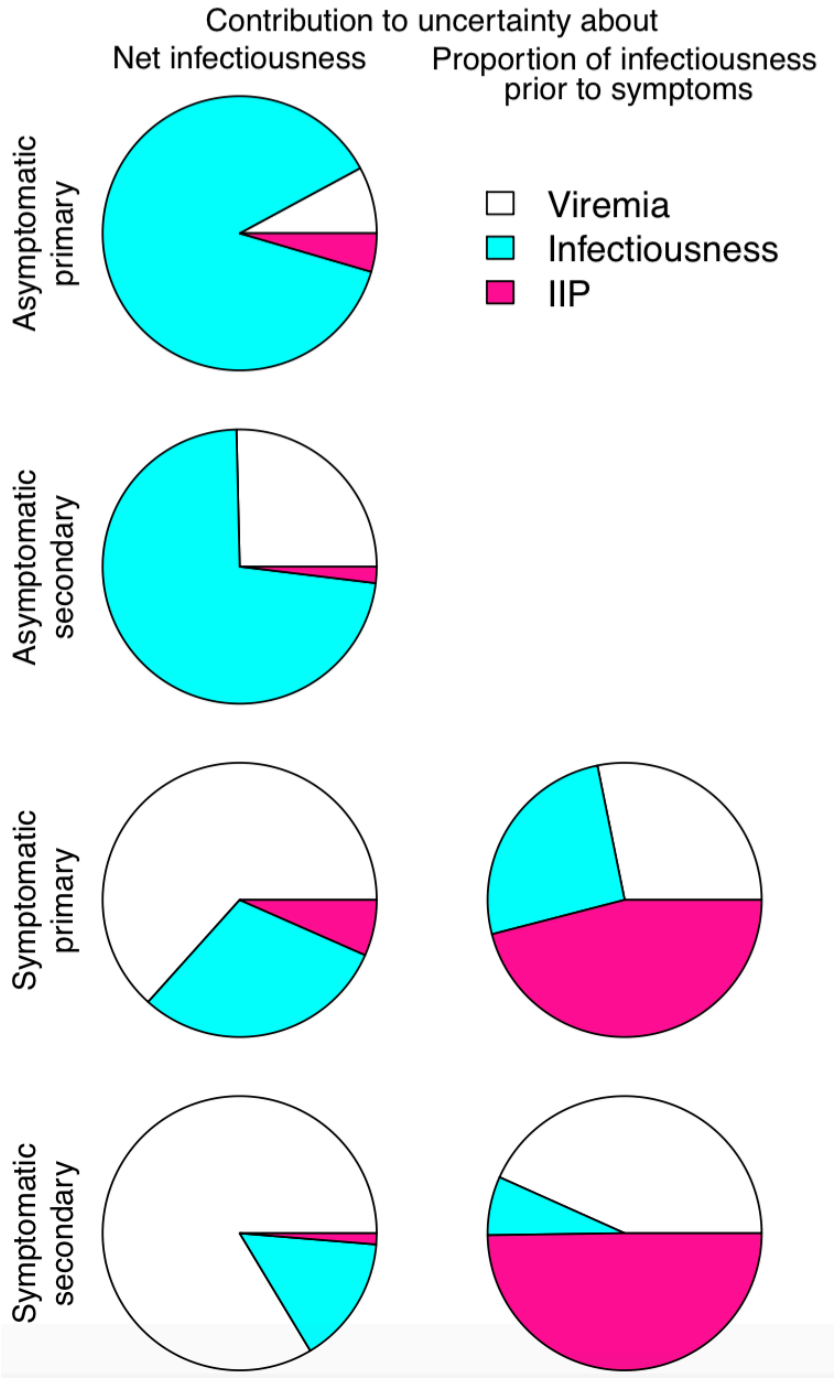

Figure S2-7: Variance-based sensitivity analysis. The contribution to the variance represents the total effect index, denoting the contribution of each source of uncertainty to the total variance, including its interactions. (IIP = intrinsic incubation period)

CHAPTER 3:

THE ROLE OF SEROTYPE INTERACTIONS AND SEASONALITY IN DENGUE MODEL SELECTION AND CONTROL: INSIGHTS FROM A PATTERN MATCHING APPROACH

Quirine A ten Bosch, Brajendra K Singh, Muhammad RA Hassan,

Dave D Chadee, Edwin Michael

3.1 Abstract

The epidemiology of dengue fever is characterized by highly seasonal, multi-annual fluctuations, and the irregular circulation of its four serotypes. It is believed that this behavior arises from the interplay between environmental drivers and serotype interactions. The exact mechanism, however, is uncertain. Constraining mathematical models to patterns characteristic to dengue epidemiology offers a means for detecting such mechanisms. Here, we used a pattern-oriented modeling (POM) strategy to fit and assess a range of dengue models, driven by combinations of temporary cross protective-immunity, cross-enhancement, and seasonal forcing, on their ability to capture the main characteristics of dengue dynamics. We show that all proposed models reproduce the observed dengue patterns across some part of the parameter space. Which model best supports the dengue dynamics is determined by the level of seasonal forcing. Further, when tertiary and quaternary infections are allowed, the inclusion of temporary cross-

immunity alone is strongly supported but the addition of cross-enhancement markedly reduces the parameter range at which dengue dynamics are produced, irrespective of the strength of seasonal forcing. The implication of these structural uncertainties on predicted vulnerability to control is also discussed. With ever expanding spread of dengue, greater understanding of dengue dynamics and control efforts (*e.g.* a near-future vaccine introduction) has become critically important. This study highlights the capacity of multi-level pattern-matching modeling approaches to offer an analytic tool for deeper insights into dengue epidemiology and control.

3.2 Author summary

The fluctuations of multi-serotype infectious diseases are often highly irregular and hard to predict. Previous theoretical approaches have attempted to disentangle the drivers that may underlie this behavior in dengue dynamics with variable success. Here, we examine the role of such drivers using a pattern-oriented modeling (POM) approach. In POM, multiple patterns observed at different scales are used to test a model's proficiency in capturing real-world dynamics. We examined dengue models with combinations of cross-immunity, cross-enhancement, seasonal fluctuations in the transmission rate, and with sensitivity analyses of asymmetric transmission rates between serotypes as well as the possibility for four subsequent heterologous infections. We demonstrate the ability of POM to model dynamical drivers that have gone unnoticed in single pattern or synthetic likelihood approaches. Further, our results present a determining role of seasonality in the selection and operation of these processes in governing dengue dynamics, in particular when full, heterologous immunity is assumed

to occur after a secondary infection. We show that this structural model uncertainty can have important practical significance, as demonstrated by the differences in control efforts required to disrupt transmission. These results highlight the importance of localized model selection and calibration using multiple data-matching, as well as taking explicit account of model uncertainty in predicting and planning control efforts for multi-serotype diseases.

3.3 Introduction

With a 30-fold increase in incidence over the last five decades, dengue poses an increasing threat to about two thirds of the world population (1). Dengue, caused by a group of viruses belonging to the *Flavivirus* genera, circulates in four major serotypes (DENV 1-4) (2), and manifests in a wide spectrum of clinical forms, from subclinical to classic dengue fever to the more serious forms of the disease, namely, dengue hemorrhagic fever (DHF) and dengue shock syndrome (DSS). In the absence of treatment, dengue can be highly fatal in subjects with DHF or DSS, with a case-fatality rate of 15%, which may be reduced to 1% with adequate medical intervention (3). Despite on-going efforts, no effective antiviral drugs are available against the disease and the potential impact of the recently licensed vaccine has yet to be determined. This limits control efforts primarily to vector control (4).

Dengue dynamics are characterized by highly seasonal, multi-annual fluctuations, with replacement of serotypes occurring at varying intervals. An example of these patterns arising in a newly emerging dengue setting is illustrated in (Figure 3-1)(5, 6). This is thought to result from a complex interplay between environmental factors, vector

ecology and host-pathogen dynamics (7). Various hypotheses have been proposed to uncover the main drivers of dengue dynamics and to reveal how such drivers interact among themselves to govern infection and disease patterns in the field. Emphasis has been on unraveling the roles that cross-immunity (CI), cross-enhancement between serotypes, and seasonal variation in the transmission rate, play in capturing the complex dynamics of dengue (8). Cross-enhancement is believed to be caused by antibody-dependent enhancement (ADE), where heterotypic antibodies facilitate cell entry through the formation of virion-antibody complexes, ultimately leading to increased viral titers upon secondary infection (9, 10). This is thought to result in increased susceptibility to a secondary heterologous infection and, upon these secondary infections, in a more serious form of disease and increased infectiousness. Enhanced disease severity is however believed to have minor impact on the dynamics as the proportion of DHF and DSS cases is substantially small (1% of confirmed cases (11)). By contrast, including sufficiently high levels of enhanced infectiousness or susceptibility (60-130%) in simulation models has been found to induce asynchronous outbreaks of different serotypes (12, 13), an outcome which has been indicated to underlie the manifestation of the 3-5 year epidemic cycles observed for dengue dynamics in Thailand (14, 15). Decomposing ADE into both enhanced infectiousness and susceptibility has further been shown to mimic this effect at lower, more realistic values of ADE, while also reducing the magnitude of oscillations to more plausible levels and decreasing the risk of stochastic extinction (15). Similarly, relaxing the common assumption of complete immunity after two heterologous infections results in asynchronous, multi-annual outbreaks at lower levels of ADE and R_0 (16). While most modeling endeavors have assumed serotypes to have identical characteristics,

allowing for a small amount of asymmetry in the transmission rate is found to increase serotype persistence in the presence of ADE (17). Furthermore, the inclusion of short-lived cross-immunity in models was found to be sufficient to reproduce the observed out-of-phase, irregular oscillations and 3-year cycles (18-21). An alternative hypothesis has been proposed by Lourenço et al., who demonstrated that spatial segregation between human hosts and its vectors can be sufficient to capture the semi-regular dengue patterns observed, even in the absence of immune interactions (22). By contrast, to mimic the distinct seasonal signature of dengue dynamics, the incorporation of seasonal forcing into the vector population dynamics or transmission rate has been found to be essential (19, 22, 23).

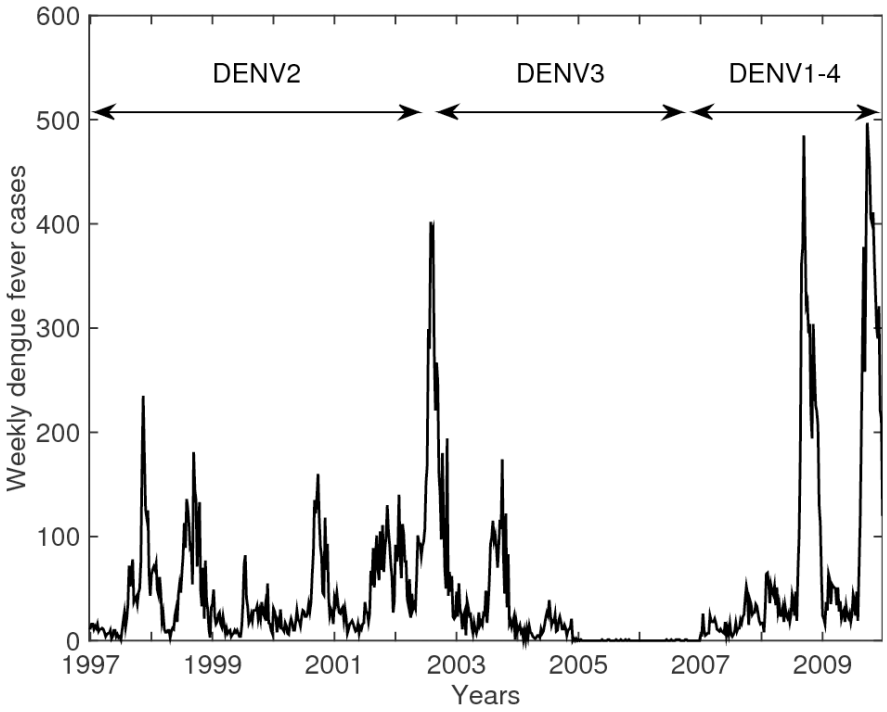

Figure 3-1: Dengue epidemiology in Trinidad and Tobago. Weekly number of confirmed dengue fever cases with circulating serotypes in Trinidad and Tobago over the period 1997-2009.

The above results hint at the complexity of dengue transmission and suggest that multiple mechanisms could underlie disease dynamics in any particular site. A key question in understanding dengue dynamics and control, therefore, is how best to use observed data in order to identify the processes governing the transmission of the disease in a given location. Recently, there has been increasing recognition that for complex systems, such as dengue, model matching to single or a few patterns is not sufficient to narrow down the range of possible explanatory mechanisms (24), and that matching to multiple patterns observed at various scales and hierarchical levels is required for identifying the mechanisms that generate such patterns, and hence are likely to be key

elements of the system's structure. Tying ecological models to multiple system patterns concurrently may also aid in detecting the right level of complexity and improve the predictive ability of such models for replicating local dynamics (24). Methods such as Pattern Oriented Modeling (POM) allow for such a multi-scope approach by facilitating the design, selection, and calibration of models of complex systems (25-30).

This study applied a POM approach to modeling global dengue infection data in order to determine whether the above proposed mechanisms related to serotype interactions and seasonal forcing of the transmission rate were able to explain all of the observed dynamical patterns in the field. We further used the modeling results to investigate the vulnerability of dengue to interruption in transmission as a result of vector control, and examined how such vulnerability was related to the identified processes governing disease transmission. We demonstrate that model selection is largely driven by the seasonality of the system, with CI being a preferred mechanism in the case of low, and ADE in the case of highly seasonal transmission regimes. At similar levels of transmission rate, resistance to control efforts was found to increase in dengue systems with CI. The results highlight the utility of the POM approach for detecting and fitting of appropriately structured disease transmission models based on observed data. In addition, they also reveal challenges in structural and parameter identifiability that would remain unnoticed when guided by individuals patterns used in isolation.

3.4 Methods

3.4.1 The patterns in the reported dengue case data

Five characteristic dengue patterns were used to filter out unrealistic model structures and reduce parameter uncertainty. The patterns were selected to reflect the breadth of characteristics used in single pattern matching approaches (12, 15, 16, 18, 22), include strong and weak patterns that are common across endemic regions and those which are relatively stable over time and encompass different levels of organization (24). The patterns (i.e. mean duration between peaks, multi-annual fluctuations, frequent replacement of one circulating serotype by another, serotype co-dominance and asynchronous serotype cycling) were derived from literature describing dengue case data and serotype epidemiology from different endemic regions across the world (5, 6, 31-42). The observed patterns are described in Table 3-1.

TABLE 3-1:

CHARACTERISTICS FOR PATTERN-ORIENTED MODELING

Characteristics	Range in the literature	Range for analysis Lower limit	Upper limit	Source
Mean inter-peak period	1.4 – 1.6	1	1.8	(6, 34, 36-39, 41, 42)
Multi-annual signals	2-6 years	2 years	6 years	(6, 31-35, 40)
Duration of serotype replacement	1-6 years	1 years	6 years	(5, 6, 22, 33, 36, 37, 39-41)
Intensity single serotype emergence	Both multi and single-serotype prevalence	0.01	0.99	(5, 6, 22, 33, 36-39, 41)
Phase-locking	Incomplete	-	-	(5, 6, 22, 33, 36, 37, 39-41)

3.4.2 The model

We used a deterministic Susceptible-Infected-Recovered (SIR) modeling framework to describe the circulation of four different dengue serotypes (DENV1-4) in a population (13). The full system of ordinary differential equations is shown in (Figure 3-2). The model consists of 26 compartments, each of which represents a fraction of the population. The population size is modeled to be stationary; hence births and deaths occur at an equal rate (μ). New-borns are assumed to be immunologically naïve to all serotypes and are born into the class of susceptibles (S). Although the presence of maternal antibodies is shown to affect the risk of infection, the impact on the overall dynamics is believed to be minimal and thus not taken into consideration (43).

Susceptibles become primarily infected by serotype *i* (I_i) at rate βSI_i and $\alpha_{TRANS}\beta SI_{ji}$ proportional to the number of primarily and secondarily infectious individuals respectively. The parameter $\alpha_{TRANS} > 1$ indicates enhanced transmissibility of secondarily infected individuals. A seasonal change in the transmission rate $(\beta(t))$ is incorporated through a sinusoidal function with a forcing period of one year: $\beta(t) = \beta_0(1 - \beta_1 \cos(2\pi t))$, where β_0 indicates the mean transmission rate and β_1 the strength of seasonal fluctuation and t time in years. The transmission rate $(\beta(t))$ is assumed to be equal across serotypes. Individuals remain infectious for a period of 1/γ. After recovery from a primary infection, individuals become immune to all serotypes (C_i) for a period 1/ρ after which they move to the partially immune stage (P_i). The P-class individuals are assumed to experience full immunity against the serotype i and enhanced susceptibility ($\alpha_{SUS}>1$) to all other serotypes. They acquire secondary infection (I_{ij}) at rates $\alpha_{SUS}\beta P_i I_j$ and $\alpha_{TRANS}\alpha_{SUS}\beta P_j I_{kj}$, proportional to the number of cases respectively primarily and secondarily infectious to a different serotype (with $k \neq j$ and $j \neq i$). The duration of the infectious period is assumed to be equal upon secondary and primary infection. To account for imported cases and prevent the ODE-models to simulate unrealistically low levels of infections, individuals (susceptible or partially immune) can also acquire infection through an infectious contact with an individual from an external population at rate $\beta\delta$, where δ signifies the import rate (23). As tertiary and quaternary infections are rarely observed (44), we assume that after recovery from a secondary infection, individuals become life-long immune to all serotypes. An adaptive time step fourth and fifth -order Runge-Kutta solver was used

with initial conditions for I_1-4 1x10-7, 2x10-7, 3x10-7 and 4x10-7 and $S = 1 - \sum_{1-4}^{i} I_i$. All other state variables were initialized at zero. The implementation of the model, as well as the analysis of its simulation results were carried out in the Matlab, version 2014b (www.mathworks.com).

$$\frac{dS}{dt} = \mu(N - S) - \sum_{i=1}^{4} \beta(t) S(I_i + a(\sum_{j=1, j\neq i}^{4} I_{ji}) + \delta)$$

$$\frac{dI_i}{dt} = \beta(t) S(I_i + a(\sum_{j=1, j\neq i}^{4} I_{ji}) + \delta) - (\gamma + \mu) I_i,\ i=1,\ldots,4$$

$$\frac{dC_i}{dt} = \gamma I_i - (\rho + \mu) C_i,\ i=1,\ldots,4$$

$$\frac{dP_i}{dt} = \rho C_i - \sum_{j=1, j\neq i}^{4} \alpha\beta(t) P_i (I_j + a(\sum_{k=1, k\neq j}^{4} I_{kj}) + \delta) - \mu P_i,\ i=1,\ldots,4$$

$$\frac{dI_{ij}}{dt} = \alpha\beta(t) P_i (I_j + a(\sum_{k=1, k\neq j}^{4} I_{kj}) + \delta) - (\gamma + \mu) I_{ij},\ i=1,\ldots,4, j(\neq i)=1,\ldots,4$$

$$\frac{dR}{dt} = \gamma(\sum_{i=1}^{4} \sum_{j=1, j\neq i}^{4} I_{ij}) - \mu R$$

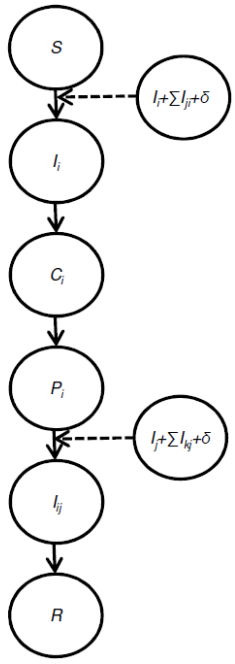

Figure 3-2: System of differential equations and flow diagram of multi-serotype model. The circles represent the infection related states: susceptible (*S*), infectious (*I*), cross-immune (*C*), partially susceptible (*P*) and recovered (*R*), solid arrows depict the transition from one state to another and the dashed arrows indicate transmission. Parameters are described in Table 3-3. Simulations are based on a four serotype (DENV1-4) model, where i, j and k denote primary (first subscript) or secondary (second subscript) infection with DENV1-4. The full system consists of 26 compartments. For simplicity, the flowchart for one serotype is shown.

3.4.3 Model hypotheses

In this analysis we assume the following hypotheses (see Table 3-2). H1: The most parsimonious hypothesis is represented by the base-model with neither ADE (α_{SUS}=1 and α_{TRANS}=1) nor CI (individuals upon recovery from primary infection go straight to the P-class). H2: The base-model with CI. H3: The base-model with enhanced susceptibility, further referred to as ADE (α_{SUS}>1 and α_{TRANS}=1). H4: H3 with CI. H5: The base-model with both enhanced susceptibility and transmissibility (i.e. ADEx2 with αSUS>1 and αTRANS>1) but no CI. H6: H5 with CI. In all models, an annual seasonal forcing in the transmission rate is assumed.

TABLE 3-2:

MODEL HYPOTHESES

	Model	Seasonality	Cross-Immunity	Enhanced susceptibility	Enhanced transmissibility
1	Base	X			
2	CI	X	X		
3	ADE	X		X	
4	ADE+CI	X	X	X	
5	ADEx2	X		X	X
6	ADEx2 + CI	X	X	X	X

Models are built as described in Figure 3-2. In the absence of cross-immunity, individuals are assumed to move straight from the infectious state (*I*) to the partially susceptible state (*P*). In the absence of enhanced susceptibility and enhanced transmissibility α_{SUS} and α_{TRANS} respectively, are set equal to 1.

3.4.4 Defining dengue characteristics in simulated data

The variables that we estimated from the simulated data to contrast the dynamics of each model against the characteristics of dengue dynamics are: 1) Mean inter-peak period; 2) Presence of a multi-annual signal; 3) Duration of serotype replacement; 4) Intensity of single-serotype emergence; and 5) Serotype phase-locking.

The *mean inter-peak period* (MIPP) is defined as: $MIPP = \frac{Y}{N}$, where Y is the number of years analysed and N the number of peaks occurring during that period. To ensure comparability of the simulated estimates with reported observations on the inter-epidemic period, peaks were defined to have a minimum proportion of infectious people of 1/4000. To assess the presence of significant *multi-annual signals* in addition to the near yearly MIPP, a spectral density approach was used. To reduce the confounding effect of very low amplitude fluctuations, the time series were smoothed using a moving average filter. The power spectral density of the smoothed time series was assessed with the Welch's overlapped segment averaging estimator (45). To evaluate the significance of the periodic signals, the signals were compared to the null-continuum. The null-continuum is a greatly smoothed version of the raw periodogram, encapsulating the underlying shape of the distribution of variance over frequency (46). A signal was assessed to be significant if the lower bound of the 90% confidence interval of the raw periodogram exceeded the null continuum (46). The *duration of serotype replacement* is defined as the mean number of years before a dominant serotype during a peak is replaced by another serotype in a subsequent peak. The intensity of single serotype emergence (ε) was defined as by Recker et al. (47): $\varepsilon = \frac{1}{N}\sum_{i}^{N}\frac{\gamma^{i}_{\max} - \gamma^{i}_{sub}}{\gamma^{i}_{\max}}$, where N defines

the number of peaks occurring during the analyzed number of years, $\gamma^{i}_{\max}$ the prevalence of the dominant serotype and γ^{i}_{sub} the prevalence of the serotype with the second-highest peak. Model runs with either complete co-dominance (ε<0.01) (*i.e.* there are multiple serotypes present at any point in time) or complete single serotype dominance (ε>0.99) were omitted. Lastly, *serotype phase-locking* here is defined as the perfect synchronization of serotypes and is detected by comparing the MIPP of serotype *i* to the aggregated MIPP. Simulations in which $MIPP = MIPP_i$ are discarded based on the presence of perfect phase-locking.

3.4.5 Data-model pattern matching

To determine which of the hypotheses or models capture the observed dengue dynamics and at which parameter values, we used a pattern oriented modeling approach (Figure 3-3) (25-28). Model performance was assessed based on the extent to which a model captured all the 5 characteristics of dengue simultaneously, as defined above (). Models were assessed using the following steps. First, Latin hypercube sampling (48) was employed to select a sample of Ω (=5,000) parameter vectors from a conjoint parameter distribution, encompassing the transmission rate (β_0), the level of seasonal forcing or seasonality (β_1) and, depending on the model, a combination of enhanced susceptibility (α_{SUS}), enhanced transmissibility (α_{TRANS}) and the rate of loss of CI (ρ) (Table 3-3). Uncertainty in the values of these parameters was addressed by assigning uniform distributions from their ranges deemed realistic according to literature (Table 3-3). The resulting ensemble of models (Model 1-6 with Ω parameter vectors) was run for 1400 years. The model outputs for the last 400 years were considered to determine

whether the model mimicked all five dengue characteristics (a model is assumed to match a characteristic if the simulated response falls within the range of that characteristic pattern given in Table 3-1). The resulting set of passing (good) parameters G (where $G \subset \Omega$) was retained as a multivariate distribution for further analysis.

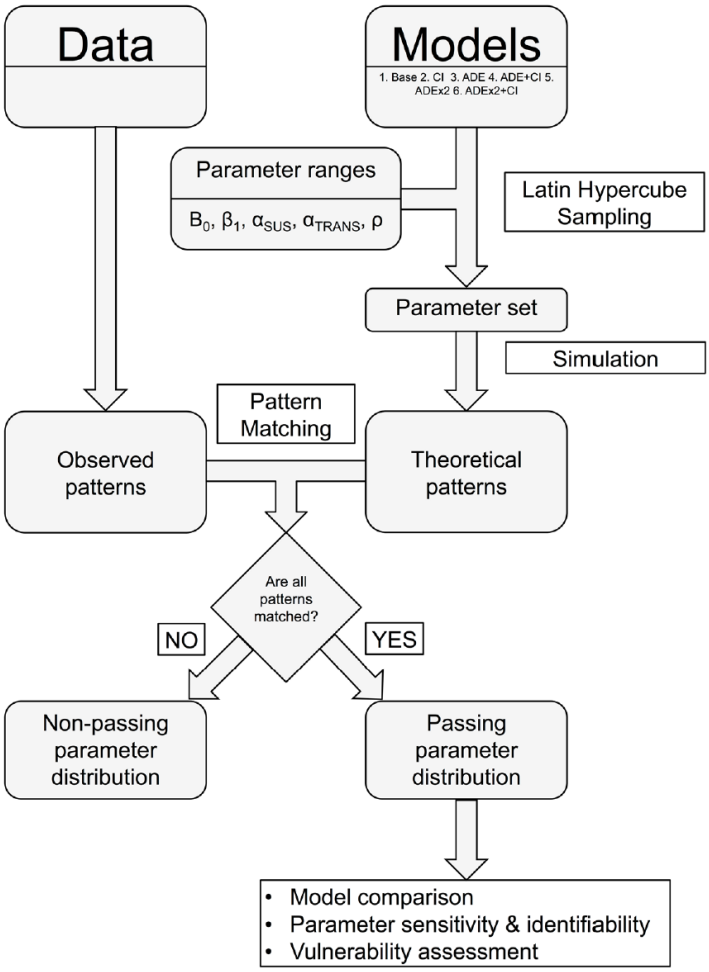

Figure 3-3: Flow chart of Pattern-Oriented Modeling approach. A set of 6 alternative models are identified and compared with respect to their ability to replicate patterns observed in dengue case data. Each model is run for a set of 5,000 different parameter combinations, sampled from plausible parameter ranges using Latin hypercube sampling. The resulting patterns from each simulation are compared to the observed patterns. The parameter sets that match all 5 patterns of interest are assembled into the passing parameter set, which forms the input for model comparison and the examination of model behavior.

TABLE 3-3:

MODEL PARAMETERS

Symbol	Description	Value	Range	Source
β_0	mean transmission rate, year-1	400	100-400	(13, 18)
β_1	seasonal forcing	0.05	0-0.35	(20, 23)
μ	host life expectancy, year-1	1/70	fixed	(13)
γ	recovery rate, year-1	100	fixed	(13, 49)
ρ	1/ duration of cross-immunity, year	2	1/3 - 3	(23)
α_{TRANS}	infectiousness enhancement	>1	1-2.4	(15)
α_{SUS}	susceptibility enhancement	>1	1-2.4	(15)
δ	import rate	1e-10	fixed	(20, 23, 50, 51)

Parameter values used in the model simulations, where Value indicates the best estimate from literature and Range depicts the boundaries of the uniform prior from which is sampled for the POM-approach.

3.4.6 Sensitivity analysis

To assess the impact of simplifying model assumptions on pattern-matching, we repeated the POM exercise for two distinct scenarios. One, we allowed for transmission rates to be uneven between serotypes (the asymmetric model). More specifically, serotype-specific transmission rates were drawn from a normal distribution with standard deviation 0.15 (17). Two, we used a model variant that allows for four heterologous infections prior to acquiring complete immunity (the 4-infection model, equations are provided in Appendix A (52)).

3.4.7 Parameter sensitivity and identifiability

We used logistic regression to assess the sensitivity of pattern-matching (binary response variable) to the parameters (independent variables). We normalized the independent variables on a 0 to 1 scale to obtain comparable regression coefficients:

coefficients larger than|3| indicate strong sensitivity while parameters with small coefficients (<<|1|) have little impact on the model matching the patterns (53). Two-way interactions were included in the construction of the logistic regression models: $\text{logit}(p) = b_0 + b_1\beta_0 + b_2\beta_1 + b_3\alpha_{SUS} + b_4\alpha_{TRANS} + b_5\rho + \text{interactions},$ with p being the probability of a pattern-match, b_0 the intercept and $b_{1\text{-}n}$ the regression coefficients.

Additionally, the identifiability of each of the parameters was examined using a principal component analysis (PCA) (54, 55). The identifiability of a parameter is a function of dependence, prior uncertainty and the model's sensitivity to the parameter and defines how well one can estimate a parameter. We assessed the parameter identifiability for the full model (ADEx2+CI), using its passing distribution (G). First, the variance-covariance matrix $(\sum)$ was constructed from the log-transformed G. Next, the principal components (PCs) were derived from $\sum$. The PCs of $\sum$ define the 5-dimensional ellipsoid that approximates the population of passing parameter values. The eigenvalues (λ_i) denote the respective radii and the eigenvectors representing how much each parameter contributes to the direction of each radius. As such, λ_i gives an indication of the variance explained by the i^{th} PC. The overall variance of all PCs was defined as $\sum_{i=1}^{5} \lambda_i = trace(\Sigma)$, thus the proportion of the total variation in G that was explained by the i^{th} PC is was estimated by: $\frac{\lambda}{trace(\sum)}$. We interpret these results as follows: A smaller λ_i indicates that the model is more sensitive to changes in the direction described by the i^{th} component, whereas a larger λ_i signifies that the model is less sensitive to changes in the direction of the component. Parameters contributing most to a large λ_i are responsible for

a big portion of the variation in the parameter space and are thus considered less identifiable.

3.4.8 Vulnerability to disruption in dengue transmission

We examined the vulnerability of the models to sudden reductions in the transmission rate that may be brought about by vector control. The models were run for all parameter sets in G for a burn-in period of 1000 years after which the system was perturbed by a reduction in the transmission rate (*i.e.* β_0 is reduced by 90%) for a control period of *w* weeks per year. We varied *w* from 1 week to 52 consecutive weeks, starting at the valley of the sinusoidal function, which mimics the onset of the rainy season. After the control period of *w* weeks, β_0 returns to its original value. These control runs were performed for 30 years after the burn-in period. The intervention of *w* weeks was assumed to be successful if no more than one peak occurred over the time-course of the model simulation. We assessed the probability of control for model *i*, where *i* represents 1 to 6, by calculating the proportion (P_{w_i}) of G_i presenting successful control as a function of the number of weeks the transmission was disrupted. Here, $P_{w_i} = \frac{N_{w_i}}{G_i}$ with N_{w_i} being the number of parameter vectors out of G_i that showed successful control for model *i* given *w* weeks of interruption in transmission. A composite average (P_w) for each control period *w* was derived by weighing the individual probability values of the models by the sizes of their passing parameter distributions (G_i), such that: $P_w = \sum_{i=1}^{6} \frac{N_{w_i}}{G_i}$.

Lastly, we estimated the values of the basic reproduction rate (R_0) for each of the parameter vectors in G to assess the relation between transmission potential and the

models' vulnerability. The R_0 of the model was derived using the next generation method (56-58) (Proof provided in Appendix B) and is defined as: $R_0 = \frac{\beta_0}{\gamma + \mu}$, where β0 defines the transmission rate, $1/\gamma$ the duration of the infectious period and $1/\mu$ the average life expectancy of the human host (59).

3.5 Results

3.5.1 Model performance

3.5.1.1 2-infection models

We compared the ability of six 2-infection models to reproduce the main characteristics of dengue epidemiology listed in Table 3-1. Table 3-4 shows the proportions of parameter sets for which the models were able to capture the dengue dynamics by reproducing the five characteristics, either all simultaneously (values in bold) or each individually. Each of the six models investigated in this study was capable of simultaneously reproducing the five patterns of dengue dynamics, albeit at different proportions of the parameter space. The percentage indicates how robustly a model could replicate the patterns across the parameter space. While each pattern, independent of the others, could be reproduced at a relatively high probability, the simultaneous reproduction of all five patterns was found to occur rarely. In general, one would expect models with increasing complexity to perform better than simpler models. Indeed, the full model performed best overall (10.98%). However, here, the base-model was found to perform nearly as good as the second best model (*i.e.* the ADE+CI model); the respective

overall proportions were similar in magnitude (5.54% versus 5.76%). Both the CI- and ADE-only models performed poorly, with overall proportions of 1.16% and 2.02%, respectively. The model with the decomposed ADEs approximately performed twice as well as either of these two models.

TABLE 3-4:

MODEL PERFORMANCE

	2-inf symmetric	2-inf asymmetric	4-inf symmetric
Base-model	**5.54**	**4.34**	**0.06**
Mean inter-peak period	74.2	65.8	95.2
Multi-annual signal	34.6	46.6	59.2
Duration of serotype replacement	49.3	43.2	12.5
Single serotype emergence	34.6	92.3	57.3
Absence of phase-locking	10.7	14.3	16.1
CI	**1.10**	**1.20**	**21.9**
Mean inter-peak period	27.9	22.3	63.4
Multi-annual signal	91.7	90.8	87.3
Duration of serotype replacement	87.6	90.6	70.2
Single serotype emergence	87.0	96.8	95.8
Absence of phase-locking	34.0	40.4	76.4
ADE	**1.88**	**7.04**	**1.94**
Mean inter-peak period	88.0	71.9	78.2
Multi-annual signal	63.7	64.2	64.6
Duration of serotype replacement	23.1	42.4	24.1
Single serotype emergence	54.8	96.9	84.7
Absence of phase-locking	18.2	33.2	74.7
ADE+CI	**5.76**	**5.70**	**12.54**
Mean inter-peak period	41.7	33.2	78.1
Multi-annual signal	91.8	88.8	83.2
Duration of serotype replacement	81.6	86.0	38.5
Single serotype emergence	86.5	97.9	98.8
Absence of phase-locking	42.0	52.6	88.7
ADEx2	**3.4**	**7.06**	**0.96**
Mean inter-peak period	47.6	38.9	28.9
Multi-annual signal	73.3	71.4	66.0
Duration of serotype replacement	45.2	62.2	53.8
Single serotype emergence	79.2	99.1	94.2
Absence of phase-locking	72.4	86.1	94.0
ADEx2+CI	**10.98**	**9.78**	**4.82**
Mean inter-peak period	50.9	50.2	76.1
Multi-annual signal	84.7	79.7	77.2
Duration of serotype replacement	62.5	62.6	20.0
Single serotype emergence	89.8	98.6	98.9
Absence of phase-locking	91.2	94.6	97.5

Percentage of runs (n=5,000) that meets the characteristics of dengue dynamics for each model structure. In the 2-infection symmetric model, heterologous immunity is assumed after a second infection and serotypes are assumed to have equal transmission rates. In the 2-infection asymmetric model, the four serotypes differ in transmission rates. In the 4-infection symmetric model, no heterologous immunity is assumed until one has recovered from all four serotypes. ADE=antigen dependent enhancement and CI=cross-immunity.

The performance of each model can also be examined by their ability to reproduce each characteristic separately. In this case, the base-model generally performed worse than the other models, yet it appeared to be equally proficient at simultaneous reproducing all characteristics or patterns as the ADE+CI-model, a more complex model than the base-model. While the MIPP is best captured by the base- and ADE-model (Table 3-4), all other characteristics demonstrate preference to the models that include CI. The model's proficiency to reproduce the multi-annual signal however interferes with its ability to capture the seasonal signature in the MIPP (Table 3-4). As such, the POM methodology appears to penalize for overly specialized model hypotheses.

Both the base-model and ADE-model are hampered in their performance by large regions of phase-locking (Figure S3-1aEA and aEC) and to a lower extent, complete single serotype dominance (Figure S3-11aDA and aDC). The parameter space in which phase-locking occurs is largely reduced by the addition of decomposed ADE as well as CI, which both induce irregular, asynchronous serotype circulation (Figure S3-1aED and aEE).

3.5.1.2 Asymmetric 2-infection models

Relaxing the assumption of symmetry in transmission rates does not affect the level of overall fit of the base-model or any of the models with CI. However, models with ADE or decomposed ADE performed better upon the inclusion of asymmetry. Across all models, the parameter space at which complete serotype co-dominance occurred was reduced by the inclusion of asymmetric transmission rates. This co-dominance seemed to

be a strong constraint on the ADE and ADEx2 models in the 2-infection case and is the reason for the markedly improved fit in the asymmetric case.

3.5.1.3 Symmetric 4-infection models

The impact of the relaxing the assumptions of full immunity after the second heterologous infection is substantial. The simple CI-model performed far better than any other models, with a 10-fold increased performance relative to its 2-infection counterpart. In the 4-infection case, the performance of the full model was about twice better than the 2-infection case. This is largely due to reduced phase-locking in the 4-infection case (16). The phase-locking was the foremost restricting factor of the CI-model in the 2-infection case. The base-model in this case, however, showed a markedly reduced performance as a result of shortened time required for serotype replacement. This indicates that the permanent heterologous immunity only after two infections was the driver of the serotype interactions sufficient to result in desynchronized oscillations in the 2-infection base-model. The few fits (0.06% of 5000, see Table 3-4) of the base-model occur because of an additional implicit serotype interaction. Since no more than one infection is assumed to occur concurrently, this introduces short cross-immunity that lasts for the infectious period. Indeed, when we allowed for more than one infection in the 4-infection base-model, the out-of-sync oscillations disappear completely (Figure S3-6).

3.5.2 Model calibration and selection

Figure 3-4 demonstrates the accepted parameter distributions (G) for the 2-infection models. While some parameters demonstrate broad distributions indicating

limited uniqueness and abundant parameter interactions, others show clear preferential values and ranges that are sensitive to the structural components of the model. Overall it appears, as can be expected, that the more complex models fit the patterns at a wider parameter range.

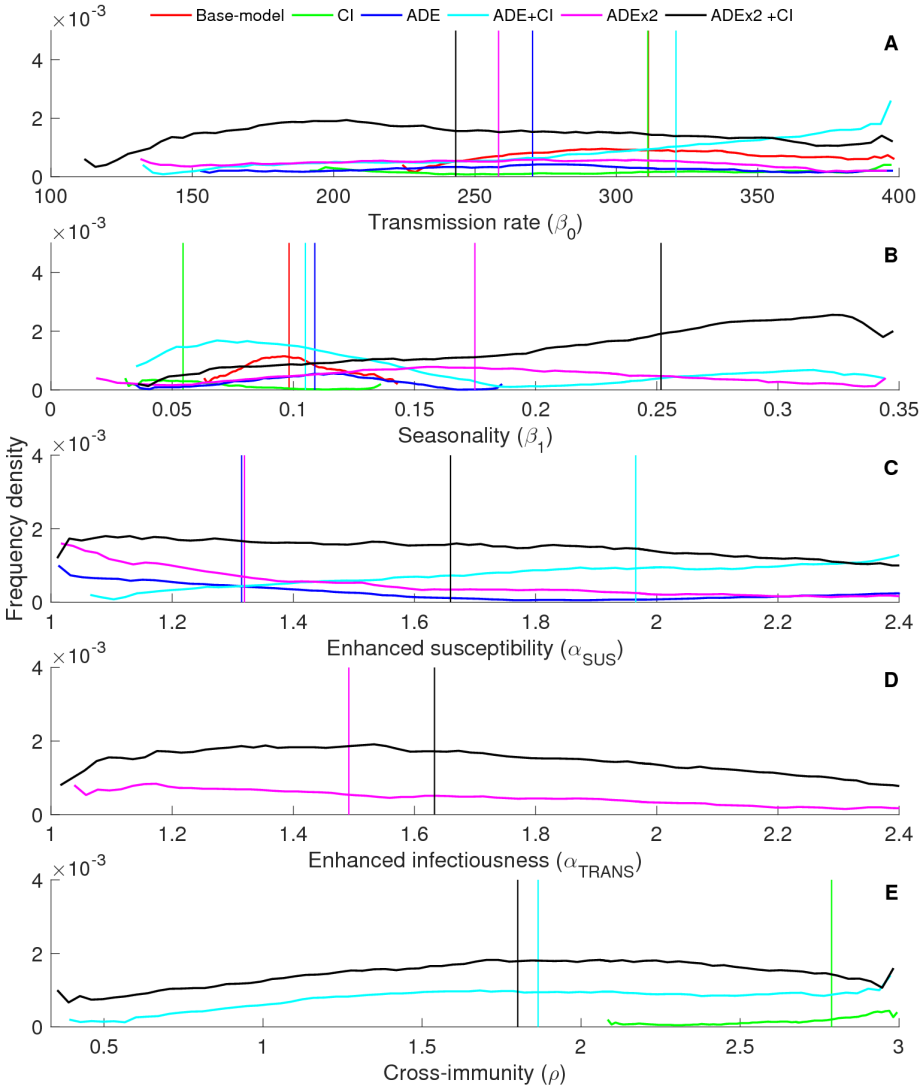

Figure 3-4: Model parameter distributions. Parameter distributions for passing parameter sets (G) for different model hypotheses (with ADE=antibody dependent enhancement, CI=cross-immunity) for (A) the transmission rate (β_0), (B) seasonality (β_1), (C) enhanced susceptibility (α_{SUS}), (D) enhanced infectiousness (α_{TRANS}), and (E) 1/duration of cross-immunity (ρ). The vertical lines depict the median values for each distribution with the colors indicating the corresponding model hypothesis.

Figure 3-4A shows that models with CI selected for relatively higher transmission levels relative to models with ADE only. For low transmission levels, the full model outcompeted all the other models, indicating that more complex models may be necessary to fit dengue dynamics at lower values of R_0. These results are insensitive to the assumption of low levels of asymmetry in transmission rates (Figure S3-2aA). In contrast to this, the 4-infection models display similar fits at lower transmission levels (Figure S3-2bA).

Seasonality appeared to be the most prominent driver of model fit and selection in the 2-infection model (Figure 3-4B). Models with CI showed a marked shift towards lower seasonal forcing relative to the base-model. In fact, at low seasonality (β_1<0.06) there is a strong preference for the inclusion of CI, as is especially notable from the elevated density levels of the ADE+CI and ADEx2+CI models. At high seasonality (β_1>0.17) only the more complex models provided an adequate fit. At intermediate levels of seasonality (β_1: 0.1-0.15) multiple models were equally proficient at replicating the dynamics, indicating a region of large model uncertainty. The model's structural sensitivity to seasonality persisted when asymmetry in transmission rates was assumed (Figure S3-2aB). However, when we allowed for tertiary and quaternary infections, the medians and shapes of the passing parameter distributions for β_1 were similar across the models (Figure S3-2bB).

The addition of CI to models with ADE results in higher levels of α_{SUS} (Figure 3-4C), yet had minor impact on the median levels of α_{TRANS} (Figure 3-4D). While previous publications suggested reduced estimates of α_{SUS} and α_{TRANS} upon the inclusion of decomposed ADE, analysis of the 2-infection model does not support this observation

(15). We did, however, observe this pattern in the 4-infection and asymmetric 2-infection model (Figure S3-2aD and bD).

The inclusion of ADE to the models with CI profoundly affects the estimated duration of cross-immunity by allowing for the selection of a much wider range of ρ (Figure 3-4E). Whereas the CI-model by itself only captures the characteristics at durations of cross-immunity shorter than half a year, the inclusion of ADE allows for cross-immune periods of up to 2 years, which is in line with the previous estimates (21). Interestingly, in the case of 4-infection, the CI-only model performed well for a wider range of durations of cross-immunity, including estimates from Reich et al. (21).

3.5.3 The role of seasonality and cross-immunity

Exploring the behavior of the models in terms of MIPP and duration of serotype replacement (Table 3-4) reveals as to why there are differences in model fits across the range of seasonal forcing (Figure S3-1aAA-aAF and Figure S3-1aCA-S1aCF). Increased levels of seasonal forcing are associated with longer MIPP. Temporary CI introduces a lag before a secondary infection can be acquired and thus generates a necessary build-up time period during which susceptible individuals accumulate in sufficient number to fuel the next outbreak. Thus, while an increase in seasonal forcing is characterized by longer inter-epidemic periods, at similar levels of seasonal forcing, the models with CI demonstrate a longer MIPP than the models without CI (Figure S3-1aAA-aAF). This allows the CI-only models capture the characteristic MIPP at lower seasonal levels than the models with just ADE. At higher levels of seasonal forcing, CI contributes to MIPPs that are longer than are characteristic to dengue. This effect is less pronounced in the 4-

infection models. The overall immune population is smaller in the 4-infection models and therefore of less influence on the frequency of outbreaks. The same can be observed for the duration of serotype replacement (Figure S3-1aCA-aCF). In contrast to CI, the inclusion of ADE to the model results in shorter cycles, thus successful fits are observed at higher levels of seasonal forcing (Figure S3-1aAA-aAF).

Lastly, we observe a prominent impact of seasonal forcing on the occurrence of phase-locking. Figure S3-1aEA-aEF demonstrate a threshold-like value of β_1 above which the system is forced into synchronized serotype dynamics. This threshold is relatively stable across the simple model structures (see also Figure 3-4B) and unaffected by the value of R_0. Only the addition of decomposed ADE disrupts this behavior, thereby being a possible driver of irregular serotype behavior at higher seasonal regions. These phase-locking thresholds are stable to some level of asymmetry in transmission rates (Figure S3-1bEA-EF), however they completely vanish in the case of 4-infection models (Figure S3-1cEA-EF).

3.5.4 Parameter sensitivity and identifiability

The logistic regression coefficients for the full-model given in Table 3-5 illustrate the differential roles each of the parameters play in explaining the dengue characteristics. β_0 is found to be an important driver of the multi-annual signal. And in conjunction with β_1 and α_{TRANS}, it is the dominant factor for the absence of phase-locking. As can be expected, β_1 is the main driver for reproducing a seasonal signature. The parameter for CI (ρ) interacts with β_1 in reproducing this pattern and is thus also an important determining factor in fitting the MIPP. The R^2-values for each of the regression models illustrate that

the separate parameter values provide reasonable information about whether a characteristic is met or not. However, when assessing the simultaneous fit, the predictive power of the parameters is negotiated by interactions between the parameters and the separate characteristics. In particular the interactions between β_1 and ρ govern simultaneous fitting (Figure S3-3a). These interactions are conserved when fitting the asymmetric 2-infection and symmetric 4-infection model (Figure S3-3b and c).

TABLE 3-5:

SENSITIVITY ANALYSIS OF MODEL FIT FULL MODEL

Pattern	**R^2**	**p-value**	**Coefficients**					
			intercept	**β_0**	**β_1**	**α_{SUS}**	**α_{TRANS}**	**ρ**
Mean inter-peak period	0.49	<0.005	**-9.84**	0.57[1]	**15.3**	1.37[2]	1.00[3]	**5.99**
Multi-annual signal	0.21	<0.005	**4.43**	**3.08**	-2.49	-2.33	**-3.25**	-2.35
Duration of serotype replacement	0.47	<0.005	**4.43**	2.09	**-4.96**	0.91[4]	-0.27[5]	0.06[6]
Intensity single serotype emergence	0.08	<0.005	0.75[7]	0.39[8]	1.09[9]	0.64[10]	1.33[11]	0.51
Phase-locking	0.52	<0.005	-0.35[12]	**6.27**	**-3.28**	2.10[13]	**4.61**	2.84
Simultaneous fit	0.07	<0.005	**-7.88**	2.93	**4.23**	**4.06**	2.69	**5.94**

Logistic regression model coefficients with pattern-match as binary response variables and the parameters (scaled 0-1) as independent variables. Two-way interactions are taken into account (coefficients in Table S3-1). Bold are high coefficient values (>|3|). Coefficients are significant ($p<0.005$) unless stated otherwise: [1]p= 0.04, [2]p=0.03, [3]p=0.12, [4]p=0.15, [5]p=0.67,[6]p=0.93,[7]p=0.1, [8]p=0.52, [9]p=0.08, [10]p=0.28, [11]p=0.40, [12]p=0.58, [13]p=0.02

Strong, multi-level parameter interactions typically result in limited parameter identifiability. Indeed, the PCA reveals that, in particular the estimates for β_1 and ρ are found to be little constrained by the characteristic patterns (Figure 3-5). The parameters β_1 and ρ dominate the first two components, which explain the largest portion of the total variance in the passing parameter space (G_{full}) (55%). While this observed lack of uniqueness may result from the limited influence the parameters have on replicating the dynamics and the substantial width of the criteria, complex interactions between patterns and parameters can also underlie this phenomenon. Indeed, as observed earlier, β_1 and ρ are correlated with each other as well with other model parameters, which substantially impedes parameterization efforts (Figure S3-3a). Parameters β_0, α_{SUS} and α_{TRANS} contribute equally to the smallest component, indicating that these are more constrained by the examined characteristics and the level of uncertainty and are less affected by dependence to other parameters (Figure 3-5). Allowing for asymmetry in transmission or tertiary and quaternary infections reduces the contribution of seasonality to the first component, leaving the duration of cross-immunity as the most important factor in explaining the variance in the passing parameter distributions (Figure S3-5a and b).

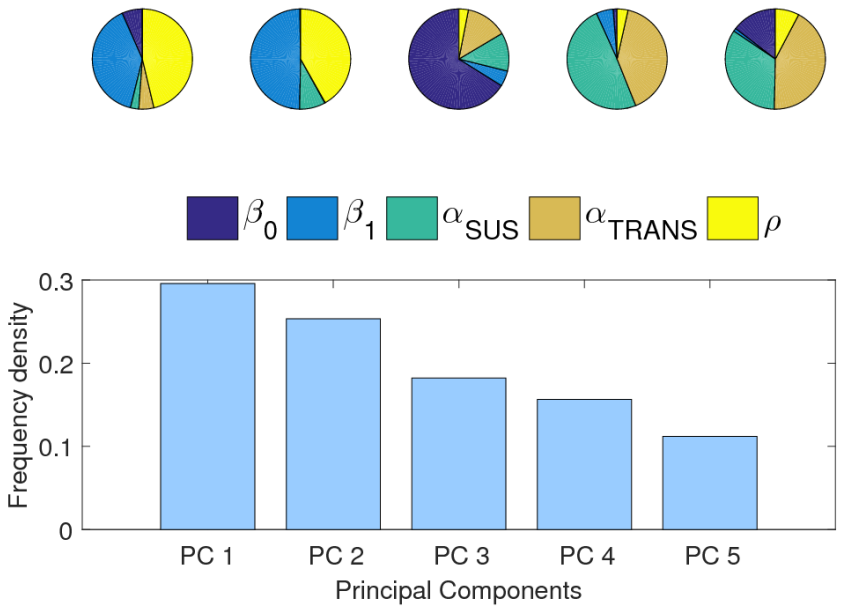

Figure 3-5: Principal component analysis. Principal component analysis of passing parameter space (G) of the full model (ADEx2+CI). The first component explains 30% of the total variance, the second 25%, the third 18% and fourth 16% and the 5th 11%. The pie charts show the contribution of the parameters to each component. β1 and ρ dominate the first component, indicating reduced identifiability. β0, αSUS and αTRANS dominates the fifth component and thus contribute most to the stiffest (i.e. most sensitive direction in the parameter space).

3.5.5 Vulnerability to disruption in dengue transmission

Figure 3-6 depicts the probability of achieving successful control (≤ 1outbreak in 30 years) as a function of *w* weeks of reduced transmission (e.g. due to implementation of vector control). The duration of control required to reach a desired probability of successful control can be used to quantify the level of resistance or vulnerability of a dynamical transmission system.

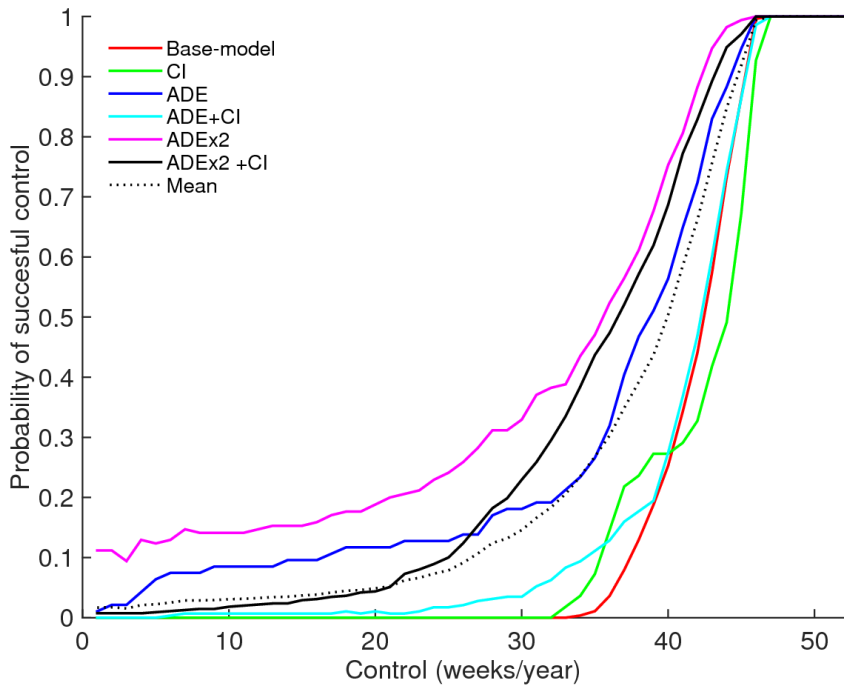

Figure 3-6: Overall vulnerability to control. Probability of successful control (a maximum of 1 outbreak during 30 years) given the duration (weeks/year) of consecutive control (temporary reduction of transmission: β_0 (1-90%) for different model hypotheses (with ADE=antibody dependent enhancement, CI=cross-immunity). The probability is defined as the proportion of the passing parameter sets (G_i) that reach successful control. Here *i* refers to the six models, shown by the individual keys. The dotted line shows the mean probability across all models.

The inclusion of ADE or ADEx2 reduces the resistance of the model to perturbations (dark blue and pink lines), provided no CI is assumed (Figure 3-6). Including CI to the model offsets this effect and demonstrates a resistance profile similar to the base-model at longer control efforts, yet shows larger vulnerability at shorter durations of control. The exception is the full-model, which converges with the ADE-model at longer control durations.

The large resistance to control in the base-model is a consequence of the high values of R_0 required for this model to meet the criteria (R_0>2.2) (Figure 3-7A). At those levels of R_0 the ADE-model demonstrates higher vulnerability to control as a result of decreased persistence (Figure 3-7C). The enhanced vulnerability of the ADE-model relative to the base-model as seen in Figure 3-6 is a consequence of low transmission rates. The inclusion of CI to either model enhances the resistance of the model especially at lower values of R_0 (Figure 3-7D). Longer durations of cross-immunity are associated with greater resistance (Figure S3-7DE), while increased enhancement results in decreased resistance (Figure S3-7CC and DC).

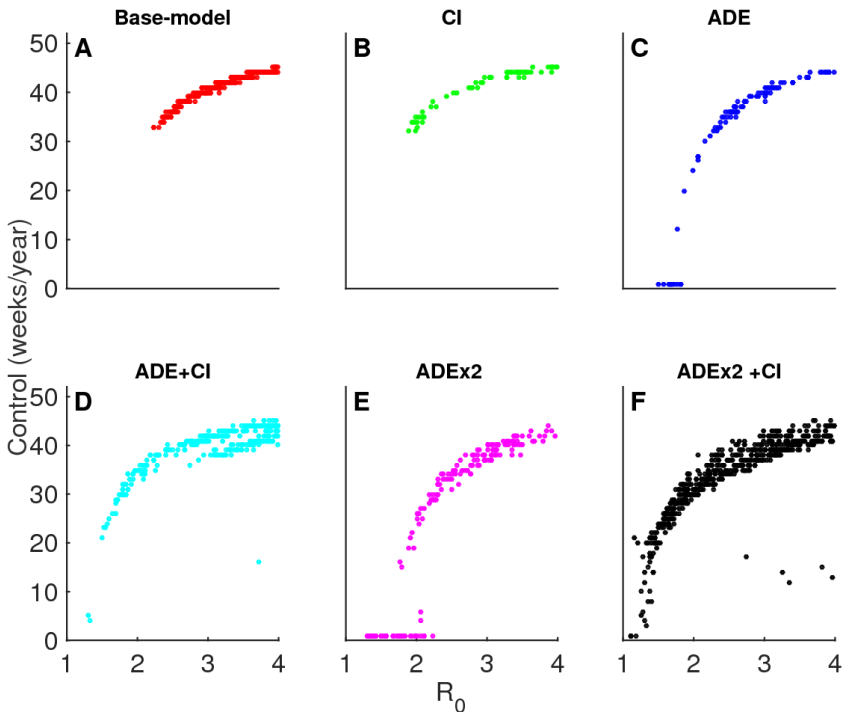

Figure 3-7: Vulnerability to control as a function of R_0. Required duration (weeks/year) for achieving successful control is shown with respect to the basic reproduction number $R_0(=\beta_0/(\gamma+\mu))$ for the different model hypotheses: are base (A), CI (B), ADE (C), ADE+CI (D), ADEx2 (E), and ADEx2+CI (F), with ADE=antibody dependent enhancement, CI=cross-immunity.

This differential vulnerability is in part due to low infection persistence levels, a typical property of models with ADE only (12, 15, 23). The addition of CI counters this effect with and without ADE (Figure 3-7C,D&F). This difference in infection persistence between CI and ADE systems, however, diminishes at high levels of seasonal forcing and R_0. At these high transmission levels, both the models with CI (ADEx2+CI) and without CI (ADEx2) represent extreme fluctuations and long periods of non-persistent dynamics (Figure S3-4aF and aG). Thus, the differential model preference affects predicted control efforts more substantially in lower than higher seasonal scenarios.

3.6 Discussion

We used a pattern-oriented modeling approach to test a range of multi-serotype models and parameter values for their ability to simultaneously replicate multiple dengue fever patterns derived from literature (Table 3-1) and case data from Trinidad and Tobago (Figure 3-1). Despite using such a multiple-pattern data fitting approach, we show that all the investigated model structures were effective at fitting each of the characteristic dengue patterns across some part of the model parameter space, suggesting the occurrence of equifinality, *i.e.* that observed infection patterns can be reproduced by more than one mechanism or combinations of mechanisms (60). This implies that there could be multiple acceptable models for describing globally observed dengue dynamics, none of which can easily be rejected and therefore should all be considered in assessing the mechanisms determining disease transmission (61-63). Three major efforts that would help disentangle the dominant drivers of dengue are: 1) better estimates of model parameters, in particular the duration of cross-immunity and the strength of seasonal forcing; 2) improved understanding on the contribution of post-secondary infections to dengue transmission dynamics; and 3) additional, more detailed patterns, such as (i) time series of serotype-specific dengue cases and (ii) levels of sero-prevalence in populations. Some of these patterns may well differ across geographic regions.

Based on the sizes of the passing parameter distributions, a preference for the most complex 2-infection model was apparent (Table 3-4). Remarkably, the model that performs best across all models is the 4-infection model with CI only. This indicates that, in some instances, the use of multiple patterns for model selection can help filter out overly specialized models and fetch simple, more generalized models that perform better

across different scales. Additionally, it helps reveal the impact of simplifying assumptions on model selection and parameterization, *i.e.,* allowing for quaternary infections enables us to reveal a simpler model framework that outcompetes its 2-infection equivalent. Also, it sheds new light on the need for ADE in replicating dengue dynamics. The role of ADE is not supported when allowing quaternary and tertiary infections while it is preferred in the 2-infection case, with and without asymmetry in transmission rates.

The performance of the base-model is noteworthy, given that it does not include the explicit serotype interactions deemed necessary to replicate asynchronous serotype oscillations. However, there are two implicit serotype interactions that likely underlie this behavior. First, in the 2-infection model, serotypes affect each other's dynamics by causing complete immunity to all serotypes after recovery from the second infection. The observed collapse in model fit of the base-model when we allowed for tertiary and quaternary infections supports this hypothesis. However, the 4-infection base-model also generates desynchronized behavior of serotypes albeit in a very sparse region of the parameter space. This may result from the other implicit serotype interaction as a result of constraining individuals from acquiring more than one infection at the same time. In other words, this second type of interaction arises because individuals infected with one serotype are cross-immune to the remaining serotypes for the duration of the infectious period. This interaction may be enough to underlie a few, sparse fits across the parameter space. Indeed, when the model is extended to include more than one concurrent infection, the out-of-sync oscillations observed in the 4-infection base-model disappear (Figure S3-6).

An additional result revealed by the POM-approach is that model preference appears to be governed by the level of seasonal fluctuations. Namely, the support for models with CI is larger in low seasonal settings, whereas the inclusion of decomposed ADE is required to reproduce the observed dengue patterns in the presence of strong seasonal fluctuations (Figure 3-4B). However, when tertiary and quaternary infections are allowed, this pattern disappears and all models apart from the base-model reveal similar median values for seasonal forcing (Figure S3-2bB). Additionally, we observe that the estimates for the duration of cross-immune period differ markedly upon inclusion of ADE or when relaxing the two infection assumption. In fact, without the inclusion of ADE, the CI-only 2-infection model does not encapsulate the best estimate of the duration of the cross-immune period, as proposed by Reich et al. (21). The CI-model in the 4-infection framework, does meet the values estimated. These findings highlight that improved understanding of the extent to which post-secondary dengue infections contribute to overall dengue transmission, may greatly aid in disentangling the dominant drivers of dengue dynamics.

The public health importance of knowing the processes governing dengue transmission in a specific setting is highlighted by our results on achieving transmission interruption by vector control. The results indicated that the vulnerability of the models to disruption in transmission at equal levels of R_0, was driven by the immune interactions incorporated in the model, with CI increasing resistance in low transmission settings, while ADE has the opposite effect. It is common practice to favor the most parsimonious model when the candidate models are equally efficient; however, the differences in model resistance we found here suggest that it is prudent to be extra cautious while

making such a decision. Given their decisive role in selecting and quantifying the predominant mechanisms as well as determining the projected effects of interventions, in addition to R_0-estimates, obtaining improved, localized estimates of seasonal forcing and the duration of cross-immunity should be prioritized towards better-informing modeling endeavors.

While efforts to disentangle the extent to which internal and external drivers influence the dynamics of multi-serotype systems have been made (64), adequately incorporating both the complex serotype interactions as well as the effects of coupling and decoupling between seasonal forcing and incidence remains an important issue. This is more so because long time series for serotype-specific incidence and vector abundance are scarce and case data are distorted by misclassification and underreporting. The core of the POM approach lies in the appreciation that single data patterns (*e.g.*, multi-annual signals) usually do not contain enough information to unambiguously identify the mechanism generating such patterns; additional patterns from data are needed to fit several model responses simultaneously (65). As pointed out above, we have shown here that, even with sparse data and relatively wide criteria, POM can be a useful tool to distinguish between different conceptual models for capturing dengue dynamics and assessing their vulnerability to control.

While the use of multiple patterns enhances the process of model selection greatly, it is not always clear whether a model capable of replicating the observed patterns can react realistically to environmental perturbations. This may especially be pertinent here as the models are fitted to macroscopic data using the average behavior of the dynamical system rather than lower level processes (24). While the proposed

framework could be extended to incorporate additional, lower level patterns, such as serotype driven variation in disease severity, age-distributions of sero-prevalence, or age at first infection, these are likely to vary across regions and would greatly enhance the parameter dimension to be studied, diminishing the transparency and insights gained into the distribution and behavior of model parameters which is our main focus. Similarly, matching to multiple patterns may not be sufficient to overcome the suspicion that the models demonstrate unrealistic resistance to control, as over 40 weeks of interrupted transmission is required to bring about an 80% probability of success (Figure 3-6). The import factor prevents the models from showing unviable dynamic behavior that results from unrealistically low levels of infections innate to ODE-systems in general and especially prevalent in models with ADE(x2), yet also enhances the resistance of models. While the absolute levels of control are thus of limited practical use, the overall conclusion of differential resistance is found to persist across models with a lower import factor as well (Figure S3-8), highlighting a fundamental challenge arising from structural model uncertainty.

The criteria derived and used in this work may be subjective. By basing the criteria on current literature and the available data and keeping the characteristics broad, we aimed to limit such subjectivity. By focusing on patterns that are common across endemic regions, the derived patterns are inherently weaker than for a localized approach, yet the outcomes are more generalizable. The broadness of the characteristics does lead to decreased uniqueness (as model fits to dengue patterns can be found across the entire parameter space)(66) and a wide range of model behaviors (Figure S3-4a-c)(67). To reduce subjectivity, we have used uniform distributions bounded by ranges informed by

literature. For model calibration, too restricted ranges may underestimate the level of uncertainty around a parameter value, whereas in model selection, the proportion of passes is sensitive to the width of the range. Also, the comparison between the models with different numbers of sampled parameters has underlying difficulties. In more complex models, the passing parameter space may be underrepresented, giving rise to a local decrease in likelihood and wider parameter bounds (68). However, given the small number of parameters and large number of parameter combinations examined, the severity of under-sampling in this exercise is limited. Finally, caution should be taken in judging the likelihood of models based on the number of passes, as no correction is made for the differential complexity between the models.

The six models examined were chosen based on their proven performance in the literature (13, 15, 19). However, the models contain some inherent limitations. The limited persistence typical in highly seasonal models with (decomposed) ADE may in part result from the lack of stochasticity in the model (12, 23). Serotype persistence is also believed to be affected by the assumed symmetry in transmission rate and or virulence between serotypes (17). We indeed observe less wild fluctuations upon the inclusion of asymmetry and a consequential increase in the fit of models with ADE (Figure S3-4b). Further, the inclusion of explicit vector dynamics has been found to increase the robustness of the system to changes in cross-immunity and ADE parameters, resulting in a larger parameter space with regular (1-2 year inter-epidemic periods) dynamics and moderate amplitude fluctuations (69). Therefore, including vector population dynamics may affect the quantitative conclusions of this study, especially when high seasonal fluctuations are assumed. The inclusion of explicit vector dynamics

would further allow for a more quantitative assessment of required control efforts, which will be a focus of future work.

Lastly, no long-term variation in parameter values was taken into account. Yet, fertility rates have decreased and life expectancy has gone up in most dengue endemic countries over the last decades (70). Cummings et al. showed that a decrease in birth rate might result in a decrease in the force of infection and increase in the mean age of infection (71). The same authors also demonstrate that this demographic shift may have induced prolonged multiannual oscillations (71). Additionally, vector control has intensified over the years with varying success (72). The on-and-off vector control is likely to act as a distorting factor in the estimation of the role of seasonality, as the climate driven signal in the incidence data may be weakened by these control measures. Therefore, ignoring on-going control measures may have had some influence in our model selection and predictions. Further research will focus on disentangling the complex interplay of dengue dynamics with non-stationary factors such as intervention efforts, demography and climate.

With the expanding spatial spread of dengue and the increase of frequency and size of outbreaks, understanding dengue disease dynamics and the consequences of control efforts (*e.g.,* a near-future vaccine introduction) has become critically important. Indeed, the present work stresses that ignoring model uncertainty in prediction exercises can skew the impact of vector control substantially. It also emphasizes that the wider use of improved data-model assimilation approaches, such as the POM method, could play a significant role in overcoming this problem.

3.7 Acknowledgments

We would like to thank the University of Notre Dame's Center for Research Computation for high performance computation support, Vijay Gupta for his advice on the use of spectral density techniques, Sarah Lukens for her help in designing the principal component analysis and Alexandra Jilkine for verification of our initial simulation results of the 4-infection models.

3.8 References

1. World Health Organization (2012) Dengue guidelines for diagnosis, treatment, prevention and control. 2009. *WHO, Geneva, Switzerland*

2. Calisher CH*, et al* (1989) Antigenic relationships between flaviviruses as determined by cross-neutralization tests with polyclonal antisera. *J Gen Virol* 70(1): 37-43.

3. Kalayanarooj S (1999) Standardized clinical management: Evidence of reduction of dengue haemorrhagic fever case-fatality rate in thailand. *Dengue Bull* 23: 10-17.

4. Murrell S, Wu SC & Butler M (2011) Review of dengue virus and the development of a vaccine. *Biotechnol Adv* 29(2): 239-247.

5. Nisalak A*, et al* (2003) Serotype-specific dengue virus circulation and dengue disease in bangkok, thailand from 1973 to 1999. *Am J Trop Med Hyg* 68(2): 191-202.

6. Campione-Piccardo J, Ruben M, Vaughan H & Morris-Glasgow V (2003) Dengue viruses in the caribbean. twenty years of dengue virus isolates from the caribbean epidemiology centre. *West Indian Med J* 52(3): 191-198.

7. Cummings DAT*, et al* (2004) Travelling waves in the occurrence of dengue haemorrhagic fever in thailand. *Nature* 427(6972): 344-347.

8. Andraud M, Hens N, Marais C & Beutels P (2012) Dynamic epidemiological models for dengue transmission: A systematic review of structural approaches. *PLoS One* 7(11): e49085.

9. Halstead SB (1979) In vivo enhancement of dengue virus infection in rhesus monkeys by passively transferred antibody. *J Infect Dis* 140(4): 527-533.

10. Halstead SB (2014) Dengue antibody-dependent enhancement: Knowns and unknowns. *Microbiol Spectr* 2(6)

11. Gubler DJ (1998) Dengue and dengue hemorrhagic fever. *Clin Microbiol Rev* 11(3): 480.

12. Cummings DA, Schwartz IB, Billings L, Shaw LB & Burke DS (2005) Dynamic effects of antibody-dependent enhancement on the fitness of viruses. *Proc Natl Acad Sci U S A* 102(42): 15259-15264.

13. Ferguson N, Anderson R & Gupta S (1999) The effect of antibody-dependent enhancement on the transmission dynamics and persistence of multiple-strain pathogens. *Proc Natl Acad Sci U S A* 96(2): 790.

14. Schwartz IB, *et al* (2005) Chaotic desynchronization of multistrain diseases. *Phys Rev E Stat Nonlin Soft Matter Phys* 72(6 Pt 2): 066201.

15. Recker M, *et al* (2009) Immunological serotype interactions and their effect on the epidemiological pattern of dengue. *P Roy Soc B-Biol Sci* 276(1667): 2541.

16. Wikramaratna PS, Simmons CP, Gupta S & Recker M (2010) The effects of tertiary and quaternary infections on the epidemiology of dengue. *PLoS One* 5(8): e12347.

17. Mier-y-Teran-Romero L, Schwartz IB & Cummings DA (2013) Breaking the symmetry: Immune enhancement increases persistence of dengue viruses in the presence of asymmetric transmission rates. *J Theor Biol*

18. Adams B, *et al* (2006) Cross-protective immunity can account for the alternating epidemic pattern of dengue virus serotypes circulating in bangkok. *Proc Natl Acad Sci U S A* 103(38): 14234-14239.

19. Wearing HJ & Rohani P (2006) Ecological and immunological determinants of dengue epidemics. *Proc Natl Acad Sci U S A* 103(31): 11802.

20. Nagao Y & Koelle K (2008) Decreases in dengue transmission may act to increase the incidence of dengue hemorrhagic fever. *Proc Natl Acad Sci U S A* 105(6): 2238-2243.

21. Reich NG, *et al* (2013) Interactions between serotypes of dengue highlight epidemiological impact of cross-immunity. *J R Soc Interface* 10(86): 20130414.

22. Lourenço J & Recker M (2013) Natural, persistent oscillations in a spatial multi-strain disease system with application to dengue. *PLoS Comput Biol* 9(10): e1003308.

23. Aguiar M, Ballesteros S, Kooi BW & Stollenwerk N (2011) The role of seasonality and import in a minimalistic multi-strain dengue model capturing differences between primary and secondary infections: Complex dynamics and its implications for data analysis. *J Theor Biol* 289: 181-196.

24. Grimm V & Railsback SF (2012) Pattern-oriented modelling: A 'multi-scope' for predictive systems ecology. *Philos T Roy Soc B* 367(1586): 298-310.

25. Spear R & Hornberger G (1980) Eutrophication in peel Inlet—II. identification of critical uncertainties via generalized sensitivity analysis. *Water Res* 14(1): 43-49.

26. Hornberger G & Spear R (1980) Eutrophication in peel Inlet—I. the problem-defining behavior and a mathematical model for the phosphorus scenario. *Water Res* 14(1): 29-42.

27. Grimm V (1994) Mathematical models and understanding in ecology. *Ecol Model* 75: 641-651.

28. Grimm V*, et al* (1996) Pattern-oriented modelling in population ecology. *Sci Total Environ* 183(1): 151-166.

29. Mitchell KM, Mutapi F, Savill NJ & Woolhouse ME (2011) Explaining observed infection and antibody age-profiles in populations with urogenital schistosomiasis. *PLoS Comput Biol*

30. Mitchell KM, Mutapi F, Savill NJ & Woolhouse ME (2012) Protective immunity to schistosoma haematobium infection is primarily an anti-fecundity response stimulated by the death of adult worms. *Proc Natl Acad Sci U S A* 109(33): 13347-13352.

31. Coudeville L & Garnett GP (2012) Transmission dynamics of the four dengue serotypes in southern vietnam and the potential impact of vaccination. *PloS One* 7(12): e51244.

32. Thai KT*, et al* (2010) Dengue dynamics in binh thuan province, southern vietnam: Periodicity, synchronicity and climate variability. *PLoS Negl Trop Dis* 4(7): e747.

33. Cuong HQ*, et al* (2013) Spatiotemporal dynamics of dengue epidemics, southern vietnam. *Emerg Infect Dis* 19(6): 945--953.

34. Nishiura H (2006) Mathematical and statistical analyses of the spread of dengue. *Dengue Bull* 30: 51.

35. Johansson MA, Dominici F & Glass GE (2009) Local and global effects of climate on dengue transmission in puerto rico. *PLoS Negl Trop Dis* 3(2): e382.

36. Mohd-Zaki AH, Brett J, Ismail E & L'Azou M (2014) Epidemiology of dengue disease in malaysia (2000–2012): A systematic literature review. *PLoS Negl Trop Dis* 8(11): e3159.

37. Limkittikul K, Brett J & L'Azou M (2014) Epidemiological trends of dengue disease in thailand (2000–2011): A systematic literature review. *PLoS Negl Trop Dis* 8(11): e3241.

38. L'Azou M, Taurel A, Flamand C & Quénel P (2014) Recent epidemiological trends of dengue in the french territories of the americas (2000–2012): A systematic literature review. *PLoS Negl Trop Dis* 8(11): e3235.

39. Bravo L, Roque VG, Brett J, Dizon R & L'Azou M (2014) Epidemiology of dengue disease in the philippines (2000–2011): A systematic literature review. *PLoS Negl Trop Dis* 8(11): e3027.

40. L'Azou M, Brett J, Marsh G & Sarti E (2014) Reviewing the literature for epidemiological trends of dengue disease: Introduction to a series of seven national systematic literature reviews. *PLoS Negl Trop Dis* 8(11): e3260.

41. Dantés HG, Farfán-Ale JA & Sarti E (2014) Epidemiological trends of dengue disease in mexico (2000–2011): A systematic literature search and analysis. *PLoS Negl Trop Dis* 8(11): e3158.

42. Su GL (2008) Correlation of climatic factors and dengue incidence in metro manila, philippines. *Ambio* 37(4): 292-294.

43. Chau TNB*, et al* (2009) Dengue virus infections and maternal antibody decay in a prospective birth cohort study of vietnamese infants. *J Infect Dis* 200(12): 1893-1900.

44. Gibbons RV*, et al* (2007) Analysis of repeat hospital admissions for dengue to estimate the frequency of third or fourth dengue infections resulting in admissions and dengue hemorrhagic fever, and serotype sequences. *Am J Trop Med Hyg* 77(5): 910-913.

45. Welch PD (1967) The use of fast fourier transform for the estimation of power spectra: A method based on time averaging over short, modified periodograms. *IEEE T Acoust Speech* 15(2): 70-73.

46. Bloomfield P (2004) *Fourier analysis of time series: an introduction,* (John Wiley & Sons,

47. Recker M, Pybus OG, Nee S & Gupta S (2007) The generation of influenza outbreaks by a network of host immune responses against a limited set of antigenic types. *Proc Natl Acad Sci U S A* 104(18): 7711.

48. Stocki R (2005) A method to improve design reliability using optimal latin hypercube sampling. *Comput Assis Mech Eng Sci* 12(4): 393.

49. Gubler DJ, Suharyono W, Tan R, Abidin M & Sie A (1981) Viraemia in patients with naturally acquired dengue infection. *Bull World Health Organ* 59(4): 623-630.

50. Ferguson NM, Donnelly CA & Anderson RM (1999) Transmission dynamics and epidemiology of dengue: Insights from age–stratified sero–prevalence surveys. *Philos T Roy Soc B* 354(1384): 757.

51. Lourenco J & Recker M (2010) Viral and epidemiological determinants of the invasion dynamics of novel dengue genotypes. *PLoS Negl Trop Dis* 4(11): e894.

52. Alfaro-Murillo JA, Towers S & Feng Z (2013) A deterministic model for influenza infection with multiple strains and antigenic drift. *Journal of Biological Dynamics* 7(1): 199-211.

53. Kramer-Schadt S, Revilla E, Wiegand T & Breitenmoser U (2004) Fragmented landscapes, road mortality and patch connectivity: Modelling influences on the dispersal of eurasian lynx. *J Appl Ecol* 41(4): 711-723.

54. Toni T, Welch D, Strelkowa N, Ipsen A & Stumpf MP (2009) Approximate bayesian computation scheme for parameter inference and model selection in dynamical systems. *J R Soc Interface* 6(31): 187-202.

55. Saltelli A*, et al* (2008) *Global sensitivity analysis: the primer,* (John Wiley & Sons,

56. Diekmann O, Heesterbeek J & Metz J (1990) On the definition and the computation of the basic reproduction ratio R 0 in models for infectious diseases in heterogeneous populations. *J Math Biol* 28(4): 365-382.

57. Van den Driessche P & Watmough J (2002) Reproduction numbers and sub-threshold endemic equilibria for compartmental models of disease transmission. *Math Biosci* 180(1): 29-48.

58. Diekmann O & Heesterbeek JAP (2000) *Mathematical epidemiology of infectious diseases: model building, analysis and interpretation,* (Wiley, West Sussex), pp 320.

59. Billings L*, et al* (2007) Instabilities in multiserotype disease models with antibody-dependent enhancement. *J Theor Biol* 246(1): 18-27.

60. Von Bertalanffy L (1968) *General system theory: Foundations, development, applications,* (George Braziller New York,

61. Beven K (2006) A manifesto for the equifinality thesis. *J Hydrol* 320(1): 18-36.

62. Singh BK, Savill NJ, Ferguson NM, Robertson C & Woolhouse MEJ (2010) Rapid detection of pandemic influenza in the presence of seasonal influenza. *BMC Public Health* 10(1): 726.

63. Pedersen EM, Stolk WA, Laney SJ & Michael E (2009) The role of monitoring mosquito infection in the global programme to eliminate lymphatic filariasis. *Trends Parasitol* 25(7): 319.

64. Koelle K, Rodo X, Pascual M, Yunus M & Mostafa G (2005) Refractory periods and climate forcing in cholera dynamics. *Nature* 436(7051): 696-700.

65. Topping CJ, Dalkvist T & Grimm V (2012) Post-hoc pattern-oriented testing and tuning of an existing large model: Lessons from the field vole. *PloS One* 7(9): e45872.

66. Spear RC (1997) Large simulation models: Calibration, uniqueness and goodness of fit. *Environ Modell Softw* 12(2): 219-228.

67. Beck M (1987) Water quality modeling: A review of the analysis of uncertainty. *Water Resour Res* 23(8): 1393-1442.

68. Dilks DW & James RT (2011) Parameter uncertainty in a highly parameterized model of lake okeechobee. *Lake Reserv Manage* 27(4): 376-389.

69. Hu K*, et al* (2012) The effect of antibody-dependent enhancement, cross immunity, and vector population on the dynamics of dengue fever. *J Theor Biol*

70. The World Bank (2011) *World Development Indicators 2011,* Washington, D.C. USA),

71. Cummings DA*, et al* (2009) The impact of the demographic transition on dengue in thailand: Insights from a statistical analysis and mathematical modeling. *PLoS Med* 6(9): e1000139.

72. Guzman MG*, et al* (2010) Dengue: A continuing global threat. *Nat Rev Microbiol* 8: S7-S16.

3.9 Supporting tables and figure

Figure S3-1: Outcome measures plane plots for the symmetric 2-infection (a), asymmetric 2-infection (b) and symmetric 4-infection model (c). Analysis of the parameter space of each model structure (with ADE=antibody dependent enhancement, CI=cross-immunity) for seasonality (β_1) and the basic reproduction number (R_0). From top to bottom, outcomes are measured with respect to (A) mean inter-peak period, (B) presence of multi-annual signal (red = present, blue = absent), (C) duration of serotype replacement, (D) single serotype emergence and (E) absence of phase-locking (red = absent, blue = present). (Pages 104- 106)

a

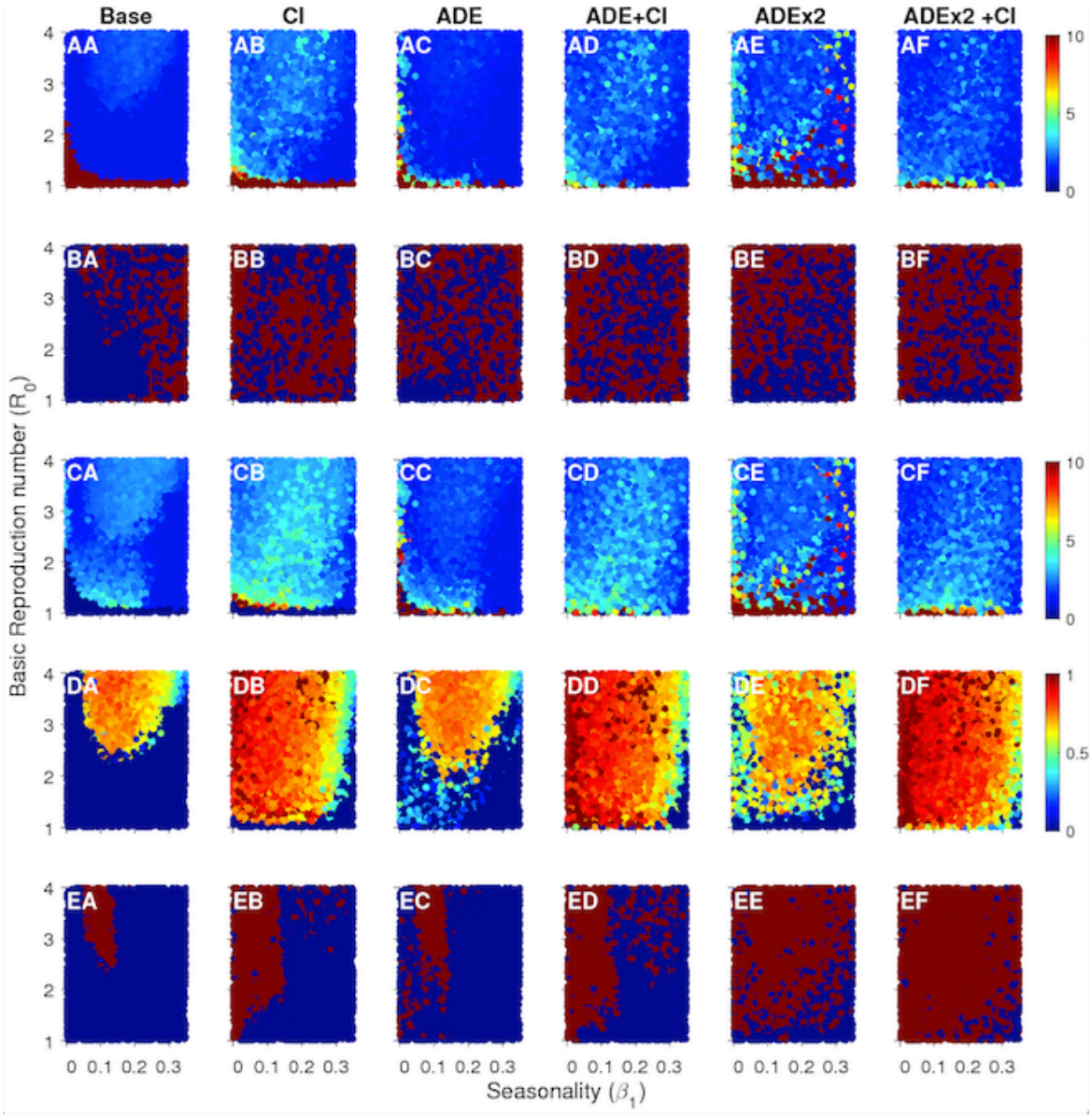
Base
CI
ADE
ADE+CI
ADEx2
ADEx2 +CI
AA
AB
AC
AD
AE
AF
BA
BB
BC
BD
BE
BF
CA
CB
CC
CD
CE
CF
DA
DB
DC
DD
DE
DF
EA
EB
EC
ED
EE
EF
Basic Reproduction number (R_0)
Seasonality (β_1)
0 0.1 0.2 0.3
1
2
3
4
10
5
0
1
0.5
0

b

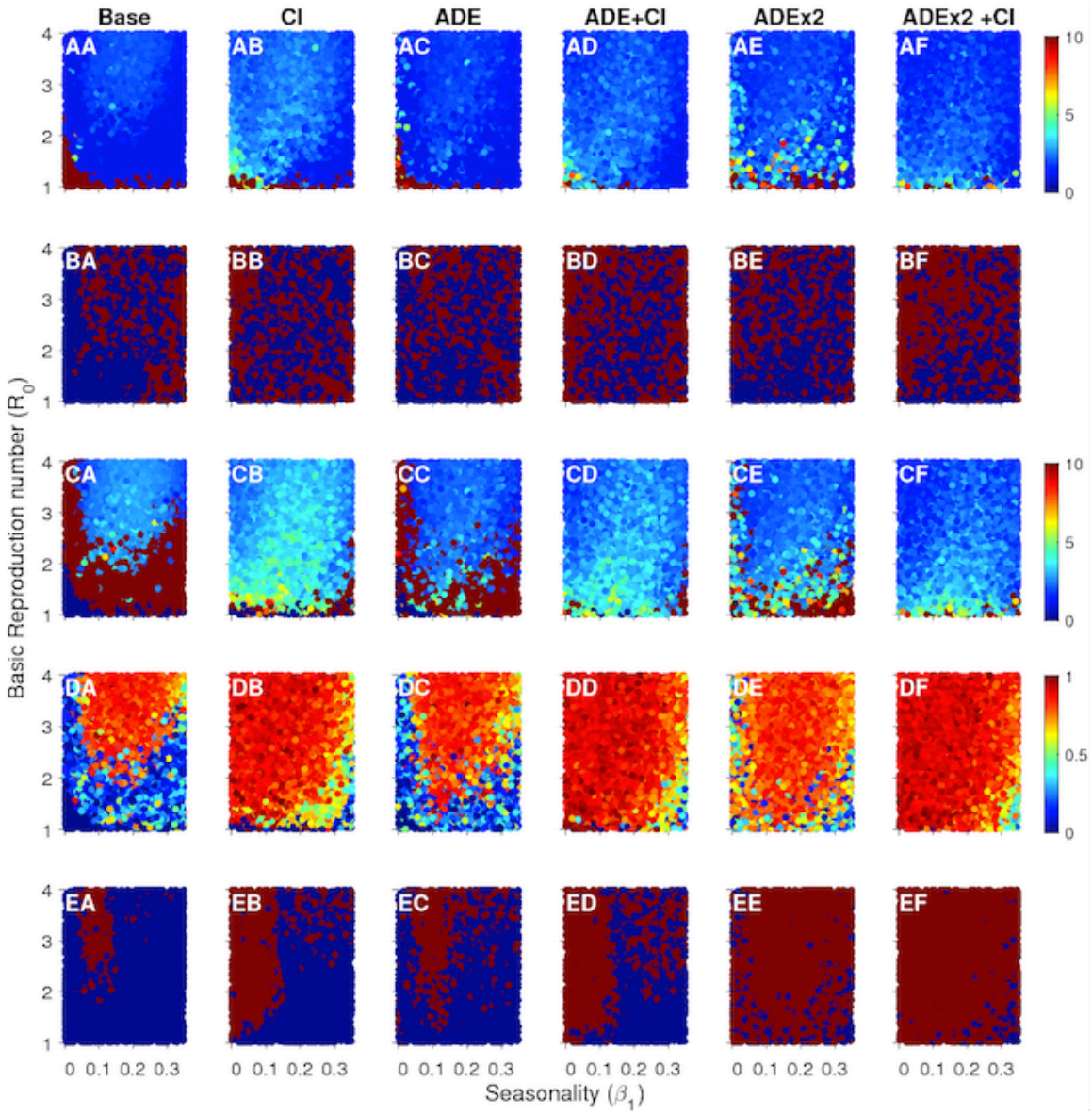
Base
CI
ADE
ADE+CI
ADEx2
ADEx2 +CI
AA
AB
AC
AD
AE
AF
BA
BB
BC
BD
BE
BF
CA
CB
CC
CD
CE
CF
DA
DB
DC
DD
DE
DF
EA
EB
EC
ED
EE
EF
Basic Reproduction number (R_0)
Seasonality (β_1)
0 0.1 0.2 0.3
1
2
3
4
0
5
10
0.5

c

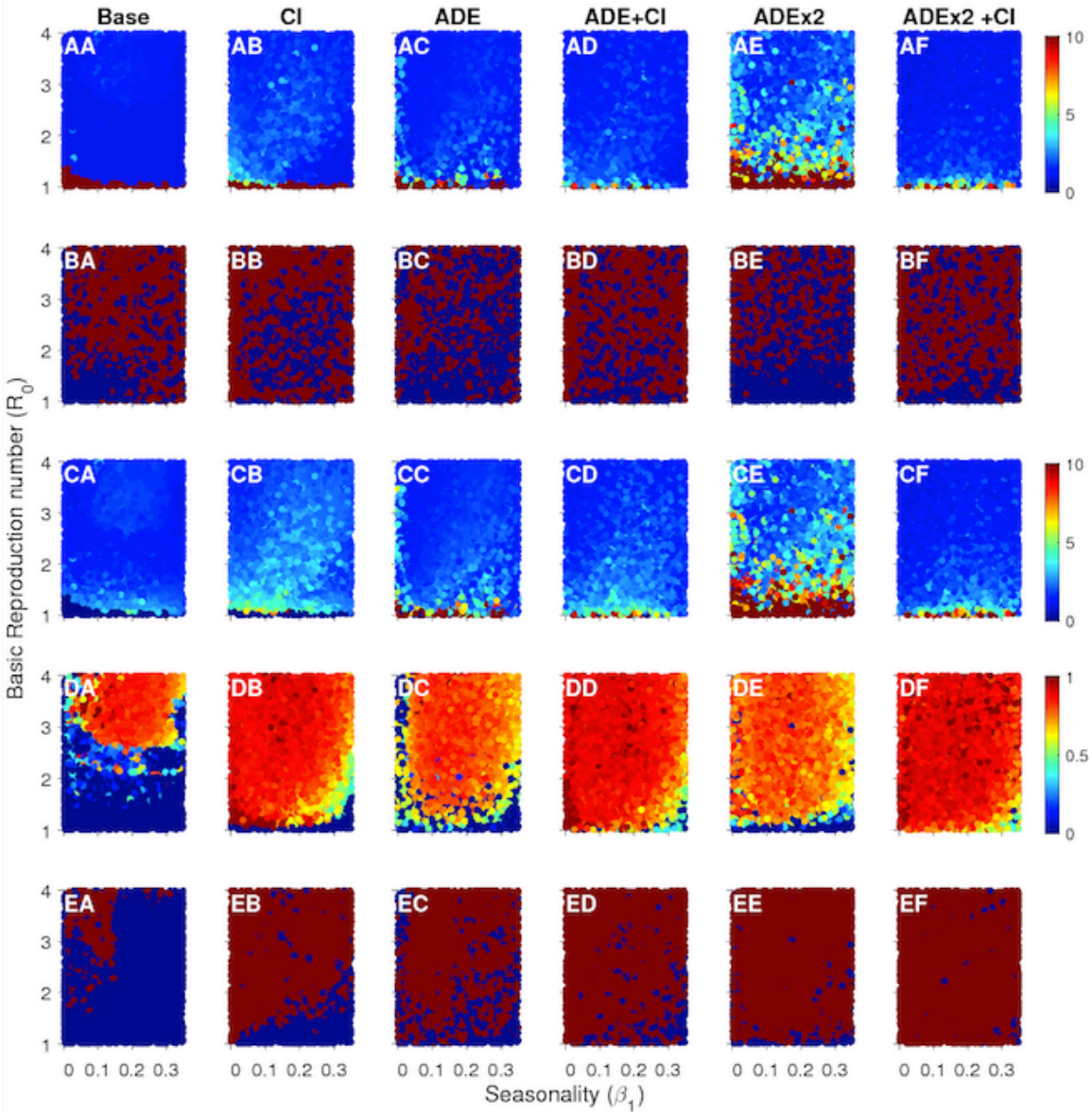
Base
CI
ADE
ADE+CI
ADEx2
ADEx2 +CI
AA
AB
AC
AD
AE
AF
BA
BB
BC
BD
BE
BF
CA
CB
CC
CD
CE
CF
DA
DB
DC
DD
DE
DF
EA
EB
EC
ED
EE
EF
Basic Reproduction number (R_0)
Seasonality (β_1)
0 0.1 0.2 0.3
1
2
3
4
0
5
10
0.5

Figure S3-2: Model parameter distributions for the asymmetric 2-infection (a) and symmetric 4-infection model (b). Parameter distributions for passing parameter sets (G) for different model hypotheses (with ADE=antibody dependent enhancement, CI=cross-immunity). The vertical lines depict the median values for each distribution with the colors indicating the corresponding model hypothesis. (Pages 108-109)

a

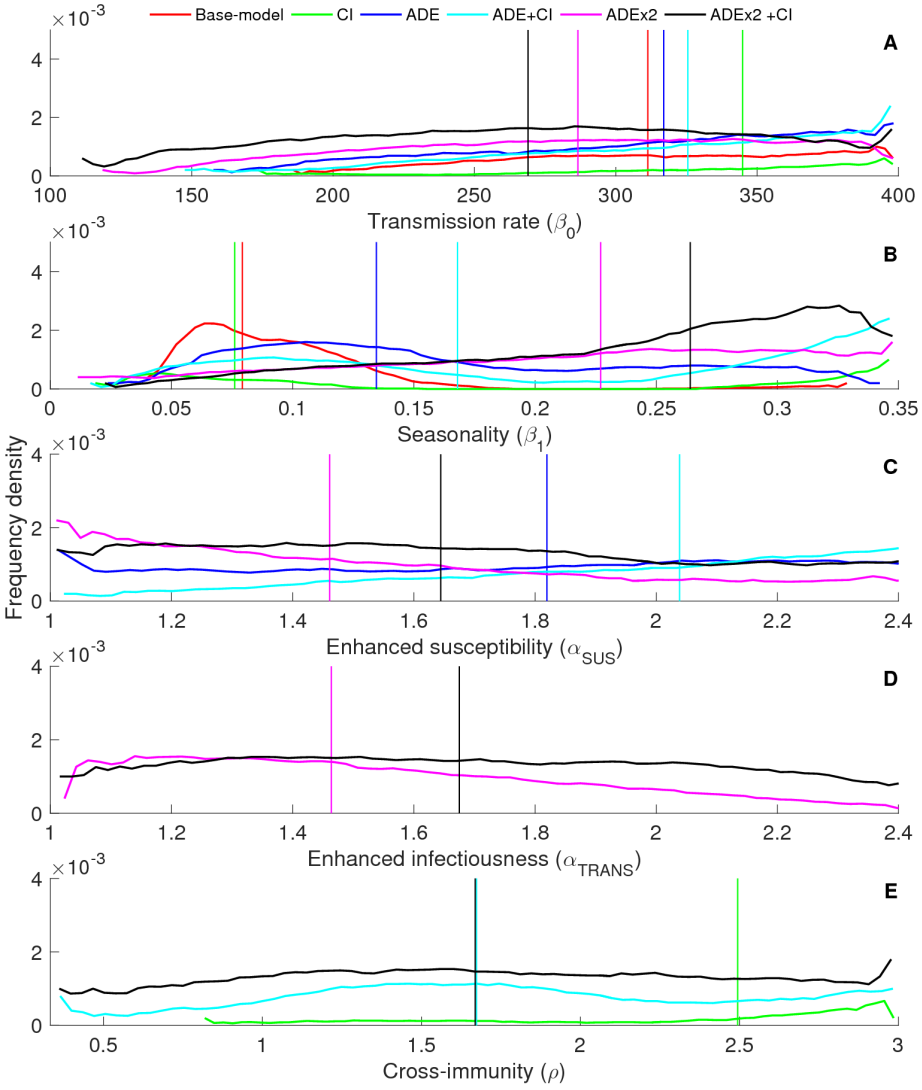
Base-model
CI
ADE
ADE+CI
ADEx2
ADEx2 +CI
A
B
C
D
E
Transmission rate (β_0)
Seasonality (β_1)
Enhanced susceptibility (α_{SUS})
Enhanced infectiousness (α_{TRANS})
Cross-immunity (ρ)
Frequency density
$\times 10^{-3}$

b

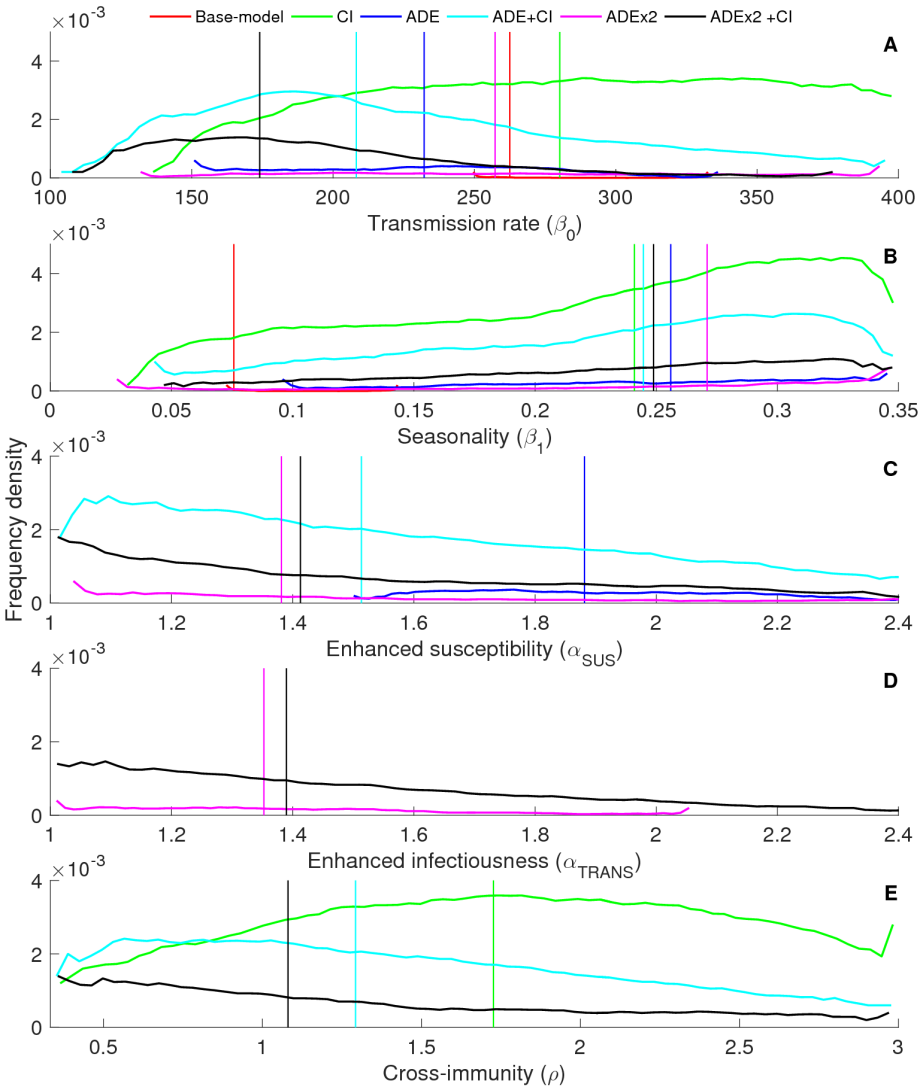
Base-model
CI
ADE
ADE+CI
ADEx2
ADEx2 +CI
A
B
C
D
E
Transmission rate (β_0)
Seasonality (β_1)
Enhanced susceptibility (α_{SUS})
Enhanced infectiousness (α_{TRANS})
Cross-immunity (ρ)
Frequency density
$\times 10^{-3}$

Figure S3-3: Correlation matrix full model for the symmetric 2-infection (a), asymmetric 2-infection (b) and symmetric 4-infection model (c). Correlation between passing parameters in full model (ADEx2+CI) with red numbers depicting a significant correlation coefficient. The respective parameter distributions are shown on the diagonal. (Pages 111-112)

a

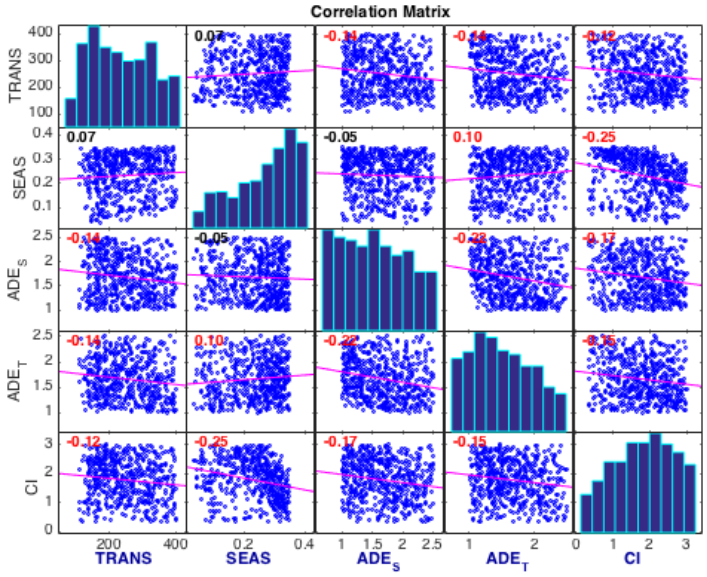
Correlation Matrix
TRANS
SEAS
ADE_S
ADE_T
CI
0.07
-0.11
-0.14
-0.12
0.07
-0.05
0.10
-0.25
-0.14
-0.05
-0.23
-0.17
-0.14
0.10
-0.22
-0.15
-0.12
-0.25
-0.17
-0.15

b

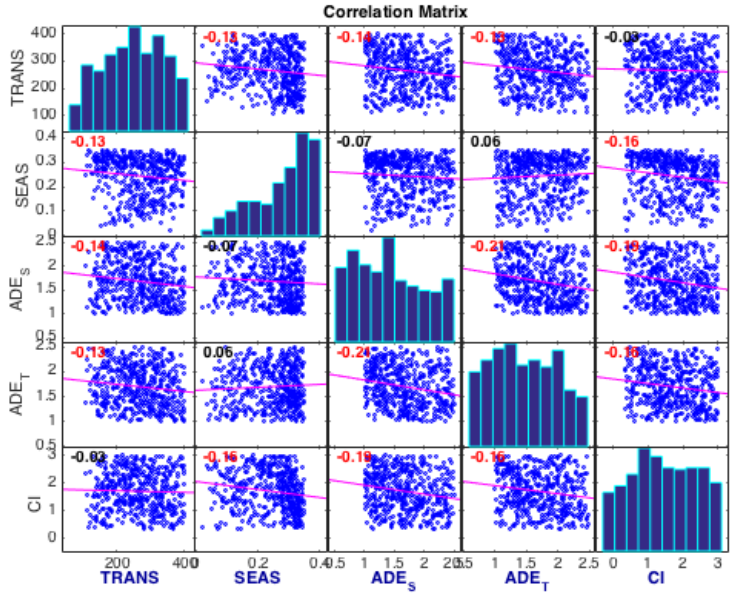
Correlation Matrix
TRANS
SEAS
ADE_S
ADE_T
CI
-0.13
-0.14
-0.12
-0.08
-0.13
-0.07
0.06
-0.16
-0.14
-0.07
-0.21
-0.13
0.06
-0.24
-0.13
-0.02
-0.16
-0.19
-0.16

c

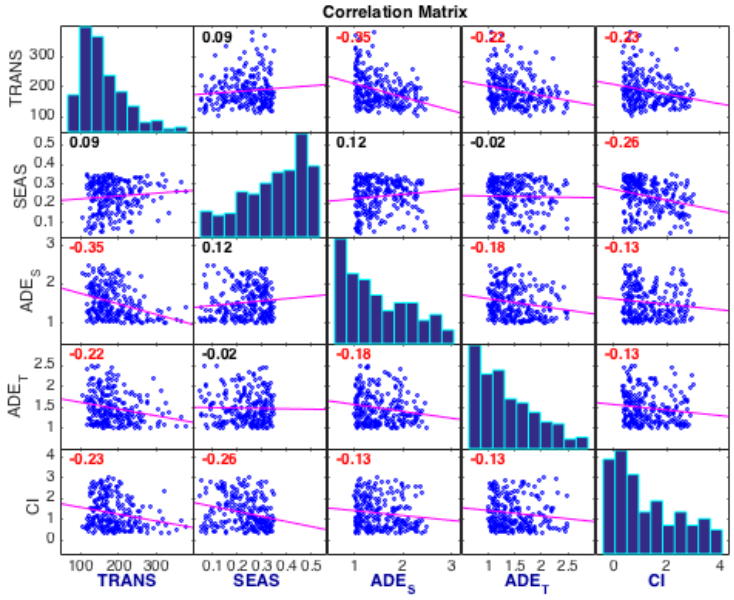
Correlation Matrix
TRANS
SEAS
ADE_S
ADE_T
CI
0.09
-0.35
-0.22
-0.23
0.09
0.12
-0.02
-0.26
-0.35
0.12
-0.18
-0.13
-0.22
-0.02
-0.18
-0.13
-0.23
-0.26
-0.13
-0.13
100 200 300
0.1 0.2 0.3 0.4 0.5
1 2 3
1 1.5 2 2.5
0 2 4

Figure S3-4: Qualitative comparison observed dengue case data and passing model simulations for the symmetric 2-infection (a), asymmetric 2-infection (b) and symmetric 4-infection model (c). Qualitative comparison between observed dengue incidence data and model simulations at median levels of seasonal forcing. Dengue incidence data from Trinidad and Tobago (1997-2009) were duplicated for comparison with model simulations (A). The dotted vertical lines indicate the length of the original dataset. Other parameter values are derived at random from the passing parameter distribution G with: (a) the symmetric 2-infection model: (A) β_0=344, β_1 =0.1, α_{SUS} =1, α_{TRANS} =1, ρ=NA (B), β_0=204, β_1 =0.06, α_{SUS} =1, α_{TRANS} =1, ρ=2.8 (C), β_0=240, β_1 =0.11, α_{SUS} =1.28, α_{TRANS} =1, ρ=NA (D), β_0=276, β_1 =0.05, α_{SUS} =1.64, α_{TRANS} =1, ρ=2.0 (E), β_0=228, β_1 = 0.16, α_{SUS} =1.05, α_{TRANS} =2.23, ρ=NA (F) and β_0=220, β_1 =0.12, α_{SUS} =1.61, α_{TRANS} =1.39, ρ=2.37 (G). (b) asymmetric 2-infection model: (A)β_0=252, β_1 =0.11, α_{SUS} =1, α_{TRANS} =1, ρ=NA (B), β_0=384, β_1 =0.24, α_{SUS} =1, α_{TRANS} =1, ρ=1.5 (C), β_0=323, β_1 =0.26, α_{SUS} =2.23, α_{TRANS} =1, ρ=NA (D), β_0=279, β_1 =0.3, α_{SUS} =1.86, α_{TRANS} =1.26, ρ=2.0 (E), β_0=228, β_1 = 0.16, α_{SUS} =1.05, α_{TRANS} =2.23, ρ=NA (F) and β_0=327, β_1 =0.30, α_{SUS} =1.16, α_{TRANS} =1.54, ρ=2.35 (G). (c) symmetric 4-infection model: (A)β_0=249, β_1 =0.07, α_{SUS} =1, α_{TRANS} =1, ρ=NA (B), β_0=308, β_1 =0.29, α_{SUS} =1, α_{TRANS} =1, ρ=1.26 (C), β_0=161, β_1 =0.09, α_{SUS} =2.08, α_{TRANS} =1, ρ=NA (D), β_0=188, β_1 =0.13, α_{SUS} =2.17, α_{TRANS} =1, ρ=1.0 (E), β_0=198, β_1 = 0.17, α_{SUS} =1.12, α_{TRANS} =1.40, ρ=NA (F) and β_0=125, β_1 =0.29, α_{SUS} =1.90, α_{TRANS} =1.68, ρ=1.04 (G). (with β_0 = mean transmission rate, β_1 = seasonal forcing, α_{SUS} = susceptibility enhancement, α_{TRANS} = transmissibility enhancement, ρ = 1/duration of cross-immunity) (Pages 114-116)

a

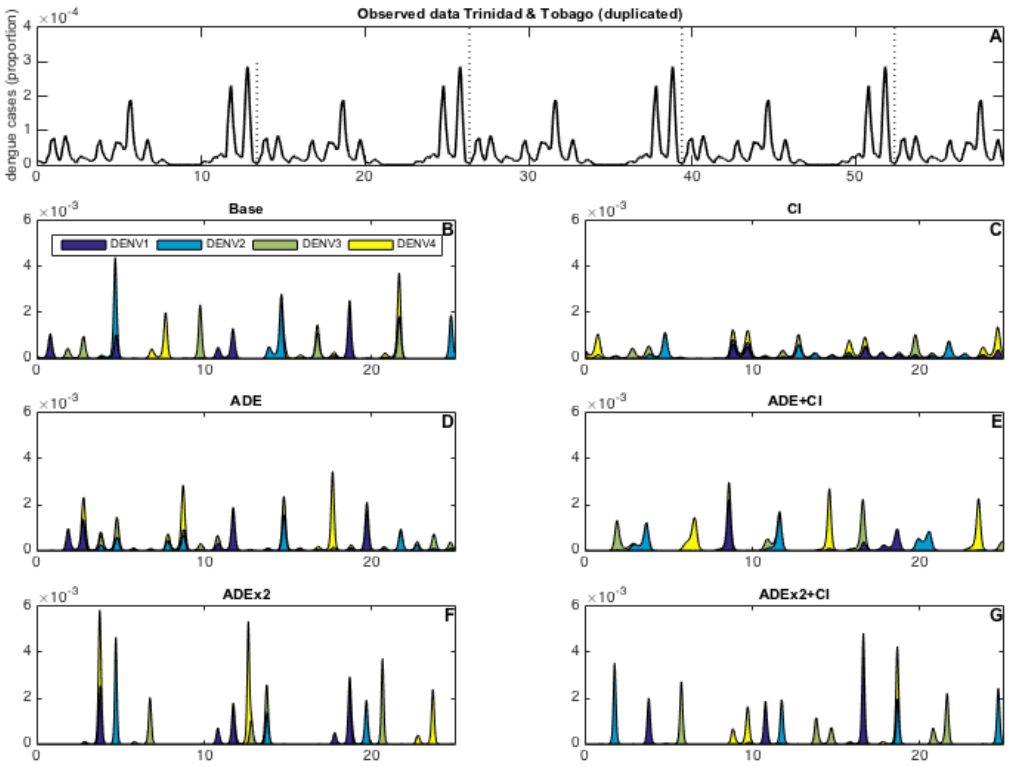
Observed data Trinidad & Tobago (duplicated)
dengue cases (proportion)
A
Base
B
DENV1
DENV2
DENV3
DENV4
CI
C
ADE
D
ADE+CI
E
ADEx2
F
ADEx2+CI
G

b

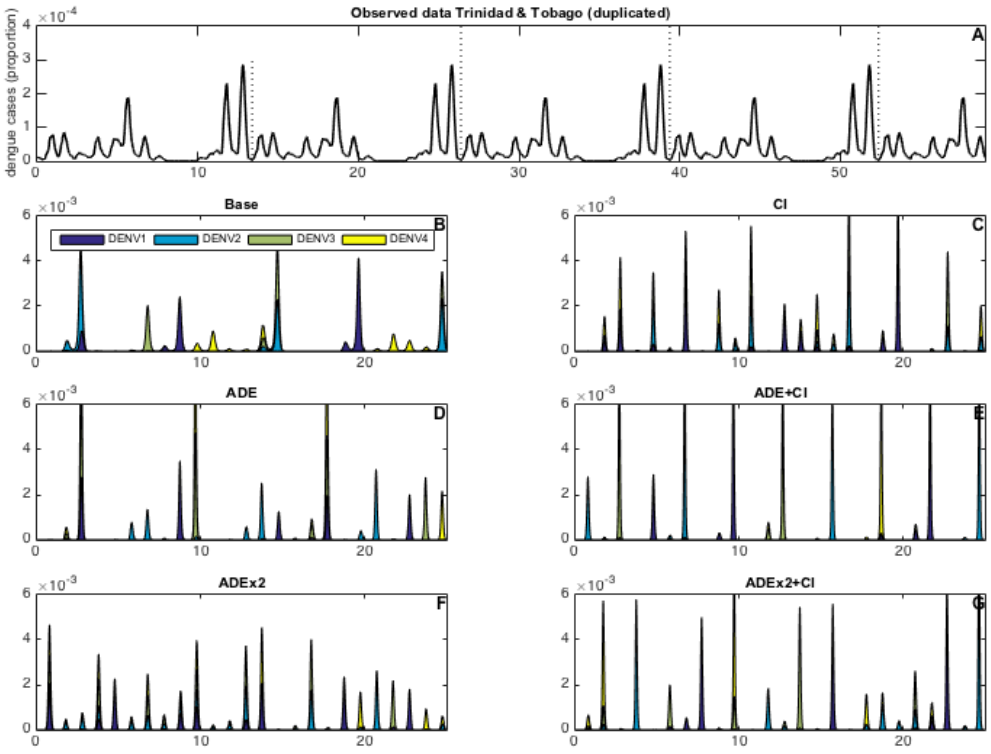
Observed data Trinidad & Tobago (duplicated)
dengue cases (proportion)
A
Base
DENV1
DENV2
DENV3
DENV4
B
CI
C
ADE
D
ADE+CI
E
ADEx2
F
ADEx2+CI
G

c

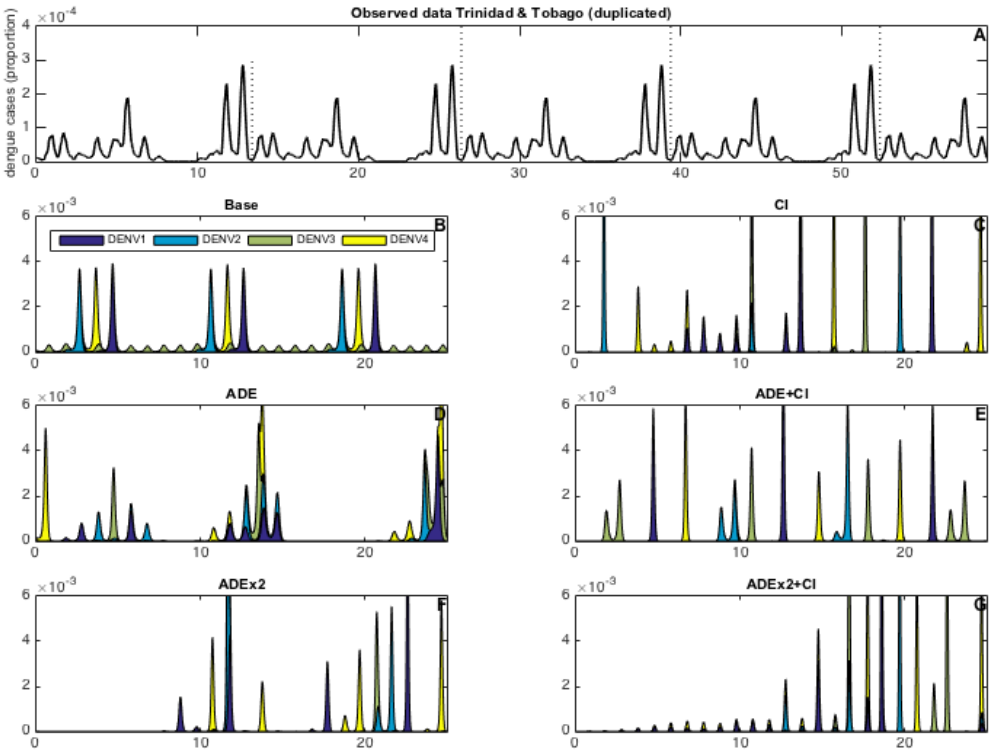
Observed data Trinidad & Tobago (duplicated)
dengue cases (proportion)
A
Base
DENV1
DENV2
DENV3
DENV4
B
CI
C
ADE
D
ADE+CI
E
ADEx2
F
ADEx2+CI
G

Figure S3-5: Principal component analysis for the asymmetric 2-infection (a) and symmetric 4-infection model (b). Principal component analysis of passing parameter space (G) of the full model (ADEx2+CI). The pie charts show the contribution of the parameters to each component. (Page 118)

a

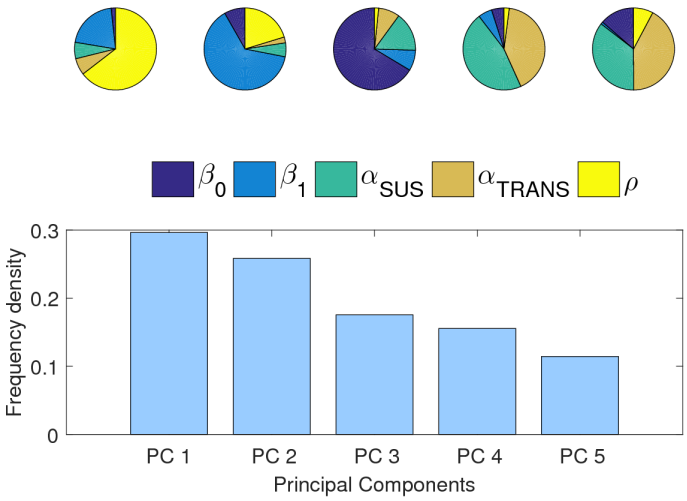
β_0 β_1 α_{SUS} α_{TRANS} ρ
Frequency density
0.3
0.2
0.1
0
PC 1
PC 2
PC 3
PC 4
PC 5
Principal Components

b

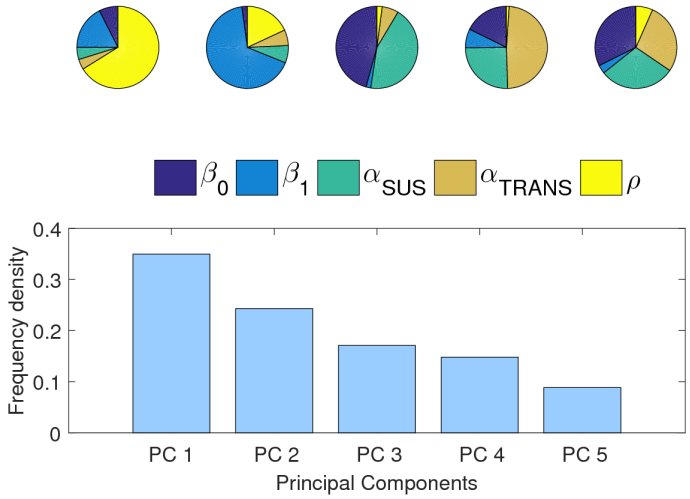
β_0 β_1 α_{SUS} α_{TRANS} ρ
Frequency density
0.4
0.3
0.2
0.1
0
PC 1
PC 2
PC 3
PC 4
PC 5
Principal Components

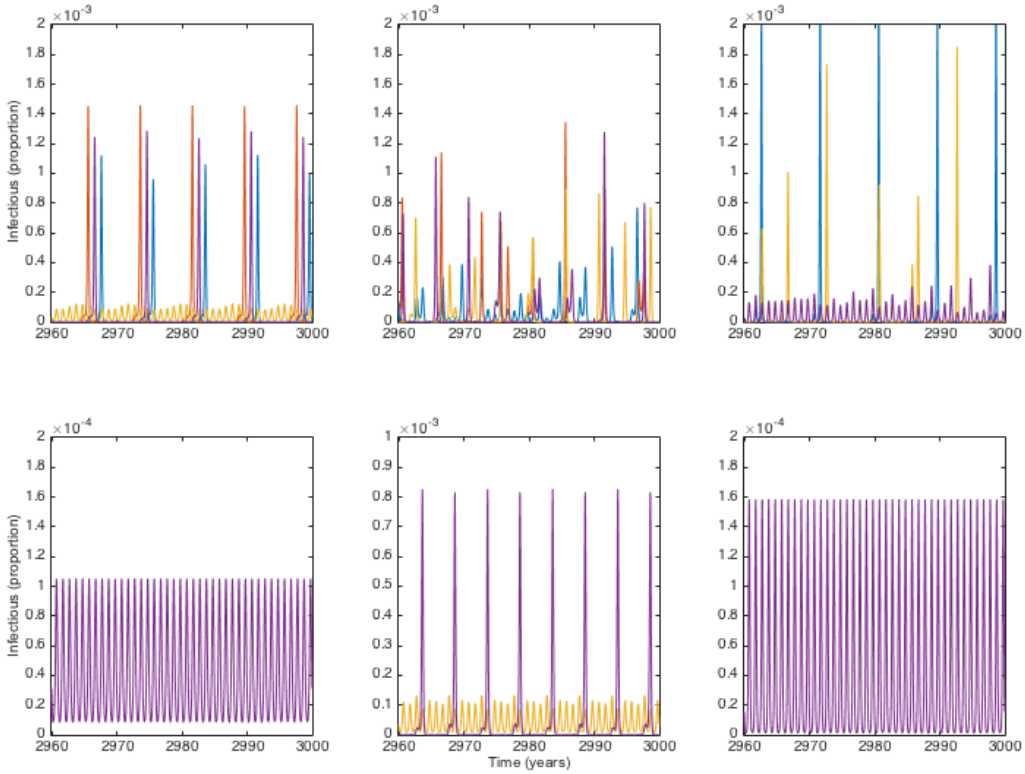

Figure S3-6: Comparative model simulations of 4-infection base-model with and without concurrent infections. Model simulations at passing parameter sets of the 4-infection base-model without concurrent infections (top row) and with concurrent infection (bottom row). The colors indicate different serotypes. Parameter values are: (left) β_0=249, β_1 =0.07, α_{SUS} =1, α_{TRANS} =1, ρ=NA (middle), β_0=333, β_1 =0.07, α_{SUS} =1, α_{TRANS} =1, ρ=NA (right), β_0=263, β_1 =0.14, α_{SUS} =1, α_{TRANS} =1, ρ=NA

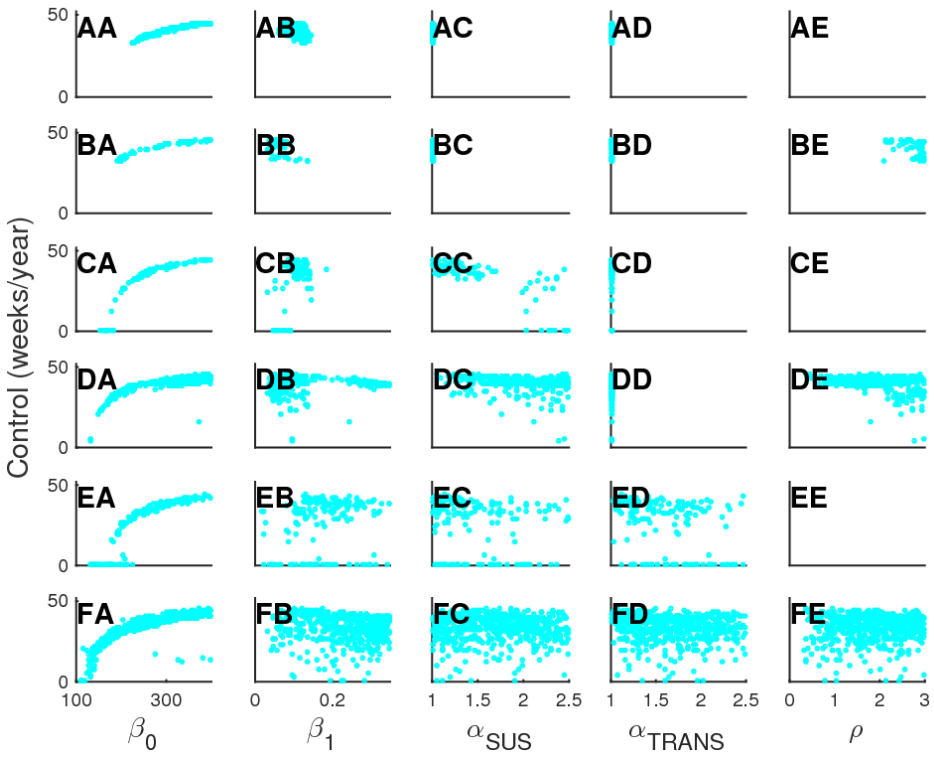

Figure S3-7: Vulnerability to control as a function of model parameters. Required duration (weeks/year) for achieving successful control is shown with respect to fitted model parameters. Different model hypotheses are (from top to bottom): base (A), CI (B), ADE (C), ADE+CI (D), ADEx2 (E), and ADEx2+CI (F), with ADE=antibody dependent enhancement, CI=cross-immunity. Model parameters assessed are (from left to right): (A) the transmission rate (β_0), (B) seasonality (β_1), (C) enhanced susceptibility (α_{SUS}), (D) enhanced infectiousness (α_{TRANS}), and (E) cross-immunity (ρ).

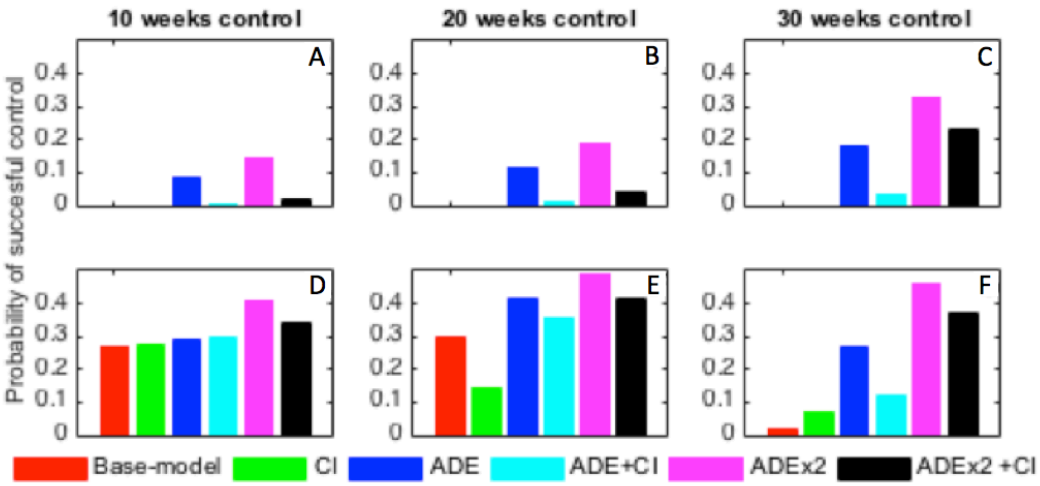

Figure S3-8: Effect of import factor on vulnerability to control. Probability of successful control (a maximum of 1 outbreak during 30 years) given different durations (10, 20, and 30 weeks/year) of consecutive control (temporary reduction of transmission: $\beta_0(1-90\%)$ for different model hypotheses (with ADE=antibody dependent enhancement, CI=cross-immunity). The probability is defined as the proportion of the passing parameter sets (G_i) that reach successful control. Here i refers to the six models, shown by the individual keys. The top row (A, B, and C) shows the results for the default import rate of 1e-10. The bottom row (D, E, and F) shows results for a decreased import rate of 1e-12. The probability of successful control for the Base-model and the CI-model in the default scenario are zero, as can also be seen in Figure 3-6.

TABLE S3-1:

SENSITIVITY ANALYSIS OF MODEL FITS ON ALL MODEL

PARAMETERIZATIONS INCLUDING INTERACTIONS

Table available in Supplemental_S3-1.xlsx

Logistic regression model coefficients with pattern match as binary response variables and the parameters (scaled 0-1) as independent variables. Red are high coefficient values (>|3|).

CHAPTER 4:

LEAVE OR DIE: MODEL-BASED ANALYSIS OF EXPERIMENTAL HUT DATA ELUCIDATES VOLATILE CHEMICAL EFFECTS ON AEDES AEGYPTI MOSQUITOES

Quirine A. ten Bosch, Fanny Castro-Llanos, Hortance Manda, Amy C. Morrison, John Grieco, Nicole L. Achee, T. Alex Perkins

4.1 Abstract

Background. – Insecticides used against *Aedes aegypti* and other disease vectors can elicit a multitude of effects on behavioral and bionomic traits, often in a dose-dependent fashion. Estimating the epidemiological impact of a product requires a thorough understanding of these different effects and how they interplay at different dosages. Volatile spatial repellent (SR) products come with an additional layer of complexity due to the potential for downstream effects in nearby premises. Here, we propose a statistical inference framework that provides a new tool to estimate these nuanced effects in a quantitative, probabilistic fashion.

Methods. – We fitted a continuous-time Markov chain model in a Bayesian framework to mark-release-recapture (MRR) data from an experimental hut study. We estimated the effects of two dosages of transfluthrin on *Aedes aegypti* repellency, expulsion, and knockdown in the hut where the product was applied, as well as

"downstream" effects in adjacent huts. We validated the framework by estimating parameters using simulated data, for which true parameter values were known.

Results. – The odds for female *Aedes aegypti* of being repelled from a treated hut (H_0) were increased at both dosages (low: 1.64, 95% highest density interval (HDI): 1.30-2.09; high: 1.35, CI: 1.04-1.67). The relative risk of exiting out of the treatment hut was reduced (RR: low: 0.70, HDI: 0.62-1.09; high: 0.70, HDI: 0.40-1.06), with this effect carrying over to as far as two huts away from the product (H_2) (RR: low: 0.79, HDI: 0.59-1.01; high: 0.66, HDI:0.50-0.87). Knockdown rates were increased in treatment as well as downstream huts, in particular under high dosage (RR: H_0: 8.37, HDI: 2.11-17.35; H_1: 1.39, HDI: 0.52-2.69; H_2: 2.22, HDI: 0.96-3.86).

Conclusion. – The novel statistical inference framework that we present is effective in elucidating multiple effects of volatile chemicals as well as their downstream effects. This offers a powerful tool for early selection of candidate product formulations worth advancing to larger, more costly epidemiological trials that are ultimately necessary for formal endorsement and widespread adoption of new products.

Keywords. – *Aedes aegypti*, Bayesian parameter estimation, Continuous-time Markov-chain models, Dengue, Transfluthrin, Vector control, Zika

4.2 Introduction

Insecticidal measures against adult mosquitoes have been used extensively in the control of mosquito-borne diseases (1). However, behavioral traits, such as outdoor and daytime biting, leave some disease vectors unaffected by traditional vector control tools such as insecticide treated nets (ITNs) and indoor residual spraying (IRS) (2). The

evolution of physiological resistance to insecticides (3) and behavioral adaptation (4, 5) also pose challenges for the effectiveness of insecticidal measures.

The effect of vector control products often goes beyond their lethal effects. ITNs can, in addition to their lethal effects, divert mosquitoes away and force them to take their blood meals on alternate hosts (6-8). Volatile chemicals such as transfluthrin and metofluthrin can also be delivered in high dosages and result in high lethality but they can likewise be used at lower dosages as "spatial repellents" (SRs) (9). SRs are designed specifically to reduce host-vector contact in a sub-lethal manner by repelling the mosquito from the environment where the product is applied (spatial repellency) and by interfering with host-seeking or blood-feeding behavior (irritancy) (9). These modes of action both on mosquito behavior and bionomic traits can have a concerted impact on disease transmission both on an individual and a community level (10-13).

Mark-release-recapture (MRR) experimental hut studies offer one way to measure repellency, irritancy, and lethality of products in a semi-natural field setting (14-17). MRR experiments in which mosquitoes, marked by release hut, are released in a configuration of multiple huts, have the potential to help elucidate downstream dosage and diversion effects. Studies such as these, however, have not yet provided the granularity required to disentangle distinct behavioral and bionomic effects. The primary challenge associated with the design and interpretation of these studies is that each mosquito is only observed once: when knocked down or when trapped in entry or exit traps. This leaves movement trajectories in between release and recapture locations unobserved, making it challenging to quantify the relative contributions of multiple

competing effects that could account for the observed data under a multitude of equally plausible scenarios.

Models used for the analysis of MRR data have a long history in ecology (18-22). Originally developed to estimate survival probabilities and population sizes (23), they are now increasingly being used to inform spatial processes (24). These models partition animal trajectories into states (e.g., breeding or foraging). When these states are reflected in the MRR data, multi-state MRR models account for the probability of the animal occupying any of the possible states at a given time. Given sufficient information (e.g., multiple sampling occasions) and appropriate model constrains (e.g., reducing the number of parameters), these models can be extended for parameter estimation in the presence of unobserved states (25). Bayesian methods are increasingly being used for these types of problems (26-28). These methods allow for formal treatment and quantification of parameter uncertainty, and they allow researchers to explicitly build on previous studies.

Here, we make a major advance in the technical capability to infer multiple nuanced effects of a vector control product on mosquito behavioral and bionomic traits by applying hierarchical Bayesian models to MRR studies performed in configurations of multiple experimental huts. We first demonstrate the accuracy of this approach using data simulated under the same experimental design as in our field experiments. We then show the dose-dependent effects on knockdown, repellency, and expulsion of *Ae. aegypti* in both treated and untreated huts. We discuss the potential use of this methodology to inform the projected impact and implementation of vector control tools.

4.3 Methods

4.3.1 Mosquitoes

Female *Aedes aegypti* test populations (F_{1}-$_{2}$ generations) of 5-7 days old were reared at the NAMRU-6 Iquitos Entomology laboratory following NAMRU-6 and USUHS protocols (29). Mosquitoes were non-blood fed but were provided with cotton soaked with sucrose solution until 24 hours before being released in the experimental huts. Prior to release, mosquitoes were marked with a fluorescent powder unique to the hut they will be released in.

4.3.2 Product

A pyrethroid insectide (transfluthrin) was applied to cotton at $1/16^{th}$ and $1/8^{th}$ dilutions of the field application rate (FAR): ($0.04g/m^2$). The solutions, prepared with acetone and neat material, were applied to the cotton using pipets to ensure complete absorption and accurate dosing. Control materials were treated with acetone alone. The cotton was applied to the interior walls of the huts using magnets and metal frames.

4.3.3 Experimental huts

A unique experimental hut design was used in which the five experimental huts were set up in a row design with the adjoining walls containing open eave gaps that create a continuum of indoor space (Figure 4-1). This design mimics a housing structure common to Iquitos - Peru and other dengue endemic areas. Each hut was 4 meters wide, 6 meters long and had 2 meter high sidewalls. They were equipped with two window exit traps and four door traps and the outermost huts had an additional three eave traps (14,

15). The study was performed at the Instituto Veterinario de Investigaciones in Iquitos Peru (73.2 °W, 7.3°S).

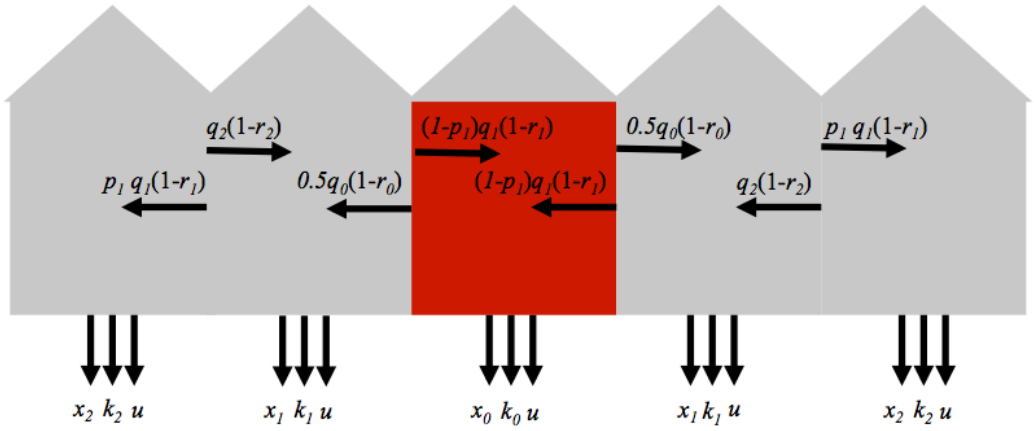

Figure 4-1: Illustration of experimental hut design and associated model parameters, with q = movement rate, p = proportion of between hut movement directed away from the treated hut, r = proportion of movement directed outdoors, $x = qr$ = exit rate, k = knock-down rate, and u = loss to follow-up rate. The red hut is where the SR or control treatment is applied. The subscripts indicate the distance from the treated hut.

4.3.4 Experiment

To quantify the spatial repellency effect of SR on *Ae. aegypti* under field conditions, an experimental hut study was performed as described in (30). The center hut (H_0) was treated with the SR product or the placebo. In each of the huts (H_0, H_{-1L}, H_{-1R}, H_{-2L}, H_{-2R}) there was a human host present under an untreated bed net to generate host-seeking cues and monitor knockdown. For each experiment 25 mosquitoes, marked according to release hut, were released inside each hut apart from the treatment hut (H_0) at 5.30 am. Exit-traps were checked every 30 minutes from 6 am until 6 pm and knockdown was monitored every hour within this time frame. At 6 pm, remaining mosquitoes were recaptured using aspirators recording their release and recapture location. The experiment was repeated five times for three different treatment schemes

(FAR 0, 1/8, 1/16). Collector teams were rotated between huts each sampling period to limit observer bias.

4.3.5 Model

Continuous-time Markov chain – A continuous-time Markov chain model was developed for the analysis of these data (31). Mosquitoes can occupy either one of five huts (transient states: $H_{2L}, H_{1L}, H_0, H_{1R}$, or H_{2R}) or have experienced one of fifteen events represented by the absorbing states: $X_{2L}, X_{1L}, X_0, X_{1R}$, or X_{2R} for the exit traps in each hut, $K_{2L}, K_{1L}, K_0, K_{1R}$, or K_{2R} for knockdown in each hut, and U_{2L}, U_{1L}, U_0, U_{1R}, or U_{2R} for those mosquitoes that are unaccounted for at the end of the experiment and are thus loss to follow-up at an unknown time point. The infinitesimal generator matrix $\boldsymbol{A}$ denotes the rates at which mosquitoes leave one state to move to the next, such that a_{ij} gives the rate at which a mosquito in state i moves to state j. These rates are assumed to be independent of time or previous trajectories and therefore the time spent in state i before leaving follows an exponential distribution with mean $1/a_i$. Note that the rates out of the absorbing states are zero and that, given symmetry in the system, the rates for hut 2L and 2R are equivalent, and similarly for 1L and 1R. Subscripts in $\boldsymbol{A}$ therefor indicate the distance from the treatment hut. **A** is defined as

$$\boldsymbol{A} = \begin{pmatrix} \boldsymbol{A}_H & \boldsymbol{A}_X & \boldsymbol{A}_K & \boldsymbol{A}_U \end{pmatrix}, \quad (1)$$

with

$$\boldsymbol{A}_H = \begin{pmatrix} -q_2(1-r_2)-q_2r_2-k_2 & q_2 & 0 & 0 & 0 \\ (1-p_1)(q_1)(1-r_1) & -q_1(1-r_1)-q_1r_1-k_1 & p_1q_1(1-r_1) & 0 & 0 \\ 0 & (1-p_0)q_0(1-r_0) & -q_0(1-r_0)-q_0r_0-k_0 & p_0q_0(1-r_0) & 0 \\ 0 & 0 & (1-p_1)q_1(1-r_1) & -q_1(1-r_1)-q_1r_1-k_1 & p_1q_1(1-r_1) \\ 0 & 0 & 0 & q_2(1-r_2) & -q_2(1-r_2)-q_2r_2-k_2 \\ \vdots & \vdots & \vdots & \vdots & \vdots \\ 0 & 0 & 0 & 0 & 0 \end{pmatrix},$$

$$\boldsymbol{A}_X = \begin{pmatrix} q_2r_2 & 0 & 0 & 0 & 0 \\ 0 & q_1r_1 & 0 & 0 & 0 \\ 0 & 0 & q_0r_0 & 0 & 0 \\ 0 & 0 & 0 & q_1r_1 & 0 \\ 0 & 0 & 0 & 0 & q_2r_2 \\ \vdots & \vdots & \vdots & \vdots & \vdots \\ 0 & 0 & 0 & 0 & 0 \end{pmatrix},$$

$$\boldsymbol{A}_K = \begin{pmatrix} k_2 & 0 & 0 & 0 & 0 \\ 0 & k_1 & 0 & 0 & 0 \\ 0 & 0 & k_0 & 0 & 0 \\ 0 & 0 & 0 & k_1 & 0 \\ 0 & 0 & 0 & 0 & k_2 \\ \vdots & \vdots & \vdots & \vdots & \vdots \\ 0 & 0 & 0 & 0 & 0 \end{pmatrix},$$

and,

$$\boldsymbol{A}_U = \begin{pmatrix} u_2 & 0 & 0 & 0 & 0 \\ 0 & u_1 & 0 & 0 & 0 \\ 0 & 0 & u_0 & 0 & 0 \\ 0 & 0 & 0 & u_1 & 0 \\ 0 & 0 & 0 & 0 & u_2 \\ \vdots & \vdots & \vdots & \vdots & \vdots \\ 0 & 0 & 0 & 0 & 0 \end{pmatrix}.$$

Here, q_i signifies the movement rate out of a hut. The direction of this movement depends on r_i (proportion of movement directed to outdoors) and, for H_1, p_1 (proportion of indoor movement direct away from SR-hut). The knockdown rate k_i is allowed to vary by hut, whereas the loss to follow-up rate u is assumed to be similar across huts. In what follows, we will refer to the exit rate qiri as xi (Figure 4-1).

The transition probabilities $\boldsymbol{P}_{ij}$ (t) satisfy a system of differential equations with rates $\boldsymbol{A}$ known as the backward Kolmogorov differential equations (31)

$$\frac{d\boldsymbol{P}}{dt} = \boldsymbol{A}\boldsymbol{P}(t)\,. \tag{2}$$

From this, we can derive the rates of change in each state

$$\begin{aligned}
\frac{dH_{2L}}{dt} &= (-q_2(1-r_2) - r_2q_2 - k_2)H_{2L} + p_1q_1(1-r_1)H_{1L} \\
\frac{dH_{1L}}{dt} &= (-q_1(1-r_1) - r_1q_1 - k_1)H_{1L} + q_2(1-r_2)H_{2L} + q_0(1-r_0)(1-p_0)H_0 \\
\frac{dH_0}{dt} &= (-q_0(1-r_0) - r_0q_0 - k_0)H_0 + q_1(1-r_1)(1-p_1)H_{1L} + q_1(1-r_1)(1-p_1)H_{1R} \\
\frac{dH_{1R}}{dt} &= (-q_1(1-r_1) - r_1q_1 - k_1)H_{1R} + q_2(1-r_2)H_{2R} + q_0(1-r_0)p_0H_0 \\
\frac{dH_{2R}}{dt} &= (-q_2(1-r_2) - r_2q_2 - k_2)H_{2R} + q_1(1-r_1)p_1H_{1R} \\
\left.\frac{dX_i}{dt}\right|_{i=2L,\ldots 2R} &= r_iq_iH_i \\
\left.\frac{dK_i}{dt}\right|_{i=2L,\ldots 2R} &= k_iH_i \\
\left.\frac{dU_i}{dt}\right|_{i=2L,\ldots 2R} &= u_iH_i.
\end{aligned} \tag{3}$$

By initializing this system in one hut (e.g., H_{2L}=1, all other states are zero), solving for this system of differential equations gives the probability that a mosquito occupies a specific state at time t conditional on release from the initial hut (here 2L) at time $t = 0$.

The absorbing states of $\boldsymbol{A}$ represent competing endpoints. Namely, an event in a certain hut only takes place if a mosquito has experienced no other event in this hut or any other hut. The Markov chain takes account of competing events since the states are discrete and mutuality exclusive. In addition, a mosquito released in 2L can only be knocked-down in 2R conditional on having moved there prior to the knock down event. The absence of non-zero rates to any of the absorbing states from other huts ensures this conditionality. As a result, the cumulative probabilities used to construct the likelihoods (next section) over the observed events account for the presence of competing risks as well as diversion conditionalities.

4.3.6 Likelihoods

To estimate A, we fitted eqn. (3) to the data based on the likelihood of the model parameters conditional on the observed data. The data collected during the experiments consist of a set of interval and right-censored time-to-event data. Outcome measures of interest include: exit, knockdown, diversion (defined as the movement to a different hut than the release hut), and loss to follow-up (ltfu), where exiting, knockdown, and loss to follow-up are competing events. Diversion can be measured either conditional on the occurrence of either of the other events ($T_{\text{diversion to H}} \leq T_{\text{knock-down in H}} \cup T_{\text{exit from H}}$) or upon recapture at the end of the experiment ($0 < T_{\text{diversion to H}} \leq T_{\text{end}}$). For each diversion event, we know that the movement from release to recapture hut has taken place at least once, though more movement events may have taken place in the mean time.

The cumulative, conditional probabilities for all events observed or inferred in the experiment can be can be directly obtained from the solutions of eqn. (3) as will be detailed in eqns. (4), (5), and (6).

Interval censored events. –Data on knockdown and exit events are interval censored between time points t_1 and t_2 , with exit events recorded at 30-minute intervals and knockdown at hourly intervals. Given model-parameter set θ, the probability that a mosquito released in *H* is observed knocked down in a specific hut at time t_2 is

$$\begin{aligned}\Pr(t_1 < T < t_2, Y = KD_H \mid H_{rel}, \theta) &= \frac{F_{KD_H}(t_2 \mid H_{rel}, \theta) - F_{KD_H}(t_1 \mid H_{rel}, \theta)}{F_{Div_H}(t_2 \mid H_{rel}, \theta) S(t_2 \mid H_{rel}, \theta)} \\ &= K_H(t_2 \mid H_{rel}, \theta) - K_H(t_1 \mid H_{rel}, \theta),\end{aligned} \tag{4}$$

where $F(t)$ denotes the probability that a specific event (here knockdown and diversion to *H*) occurred in hut *H* by time *t* and $S(t)$ denotes the survival function (i.e., the probability that no knockdown, exit, or loss to follow-up has occurred by time *t*). Exit and knockdown events contain indirect information on the diversion event, namely that the mosquito has moved from its release location to the hut where the event took place before the event occurred. This condition, as illustrated by F_{Div} in the denominator of eqn. (4), is implicitly accounted for within the system of eqn. (3), hence the absence of conditioning in the second part of eqn. (4).

Loss to follow-up. – Of mosquitoes that are not retrieved at the end of the experiment, we know they were loss to follow-up at some point between the start and the end of the experiment

$$\Pr(t_{start} < T < t_{end}, Y = U \mid H_{rel}, \theta) = F_U(t_{end} \mid H_{rel}, \theta) = \sum_{i=2L}^{2R} U_i(t \mid H_{rel}, \theta). \tag{5}$$

Right censored data. – Mosquitoes retrieved by the end of the experiment are treated as right censored. While it is unknown when an event would have occurred, we do

know it did not occur during the duration of the study. In addition, we know the mosquito moved from the release hut to the hut where it was retrieved

$$\Pr(T > t_{end} \mid H_{rel,}\theta) = S(t_{end} \mid H_{rel},\theta) F_{Div_H}(t_{end} \mid H_{rel},\theta) = H_H(t_{end} \mid H_{rel},\theta). \quad (6)$$

Likelihood function. – The overall likelihood is the product of the individual likelihoods conditional on the observations. These include, for different release huts, event huts, and experiment days, the number of mosquitoes exited or knocked down during specific time intervals during the experiment, as well as numbers recaptured or loss to follow-up at the end of the experiment

$$L = P_{multinom}(k_{exit_{t=i,H=j,rel=k,day=l}}, k_{kd_{t=i,H=j,rel=k,day=l}}, k_{hut_{t=750,H=j,rel=k,day=l}}, k_{u_{t=750,rel=k,day=l}} \mid p_{exit_{t=i,H=j,rel=k}}, p_{kd_{t=i,H=j,rel=k}}, p_{hut_{t=750,H=j,rel=k}}, p_{u_{t=750,rel=k}}), \quad (7)$$

with $\forall i : i \in [30,60,90,\ldots,750]$ time points for k_{exit} and $\forall i : i \in [30,90,150,\ldots,750]$ for k_{kd}, event huts H $\forall j : j \in [2\mathrm{L},1\mathrm{L},0,1\mathrm{R},2\mathrm{R}]$, release hut $\forall k : k \in [2\mathrm{L},1\mathrm{L},0,1\mathrm{R},2\mathrm{R}]$ for control experiments and $\forall k : k \in [2\mathrm{L},1\mathrm{L},1\mathrm{R},2\mathrm{R}]$ for treatment experiments, and finally experiment days $\forall l : l \in [1,2,3,4,5]$. Here, each k_{exit} denotes the number of exited mosquitoes in hut H observed at time t, by release hut and experiment day. The corresponding probabilities p are derived as detailed before (eqn. (4), (5), and (6)) and are assumed to be independent of the experiment day.

4.3.7 Model fitting

We used a Bayesian Markov chain Monte Carlo (MCMC) approach for parameter estimation. Using Bayes' theorem, we define the posterior probability density of the model's parameters (θ) given the data as

$$\pi = P(\theta \mid data) = \frac{P(data \mid \theta) P(\theta)}{\int P(data \mid \theta) P(\theta) d\theta}, \quad (8)$$

where P(θ) is the prior distribution. We applied beta distributed priors with median 0.5 for p_1 and median 0.25 on r_i (i.e., a mosquito is twice as likely to move to a adjacent hut than to move outside), a gamma distributed prior with mean 0.02 (average residence time of 50 minutes) on the movement rates q_i, and uniform priors for the remaining parameters (Table 4-1). Average residential times ($1/q_i$) in each hut were constrained between 5 minutes and 20 hours and the average time until knock down ($1/k_i$) between 12 hours and 10 days (14, 32). We explored the full parameter space of θ using the Metropolis-Hastings algorithm.

Starting from an initial parameter set θ_1, a new parameter was proposed such that $\theta_2 = \theta_1 + X$, where X is a random value from a truncated normal proposal distribution *g* with mean θ_1 with a standard deviation formulated relative to θ_1 and selected so as to ideally have an acceptance rate between 10 and 50% (33). The probability for θ_2 to be accepted depends on the likelihood of both θ_1 and θ_2

$$A(\theta_1,\theta_2)=\min\left(1,\frac{\pi_2}{\pi_1}\frac{g(\theta_1|\theta_2)}{g(\theta_2|\theta_1)}\right). \quad (9)$$

Here, the proposal probability $g(\theta_1|\theta_2)$ accounts for truncation of the normal proposal distributions (between zero and one for the *p*'s and *r*'s, and from zero to infinity otherwise):

$$\begin{aligned} g(\theta_2|\theta_1)&=\frac{P(X=\theta_2)}{P(X\le 1)-P(X\le 0)} \text{ for } p_1 \text{ and} \\ g(\theta_2|\theta_1)&=\frac{P(X=\theta_2)}{1-P(X\le 0)} \text{ for all others parameters,} \end{aligned} \quad (10)$$

where X is a normal distribution with mean θ_1 and standard deviations corresponding to each parameter's proposal distribution.

If the acceptance probability is larger than a randomly generated uniform value between zero and one, θ_2 was accepted into the chain. Otherwise, θ_1 was retained. Multiple iterations of this routine were performed (n = 90,000). This process was repeated five times starting from different initial parameter sets. The resulting chains of accepted parameters (φ), after discarding a burn-in period (10,000), were combined to represent our sample from the posterior distribution (π). Convergence was assessed using the Gelman-Rubin (GR) statistic (34).

4.3.8 Simulation experiments

To test the performance of the fitting algorithm, we simulated data with a known underlying process and known model parameters. Probabilities for released mosquitoes to occupy a specific state over time are derived using eqn. (3). As follows from eqs. (4), these probabilities are defined for interval- and right-censored events. Random draws from a multinomial distribution with the simulated probabilities and a given number of released mosquitoes are taken to simulate numbers of mosquitoes occupying each state at sampling time points. Parameter sets (n=10) are sampled across the composite parameter space θ using the Sobol algorithm (35, 36), where the same bounds are applied as for the prior distributions (Table 4-1). Data are simulated for different numbers of released mosquitoes (25: field scenario, and 1,000: large sample size scenario) for five replicates per parameter set and fitted to eqn. (3) as described before.

4.4 Results

4.4.1 Testing the inference methodology

Large sample size scenario.–The inference framework was tested against data simulated with the system of ordinary differential equations described in eqn. (3), with an observation process that mimicked the field experiment and with parameters reflecting the range of values in the prior distributions. In the large sample size scenario (five replicates with 1,000 released mosquitoes each), we accurately estimated the values of all parameters used in the simulations. All true parameter values fell within the 95% highest density interval (HDI) of the estimated posterior distributions (Figure 4-2). Most posterior medians approximated the true parameter well (Pearson R^2>0.98), but somewhat less so for knockdown in the treated hut (Pearson R^2=0.74). Posterior distributions were relatively wider for rate parameters associated with the treated hut (x_0 and k_0). Standard deviations of these parameters were a fraction (i.e., 11% and 12%) of their respective medians, whereas the s.d.:median ratio was below 3.5% for all other parameters. This reduced precision may be a consequence of the fact that rate parameters associated with huts other than the treated hut were informed by twice as much data as were the rate parameters associated with the treated hut, which derives from our assumption of shared parameters for huts a given distance from the treated hut (Figure 4-1). Gelman-Rubin statistics were below 1.1 for most simulation sets (average 1.04). When simulation sets resulted in parameters with GR statistics above 1.1, these were related to mosquito movement (q_i, r_i, and p_1) and were most commonly associated with the untreated huts (Table S4-1).

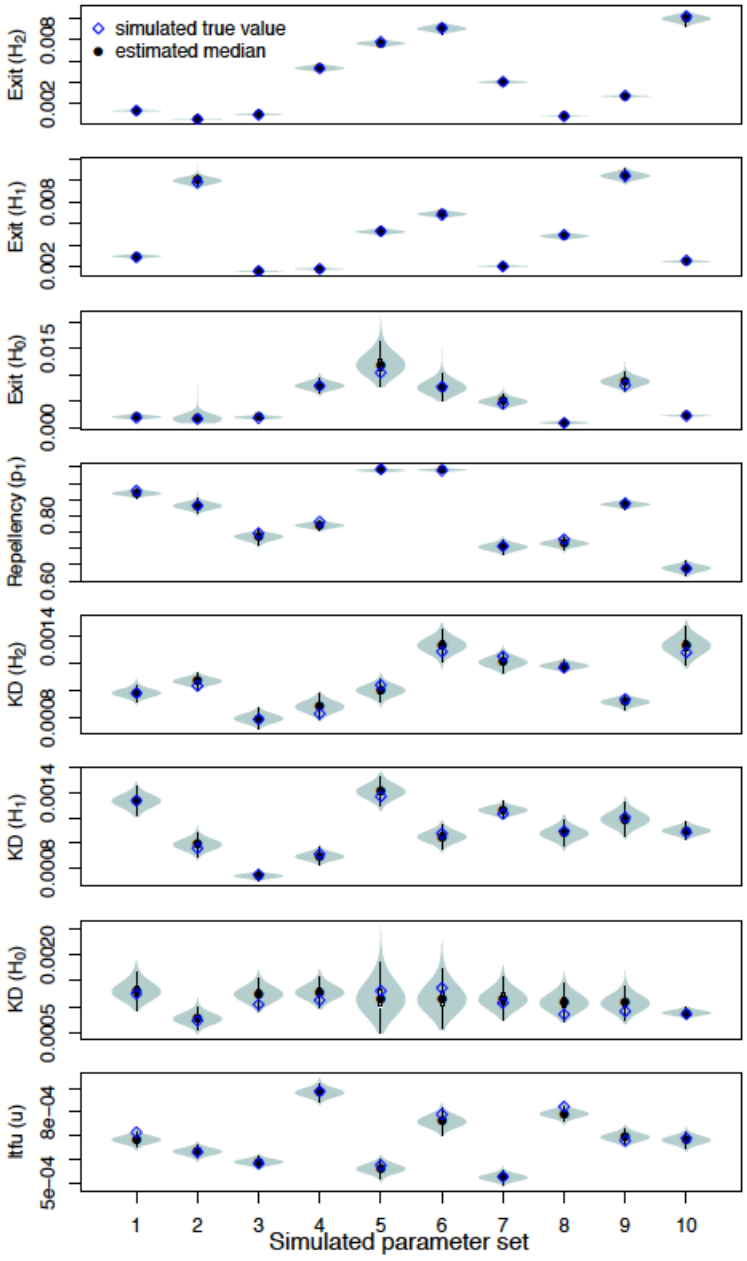

Figure 4-2: Estimated parameters from simulation experiments for five replicates of 1,000 released mosquitoes (large sample size scenarios) with the true value (blue diamonds) and the estimated median (black circles). Each estimation is based on 5 chains with distinct starting conditions. 50,000 MCMC iterations were performed following a burn-in period of 10,000.

Field scenario.–We also tested the performance of the inference framework on data simulated under conditions that closely resembled the conditions under which the experimental data were collected (Figure 4-3). All true parameter values fell within the 95% HDI, but the posterior medians were less consistent with the simulated values (R^2>0.8 for all but x_0: 0.68; k_2:0.03, and k_0: -0.29) than under the large sample size scenario. The low correlation coefficients on the knockdown rates appear to be driven by a few outliers (Figure 4-3). No systematic underestimation or overestimation was observed based on these simulations, suggesting that the additional discrepancy between simulated and inferred parameter values in the field scenario relative to the large sample size scenario is due to stochasticity associated with the smaller sample size in the field scenario (i.e., n = 25 vs n = 1,000). Gelman-Rubin statistics were, across all parameters and simulation sets, close to 1 (average GR 1.01) (Table S4-1).

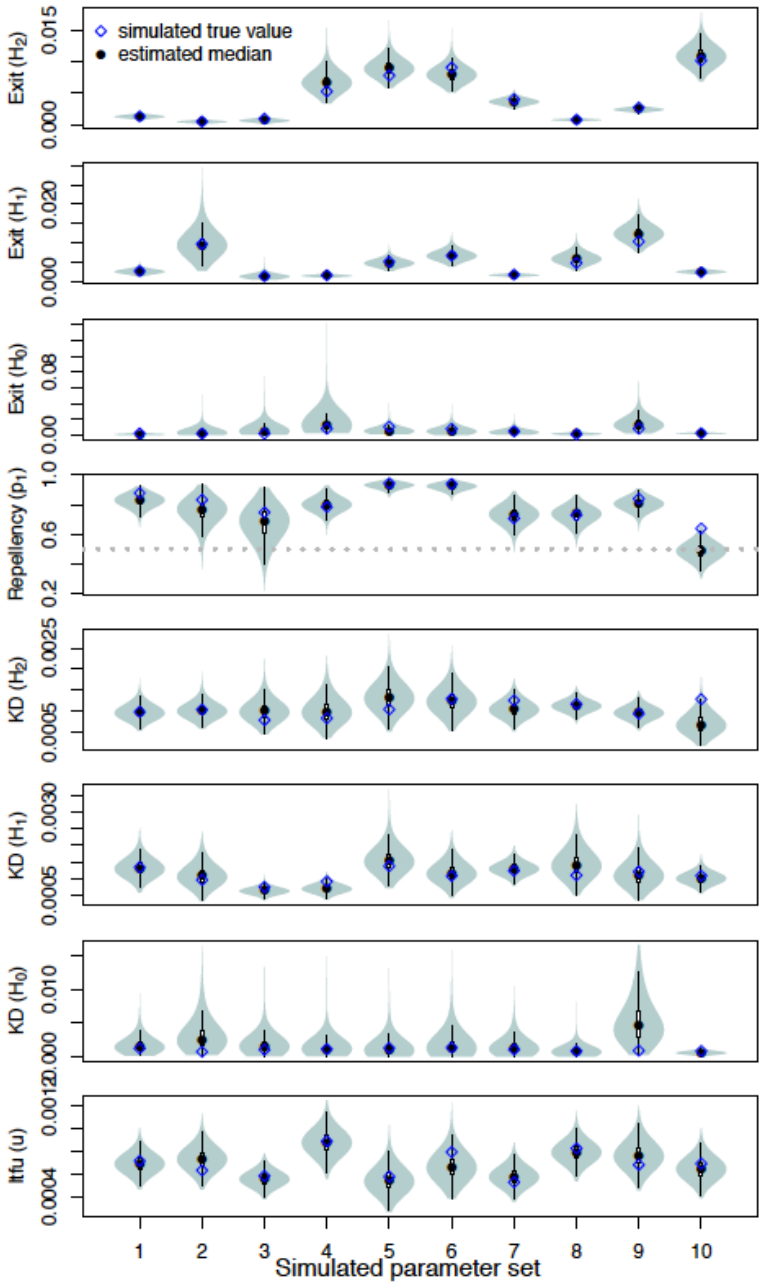

Figure 4-3: Estimated parameters from simulation experiments for five replicates of 25 released mosquitoes (field scenarios) with the true value (blue diamonds) and the estimated median (black circles). Each estimation is based on 5 chains with distinct starting conditions. 50,000 MCMC iterations were performed with a burn-in period of 10,000.

4.4.2 Product effects on mosquito bionomics

We first fitted the Markov chain model to the experimental hut data with all parameters allowed to vary. Strong correlations between r_i, q_i, and p_i indicated that these parameters were not identifiable given that a wide range of combinations of values of these parameters explained the data equally well (Figure S4-1). To resolve this identifiability issue, we fitted the exit rate x_i as a single composite parameter ($q_i r_i$). The rate of movement between huts is directly related to the exit rate, namely it is a proportion ($1-r_i$) of the overall movement rate out of a specific hut (q_i). In doing so, we fixed the values of r_i at the medians of the posterior marginal density of the r_i corresponding to each hut that was obtained from the full parameter fit on the control data set (Figure S4-1). This reduced the amount of cross-correlation from Pearson R^2 as high as 0.84 in the original to up to 0.72 upon fixing r_i. Most importantly, it markedly improved convergence from GR statistics as high as 1.38 (q_2, low dosage) to 1.00 for all parameters after fixing r_i, indicating that other parameters are identifiable once this adjustment is made (Figure S4-7-9). Choosing either the 2.5^{th} or 97.5^{th} percentile of r_i instead did not affect this conclusion (Figure S4-5 and 6). Acceptance rates for each chain tended to remain relatively constant following a burn-in period and varied across chains and parameters within the range of 21-54%.

Exit rates.–In the control, exit rates (x_i) from huts at different distances i from the treatment hut were relatively similar (medians for x_0: $2.2\text{x}10^{-3}$, x_1: $1.6\text{x}10^{-3}$, x_2: $1.8\text{x}10^{-3}$) (Figure 4-4A-C). In the treatments, exit rates out of the treated hut were reduced relative to the control in response to both the low (relative risk, RR:0.70, HDI:0.62-1.09) and the high dosage (RR:0.70, HDI:0.40-1.06), with no perceptible difference in the respective

effects of the two dosages (Figure 4-4C). This effect carried over to the adjacent huts (H_1) with exit rates that were lower than in the control experiment (RR: low: 0.79, HDI:0.59-1.01, high: 0.66, HDI:0.50-0.87) (Figure 4-4B). In the huts furthest from the SR (H_2), the low dosage had no effect on exit rates relative to the control (RR: 0.94, HDI:0.72-1.18), whereas the high dosage reduced exit rates (RR: 0.71, HDI:0.54-0.92) even at a relatively far distance from the product (Figure 4-4A).

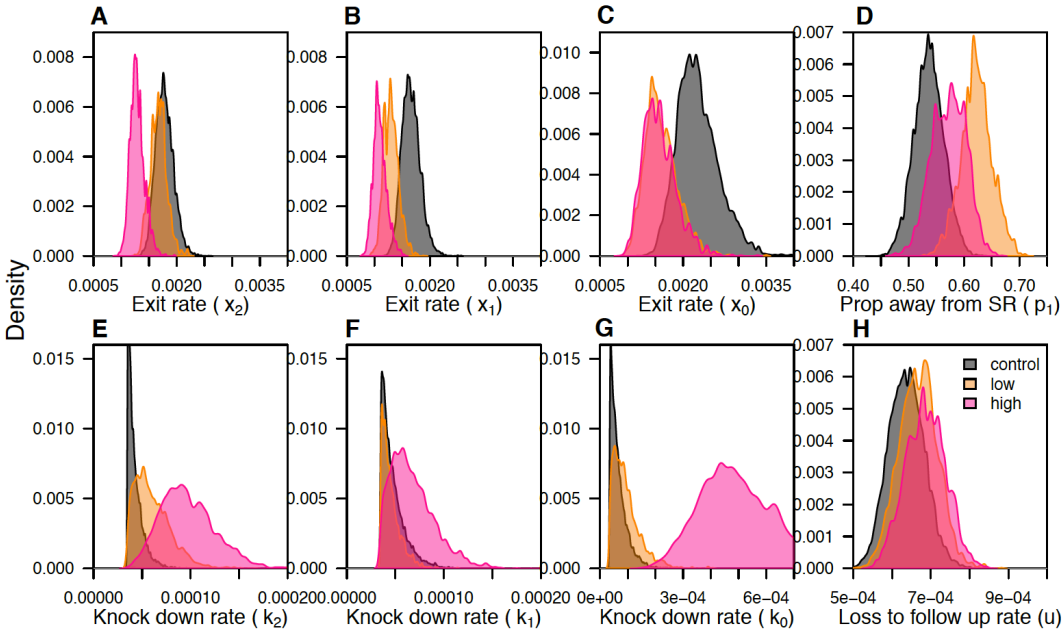

Figure 4-4: Posterior distributions of model parameters fitted to experimental data for the control (gray), low dosage (orange) and high dosage (pink) for the SR-hut (subscript 0) and huts 2 or 1 removed (subscript 2 and 1 respectively). A-C) rates at which mosquitoes exit the huts D) proportion of movement from H_1 (hut directly adjacent to the treatment hut) away from the SR-product. E-G) knockdown rates, and H) loss to follow-up rates. The algorithm was run for 90,000 iterations with a burn-in period of 10,000.

Repellency.–In the control, mosquitoes moved away from or towards the treated hut with roughly equal probability (p_1=0.54, HDI:0.48-0.59), although with a possible slight preference for movement away from H_0 (odds of moving away: 1.16, HDI:0.92-1.41) (Figure 4-4D). In the low-dosage treatment, significant repellency was observed (odds: 1.64, HDI:1.30-2.09), with a median probability of moving away from the SR hut of 0.62 (HDI:0.57-0.68) (Figure 4-4D). In the high-dosage treatment, repellency was still clear (odds: 1.35, HDI:1.04-1.67), but the effect was somewhat smaller (p_1=0.57, HDI:0.52-0.63) (Figure 4-4D).

Knockdown.–Knockdown was a very rare event in the control (2/125 mosquitoes across all five replicates). As a consequence, estimates of knockdown rates in the control resembled the lower boundary of the prior distribution (medians for H_0: $5.8\text{x}10^{-5}$, H_1: $4.4\text{x}10^{-5}$, H_2: $4.0\text{x}10^{-5}$) (Figure 4-4E-8G). There was no effect of the low dosage on knockdown rates relative to the control, both in the treated hut H_0 (RR: 1.39, HDI:0.26-3.84) (Figure 4-4G) and in the H_1 huts directly adjacent (RR: 1.00, HDI:0.45-1.76) (Figure 4-4F). In the H_2 huts furthest away from the treatment, a somewhat increased knockdown rate was observed in response to the low dosage relative to the control (RR: 1.37, HDI:0.64-2.46) (Figure 4-4E). Knockdown rates in the high-dosage scenario were elevated in all huts, in particular in the H_0 treatment huts (RR: 8.37, HDI:2.11-17.35) (Figure 4-4G) but also in the H_1 and H_2 huts (RR: H_1: 1.39, HDI:0.52-2.69, H_2: 2.22, HDI:0.96-3.86) (Figure 4-4E and 8F).

Loss to follow-up.–Rates of loss to follow-up were similar across the control and two treatments, although there was a signal for a small increase in these rates with increasing dosage (low: 5%, high: 8%) (Figure 4-4H). In comparing posterior samples

across dosages, a signal for a positive dose-response relationship (i.e., u(high) > u(low) > u(control)) was confirmed in 61% of samples from the posterior.

Residence times.–The proportion of time a mosquito spent in each hut results from the composite of treatment effects. Using simulations of the system of ordinary differential equations (eqn. (3)), we derived a posterior estimate of the proportion of time spent in the H_0 treated hut, which was similar but slightly reduced in either treatment scenario relative to the control (Figure 4-5E) and without any effect in the downstream huts H_1 and H_2 (Figure 4-5A and 9C). However, when considering the total duration of the experiment, the proportion of time spent in the downstream huts H_1 and H_2 was higher in the treatments than in the control (Figure 4-5B and 9D). This was a result of reduced exit rates and thus an overall increase in time spent in the hut system as a whole (Figure 4-4A and 8B).

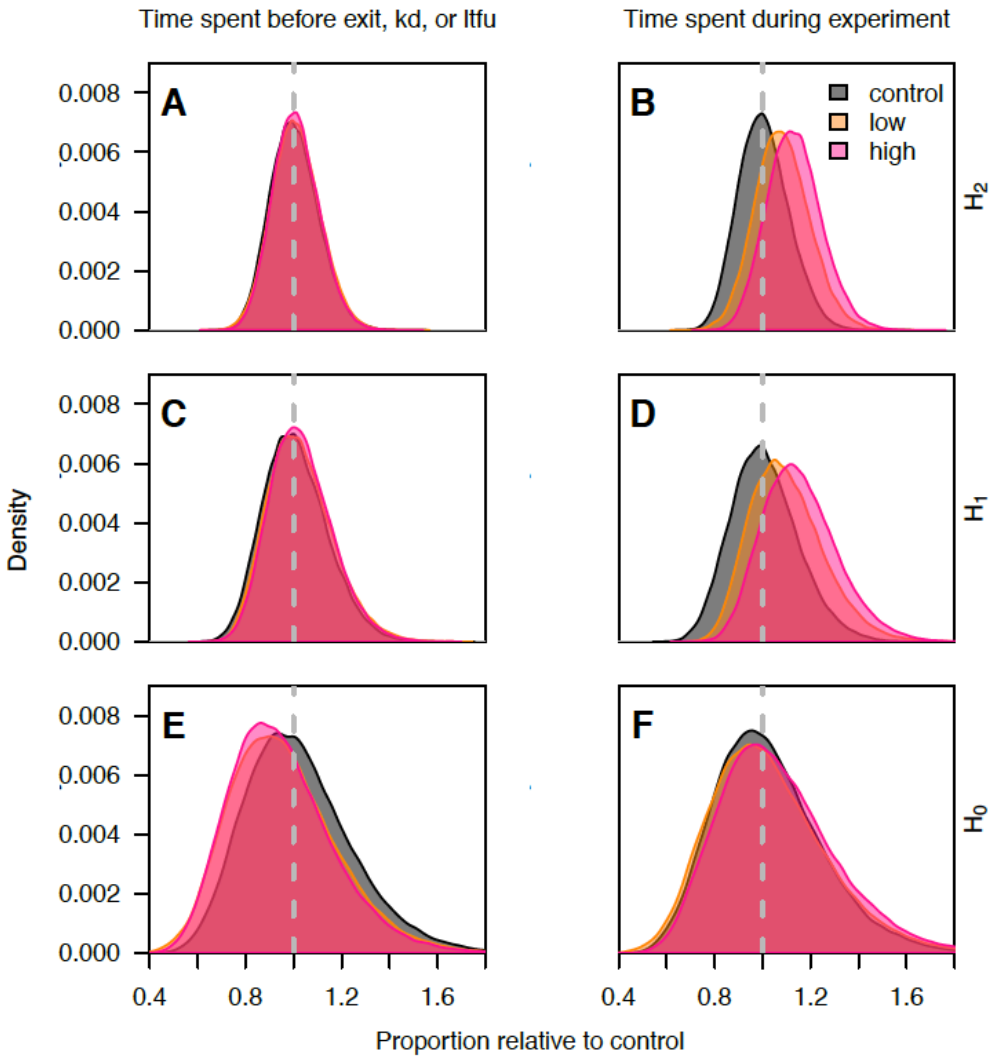

Figure 4-5: Distributions of time spent in each hut relative to the control (gray), low dosage (orange), and high dosage (pink) for the huts 2 (A and B) or 1 (C and D) removed from the SR and the SR-hut (E and F). The left column signifies the proportion of time spent in each hut before having experienced an event (A,C, and E), where kd is knockdown and ltfu is loss to follow-up. The right column signifies the proportion of the total experiment time spent in each hut relative to the control (B, D, F).

4.5 Discussion

We used a continuous-time Markov chain model informed by experimental data under a Bayesian inference framework to quantify concurrent and downstream effects of a transfluthrin-based spatial repellent (SR) product on female *Aedes aegypti* mosquito behavior and bionomics. Examination of posterior estimates of model parameters showed that mosquitoes were deterred from entering the experimental hut where the product was located and that this effect was stronger for the lower dosage SR. Posterior estimates of model parameters also indicated lower exit rates out of the treatment hut under both treatments, presumably due to irritancy effects of the product on mosquitoes. Under the higher dosage SR, this effect was noticeable as far as two huts away from the treated hut. Similarly strong downstream effects were observed for knockdown rates, which were markedly increased in all huts in the presence of the higher dosage SR. The lower dosage SR had a detectable, but lower, effect on knockdown.

We validated our inference method by demonstrating its ability to accurately estimate the model's parameters given simulated data. This assessment was conditional, however, on the assumption that the model is an accurate representation of reality. Some of the known limiting assumptions of our analysis include (1) effects that depend on distance from the treated hut rather than on each hut individually, (2) equal loss to follow-up across huts, and (3) time-invariant parameters. Of these, the first may be most problematic given that wind and other factors could result in asymmetric effects of the SR on huts of the same distance from the treated hut but on different sides of it (37). In principle, it would be possible to account for such factors in future studies. For example, repellency (ρ) could be treated as a function of readings from a wind gauge. Posterior

estimates of the parameters governing the relationship between wind and ρ would then allow for inferences about the repellency of the product under wind conditions different than those in the experiment. Required sample sizes and sampling schemes for such experiments could be informed ahead of time by our model and results (38).

Repellency and increased knockdown reduced the overall time mosquitoes spent in the experimental hut in which the SR was located and thus appear to have the potential to limit transmission. The reduced time spent in the SR hut was offset by reduced exit rates upon exposure to the product. However, it is uncertain to what extent the host-seeking and blood-feeding behaviors of these irritated mosquitoes are affected. Laboratory experiments using similar volatile products showed these effects to also be associated with reduced rates of human landing (39). The inclusion of blood-feeding assays in the design of experimental hut studies would be valuable for resolving questions such as this, which are still outstanding following our study.

The effect of SR products on neighboring premises is also critical to know about, given concerns that mosquitoes could be diverted to untreated houses and increase blood-feeding there (40). Three aspects of our results suggest that the risk of diversion for the formulation used in our experiments may be limited. First, SR exposure reduced movement rates. Second, mean residence time in the untreated huts relative to the treated hut was unaffected by treatment, once reduced exit rates were accounted for. Third, there was a marked increase in knockdown in untreated huts. At the same time, there was also a marked reduction in expellency in untreated huts, which resulted in prolonged time spent in adjacent huts. Evaluating the overall potential for diversion based on these

effects will require pairing experimental results such as ours with new theory that is capable of accounting for this range of behavioral and bionomic effects (10, 41, 42).

The net increase in time spent in untreated huts is likely a result of downstream effects of the SR product rather than diversion. Under our experimental design, we cannot distinguish between downstream effects caused by volatile particles in untreated huts or by the residual effect of the product on mosquitoes that are exposed in the treated hut but exit or are knocked down elsewhere. The reduced repellency effect observed at high relative to low dosage may not result from reduced sensitivity of mosquitoes to this effect per se, but may instead be a result of saturation of all experimental huts with the volatile chemical. Alternative experimental designs, combined with our new inference framework, could be capable of quantifying the extent to which downstream effects result from movement of the volatile chemical or exposed mosquitoes with lingering effects.

The need for new vector control formulations and efficient testing thereof is evident (2, 43). The framework we proposed provides a flexible tool to estimate a product's effects on movement in a quantitative and probabilistic fashion, without the need for expensive, technologically advanced tracking devices. In addition, the context-specific balance between adverse diversion effects and the positive consequences of downstream dosing can be estimated at early stages of the product development and in a variety of settings. This enables a cheap, efficient selection of products (or combinations thereof) worth advancing to entomological and clinical field trials, and it strengthens a proof of concept required for approval by the WHO vector control advisory group (44).

4.6 References

1. Eldridge BF & Edman J (2012) Medical entomology: a textbook on public health and veterinary problems caused by arthropods, (Springer Science & Business Media,

2. Achee NL, et al (2015) A critical assessment of vector control for dengue prevention. PLoS Negl Trop Dis 9(5): e0003655.

3. Corbel V & N'Guessan R (2013) Distribution, mechanisms, impact and management of insecticide resistance in malaria vectors: A pragmatic review. Anopheles Mosquitoes-New Insights into Malaria Vectors 633

4. Gatton ML, et al (2013) The importance of mosquito behavioural adaptations to malaria control in africa. Evolution 67(4): 1218-1230.

5. Russell TL, et al (2011) Increased proportions of outdoor feeding among residual malaria vector populations following increased use of insecticide-treated nets in rural tanzania. Malaria Journal 10(1): 1.

6. Fanello C, et al (2003) Comparative evaluation of carbosulfan-and permethrin-impregnated curtains for preventing house-entry by the malaria vector anopheles gambiae in burkina faso. Med Vet Entomol 17(3): 333-338.

7. Pleass R, Armstrong J, Curtis C, Jawara M & Lindsay S (1993) Comparison of permethrin treatments for bednets in the gambia. Bull Entomol Res 83(01): 133-139.

8. Lindsay S, Adiamah J & Armstrong J (1992) The effect of permethrin-impregnated bednets on house entry by mosquitoes (diptera: Culicidae) in the gambia. Bull Entomol Res 82(01): 49-55.

9. Achee NL, et al (2012) Spatial repellents: From discovery and development to evidence-based validation. Malar J 11(1): 164.

10. Killeen GF & Smith TA (2007) Exploring the contributions of bed nets, cattle, insecticides and excitorepellency to malaria control: A deterministic model of mosquito host-seeking behaviour and mortality. Trans R Soc Trop Med Hyg 101(9): 867-880.

11. Kiware SS, et al (2012) Simplified models of vector control impact upon malaria transmission by zoophagic mosquitoes. PLoS One 7(5): e37661.

12. Briët OJ, Smith TA & Chitnis N (2012) Measurement of overall insecticidal effects in experimental hut trials. Parasites & Vectors 5(1): 1.

13. Chitnis N, Schapira A, Smith T & Steketee R (2010) Comparing the effectiveness of malaria vector-control interventions through a mathematical model. Am J Trop Med Hyg 83(2): 230-240.

14. Chareonviriyaphap T, et al (2010) An improved experimental hut design for the study of aedes aegypti (diptera: Culicidae) movement patterns in thailand. Journal of Vector Ecology 35(2): 428-431.

15. Achee NL, Grieco JP, Andre RG, Rejmankova E & Roberts DR (2005) A mark-release-recapture study using a novel portable hut design to define the flight behavior of anopheles darlingi in belize, central america 1. J Am Mosq Control Assoc 21(4): 366-379.

16. Massue DJ, et al (2016) Comparative performance of three experimental hut designs for measuring malaria vector responses to insecticides in tanzania. Malaria Journal 15(1): 1.

17. Randriamaherijaona S, et al (2015) Do holes in long-lasting insecticidal nets compromise their efficacy against pyrethroid resistant anopheles gambiae and culex quinquefasciatus? results from a release–recapture study in experimental huts. Malaria Journal 14(1): 1.

18. Chapman DG & Junge Jr CO (1956) The estimation of the size of a stratified animal population. The Annals of Mathematical Statistics : 375-389.

19. Jolly GM (1965) Explicit estimates from capture-recapture data with both death and immigration-stochastic model. Biometrika 52(1/2): 225-247.

20. Arnason AN (1972) Parameter estimates from mark-recapture experiments on two populations subject to migration and death. Researches on Population Ecology 13(2): 97-113.

21. Arnason AN (1973) The estimation of population size, migration rates and survival in a stratified population. Researches on Population Ecology 15(2): 1-8.

22. Seber GA (1965) A note on the multiple-recapture census. Biometrika 52(1/2): 249-259.

23. Lebreton J, Nichols JD, Barker RJ, Pradel R & Spendelow JA (2009) Modeling individual animal histories with multistate capture–recapture models. Adv Ecol Res 41: 87-173.

24. Lebreton J & Cefe RP (2002) Multistate recapture models: Modelling incomplete individual histories. Journal of Applied Statistics 29(1-4): 353-369.

25. Kendall WL & Nichols JD (2002) Estimating state-transition probabilities for unobservable states using capture–recapture/resighting data. Ecology 83(12): 3276-3284.

26. Ergon T & Gardner B (2014) Separating mortality and emigration: Modelling space use, dispersal and survival with robust-design spatial capture–recapture data. Methods in Ecology and Evolution 5(12): 1327-1336.

27. Villela DA, et al (2015) A bayesian hierarchical model for estimation of abundance and spatial density of aedes aegypti. PloS One 10(4): e0123794.

28. Ovaskainen O (2004) Habitat-specific movement parameters estimated using mark–recapture data and a diffusion model. Ecology 85(1): 242-257.

29. McLean-Cooper N, Achee N, Foggie T, Grieco J & Williams J (2008) Space optimizing methods for laboratory rearing of aedes aegypti. J Am Mosq Control Assoc 24(3): 460-462.

30. Grieco JP, Achee NL, Andre RG & Roberts DR (2000) A comparison study of house entering and exiting behavior of anopheles vestitipennis (diptera: Culicidae) using experimental huts sprayed with DDT or deltamethrin in the southern district of toledo, belize, C.A. J Vector Ecol 25(1): 62-73.

31. Taylor HM & Karlin S (2014) An introduction to stochastic modeling, (Academic press,

32. Grieco JP, et al (2007) A new classification system for the actions of IRS chemicals traditionally used for malaria control. PLos One 2(8): e716.

33. Gilks WR (2005) Markov chain monte carlo, (Wiley Online Library,

34. Gelman A & Rubin DB (1992) Inference from iterative simulation using multiple sequences. Statistical Science 7(4): 457-472.

35. Sobol IM (1967) On the distribution of points in a cube and the approximate evaluation of integrals. Zhurnal Vychislitel'Noi Matematiki i Matematicheskoi Fiziki 7(4): 784-802.

36. King A, et al (2010) Pomp: Statistical inference for partially observed markov processes (R package). URL Http://Pomp.R-Forge.R-Rproject.Org

37. Hoffmann EJ & Miller JR (2002) Reduction of mosquito (diptera: Culicidae) attacks on a human subject by combination of wind and vapor-phase DEET repellent. J Med Entomol 39(6): 935-938.

38. Restif O, et al (2012) Model-guided fieldwork: Practical guidelines for multidisciplinary research on wildlife ecological and epidemiological dynamics. Ecol Lett 15(10): 1083-1094.

39. Ritchie SA & Devine GJ (2013) Confusion, knock-down and kill of aedes aegypti using metofluthrin in domestic settings: A powerful tool to prevent dengue transmission. Parasit Vectors 6: 262-280.

40. Maia MF, et al (2013) Do topical repellents divert mosquitoes within a community?–Health equity implications of topical repellents as a mosquito bite prevention tool. PLoS One 8(12): e84875.

41. Brady OJ, et al (2016) Vectorial capacity and vector control: Reconsidering sensitivity to parameters for malaria elimination. Trans R Soc Trop Med Hyg 110(2): 107-117.

42. Briët OJ, et al (2013) Effects of pyrethroid resistance on the cost effectiveness of a mass distribution of long-lasting insecticidal nets: A modelling study. Malaria Journal 12(1): 1.

43. Bowman LR, Donegan S & McCall PJ (2016) Is dengue vector control deficient in effectiveness or evidence?: Systematic review and meta-analysis. PLoS Negl Trop Dis 10(3): e0004551.

44. Vontas J, et al (2014) Framework for rapid assessment and adoption of new vector control tools. Trends Parasitol 30(4): 191-204.

TABLE 4-1:

PARAMETER DEFINITIONS AND PRIOR PROBABILITY DISTRIBUTIONS FOR

EACH

Parameter	Description	Distribution	Parameters	Ref	Note
q_i	Movement rate	gamma	shape = 1.5 mean = 0.02 rate = shape/ mean	(32)	Assuming symmetry
p_1	Proportion of movement away from SR	beta	mean = 0.5 shape1 = 4 shape2 = shape1 / (mean – shape1)	-	
r	Exit rate	beta	mean = 0.25 shape1 = 1.25 shape2 = shape1 / (mean – shape1)	(32)	Assuming symmetry
k	Knockdown rate	uniform	min = 1 $hours^{-1}$ max = 16 $days^{-1}$	(14, 32)	Assuming symmetry
u	Loss to follow-up rate	uniform	min = 30 min^{-1} max = 100 $days^{-1}$	-	Assumed the same between huts

4.7 Supportings and figures

TABLE S4-1:

AVERAGE GELMAN-RUBIN STATISTICS ACROSS SIMULATED DATA SETS

(MEDIAN AND THE UPPER BOUND OF THE 95% CONFIDENCE INTERVAL)

	Large sample size scenario		**Field scenario**	
Parameter	**Median**	**Upper bound 95% CI**	**Median**	**Upper bound 95% CI**
q_2	1.01	1.02	1.02	1.03
q_1	1.02	1.05	1.00	1.01
q_0	1.01	1.03	1.00	1.01
p_1	1.09	1.21	1.01	1.02
r_2	1.01	1.02	1.01	1.02
r_1	1.07	1.18	1.01	1.02
r_0	1.08	1.20	1.01	1.03
k_2	1.01	1.03	1.01	1.01
k_1	1.08	1.20	1.01	1.02
k_0	1.09	1.21	1.01	1.02
u	1.00	1.01	1.00	1.01

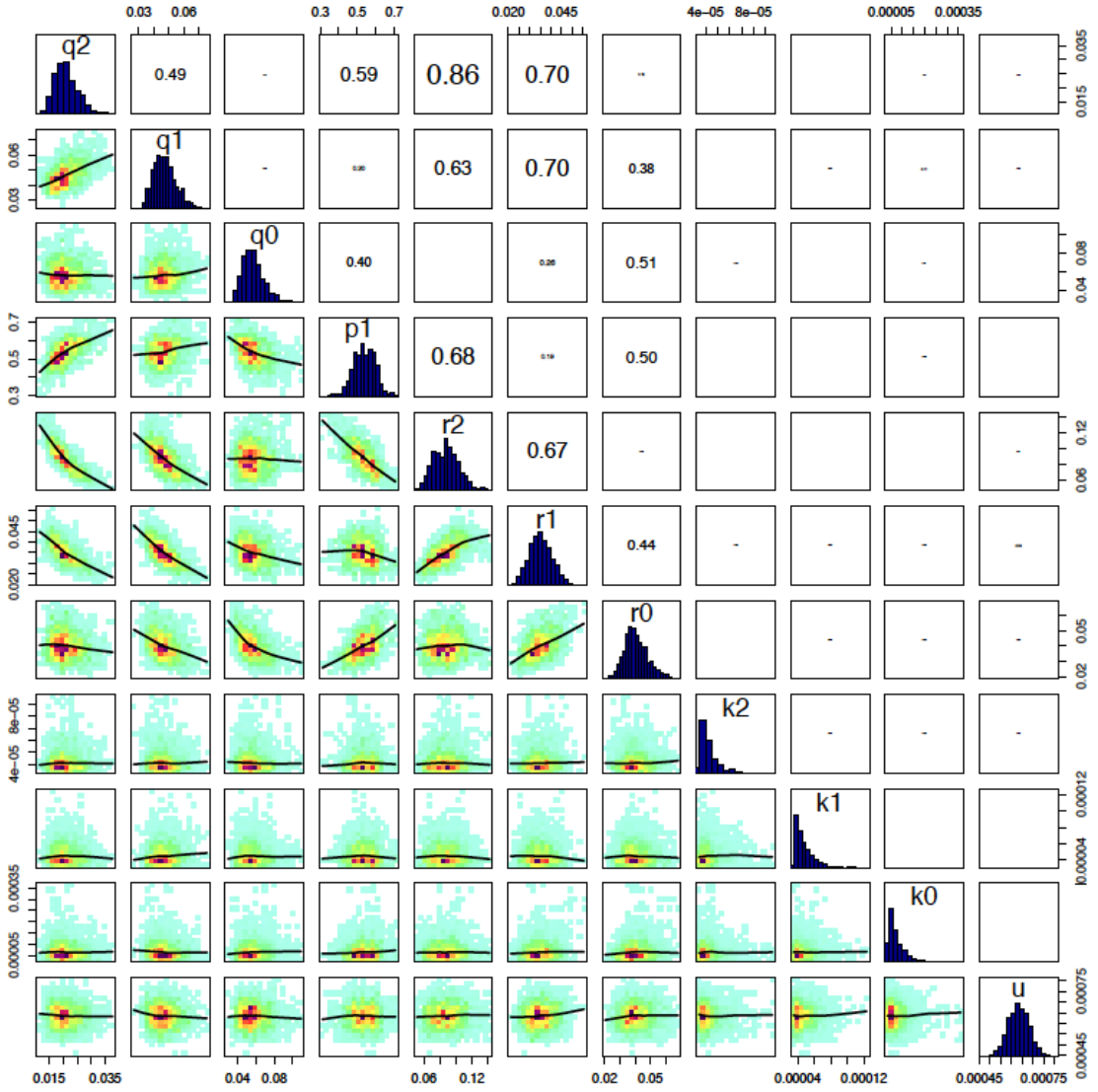

Figure S4-1: Correlations between parameter posteriors of model fit on control scenario with all parameters estimated. Marginal posteriors are depicted on the diagonals. The numbers on the right of the diagonal depict the correlation coefficients for each side by side comparison.

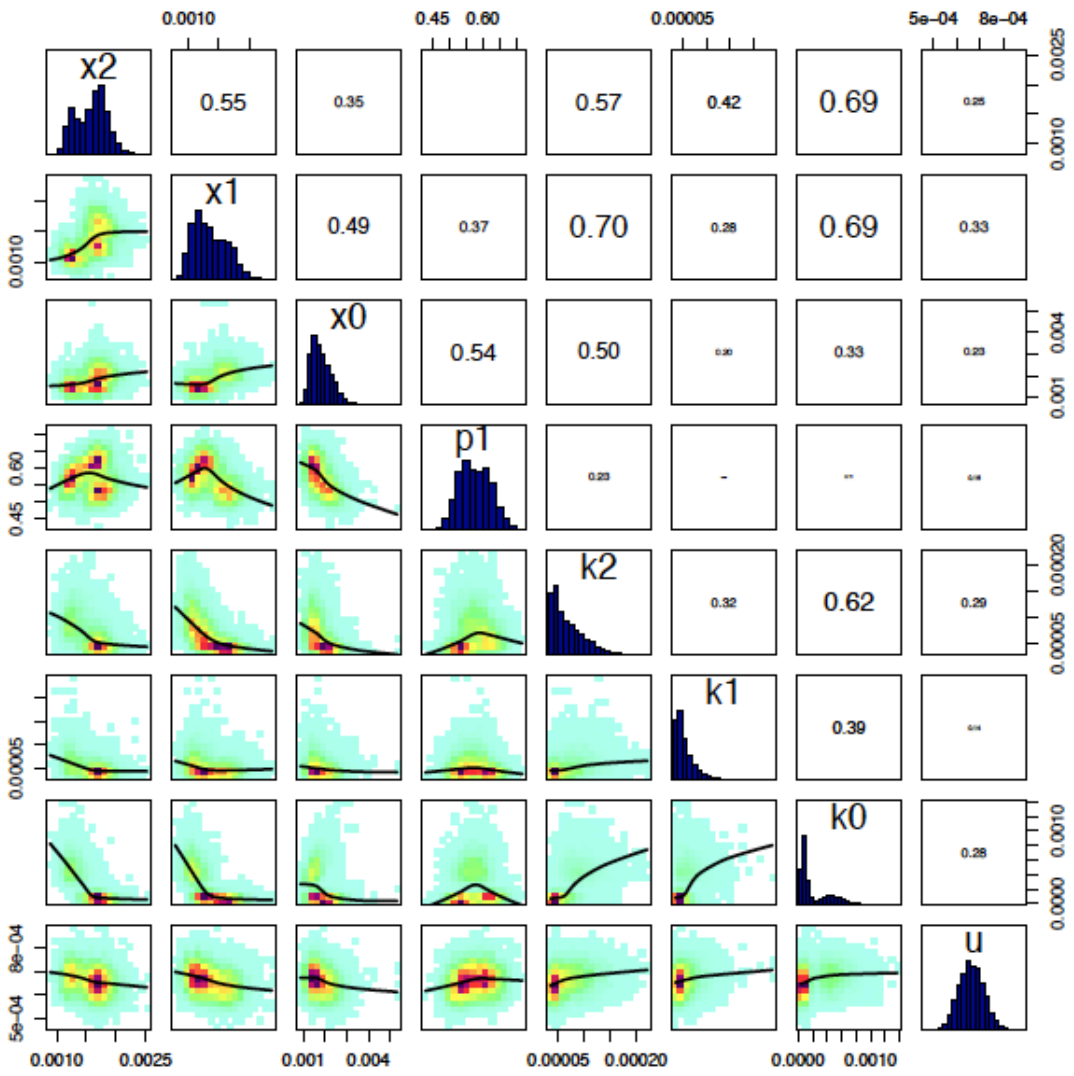

Figure S4-2: Correlations between parameter posteriors of model fit on control scenario with r_i fixed. Marginal posteriors are depicted on the diagonals. The numbers on the right of the diagonal depict the correlation coefficients for each side by side comparison.

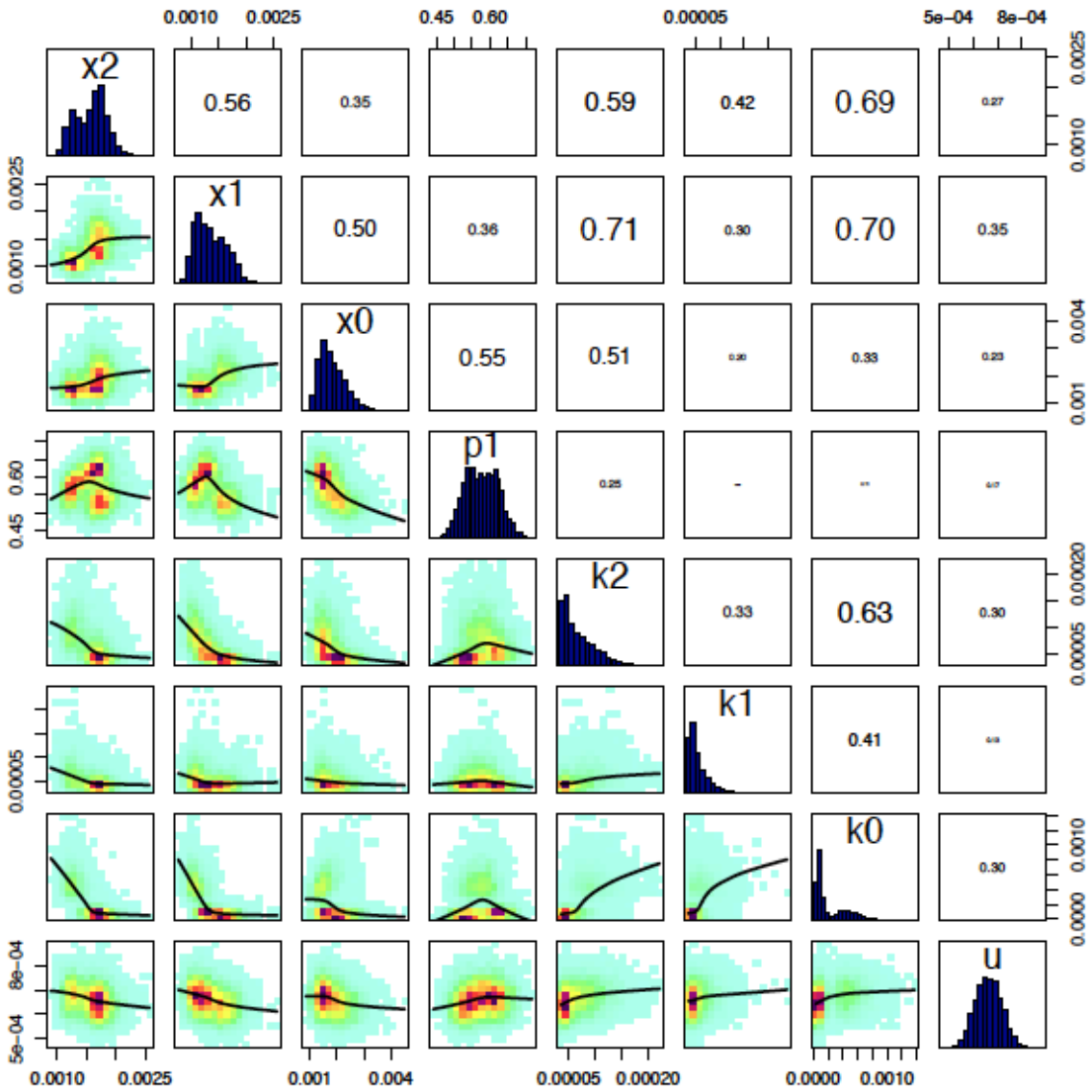

Figure S4-3: Correlations between parameter posteriors of model fit on low dosage scenario with r_i fixed. Marginal posteriors are depicted on the diagonals. The numbers on the right of the diagonal depict the correlation coefficients for each side by side comparison.

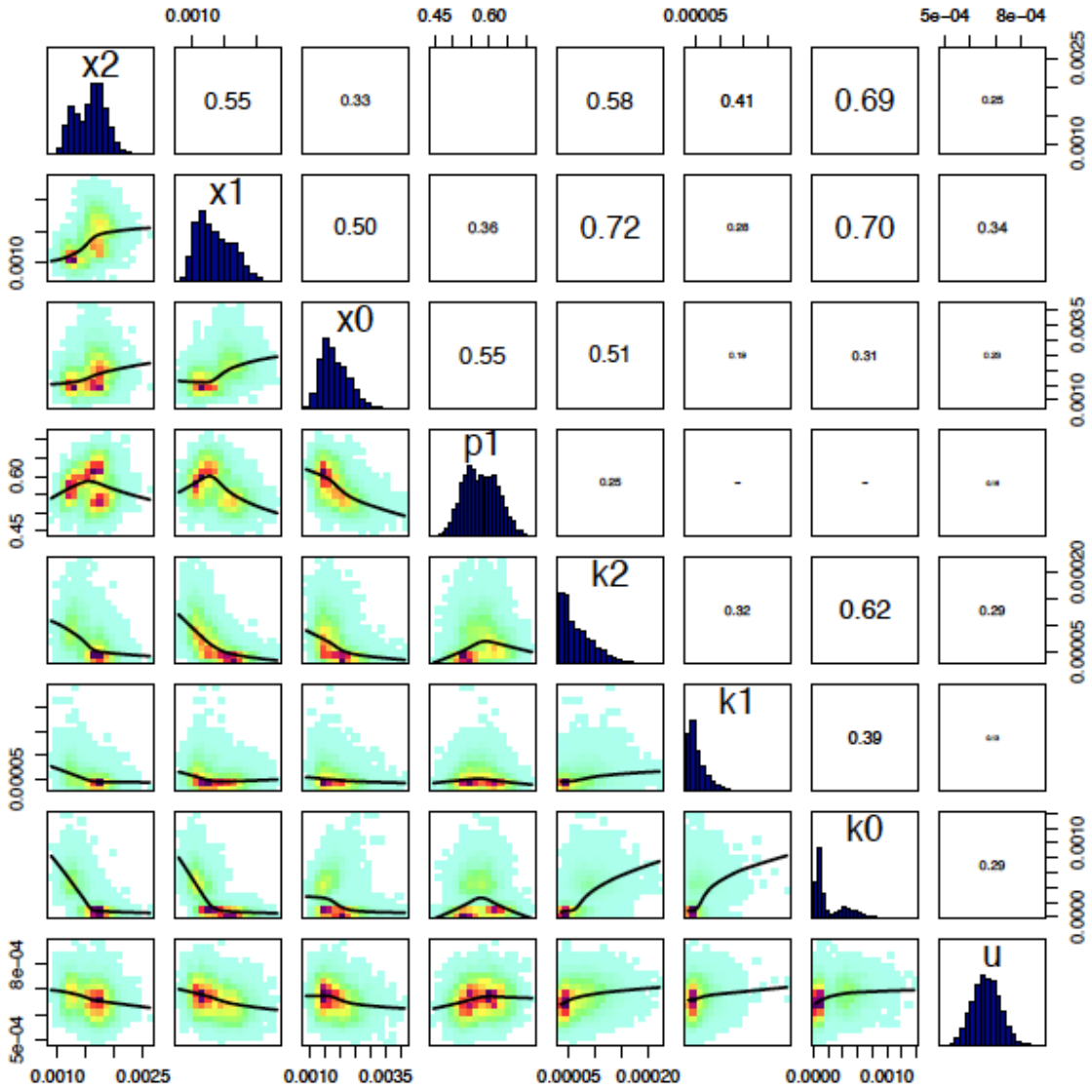

Figure S4-4: Correlations between parameter posteriors of model fit on high dosage scenario with r_i fixed. Marginal posteriors are depicted on the diagonals. The numbers on the right of the diagonal depict the correlation coefficients for each side by side comparison.

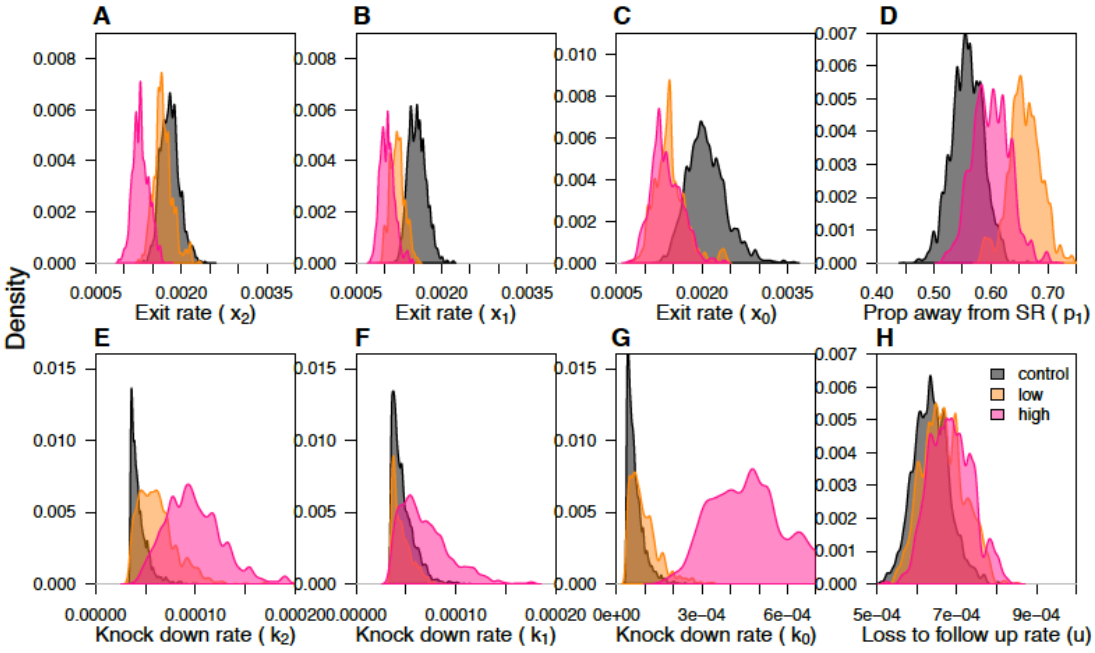

Figure S4-5: Posterior distributions of model parameters fitted to experimental data while fixing the values of r_i at the 2.5th percentile of the posterior from the full parameter fit to the control data. Posteriors are shown for the control (gray), low dosage (orange) and high dosage (pink) for the SR-hut (subscript 0) and huts 2 or 1 removed (subscript 2 and 1 respectively). A-C) rates at which mosquitoes exit the huts D) proportion of movement from H_1 (hut directly adjacent to the treatment hut) away from the SR-product. E-G) knockdown rates, and H) loss to follow-up rates. The algorithm was run for 25,000 iterations with a burn-in period of 10,000.

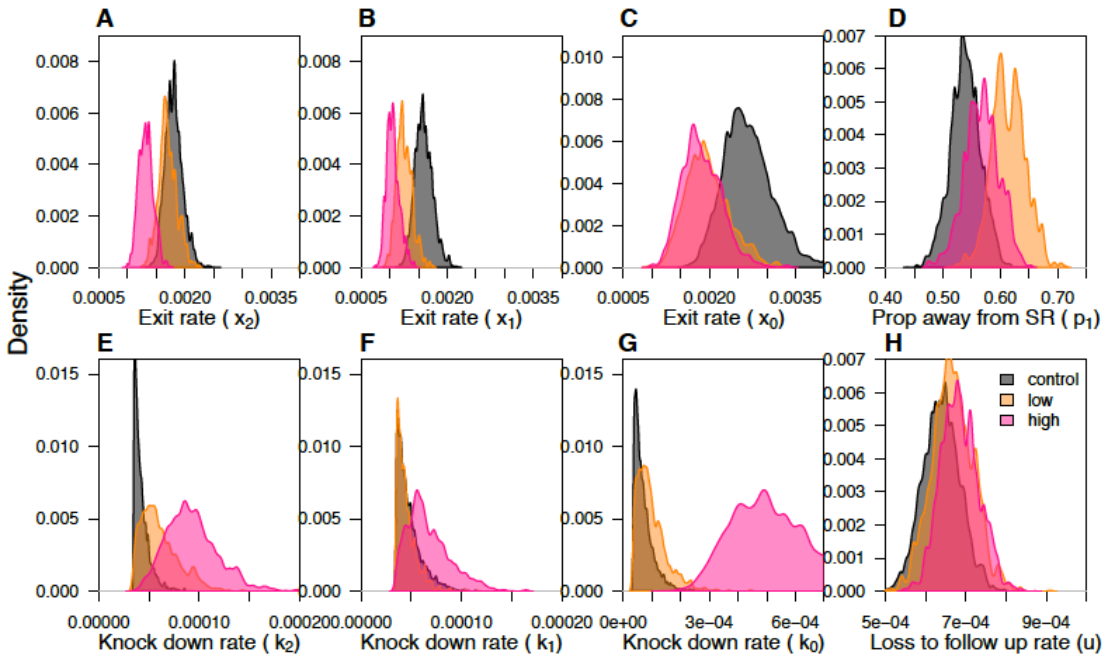

Figure S4-6: Posterior distributions of model parameters fitted to experimental data while fixing the values of r_i at the 97.5th percentile of the posterior from the full parameter fit to the control data. Posteriors are shown for the control (gray), low dosage (orange) and high dosage (pink) for the SR-hut (subscript 0) and huts 2 or 1 removed (subscript 2 and 1 respectively). A-C) rates at which mosquitoes exit the huts D) proportion of movement from H_1 (hut directly adjacent to the treatment hut) away from the SR-product. E-G) knockdown rates, and H) loss to follow-up rates. The algorithm was run for 25,000 iterations with a burn-in period of 10,000.

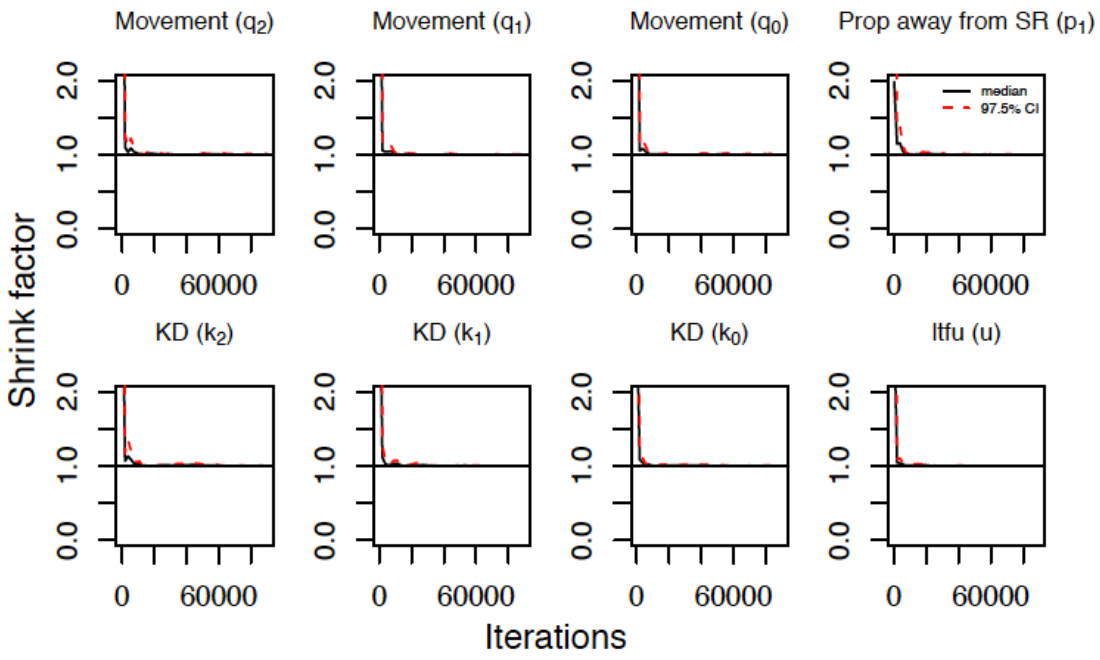

Figure S4-7: Gelman-Rubin convergence diagnostics by iteration for the control scenario.

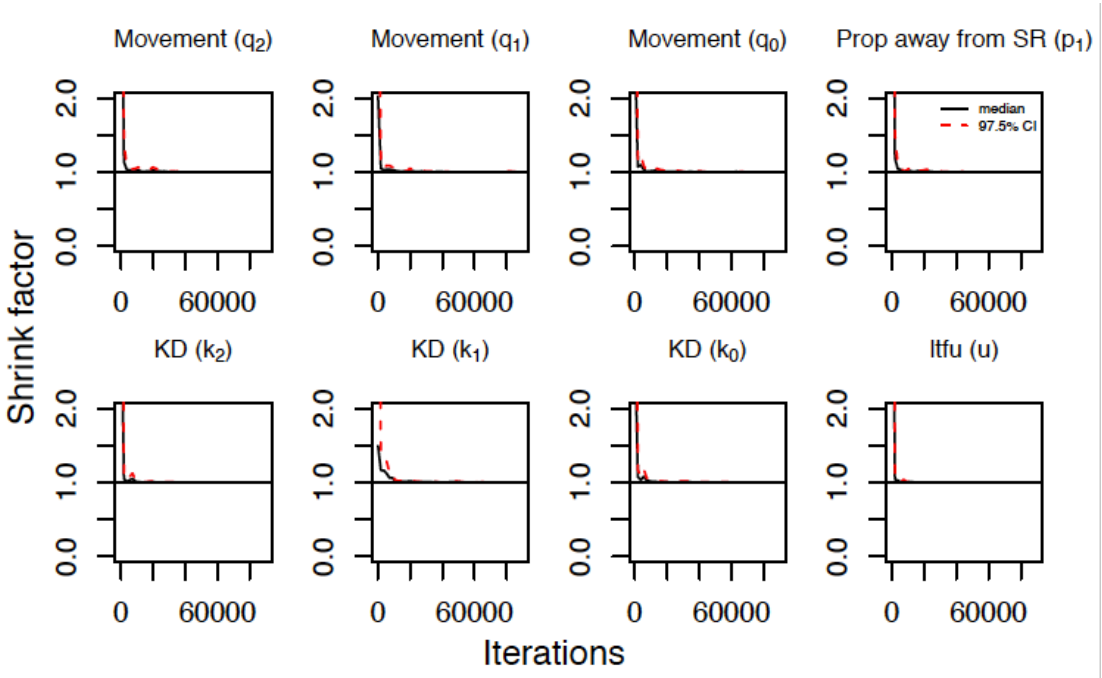

Figure S4-8: Gelman-Rubin convergence diagnostics by iteration for the low dosage scenario.

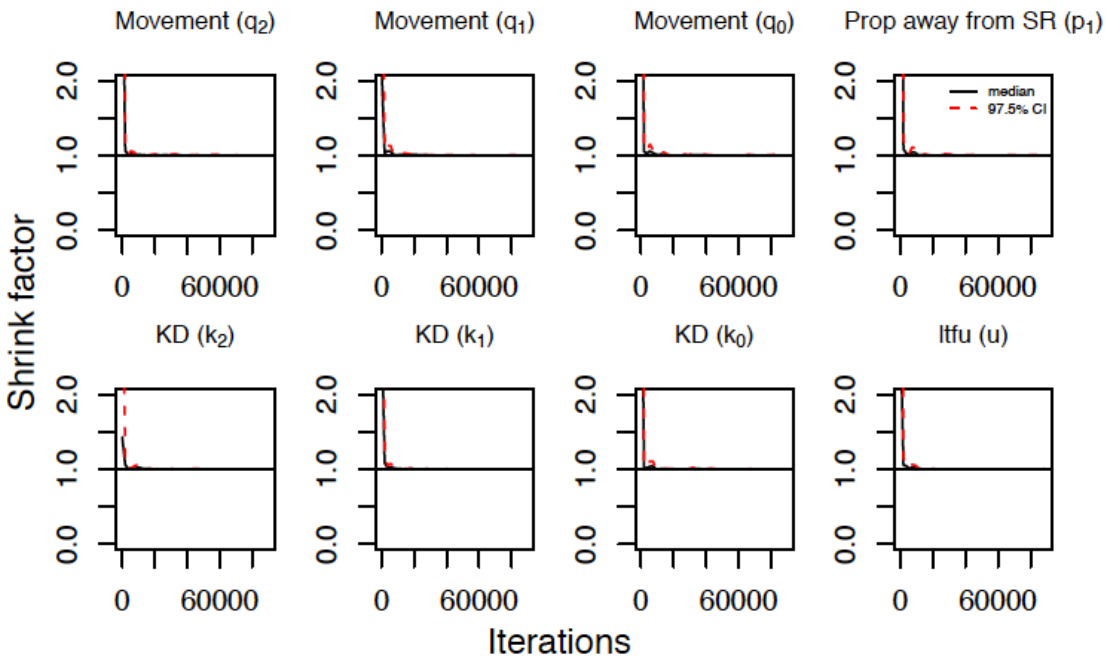

Figure S4-9: Gelman-Rubin convergence diagnostics by iteration for the high dosage scenario.

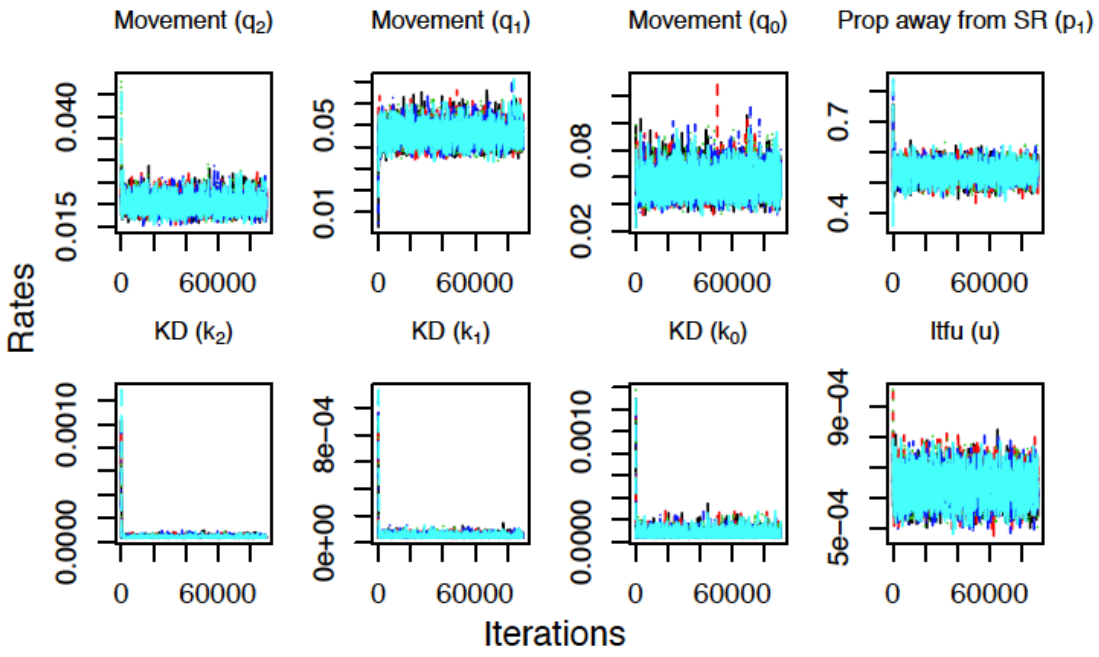

Figure S4-10: Trace plots for the control scenario.

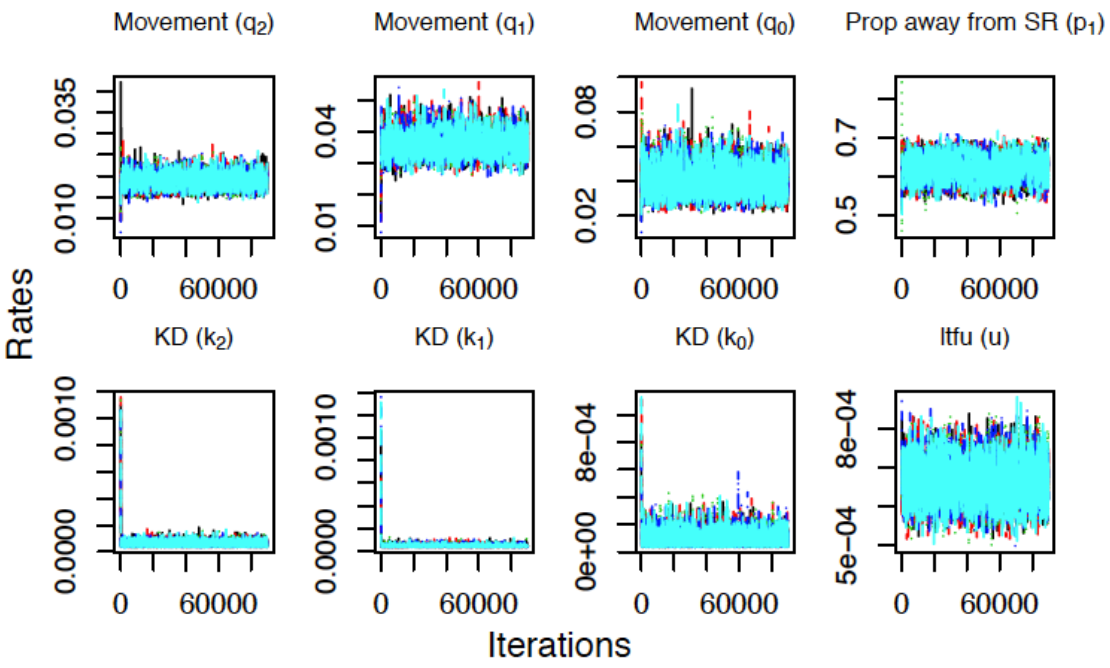

Figure S4-11: Traceplots for the low dosage scenario.

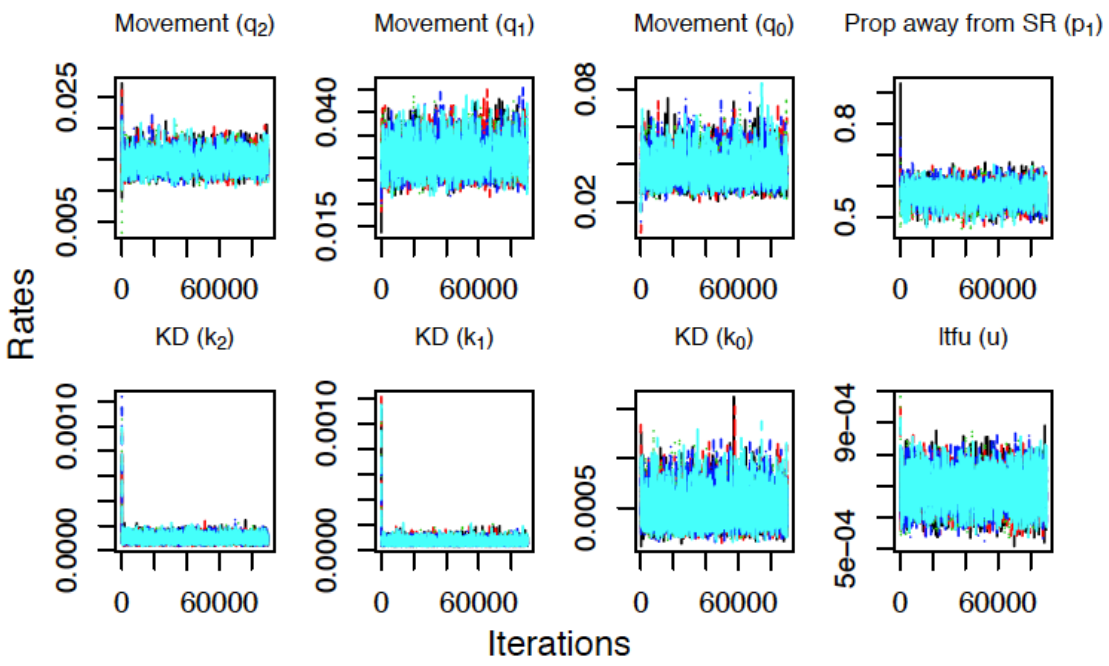

Figure S4-12: Traceplots for the high dosage scenario.

CHAPTER 5:

IT TAKES A VILLAGE: COMMUNITY-LEVEL IMPACTS OF SPATIAL REPELLENTS FOR MOSQUITO-BORNE DISEASE CONTROL

Quirine A. ten Bosch, Joseph Wagman, Fanny Castro-Llanos, Steven T. Stoddard, Amy C. Morrison, Neil F. Lobo, Nicole L. Achee, John Grieco, T. Alex Perkins

5.1 Abstract

Despite some limited successes, vector control has not been able to curb the spread of dengue and other arthropod-borne viruses (arboviruses). One important component of future strategies for arboviral disease control is the development of new, broadly applicable tools to augment currently available options. Spatial repellents (SRs) constitute one set of tools that could play an important role moving forward. These sub-lethal products are aimed at reducing human-vector contact by preventing the entrance of mosquitoes into human-occupied spaces or by interfering with host detection and blood feeding. Many compounds exhibit a combination of these modes of actions. Complex interactions thereof exceed the capability of existing theory for vector-borne disease control to make quantitative projections of epidemiological impact. Here, we used data from entomological experiments involving a transfluthrin-based SR product on *Aedes aegypti* behavior and bionomics to estimate the proportional reduction in dengue virus force of infection due to the combined effects of repellency, irritancy, and toxicity. Our results show that the greatest contribution to the SR's impact derives from toxicity but

that substantial impact is still possible in the absence of toxic effects, due to delayed biting and associated negative population feedbacks. The extent of this impact varies by population coverage, product formulation, and the density of housing within a covered area. In addition, we demonstrate adverse impacts of probing (increased partial blood meals per feeding cycle) and reduced exit rates, and we highlight how those effects could offset gains achieved by other effects. Our theoretical framework provides a way to leverage results from small-scale experiments to derive expectations of how multiple behavioral and bionomic effects of novel vector control products may impact arbovirus epidemiology when deployed at much larger scales.

5.2 Introduction

In recent decades, significant progress has been made in reducing the burden of malaria, in part due to the success of insecticide treated nets (ITNs) (1). Similar public health successes of vector control have been achieved in the control of dengue (DENV) and yellow fever viruses (2-4), but none of these were sustainable (5). The unabated rise of DENV, as well as the recent emergence of other *Aedes aegypti* borne diseases such as Zika and chikungunya, highlights the failure of vector control to prevent outbreaks and global expansion (6). Nonetheless, it has been recognized that even as alternative tools such as vaccines become available, vector control will remain an indispensable tool in the control of mosquito-borne pathogens (MBPs) (7). Hence, there is an eminent need for new, broadly applicable vector control tools and more effective implementation strategies.

Spatial repellents (SRs) constitute one such paradigm for vector control in a public health context. SRs consist of sub-lethal products aimed at reducing human-vector contact through either movement away from the product or interference with host detection and/or blood feeding. The effectiveness of SR products has been shown in several entomological studies, demonstrating significantly reduced blood feeding in *Ae. aegypti* (8, 9). Studies on epidemiological effects of SRs on DENV transmission are in their early stages of implementation, but promising results have been shown in reducing malaria transmission (10-12).

Diversion of mosquitoes to untreated houses has been found to offset beneficial community-level effects in some cases (13, 14) but were found to be outweighed by other

beneficial effects in others (15-17). As such, the community-level effects of SRs are yet to be determined and likely to be context- and product-specific.

Spatial repellency is distinct from other chemically induced effects such as contact irritancy and lethality. However, most compounds exhibit a combination of these modes of action; i.e., repellency (preventing entry), expellency (promoting exit), reduced biting, and lethality. In addition, irritant effects could promote adverse behaviors such as reduced exiting or probing, wherein irritated mosquitoes take multiple, partial blood meals prior to full engorgement and oviposition (18). This could result in an increased overall biting rate but may still delay the time until oviposition or increase the risk of dying associated with blood feeding. Similarly, reduced exiting does not per se result in an increased probability of blood feeding at a particular house, as the irritancy that leads to reduced exiting may also be accompanied by reduced blood feeding (9). The combination and magnitude of these various effects depend on the formulation of the SR product and the dosage used (19). In addition, the community-level impact may differ substantially across settings with different types of structures and housing density, outdoor and indoor mosquito predators, and additional vector control efforts, among other factors. The complex interplay of these effects complicates predictions of the epidemiological impact of SRs and other vector control products.

Examining the many possible combinations of effects that different products have and addressing their context-specificity in field trials would be extremely costly, if not altogether unfeasible (20). Modeling has therefore been used as a tool to augment our understanding of the epidemiological impact of combinations of effects of other vector control tools, namely insecticide-treated nets (ITNs) (21-23). Insights have been gained

on both the individual- and community-level impact of various products and combinations thereof (24, 25), including explorations of circumstances with adverse diversion effects (22), the impacts of insecticide resistance (26, 27), and product decay (27).

Here, we extend previous models of the combined effects of vector control products by considering a broader range of effects, including repellency and expellency, irritant effects on biting, distinguishing probing from time until oviposition, and examining the context specificity of the epidemiological impact. Specifically, we use data from small-scale entomological experiments of a transfluthrin formulation on *Aedes aegypti* bionomics to estimate the relative change in dengue virus (DENV) force of infection (a variable we denote as *FoI*) brought about by a product with such properties introduced into a community at a given coverage. This integration of experimental results and novel metrics of transmission serves as a proof of principle of how modeling can be used to scale up results from small-scale experiments into estimates of community-level impacts.

5.3 Methods

Our approach involved 1) the development of new mathematical theory to project the epidemiological impact of vector control products with multiple effects on mosquito behavioral and bionomic traits; 2) the collection and analysis of experimental data to quantify those effects; and 3) sensitivity analyses of the model-based estimates of community-level impact informed by experimental results. At the time of publication, code used to perform the statistical and mathematical analyses will be made available on GitHub, and experimental data will be made available on DataDryad.

5.3.1 Mathematical framework

To estimate the community-level impact of vector control (VC) products that potentially affect transmission through multiple behavioral and bionomic traits, we extended a modeling framework rooted in classical epidemiological theory (28). We assumed a well-mixed community in which each house has a probability of being protected by the VC product at any given time equal to coverage *C*. Consequently, upon searching for a blood meal, mosquitoes encounter a treated house with probability *C*, assuming the possibility of repellency or attraction of the product can only occur once the mosquito has "encountered" the house at close proximity. Below, we describe the effects that the product may have on a mosquito once it makes such an encounter, how those effects scale with coverage *C*, and how those scaled effects impact the force of infection of a mosquito-borne pathogen transmitted in a community in which these interventions are deployed (Figure 5-1).

Figure 5-1: Schematic of multiple effects of SR products on mosquito behavioral and bionomic traits and their impact on mosquito-borne pathogen transmission. Each row presents a potential scenario for a mosquito after it has become infected, in the absence (top row) or presence (other rows) of the SR. On the left, flight behavior in search for blood meals or oviposition sites (containers) is depicted in untreated (gray) and treated houses (pink). On the right, the mosquito's life span after human-to-mosquito transmission is shown, with the duration of the extrinsic incubation period (EIP) (dashed white line) and the infectious period (solid white line). Blood meals (full or partial) may result in mosquito-to-human transmission (red human) once the EIP is over, but not before (white humans). Once a mosquito is fully blood fed, it searches for an oviposition site, after which the next gonotrophic cycle starts. Scenarios presented from top to bottom are: A) the baseline in the absence of the SR, B) reduced mosquito life span as a result of toxic effects of the SR (μ or ϕ), C) reduced blood feeding and prolonged gonotrophic cycle as a result of repellency (ρ), irritancy (α and o), and expellency (increase in exit rate q), and D) increased blood feeding and prolonged gonotrophic cycle due to increased partial blood feeding (α) but prolonged time until fully blood fed (o). (Page 175)

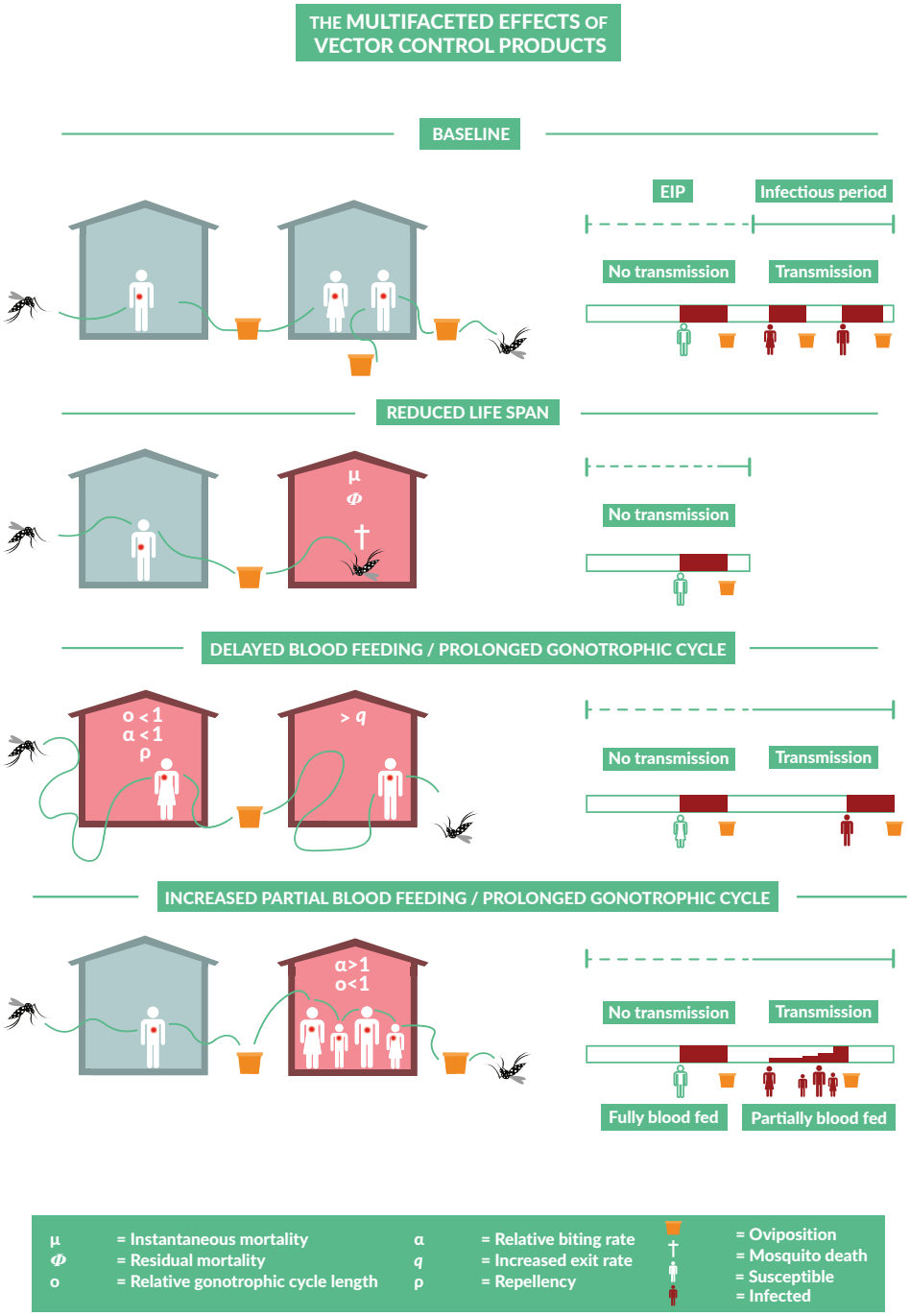
THE MULTIFACETED EFFECTS OF VECTOR CONTROL PRODUCTS
BASELINE
EIP
Infectious period
No transmission
Transmission
REDUCED LIFE SPAN
μ
Φ
†
No transmission
DELAYED BLOOD FEEDING / PROLONGED GONOTROPHIC CYCLE
o < 1
α < 1
ρ
> q
No transmission
Transmission
INCREASED PARTIAL BLOOD FEEDING / PROLONGED GONOTROPHIC CYCLE
α>1
o<1
No transmission
Transmission
Fully blood fed
Partially blood fed
μ = Instantaneous mortality
Φ = Residual mortality
o = Relative gonotrophic cycle length
α = Relative biting rate
q = Increased exit rate
ρ = Repellency
= Oviposition
= Mosquito death
= Susceptible
= Infected

5.3.1.1 Entomological effects: Delayed blood-feeding

Mosquitoes seeking a human blood meal encounter an SR product with probability C, upon which the product may repel them with probability ρ. It is expected that when this occurs, mosquitoes will take an average amount of time τ to move to another house. Due to various behavioral and physiological responses associated with the irritancy effect of the product, a mosquito that does enter a treated house may delay its feeding by a proportion $1/\alpha$ of the entire feeding cycle, which has an average length $1/a$ in the absence of the SR. In addition, the expellency effect of the intervention may reduce the time a mosquito spends in the house from $1/q_U$ to $1/q_T$, on average.

To arrive at an estimate of the overall delay in blood feeding that results from the combination of these aforementioned effects, we first calculated the average delay associated with each of these events weighted by the probability of each such event. In the event that a mosquito encounters a treated house but does not enter it, which occurs with probability $C\rho$, the delay before the next house is visited is simply the transit time τ. In an untreated house, which mosquitoes enter with probability $1-C$, a mosquito may not blood feed before leaving the house with probability $e^{-\frac{a}{q_U}}$. The delay associated with this is $1/q_U+\tau$. In a treated house, which mosquitoes enter with probability $C(1-\rho)$, a mosquito may not bite before leaving the house with probability $e^{-\frac{a\alpha}{q_T}}$. The delay associated with this is $1/q_T+\tau$. Together, the probability of one of these three events occurring is $D=C\rho+C\left(1-\rho\right)e^{-\frac{a\alpha}{q_T}}+\left(1-C\right)e^{-\frac{a}{q_U}}$, and the expected delay conditional on one of these events occurring is

$$\delta = \frac{\tau C\rho + \left(\frac{1}{q_T} + \tau\right)\left(C(1-\rho)e^{-\frac{a\alpha}{q_T}}\right) + \left(\frac{1}{q_U} + \tau\right)\left(\left(1-C\right)e^{-\frac{a}{q_U}}\right)}{D}. \quad (11)$$

We next considered that multiple such delays could occur consecutively. If the probabilities of experiencing one of these delays from one blood-feeding attempt to the next are independent, then the expected number of delays before successful blood feeding is D / (1 – D). To capture these effects within a single modified biting rate a_C, we can equate the reciprocal of that biting rate with the average time until a successful blood meal, which is

$$\frac{1}{a_C} = \delta\frac{D}{1-D} + \frac{1}{a}. \quad (12)$$

5.3.1.2 Entomological effects: Mortality

Mosquitoes exposed to the lethal effects of the product are assumed to die with probability μ within a relatively short timeframe after entering the house in the event that they are undeterred by the repellent effect of the product. In addition, exposure to the product may have additional overall fitness costs that increase the death rate of the mosquito (g_T). Lastly, a mosquito that is successfully repelled by the product may experience additional hazards while it is transitioning to another house, experiencing a death rate g_τ during transition. The interplay of these lethal effects augments the background mortality rate g in the absence of vector control to result in a new overall mortality rate g_c in the presence of an SR product at coverage C. The new overall mortality rate follows from the sum of the death rates associated with each of three states

(in transit (Δ), present in a treated (T) or untreated house (U)), weighted by the proportion of time spent in each state.

To derive the proportion of time spent in each state, we consider a Markov chain with states {Δ, U, T} and infinitesimal matrix (29)

$$\boldsymbol{A}=\begin{pmatrix} \frac{1}{\tau}\left(\rho C-1\right) & \frac{1}{\tau}\left(1-C\right) & \frac{1}{\tau}\left(1-\rho\right)C \\ q_U & -q_U & 0 \\ q_T & 0 & -q_T \end{pmatrix}. \tag{13}$$

The transition probabilities $\mathbf{P}_{ij}$ (t) satisfy a system of differential equations with rates **A** known as the backward Kolmogorov differential equations (29)

$$\frac{dP}{dt}=\boldsymbol{A}\boldsymbol{P}(t), \tag{14}$$

where $\frac{dP}{dt}$ follows from the rates of change in each state

$$\begin{aligned} \frac{d\Delta}{dt}&=\frac{1}{\tau}\left(\rho C-1\right)\Delta+q_U U+q_T T \\ \frac{dU}{dt}&=-q_U U+\frac{1}{\tau}\left(1-C\right)\Delta \\ \frac{dT}{dt}&=-q_T T+\frac{1}{\tau}\left(1-\rho\right)C\Delta. \end{aligned} \tag{15}$$

At equilibrium $\frac{dP}{dt}=0$ and so the stationary distribution $\lim_{t\to\infty}\boldsymbol{P}(t)=\pi=\left(\pi_\tau,\pi_U,\pi_T\right)$ follows from eqn. (14) and the notion that the probabilities must sum to one. Solving $0=\boldsymbol{A}\boldsymbol{P}(t)$ under that condition gives a description of the probability at any given time that a mosquito is in a given state

$$\pi_\tau = -\frac{\tau q_U q_T}{q_U C(\rho-1)+q_T(C-\tau q_U-1)}$$
$$\pi_U = \frac{(1-C)\pi_\Delta}{\tau q_U} = \frac{(C-1)q_T}{q_T(C-\tau q_U-1)+C(\rho-1)q_U} \quad (16)$$
$$\pi_T = \frac{(1-\rho)C\pi_\Delta}{\tau q_T} = \frac{C(\rho-1)q_T}{q_T(C-\tau q_U-1)+C(\rho-1)q_U}.$$

The average mortality rate g_c under coverage C then follows by taking the probabilities from eqn.(16) and using them to weight the state-specific probabilities μ, gT, and gU according to

$$g_c = \pi_T(\mu q_T + g_T)+\pi_U g_U + \pi_\tau g_\tau. \quad (17)$$

5.3.1.3 Entomological effects: Mosquito density

We assume that effects of the SR product on mosquito density act through effects on demographic processes; i.e., birth and death. A general form for equilibrium mosquito density is $m = \varepsilon / g$, where ε is the rate of emergence of new adult mosquitoes and g is death rate. One formulation of the emergence rate ε is that it is the product of the expected number of blood meals that each mosquito takes over the course of its lifetime and a combination of immature-stage mortality and development rates(30). We treat the latter as an unspecified constant and the former as the product of the rate of oviposition o and the expected lifetime $1/g$, implying that $m_c \propto o_c / g_c^2$.

5.3.1.4 Epidemiological impact

We use the force of infection (*FoI*) as our focal metric for quantifying the epidemiological impact of the SR product. *FoI* is defined as the rate at which susceptible

individuals become infected. In Ross-Macdonald models of mosquito-borne pathogen (MBP) transmission, $FoI = bmaY$, where b is the probability that a human becomes infected after being bitten by an infectious mosquito, m is the ratio of mosquitoes to humans, a is the rate at which a mosquito engages in blood feeding (either partial or full blood-feeding), and Y is the prevalence of infection among mosquitoes (31, 32). The latter depends further on the daily mosquito mortality rate g, the incubation period n in the mosquito, the probability c that a mosquito becomes infected upon biting an infectious human, and the prevalence of infection in humans according to

$$FoI = bmaY = \frac{bma^2cXe^{-gn}}{g+acX}. \tag{18}$$

Under equilibrium assumptions in an *SIS-SI* malaria model, X can in turn be solved for as a function of model parameters (32). Under non-equilibrium assumptions, however, the formulation in eqn. (18) is equally valid for other types of compartmental models (e.g., SEIR-SEI) provided that X is regarded as an unknown parameter, which is appropriate given its highly dynamic and uncertain nature for many MBPs.

To derive an expectation for how FoI will change in response to an SR, we can take the ratio of the expression in eqn. (8) evaluated with parameter values reflecting the intervention at a given coverage C against the expression evaluated with parameter values reflecting conditions in the absence of the SR. We allow for the possibility that any or all of m, a, o, and g may change in response to the SR. This results in a ratio of FoIs of

$$FoI_{rel} = \frac{FoI_c}{FoI} = \frac{m_c o_c a_c}{moa}\frac{g+acX}{g_c+a_cX}e^{-(g_c-g)n}. \tag{19}$$

Substituting the result $m_c \propto o_c / g_c^{\,2}$ into eqn.(19), we obtain

$$FoI_{rel} = \frac{o_c a_c^2 g_c^2}{o a^2 g^2} \frac{g + acX}{g_c + a_c cX} e^{-(g_c - g)n}, \quad (20)$$

which effectively depends on the effects of the intervention on rates of blood feeding and mortality, as well as three free parameters, C, X, and n.

5.3.2 Collection of experimental data

5.3.2.1 SR effect on blood feeding

Ae. aegypti populations from Thailand (n=125 for each arm, F_5) were exposed to the SR product (transfluthrin) or a placebo for 10 minutes using a high-throughput screening mechanism (33). An hour after exposure, mosquitoes were allowed to blood feed (membrane feeding). After a predefined follow up time, mosquitoes were dissected and recorded as fully blood-fed, partially blood-fed, or not blood-fed. The experiment was repeated for seven follow-up times (0, 1, 3, 6, 12, 24, and 48 hours) and 3 different dosages (0, 1, and 1.5 times the field application rate, FAR=8.4×10^{-7} g/L). Each experiment was performed at 80 °F and 75% humidity.

5.3.2.2 SR effect on mortality

Ae. aegypti mosquitoes (n=120 for each arm, F_5) from the same population as those used in the blood-feeding experiment were exposed to the SR product or a placebo as described above, after which they were returned to the insectary. Adult survival was monitored on a daily basis for a total duration of 25 days. The experiment was repeated for a control regimen and five different treatment dosages (FAR 0, 0.5, 0.75, 1, 1.25, 1.5). Each experiment was performed at 80 °F and 75% humidity.

5.3.2.3 SR effect on repellency and expellency

To quantify the spatial repellency effect of SR on *Ae. aegypti* under field conditions, an experimental hut study was performed similar to the one described by Grieco et al. (34). A unique design was employed in which five experimental huts were set up in a row design with the adjoining walls containing open eave gaps that create a continuum of indoor space. This design mimics a housing structure common to Iquitos, Peru, as well as other dengue-endemic areas. Each 4 m x 6 m x 2 m hut was equipped with two exit traps. The center hut was treated with the SR product or the placebo. In each of the huts, a human was present under an untreated bed net to generate host-seeking cues and to monitor knockdown. For each experiment, 5-7 day old, sugar-fed mosquitoes (n=25, $F_{2\text{-}3}$), marked according to release hut, were released inside each hut except the treated hut at 5:30 AM. Exit traps were checked every 30 minutes from 6:00 AM until 6:00 PM, and knockdown was monitored hourly within this time frame. At 6:00 PM, remaining mosquitoes were recaptured using aspirators, and their release and recapture locations were recorded. The experiment was repeated five times for three different treatments relative to the field application rate of 0.04g/m^2 (FAR 0, 1/8, 1/16) (see Chapter 4 for a full description of the experiment).

5.3.3 Analysis of experimental data

5.3.3.1 SR effect on blood feeding

Mosquitoes in the blood-feeding experiment could have experienced three different outcomes: partially blood-fed, fully blood-fed, or not blood-fed. We consider the biting rate *a* referred to previously as the sum of the rates of partial and full blood

feeding, a_p and a_f, respectively. We modeled these rates as functions of the dose of transfluthrin, x_{dose}, as

$$a_p(x_{dose}) = \frac{1}{e^{(\beta_{p,0}+\beta_{p,1}x_{dose})}} \tag{21}$$

and

$$a_f(x_{dose}) = \frac{1}{e^{(\beta_{f,0}+\beta_{f,1}x_{dose})}}. \tag{22}$$

We assume that a mosquito can potentially take multiple partial blood meals, with a single partial blood meal having no impact on the probability of taking another partial blood meal or a full blood meal. We assume that full blood meals are absorbing states, however, in the sense that a full blood meal prevents any further blood feeding thereafter within the timeframe of the experiment.

Under these assumptions, the expected number of partial blood meals after time t given $a_{\text{p}}(x_{\text{dose}})$ is $a_{\text{p}}(x_{\text{dose}})t$, provided that blood feeding follows a Poisson process. This results in the probability of k partial blood meals after time t being described by a Poisson distribution with rate parameter $a_{\text{p}}(x_{\text{dose}})t$. Similarly, the probability of a full blood meal to have occurred by time t is the complement of the probability that no full blood meal has occurred by that time; i.e., $1-e^{-a_f(x_{dose})t}$.

The number of fully blood-fed mosquitoes observed in the experiment includes both mosquitoes that were fully engorged after one meal, as well as those that became fully engorged after multiple partial blood meals. Therefore, the probability for a mosquito to be partially blood-fed is the probability of the intersection of $k_p > 0$ and $k_f = 0$, which is

$$\Pr(B_p) = \Big(1 - \Pr(k_p = 0)\Big)\Big(\Pr(k_f = 0)\Big). \quad (23)$$

$\Pr(k_f = 0)$ is the probability of observing a mosquito that is not blood fed and equals

$$\Pr(B_0) = \Pr(k_p = 0)\Pr(k_f = 0), \quad (24)$$

and the probability of observing a fully blood-fed mosquito is

$$\Pr(B_f) = 1 - \Pr(B_p) - \Pr(B_0). \quad (25)$$

Using the probabilities in eqns. (23)-(25) and the observed number of mosquitoes (n) in each feeding category, we calculated the likelihood of the model parameters given the observed data as

$$L = P_{multinom}(\beta_{p,0}\beta_{p,1}\beta_{f,0}\beta_{f,1} \mid n_p, n_f, n_0). \quad (26)$$

We optimized this likelihood using the bbmle package (35) in R to derive our best estimates of the coefficients $\beta_{p,0}$, $\beta_{\mathrm{p},1}$, $\beta_{f,0}$, and $\beta_{\mathrm{f},1}$ in eqns. (21) and (22) that describe the dosage effects of the SR on the biting rates a_p and a_f.

5.3.3.2 SR effect on mortality

We used the data collected during the longevity experiments to estimate two distinct lethality effects: instantaneous (μ) and residual (g_{T}) lethality. To disentangle these effects, we consider observed death and survival over the course of day 1 to be informative of μ and any death and survival thereafter to be informative of g_{T}.

Over the course of day 1, we assumed that the number of mosquito deaths was a binomial random variable with probability μ with relationship to transfluthrin dose x_{dose} defined by

$$\mu(x_{dose}) = e^{\left(\beta_0 + \beta_1 x_{dose}\right)}. \quad (27)$$

We obtained maximum-likelihood estimates of β_0 and β_1 using the bbmle package (35) in R (36).

Conditional on surviving day 1, the data consist of a set of interval- and right-censored time-to-event data (37). Let T be a random variable representing the time until death, $f(T=t)$ its probability density function (pdf), and $F(T=t)$ its cumulative distribution function (cdf). The complement of the cdf is the survival function $S(t)$; i.e.,

$$S(t) = \Pr\{T \geq t\} = 1 - F(t) = \int_t^{\infty} f(x)dx, \tag{28}$$

which describes the probability that death has not yet occurred by time t. A related characterization of the distribution of T, and fundamental to survival analysis, is the hazard function, $\lambda(t)$ (37). The hazard denotes the instantaneous rate at which death occurs and is described as the probability that death occurs between time t and time $t+dt$, given that it has not occurred before t, taking the form

$$\lambda(t) = \lim_{dt \to 0} \frac{\Pr\{t \leq T < t + dt \mid T \geq t\}}{dt}. \tag{29}$$

The hazard rate can be written as the ratio of the joint probability that T is in the interval $[t,t+dt]$ and that $T>t$

$$\lambda(t) = \frac{f(t)}{S(t)}. \tag{30}$$

To estimate the effect of dosage on the hazard rate over time, we fitted different survival models to the time-to-event data collected in the laboratory experiments. A specific feature of these data is censoring; for some mosquitoes, death has not yet occurred by the end of the study and thus we only know that T exceeds the observation time. An

important assumption here is that this censoring – i.e., the end of the observation time – is independent of the probability of an event occurring after the censoring time.

For uncensored mosquito *i*, we can express the likelihood of a given model of the hazard conditional on an observed event time $T=t_i$ as the product of $S(t)$ (i.e., the probability of surviving to t) and $\lambda(t)$ (i.e., the probability that the event occurs at time t) as

$$L_i = f(t_i) = S(t_i)\lambda(t_i). \tag{31}$$

For censored observations, the likelihood function only reflects that T exceeds t_i

$$L_i = S(t_i). \tag{32}$$

We can write this into a single expression

$$L = \prod_{i=1}^{n} L_i = \prod_i \lambda(t_i)^{d_i} S(t_i), \tag{33}$$

where d_i is the event indicator and takes a value of 1 if the event has occurred before the end of the observation time and 0 otherwise.

The specific form of the hazard model that we seek to estimate is a function of the transfluthrin dose x_{dose}, expressed at time t as

$$\lambda_i(t \mid x_{dose}) = \lambda_0(t) e^{\beta_1 x_{dose}}, \tag{34}$$

where $\lambda_0(t)$ is the baseline hazard for individuals with x_{dose} equal to zero (i.e., the control group) and $e^{\beta_1 x_{dose}}$ is the relative risk associated with a specific dosage, which is assumed to be stable over time. Such proportional hazard (PH) models allow for a distinct separation of the effect of time from the effect of the covariate. This becomes clearer when we express the model in terms of the log of the hazards, finding a simple additive

model $\log \lambda_i(t \mid x_{dose}) = \alpha_0(t) + \beta x_{dose}$. We will assume that PH holds in this analysis, namely that the relative effects of the products do not change over time. We verified this assumption by performing a log transformation on the survival data (Figure S5-1) and assessed whether, under this transformation, the observations were parallel across dosages. Doing so tests our assumption that the effect of dosage on survival is additive.

The shape of the baseline hazard λ_0(t) affects the results of the final proportional hazards model. Under the assumption that the distribution of survival times is the result of a continuous-time stochastic process, one can use parametric survival models to describe λ_0(t) (37). We examined the performance of five candidate models with different assumptions about λ_0(t) (Table 5-3). The exponential model assumes a stable baseline hazard λ(t) = λ. Alternatively, the Weibull model allows λ(t) to monotonically increase or decrease over time: $\lambda(t) = v\lambda\left(\lambda t\right)^{v-1}$. The gamma distribution too allows for λ(t) to monotonically increase or decrease. There is no closed form for the hazard function of the gamma distribution. Whereas the exponential model describes the waiting time until the first event occurs in a Poisson process, the gamma describes the waiting time until *k* events occur. For comparable rate parameters *k* or *v* (Table 5-3), the hazard described by the Weibull distribution decreases more rapidly than in a gamma distribution. The lognormal model allows for an initial increase in λ(t) to be followed by a decrease as time progresses. Lastly, the generalized gamma distribution is an extension of the gamma distribution with an added scale parameter that allows for increased flexibility in λ(t). The gamma (v =1), Weibull ($\kappa = 1$), lognormal ($\kappa \to \infty$), and exponential ($\kappa = 1$ and v =1) models are all special, nested cases of the generalized gamma distribution. We used the Akaike Information Criterium (38) to select the best model, thereby accounting for

different numbers of parameters across models. The models were fitted and assessed using the survival package 2.27-7 (39) and the flexsurv package (40) in R 3.2.3 (36).

5.3.3.3 SR effect on repellency and expellency

The data collected in this experiment include competing interval-censored data on exit (30-minute intervals) and knockdown (hourly intervals) by event hut and release hut. In addition, mosquitoes recaptured at the end of the experiment represent right-censored data. Lastly, the mosquitoes not recaptured at any point during the experiment are considered to have been loss to follow-up at some unknown time before the end of the experiment.

The analysis of these data is detailed in Chapter 4. In brief, a continuous-time Markov Chain (CTMC) model is used to describe the probability for mosquitoes, over time and given their release location, to be in either hut or have experienced an outcome. At any time, a mosquito can either be in one of the five huts (transient states: H_{2L}, H_{1L}, H_0, H_{1R}, or H_{2R}), or have already experienced one of 15 events: exit, knocked-down, or loss to follow-up in any of the five huts (absorbing states: X_i, K_i, and U_i for $\forall i : i \in [2L,1L,1R,2R]$). The rates at which mosquitoes move either to adjacent huts or to an absorbing state are assumed to be independent of time or previous trajectories and thus the time spent in each transient state is exponentially distributed.

The parameters of the CTMC model were fitted to the data using a Bayesian Markov chain Monte Carlo (MCMC) approach, using the coda package (41) for processing of the results.

5.3.4 Sensitivity analysis of mathematical framework informed by experimental data

5.3.4.1 Baseline model parameterization

Six distinct entomological effects of the SR are defined by the probability of death upon encountering an SR (μ), increased mortality (ϕ), the probability of repellency (ρ), expellency (q_U/q_T), delayed blood feeding (α) expressed as a proportion of the mean rate of blood feeding in the absence of SR, and delayed oviposition (o) (Table 5-2). These parameters were derived from the longevity, blood feeding, and repellency experiments described above.

The probability of instantaneous death (μ) follows directly from eqn. (27). From the second part of the analysis of the mortality experiment, we estimated the reduction in time until death in response to the SR relative to the control group (ϕ) from the accelerated failure time survival models. The treatment-adjusted mortality rate is

$$g_T = g_U / \phi . \tag{35}$$

From the blood-feeding experiment, we estimated the blood feeding rate (aT) in a treated house as the fraction α of this quantity relative to the biting rate (a_U) in an untreated house, where we assume that the ratio of biting rates in treated and untreated houses is the same as the ratio of the biting rates in the treatment and control arms of the laboratory blood-feeding experiment. The oviposition rate (o) is estimated similarly, but solely relies on the rate at which mosquitoes become fully blood fed.

Repellency (ρ) is informed by the proportion of mosquitoes leaving an adjacent hut ($H_{1L \text{ or } 1R}$) that move away from rather than towards the treated hut (p_1 in Chapter 4). Assuming that in an untreated environment mosquitoes move to either neighboring hut

with an equal probability (i.e., p_1=0.5), the repellency effect relative to the untreated scenario is $\rho = 1 - \left(1 - p_{1_T} / 0.5\right)$. The rate at which a mosquito leaves a treated house relative to an untreated house follows from the fitted exit rates in (Chapter 4). The relative exit rate out of the treated house is a fraction q_U/q_T of the default rate q_U (Table 5-1).

5.3.4.2 Sensitivity and scenario analysis

For the baseline parameterization of the model, we assumed that exposures across experiments map to similar dosages in the population setting. This assumption is necessary for illustrative purposes, but it should be kept in mind that the level of exposure in real-life settings will differ from any experimental setting, in particular for the laboratory experiments. We examined a range of different combinations of bionomic effects to assess the sensitivity of our estimates to different product profiles and to quantify the uncertainty of our estimates. Further, we examined the impact of different assumptions on the free parameters (Table 5-1). We investigated the sensitivity of our relative *FoI* estimates across the range of realistically plausible values. In addition, the population-level effects of SRs may vary across settings. For instance, whereas densely populated areas could result in shorter travel times between houses (τ), this duration and associated hazards could be elevated in less densely populated settings due to increased distance and more abundant predators. The impacts of different transition times (τ), transition hazards (g_τ), and residence times ($1/q$) on our estimates of relative *FoI* by coverage were assessed in a similar fashion as the other free parameters.

5.4 Results

5.4.1.1 SR effect on blood feeding

Estimates of a_c were significantly reduced in comparison to estimates from the control ($\beta_{1,f}$: p=1.6x10^{-2}, $\beta_{1,p}$: p=6.3x10^{-17}, t-test, df = 24) (Table 5-2). The average time until blood feeding was increased by 22% (95% highest density interval HDI: 12-30%) after exposure to the SR product at FAR 1 and by 31% (HDI: 16-46%) at FAR 1.5 (Figure 5-2). This result was largely driven by a reduction in the rate at which full blood meals were taken, with the average time until a full blood meal increasing relative to the control by 45% (HDI: 33-58%) (FAR 1) and 75% (HDI: 52-97%) (FAR1.5). Part of this reduction in the rate at which full blood meals were taken was offset by an increase in partial blood meals (probing effect), but not enough to result in a net increase in blood-feeding rate. The partial blood-feeding rate increased in response to exposure by 17% (HDI: 4-29%) (FAR 1) and 24% (HDI: 6-40%) (FAR 1.5) relative to the control. The probability of blood feeding over time extrapolated by dosage was derived using eqns. (23) and (25) (Figure 5-2). We parameterized the biting rate (a_c) to be a fraction α of 0.82 (HDI: 0.76-0.89) (FAR 1) and 0.77 (HDI: 0.68-0.89) (FAR 1.5) and the oviposition rate (o_c) a fraction 0.69 (HDI: 0.63-0.75) (FAR 1) and 0.57 (HDI: 0.50-0.66) (FAR 1.5) (Table 5-2).

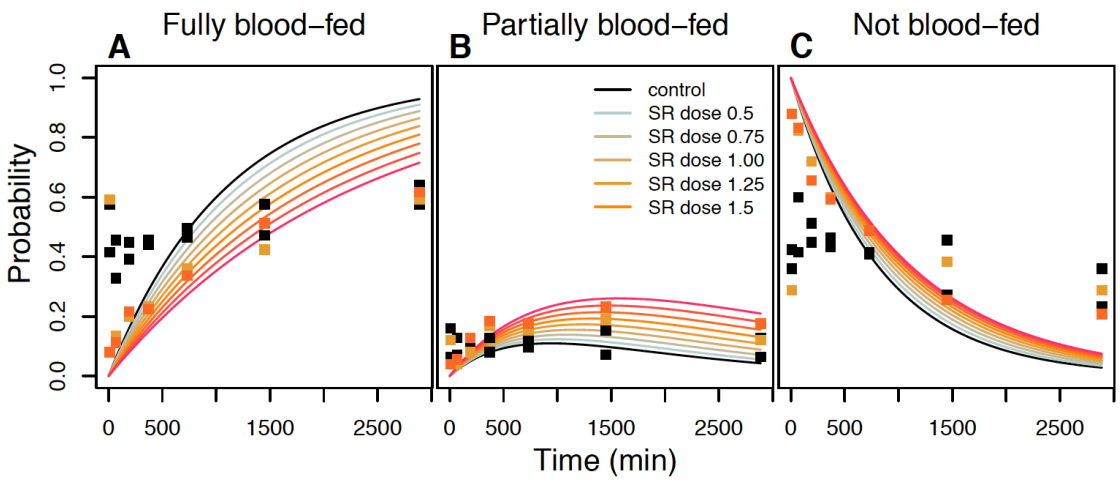

Figure 5-2: Dose effect of SR product on the probability of blood feeding over time for A) fully blood-fed, B) partially blood-fed, and C) not blood-fed *Aedes aegypti* mosquitoes.

5.4.1.2 SR effect on mortality

Deaths that occurred during the first day of the mortality experiments showed that there was a significant effect of transfluthrin, and its dosage, on what we regarded in our model as "instantaneous" lethality (μ) (p=2.8x10^{-14},t-test, df=74), with probability of first-day mortality of 8% (HDI: 5-11%) (FAR 1) and 38% (HDI: 28-49) (FAR 1.5) (Table 5-2).

Deaths that occurred after the first day showed a significant effect of transfluthrin, and its dosage, on what we regarded in our model as "residual" lethality (ϕ) (p=3x10^{-9} , LRT, df=1, X^2=35.16) (Table 5-2), with mean time until death reduced by a ϕ of 71% (HDI: 64-79) at FAR 1 and 60% (HDI:51-70%) at FAR 1.5. Although these results are based on an assumption of exponentially distributed time until death, estimates of ϕ based on alternative parametric models with different assumptions about time-varying hazards of mortality were similar (Table S5-1 and Figure 5-3).

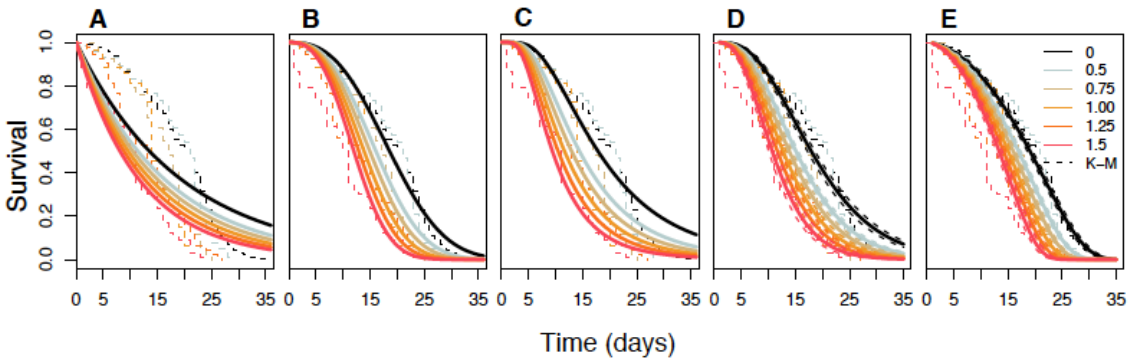

Figure 5-3: Estimated dose effects of spatial repellent on mosquito longevity for A) exponential, B) Weibull, C) lognormal, D) gamma, E) generalized gamma models. The dashed lines depict the Kaplan-Meier curves at associated dosages, presented relative to the field application rate (FAR).

5.4.1.3 SR effect on repellency and expellency

Analysis of data from the experimental hut studies showed that repellency (ρ) was highest at a low dosage of transfluthrin, with a median proportion of 19% (HDI: 3-36%) of mosquitoes being deterred by the product and opting to move away from rather than towards the treated hut. Repellency was lower at the higher dosage of transfluthrin, with a median of 8% repellency (HDI: -9-25%) (Figure 5-4A). The mosquitoes that did enter the treated hut were estimated to have exited at a lower rate, suggesting irritating effects of transfluthrin in the experimental hut study. At low dosage, median exit rates (q_T) were a factor 0.70 (HDI: 0.41-0.1.09) relative to an untreated hut. A similar effect was estimated at high dosage (0.69, HDI: 0.40-1.06).

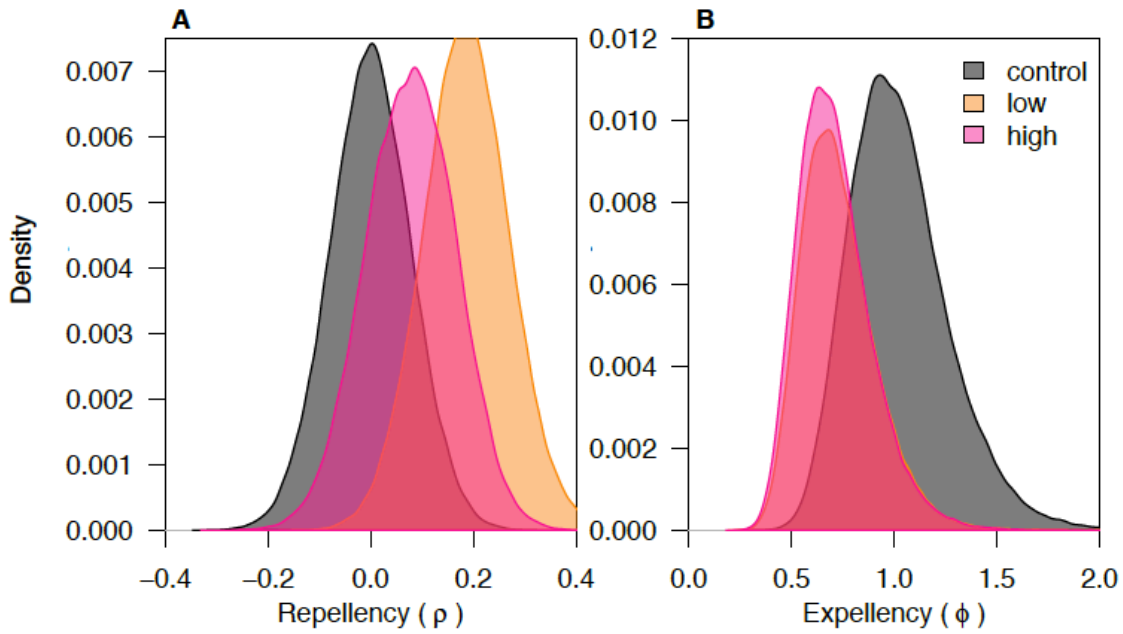

Figure 5-4: Posterior estimates of SR effects on A) repellency and B) expellency for the control, low, and high dose regimen.

5.4.1.4 Epidemiological impact

The total estimated community-level impact of the SR product on relative *FoI* is substantial, with a 50% reduction in *FoI* estimated at 25% coverage (HDI: 18-33%) at low dosage (low dosage for ρ and q_U/q_T and FAR=1 for other parameters) and 9% coverage (HDI: 6-12%) at high dosage (high dosage for ρ and q_U/q_T and FAR=1.5 for other parameters) (Figure 5-5A). The nonlinear relationship of this effect indicates strong indirect effects of the SR when community-level effects are accounted for (42). A large portion of this effect is attributable to the mortality effects of the product (Figure 5-5B). This is a result of the cubic scaling of reductions in mosquito lifespan on *FoI*; i.e., reducing mosquito density, reducing the probability that a mosquito becomes infected in its lifetime, and reducing the probability of surviving the incubation period and thus being able to transmit the virus.

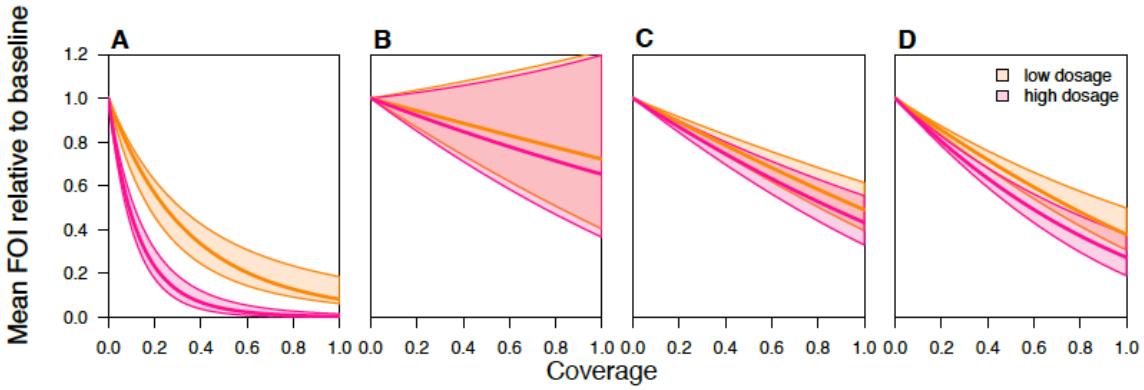

Figure 5-5: Composite effects of SR on relative force of infection (*FoI*) as a function of population coverage for different modes combined for A) all effects, B) as A without mortality, C) as B without expellency, and D) as C without probing effect, with the median defaults estimates (solid lines) and the 2.5th and 97.5th percentile for the low dosage (orange) and the high dosage (pink).

The SR without any mortality effects was estimated to have a much more modest impact on *FoI* (Figure 5-5B). When considering the combined effects on blood-feeding rates and repellency, but not expellency, the maximum estimated reduction in *FoI* at FAR 1 was 51% (HDI: 39-63%) at 100% coverage and similar for high dosage (57, HDI: 46-68%) (Figure 5-5C). The increased propensity for partial blood feeding limits the community-level impacts of the SR in our model. In the absence of a partial blood-feeding effect (i.e., o_c=a_c), the maximum impact of this product would increase at low dosage to 62% (HDI: 52-71%) at 100% coverage and to 75% (HDI: 64-80%) at high dosage (Figure 5-5C).

Exposure to the SR product investigated in the hut experiments reduced the rate at which mosquitoes exited the huts. This negative expellency effect (q_U/q_T = 0.71) prolongs the time a mosquito has to blood feed, thereby increasing the probability of transmission

at that location. This relative enhancement of *FoI* (Figure 5-6F) is greater if outdoor mortality is higher relative to indoor mortality (Figure 5-7J), because the prolonged time spent indoors reduces exposure to outdoor hazards. Conversely, if an SR has strong effects on residual mortality, reduced exit rates can increase exposure to the product, resulting in substantial reduction in the *FoI* (Figure 5-6DF). If an SR with a positive expellency effect (e.g., $q_U/q_T = 1.30$) were to be used, the result of more bouts transitioning between houses outdoors would enhance the maximum population-level impact of the SR from a 28% (HDI: -17- 64%) reduction in *FoI* at low dosage to a 63% (HDI: 54-72%) reduction at similar indoor and outdoor death rates ($g_U/g\tau=1$). If outdoor mortality were three times higher than indoor mortality, this would enhance the maximum population-level impact of the SR to an 83% (HDI: 74-93%) reduction in FoI. Similar reasoning holds for the impact of repellency effects.

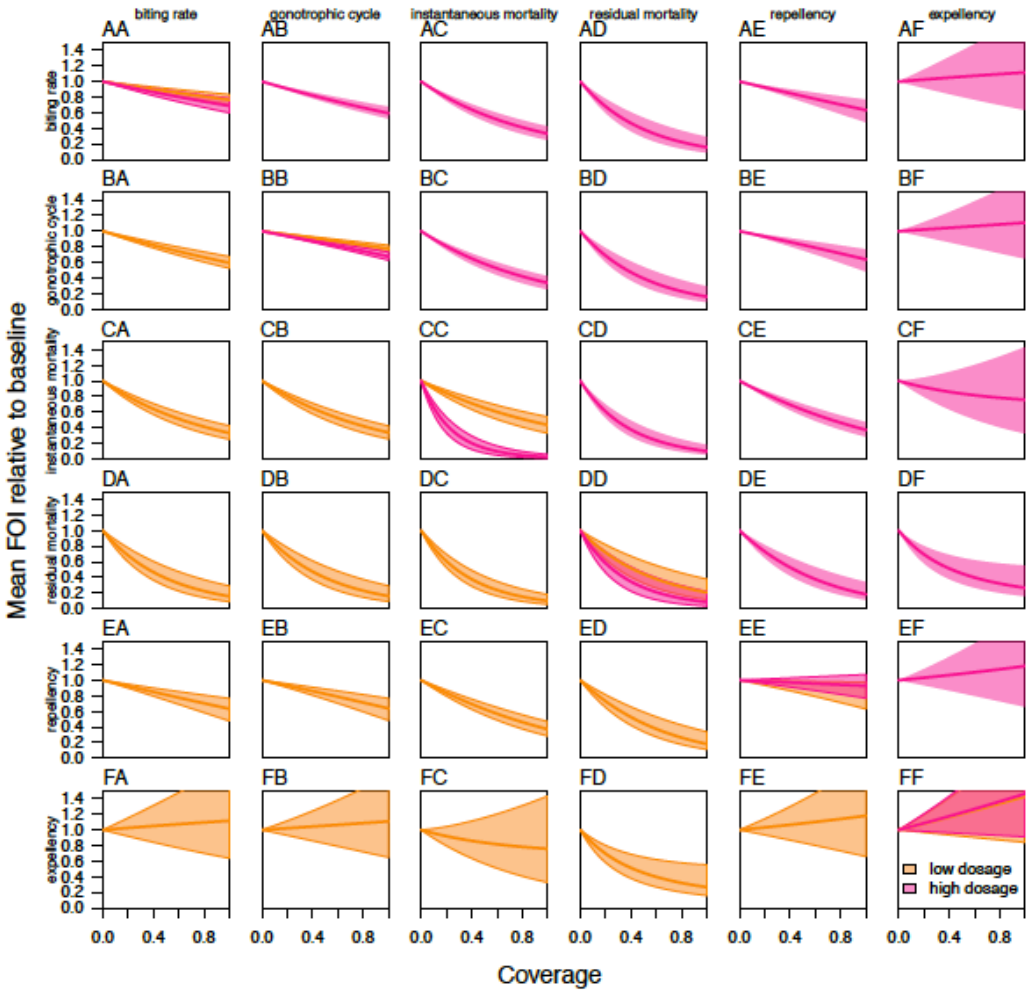

Figure 5-6: Composite effects of SR on relative force of infection (*FoI*) as a function of population coverage for different modes of action in isolation (diagonal) and combined with another with the mean default estimates (solid lines) and the the 2.5th and 97.5th percentile for the low dosage (orange) and the high dosage (pink).

5.4.1.5 Sensitivity analysis

Overall, we found that the estimated effects of the SR were robust to some but not all free parameters. The results were sensitive to the extrinsic incubation period (EIP, n), the baseline mortality rate (g_U), the ratio between the indoor and outdoor mortality rate (g_U/g_τ), and the ratio between indoor and outdoor time (q_U/q_τ). We found that the SR in our model was less effective in a relative sense at shorter durations of the EIP (n) and higher baseline mortality rates (g_U). The risk of not surviving the EIP and thus successfully transmitting the infection is much increased under such assumptions, resulting in relatively smaller impacts on *FoI* of the mortality effects of the SR. When mortality outdoors is relatively higher than indoors, the effect of the SR is also reduced. This is a result of the negative expellency effect of the product, which results in a lower proportion of time spent outdoors than in the absence of treatment. This pattern is reversed when a product with positive expellency or stronger repellency is assumed. Lastly, the effect of the product is reduced when mosquitoes spend a longer time in transit to another house, relative to their residence time indoors. In such a setting, the mosquitoes encounter the SR less often over the course of their lifetimes, thereby diminishing the effect of the SR.

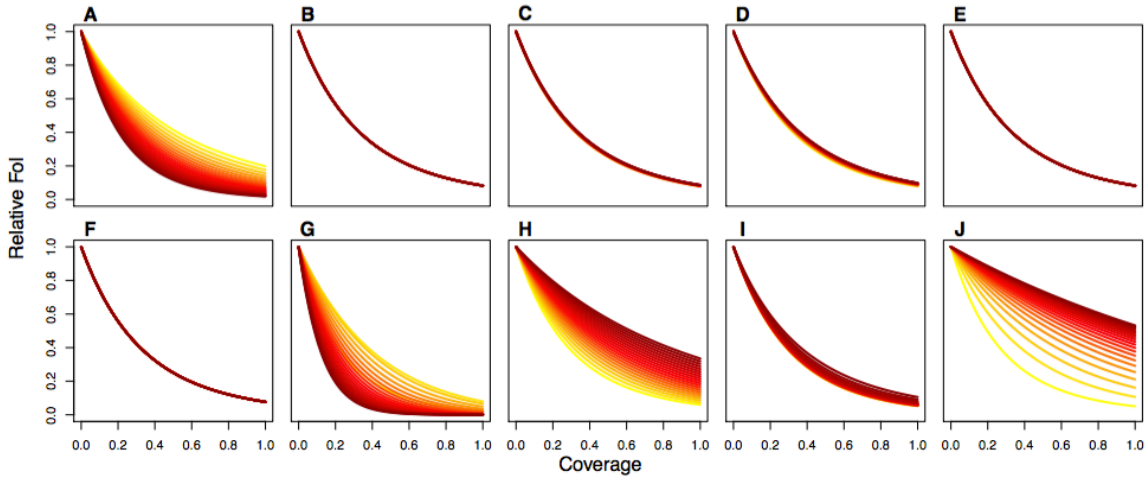

Figure 5-7: Sensitivity of relative force of infection (*FoI*) estimates to the baseline parameters as a function of population coverage, with A) extrinsic incubation period from 3 to 33 days, B) transmission probability from mosquito to human from 0.01 to 1, C) as B but from human to mosquito, D) human infection prevalence from 1 to 99%, E) the duration of the gonotrophic cycle from 1 to 14 days, F) the baseline biting rate from 0.2 to 10, G) the baseline mosquito mortality rate from 0.025 to 2.5, H) mortality rate during transit relative to indoor mortality rate from 0.1 to 10, I) average time spent in an untreated house from 0.05 to 5 days, and J) the proportion of time a transit event takes relative to the baseline residence time, from 0.01 to 10. Yellow depicts the low estimates, whereas red signifies higher values of the examined ranges.

5.5 Discussion

We have introduced a novel modeling framework for estimating the epidemiological impacts at the community level of spatial repellent (SR) products that derive not only from individual protection but from a combination of direct and indirect effects at different levels of product coverage within a community. Using a suite of laboratory and semi-field experiments, we parameterized six distinct effects of a transfluthrin-based SR product on mosquito behavioral and bionomic traits. We showed that the product could have a substantial epidemiological impact by way of reducing the

force of infection (*FoI*) of a pathogen transmitted by *Aedes aegypti* mosquitoes in a community with appreciable coverage of the SR product. This is largely driven by the product's effects on mosquito mortality, but not completely. For instance, when employed in a mosquito population that has gained partial resistance to the lethal effects (43) an SR product such as the one in our model could still lead to a meaningful reduction in *FoI* due to delayed blood feeding induced in multiple distinct ways.

One potential use of our modeling framework is as a tool to guide the design of new products and to assess their potential impact when deployed at scale. In particular, the transfluthrin formulation examined in this study was found to significantly increase mortality and to reduce overall biting and hut entry. However, the product was also found to result in increased partial blood feeding and a delay in exiting the experimental huts. The relative transmission potential of partial and full blood meals is unclear, but increased partial blood feeding very well could negatively affect the epidemiological impact of the product (44). Such irritant effects are common at low, sub-lethal dosages (19) and could compromise the potential net benefit of the product. This underscores the importance of understanding how dosage affects multiple distinct behavioral and bionomic effects, as well as how these effects decay over time as dosages decay and how they affect neighboring premises via downstream effects.

The projected epidemiological impact of SRs and other vector control products depend in some ways on the properties of the products and the context of their deployment (45). We found the potential for the SR product in this study to be highest in densely populated urban areas where mosquitoes spend a relatively large portion of time indoors and transition relatively quickly between houses (18). In these settings,

mosquitoes may be more likely to have frequent encounters with the SR and to be affected by its lethal and irritant effects. However, if the SR has stronger repellency and expellency effects, longer transit times in sparsely populated areas would result in longer biting delays and increased transit-related mortality, resulting in a larger impact on transmission. Notably, high-dosage SRs could have reduced impacts in very densely populated areas at low coverage. In that situation, the repellency effect could protect mosquitoes from entering a house with high SR-associated mortality. A delay in biting as a result of the SR would then be offset by the reduced life span it would have experienced if it had entered the house. At low coverage, densely populated settings could be most prone to the adverse effects of diversion to untreated homes. The potential for diversion is strongly tied to the risks a mosquito experiences both from its exposure to the product and from its transit between houses. In settings where transit is relatively hazardous, SRs that reduce time indoors are expected to have a greater impact. Push-pull strategies, which trap mosquitoes in sentinel traps after they have been repelled or expelled from a house (46), may therefore be an especially promising candidate in this context.

We made a number of simplifying assumptions that may affect the outcome of SR implementation. First, our framework assumes homogeneous mixing such that each house has an equal probability of being visited by a mosquito, irrespective of its proximity to the house where the mosquito was previously. In addition, the model assumes that no biting occurs in transit. This does not, however, exclude the possibility of outdoor biting. The houses in the model should be regarded as the totality of all space affected by the SR and may thus include semi-enclosed and open areas in sufficiently close proximity of the product (47). Further, we assumed that placement of the product is

random. A clustered rollout may be logistically desirable and could, depending on the context and the formulation of the product, result in community-level impacts that differ from our estimates. One possible advantage of clustered rollout could occur if the product has beneficial downstream effects to adjacent, untreated houses. Such effects are currently not included in our framework, but they could enhance the impact of the product unless adverse, irritating effects such as partial blood feeding or reduced expellency occur downstream.

Downstream effects of this product have been observed in the experimental hut study (Chapter 4). These include expellency (for both dosages) and mortality (only for the high dosage) effects. Downstream effects on blood-feeding rates are currently unknown but may well occur in tandem with other irritating effects such as reduced expellency (9). In addition, dosage decay over time may alter the product profile by increasing irritating effects and decreasing effects on mortality as the product expires. Although our framework does not allow for temporal changes in treatment effects, it does allow for the exploration of a suite of different profiles. Given appropriate experimental data on effects following the decay of the product, our framework could be used to estimate the cross-sectional effects of an SR at different stages of the product's lifetime as a way to inform best practices for replacement timing. Coupling more detailed models with additional laboratory and semi-field experiments would aid in capturing the full effects of heterogeneity in exposure and protection, both on the treated and untreated population. The framework presented here provides a general way to gain insights on the projected interplay of different behavioral and bionomic effects of an SR in a variety of settings.

The sustained burden of dengue and the emergence of other pathogens transmitted by *Aedes aegypti* mosquitoes highlight the need for novel vector control paradigms (6, 48). Spatial repellents are one promising tool for settings where other vector control products are insufficient, such as the control of day- and outdoor-biting mosquitoes, in settings with high potential for resistance against lethality, or as an additional tool in outbreak response. Our framework could likewise be extended to other vector control tools with multi-facetted impacts on mosquito behavioral and bionomic traits, including long-lasting insecticidal bed nets, push-pull regimens, and window screening. Whereas lethal products are more effective in many cases, outstanding challenges such as resistance evolution and outdoor blood feeding necessitate the development and assessment of new tools. Our new framework offers a way of synthesizing the results of feasible experiments at small scales to meet daunting public health challenges at large scales.

TABLE 5-1:

BASELINE PARAMETERS FOR FORCE OF INFECTION FRAMEWORK

Symbol	Description	Units	Default	Reference
a	Biting rate	$days^{-1}$	0.76	(18)
1/o	Duration of gonotrophic cycle	days	4	(49)
g_U	Daily mortality rate (indoors)	$days^{-1}$	0.18	(50)
g_τ	Daily mortality rate (outdoors)	$days^{-1}$	0.18	
τ	Time spent per transit event	days	0.3 q_U	(51)
n	Duration of the extrinsic incubation period	days	14	(52)
b	Probability of mosquito to human infection		0.5	
c	Probability of human to mosquito infection		0.5	
X	Human infection prevalence		12.5	

TABLE 5-2:

FITTED MODEL PARAMETERS DEPICTING SR EFFECTS

Experiment	Model framework parameter description	Model framework parameter symbol	Fitted equation	Fitted parameters (95% confidence interval: lower bound, higher bound)	Model framework default (HDI)
Blood feeding	Fraction of baseline blood feeding rate	$\alpha(x_{dose}) = \frac{a(x_{dose=0})}{a(x_{dose})} - 1$	$a = \frac{1}{e^{(\beta_{p,0}+\beta_{p,1}x_{dose})}} + \frac{1}{e^{(\beta_{f,0}+\beta_{f,1}x_{dose})}}$	$\beta_{p,0}$=8.05 (7.91, 8.20) $\beta_{p,1}$=-0.18(-0.33, -0.03) $\beta_{f,0}$=7.00 (6.93, 7.07) $\beta_{f,1}$= 0.37(0.28, 0.46)	0.82 (0.76, 0.89)
	Fraction of baseline oviposition rate	$o(x_{dose}) = \frac{a_f(x_{dose=0})}{a_f(x_{dose})} - 1$	$a_f = \frac{1}{e^{(\beta_{f,0}+\beta_{f,1}x_{dose})}}$		0.69 (0.63, 0.75)
Longevity	Probability of first day mortality	$\mu(x_{dose})$	$\mu = e^{(\beta_0+\beta_1 x_{dose})}$	β_0=-5.68 (-6.84, -4.67) β_1= 3.14(2.38, 4.00)	0.08 (0.05, 0.11)
	Fraction time until death relative to baseline	$\phi(x_{dose})$	See Table 5-3	See Table 5-3	0.71 (0.64, 0.79)
Movement	Probability of being repelled	$\rho(x_{dose})$	See Chapter 4	ρ	0.19 (0.03, 0.36)
	Fraction of baseline exit rate	$q_{\underline{U}}/q_T(x_{dose})$	See Chapter 4	$q_{\underline{U}}/q_T$	0.71 (0.40, 1.06)

TABLE 5-3:

SURVIVAL FUNCTIONS

Model	Probability density function (f(t))	Survival function	Parameters	With covariates	Mean (95% Confidence interval: lower bound, higher bound)	AIC	ΔAIC
Exponential	$\lambda e^{-\lambda t}$	$e^{-\lambda t}$	λ =rate	$\lambda = \lambda(x)$ $\lambda(x) = \frac{1}{e^{\beta_0+\beta_i x_i}}$	β_0=2.97 (2.89, 3.05) β_1= -0.34(-0.45, -0.23)	8623	1201
Weibull	$v\lambda t^{v-1}e^{-\lambda t^v}$	$e^{-\lambda t^v}$	λ=rate v = shape	$\lambda = \lambda(x)$ $\lambda(x) = e^{\beta_0+\beta_i x_i}$	v = 0.07 (0.06, 0.08) β_0=3.06 (3.02, 3.08) β_1=-0.29(-0.33, 00.25)	7564	143
Log-normal	$\frac{1}{x\sigma\sqrt{2\pi}} e^{-\frac{(\ln(t-\mu)^2}{2\sigma^2}}$	$\frac{1}{2}+\frac{1}{2}erf\left[\frac{\ln(x-\mu)}{\sqrt{2\sigma}}\right]$	μ = location σ = scale	$\mu = \mu(x)$ $\mu(x) = e^{\beta_0+\beta_i x_i}$	σ =0.59(0.56, 0.61) β_0=2.88 (2.83, 2.93) β_1=-0.43(-0.49, -0.36)	8078	656
Gamma	$\frac{\lambda(\lambda t)^{\kappa-1}e^{-\lambda t}}{\Gamma(\kappa)}$	No closed form	λ=rate κ = shape	$\lambda = \lambda(x)$ $\lambda(x) = v / e^{\beta_0+\beta_i x_i}$	κ = 4.08 (3.77, 4.42) β_0= 0.21(0.19, 0.23) β_1=0.34(0.29, 0.40)	7786	364
Generalized Gamma	$\frac{\lambda v(\lambda t)^{v\kappa-1}e^{-(\lambda t)^v}}{\Gamma(\kappa)}$	$1-(\gamma\{\kappa,(\lambda t)^v\}/\Gamma(\kappa))$ $\gamma(s,x)=\int_0^x t^{s-1}e^{-t}\,dt$	λ =rate v = shape 1 κ = shape 2	$\lambda = \lambda(x)$ $\lambda(x) = e^{\beta_0+\beta_i x_i}$	κ = 0.23 (0.18, 0.28) v = 7.99 (6.76, 9.43) β_0= 29.20(28.42, 30.00) β_1=-0.24(-0.26, -0.21)	7421	0

5.6 References

1. Bhatt S*, et al* (2015) The effect of malaria control on plasmodium falciparum in africa between 2000 and 2015. *Nature* 526(7572): 207-211.

2. Strode GK (1951) Yellow fever. *Yellow Fever*

3. Monath TP (1994) Yellow fever and dengue—the interactions of virus, vector and host in the re-emergence of epidemic disease5(2): 133-145.

4. Armada Gessa JA & Gonzalez RF (1987) Application of environmental management principles in the programme for eradication of aedes (stegomyia) aegypti (linneus, 1762) in the republic of cuba, 1984.

5. Gubler DJ (2011) Dengue, urbanization and globalization: The unholy trinity of the 21(st) century. *Trop Med Health* 39(4 Suppl): 3-11.

6. Achee NL*, et al* (2015) A critical assessment of vector control for dengue prevention. *PLoS Negl Trop Dis* 9(5): e0003655.

7. Christofferson RC & Mores CN (2015) A role for vector control in dengue vaccine programs. *Vaccine* 33(50): 7069-7074.

8. Rapley LP, Russell RC, Montgomery BL & Ritchie SA (2009) The effects of sustained release metofluthrin on the biting, movement, and mortality of aedes aegypti in a domestic setting. *Am J Trop Med Hyg* 81(1): 94-99.

9. Ritchie SA & Devine GJ (2013) Confusion, knock-down and kill of aedes aegypti using metofluthrin in domestic settings: A powerful tool to prevent dengue transmission. *Parasit Vectors* 6: 262-280.

10. Ogoma SB, Moore SJ & Maia MF (2012) A systematic review of mosquito coils and passive emanators: Defining recommendations for spatial repellency testing methodologies. *Parasit Vectors* 5: 287.

11. Hill N*, et al* (2014) A household randomized, controlled trial of the efficacy of 0.03% transfluthrin coils alone and in combination with long-lasting insecticidal nets on the incidence of plasmodium falciparum and plasmodium vivax malaria in western yunnan province, china. *Malaria Journal* 13: 208.

12. Syafruddin D*, et al* (2014) Impact of a spatial repellent on malaria incidence in two villages in sumba, indonesia. *Am J Trop Med Hyg* 91(6): 1079-1087.

13. Maia MF*, et al* (2013) Do topical repellents divert mosquitoes within a community?–Health equity implications of topical repellents as a mosquito bite prevention tool. *PLoS One* 8(12): e84875.

14. Maia MF, *et al* (2016) A crossover study to evaluate the diversion of malaria vectors in a community with incomplete coverage of spatial repellents in the kilombero valley, tanzania. *Parasites & Vectors* 9(1): 451.

15. Binka FN, Indome F & Smith T (1998) Impact of spatial distribution of permethrin-impregnated bed nets on child mortality in rural northern ghana. *Am J Trop Med Hyg* 59(1): 80-85.

16. Gimnig J, *et al* (2002) Density-dependent development of anopheles gambiae (diptera:Culicidae) larvae in artificial habitats. *Journal of Medical Entomology* 39(1): 162-172.

17. Hawley WA, *et al* (2003) Community-wide effects of permethrin-treated bed nets on child mortality and malaria morbidity in western kenya. *Am J Trop Med Hyg* 68(4 Suppl): 121-127.

18. Scott TW, *et al* (2000) Longitudinal studies of aedes aegypti (diptera: Culicidae) in thailand and puerto rico: Blood feeding frequency. *J Med Entomol* 37(1): 89-101.

19. Grieco JP, *et al* (2007) A new classification system for the actions of IRS chemicals traditionally used for malaria control. *PLos One* 2(8): e716.

20. Reiner Jr RC, *et al* (2016) Quantifying the epidemiological impact of vector control on dengue. *PLOS Negl Trop Dis* 10(5): e0004588.

21. Roberts DR, *et al* (2000) A probability model of vector behavior: Effects of DDT repellency, irritancy, and toxicity in malaria control. *J Vector Ecol* 25(1): 48-61.

22. Killeen GF & Smith TA (2007) Exploring the contributions of bed nets, cattle, insecticides and excitorepellency to malaria control: A deterministic model of mosquito host-seeking behaviour and mortality. *Trans R Soc Trop Med Hyg* 101(9): 867-880.

23. Yakob L, Bonsall MB & Yan G (2010) Modelling knowlesi malaria transmission in humans: Vector preference and host competence. *Malar J* 9: 329.

24. Kiware SS, *et al* (2012) Simplified models of vector control impact upon malaria transmission by zoophagic mosquitoes. *PLoS One* 7(5): e37661.

25. Chitnis N, Schapira A, Smith T & Steketee R (2010) Comparing the effectiveness of malaria vector-control interventions through a mathematical model. *Am J Trop Med Hyg* 83(2): 230-240.

26. Killeen GF, *et al* (2011) The importance of considering community-level effects when selecting insecticidal malaria vector products. *Parasites & Vectors* 4(1): 1.

27. Briët OJ*, et al* (2013) Effects of pyrethroid resistance on the cost effectiveness of a mass distribution of long-lasting insecticidal nets: A modelling study. *Malaria Journal* 12(1): 1.

28. Smith DL*, et al* (2012) Ross, macdonald, and a theory for the dynamics and control of mosquito-transmitted pathogens. *PLoS Pathogens* 8(4): e1002588.

29. Taylor HM & Karlin S (2014) *An introduction to stochastic modeling,* (Academic press,

30. Parham PE & Michael E (2010) Modeling the effects of weather and climate change on malaria transmission. *Environ Health Perspect* 118(5): 620-626.

31. Smith D & McKenzie FE (2004) Statics and dynamics of malaria infection in anopheles mosquitoes. *Malaria Journal* 3(1): 13.

32. Smith DL, McKenzie FE, Snow RW & Hay SI (2007) Revisiting the basic reproductive number for malaria and its implications for malaria control. *PLoS Biol* 5(3): e42.

33. Grieco JP, Achee NL, Sardelis MR, Chauhan KR & Roberts DR (2005) A novel high-throughput screening system to evaluate the behavioral response of adult mosquitoes to chemicals 1. *J Am Mosq Control Assoc* 21(4): 404-411.

34. Grieco JP, Achee NL, Andre RG & Roberts DR (2000) A comparison study of house entering and exiting behavior of anopheles vestitipennis (diptera: Culicidae) using experimental huts sprayed with DDT or deltamethrin in the southern district of toledo, belize, C.A. *J Vector Ecol* 25(1): 62-73.

35. Bolker B (2016) Package 'bbmle'

36. Team RC (2014) . *R: A Language and Environment for Statistical Computing.R Foundation for Statistical Computing, Vienna, Austria.2013*

37. Woodward M (2014) *Epidemiology: study design and data analysis,* (CRC Press,

38. Akaike H (1973) Information theory and an extension of the maximum likelihood principle: 267-281.

39. Therneau T (2013) A package for survival analysis in S. R package version 2.37-4. *URL Http://CRAN.R-Project.Org/Package= Survival.Box* 980032: 23298-20032.

40. Jackson CH (2016) Flexsurv: A platform for parametric survival modelling in R. *Journal of Statistical Software* 70(8): 1-33.

41. Plummer M, Best N, Cowles K & Vines K (2006) CODA: Convergence diagnosis and output analysis for MCMC. *R News* 6(1): 7-11.

42. Keeling MJ & Rohani P (2008) *Modeling infectious diseases in humans and animals,* (Princeton Univ Pr,

43. Sharma S, Shukla R, Raghavendra K & Subbarao SK (2005) Impact of DDT spraying on malaria transmission in bareilly district, uttar pradesh, india. *Journal of Vector Borne Diseases* 42(2): 54.

44. Putnam JL & Scott TW (1995) The effect of multiple host contacts on the infectivity of dengue-2 virus-infected aedes aegypti. *J Parasitol* : 170-174.

45. Smith DL, Perkins TA, Tusting LS, Scott TW & Lindsay SW (2013) Mosquito population regulation and larval source management in heterogeneous environments. *PLoS One* 8(8): e71247.

46. Salazar FV*, et al* (2012) Evaluation of a peridomestic mosquito trap for integration into an aedes aegypti (diptera: Culicidae) push-pull control strategy. *Journal of Vector Ecology* 37(1): 8-19.

47. Hoffmann EJ & Miller JR (2002) Reduction of mosquito (diptera: Culicidae) attacks on a human subject by combination of wind and vapor-phase DEET repellent. *J Med Entomol* 39(6): 935-938.

48. Bowman LR, Donegan S & McCall PJ (2016) Is dengue vector control deficient in effectiveness or evidence?: Systematic review and meta-analysis. *PLoS Negl Trop Dis* 10(3): e0004551.

49. Focks DA, Brenner RJ, Hayes J & Daniels E (2000) Transmission thresholds for dengue in terms of aedes aegypti pupae per person with discussion of their utility in source reduction efforts. *Am J Trop Med Hyg* 62(1): 11.

50. Harrington LC*, et al* (2001) Analysis of survival of young and old aedes aegypti (diptera: Culicidac) from puerto rico and thailand. *J Med Entomol* 38(4): 537-547.

51. Scott TW*, et al* (2000) Longitudinal studies of aedes aegypti (diptera: Culicidae) in thailand and puerto rico: Population dynamics. *J Med Entomol* 37(1): 77-88.

52. Chan M & Johansson MA (2012) The incubation periods of dengue viruses. *PloS One* 7(11): e50972.

5.7 Supporting tables and figures

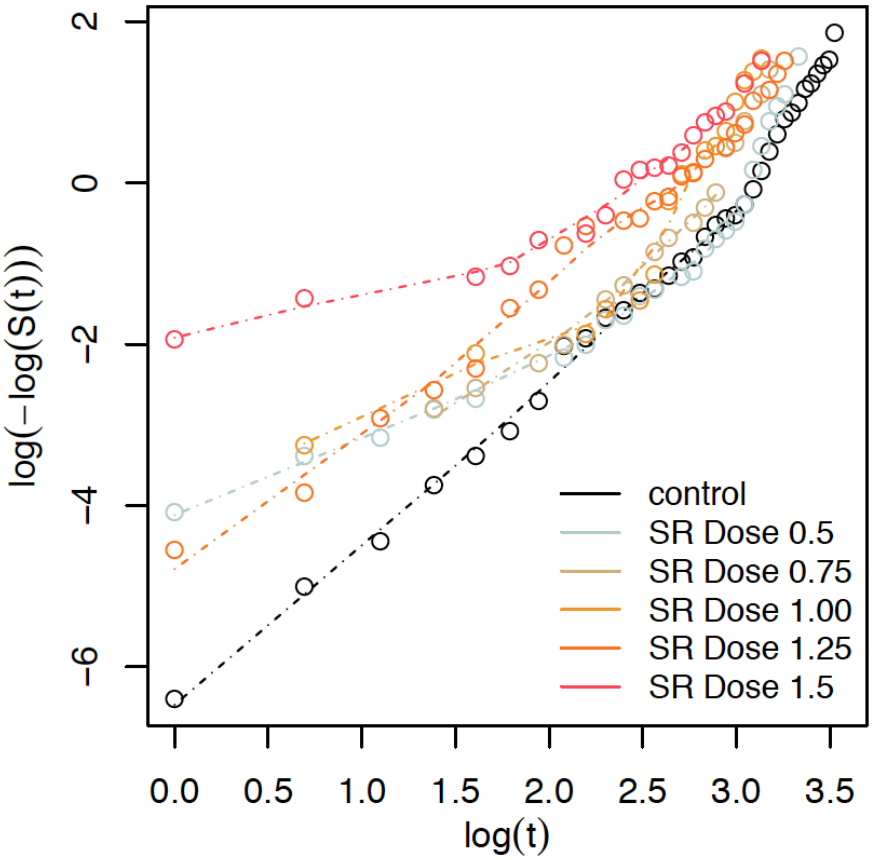

Figure S5-1: Proportional hazard test for longevity data conditioned on first day survival. The proportional hazards assumption holds for dosage regimen that are parallel to each other when plotted with these transformations.

TABLE S5-1:

SR EFFECTS ON MORTALITY BY SURVIVAL MODEL (FAR 1)

Model	**ϕ**	**95% confidence interval**
exponential	0.71	(0.63, 0.79)
Weibull	0.75	(0.72, 0.78)
log-normal	0.65	(0.61, 0.70)
gamma	0.71	(0.67, 0.75)
generalized gamma	0.79	(0.77, 0.81)

CHAPTER 6:

CONCLUSION

Mathematical models have a long history in infectious disease research (1, 2), with applications in prediction (3, 4), control (5-7), and elimination efforts (8, 9). They are used across different scales, from the examination of within-host dynamics of viruses and their interactions with the human immune response (10, 11), to making estimations of the burden of a disease worldwide (12, 13). In this dissertation, I used techniques from the field of mathematical epidemiology to answer a wide range of questions pertaining to the spread and control of the mosquito-borne dengue virus.

Most dengue virus infections result in either no perceptible symptoms or symptoms that are so mild that they go undetected by surveillance systems (12). It is unclear how much these infections contribute to the overall transmission and burden of dengue. In Chapter 2, I parsed data on the viremia and infectiousness of dengue-infected individuals to estimate the net infectiousness of individuals across the range of clinical outcomes. While viremia levels in asymptomatic individuals were on average lower than in individuals that do present with symptoms, a recent study found that, at a given level of viremia, asymptomatic individuals were more likely to transmit the virus to a mosquito when bitten (14). I synthesized these empirical findings to perform calculations that suggest that the net infectiousness of individuals with asymptomatic infections is not significantly different from that of their symptomatic counterparts. Due to their numerical

prominence in the population and their appreciable infectiousness, I estimated that 80% of infections result from individuals who display no apparent symptoms at the time of transmission. If individuals that experience their third or fourth infection (post-secondary) were to contribute to transmission too, the relative contribution of silent infections would even be larger. These results suggest that individuals with clinically inapparent or no symptoms whatsoever may be the primary reservoir of dengue virus transmission and that policy for dengue control and prevention must be revised accordingly.

Predicting dengue epidemics is another field of research that mathematical models have been used for. The dynamics of dengue are highly irregular and particularly hard to predict. This is thought to result from a complex interplay between environmental factors, mosquito ecology, and host-pathogen dynamics. Mathematical models have been used to uncover the main drivers and examine how they interplay to govern the complex dynamics of dengue that we see worldwide. In Chapter 3, I compiled hypotheses on the driving factors of dengue epidemiology as proposed in the modeling literature and performed a comprehensive comparison between those (15). Specifically, I used an approach called pattern-oriented modeling (POM) in which I used multiple dengue-specific patterns observed at different scales to test a model's proficiency in capturing the real-world dynamics. I compared models with different combinations of cross-immunity, cross-enhancement, and seasonal fluctuations, as well as explored the impact of asymmetry in the transmission potential of different serotypes and the impact of active transmission by tertiary and quaternary infections. All proposed models were capable of reproducing the typical dengue dynamics, but the level at which seasonal forcing acted on

the system determined which model best supported the dengue dynamics. Further, when tertiary and quaternary infections were assumed to contribute to transmission, the inclusion of temporary cross-immunity alone was strongly supported, whereas there was much less support for the hypothesis that cross-enhancement governs typical dengue dynamics. These post-secondary infections are often not considered in dengue models, due to their low rates of apparent disease (16). How infectious these post-secondary infections are, is however unknown. My work in both Chapter 2 and 3 highlights the importance of unraveling the transmission potential of these infections, both to better predict and understand dengue dynamics, as well as to better focus control efforts.

While the first dengue vaccine (17) has been licensed recently and more are in advanced stages of the development pipeline (18), it has been recognized that mosquito control will remain a crucial component in the control of this, and other mosquito-borne viruses (MBV) (19). Mosquito-control has not been able to curb the rapid emergence and growing burden of MBVs (20) and with the emergence of insecticide resistance (21) and behavioral adaptation (22, 23), the mosquito control community is challenged to develop new strategies that can augment currently available options. Mathematical models can be used to guide several stages of the development and implementation process of such new mosquito control strategies. In Chapter 4 and 5, I used models to investigate the potential for community-level implementation of spatial repellents (SR). SR products are designed to reduce human-mosquito contacts by either repelling mosquitoes from human dwellings or by interfering with their ability to find a human to feed on (24). Repellency is a distinct mode of action of these products, but most chemicals elicit a combination of, often dose-dependent, effects, including toxicity and irritancy (25-27). Examining how these effects

interplay at different dosages and how this translates into epidemiological outcomes is a major challenge for which mathematical models are indispensable.

In Chapter 4, a mark-release-recapture experimental-hut study was performed to examine the effects of SR on mosquito movement between and out of huts. A challenge of such experiments is that, even though we know where a mosquito is released (based on the color it was marked with), and where it gets captured (either in traps, upon knockdown in a hut, or by aspirators), its whereabouts in between are unobserved. This unobserved behavior harbors a lot of important information on the effects of the product. For instance, if fewer mosquitoes were to be recaptured in a treated hut, this could have been a result of reduced entry, or increased exiting. Which of these processes were in play has implications for the level of product a mosquito gets exposed to and the effect a product could have on neighboring premises. In Chapter 4, I used a Bayesian model framework to estimate such concurrent, indirectly observed effects of SR products. I found that the transfluthrin product used in the study reduced entry into a treated hut, but mosquitoes that did enter the hut exited at reduced rates due to irritancy effects. In addition, I showed that the effect of this volatile product, especially at high dosage, extended up to two huts away from the treated hut. This type of downstream effect could be beneficial for community-level rollout of the product. The framework proposed in Chapter 4 can aid to unravel these types of processes and can be adapted to a variety of settings.

In Chapter 5, I used the findings from Chapter 4 and additional laboratory experiments on this transfluthrin formulation to examine how different modes of action of a mosquito control product may act in symphony to affect epidemiological outcomes.

For this effort, I proposed a new description of the force of infection. The force of infection describes the rate at which susceptible individuals become infected and depends on, among other factors, a variety of mosquito behavioral and bionomic traits. Mosquito control products affect many of these traits. I parsed data from several experiments performed by collaborators to parameterize the new modeling framework and to project the epidemiological impact of the SR product at different dosages and coverage levels. While toxic effects contribute most to the impact of the product, I showed that in the absence of these toxic effects, this SR product could still reduce transmission appreciably. This is particularly relevant in light of the emergence of insecticide resistance (24). In addition, the modeling framework also allows the investigation of adverse effects of a product. One such potentially adverse effect is that the product I investigated resulted in increased probing behavior. Probing indicates that mosquitoes are taking multiple partial bites before they are fully blood fed. Irritancy effects of mosquito control products can induce such behavior, thereby increasing the number of bites and thus potential transmission events. I demonstrated that, for this specific formulation, the probing effect is offset by other modes of action, but outcomes can be markedly improved if effects on probing are limited. The framework can be a helpful tool in the development and implementation of new products in providing a way to leverage results from small-scale experiments to derive expectations of community-level epidemiological impact.

With the recent emergence of Zika virus and the global expansion of dengue and chikungunya, the public health threat of mosquito-borne viruses is evident. A greater understanding of the processes that drive the spread of these diseases is critical for

improving control and outbreak response efforts. In this dissertation, I presented a suite of studies that highlight the role that mathematical modeling can play in bridging core results from different disciplines, informing data collection and interpretation, and translating such empirical results into meaningful and actionable epidemiological outcomes.

6.1 References

1. Ross R (1911) The prevention of malaria

2. Ross R (1911) Some quantitative studies in epidemiology. *Nature* 87: 466-467.

3. Fraser C*, et al* (2009) Pandemic potential of a strain of influenza A (H1N1): Early findings. *Science* 324(5934): 1557-1561.

4. Ferguson NM*, et al* (2016) EPIDEMIOLOGY. countering the zika epidemic in latin america. *Science* 353(6297): 353-354.

5. Cauchemez S*, et al* (2009) Closure of schools during an influenza pandemic. *The Lancet Infectious Diseases* 9(8): 473-481.

6. Donnelly CA*, et al* (2003) Impact of localized badger culling on tuberculosis incidence in british cattle. *Nature* 426(6968): 834-837.

7. Stolk WA*, et al* (2013) Modeling the impact and costs of semiannual mass drug administration for accelerated elimination of lymphatic filariasis. *PLoS Neglected Tropical Diseases* 7(1): e1984.

8. Mayer BT*, et al* (2013) Successes and shortcomings of polio eradication: A transmission modeling analysis. *Am J Epidemiol* 177(11): 1236-1245.

9. Keeling MJ & Grenfell BT (1997) Disease extinction and community size: Modeling the persistence of measles. *Science* 275(5296): 65-67.

10. Clapham HE, Tricou V, Van Vinh Chau N, Simmons CP & Ferguson NM (2014) Within-host viral dynamics of dengue serotype 1 infection. *J R Soc Interface* 11(96): 10.1098/rsif.2014.0094.

11. Ben-Shachar R & Koelle K (2015) Minimal within-host dengue models highlight the specific roles of the immune response in primary and secondary dengue infections. *J R Soc Interface* 12(103): 10.1098/rsif.2014.0886.

12. Bhatt S, *et al* (2013) The global distribution and burden of dengue. *Nature* 496: 504-507.

13. Stanaway JD, *et al* (2016) The global burden of dengue: An analysis from the global burden of disease study 2013. *The Lancet Infectious Diseases* 16: 712-723.

14. Duong V, *et al* (2015) Asymptomatic humans transmit dengue virus to mosquitoes. *Proc Natl Acad Sci U S A* 112: 14688-14693.

15. ten Bosch QA, Singh BK, Hassan MR, Chadee DD & Michael E (2016) The role of serotype interactions and seasonality in dengue model selection and control: Insights from a pattern matching approach. *PLoS Negl Trop Dis* 10(5): e0004680.

16. Olkowski S, *et al* (2013) Reduced risk of disease during postsecondary dengue virus infections. *J Infect Dis* 208(6): 1026-1033.

17. Hadinegoro SR, *et al* (2015) Efficacy and long-term safety of a dengue vaccine in regions of endemic disease. *N Engl J Med* 373(13): 1195-1206.

18. Vannice KS, Durbin A & Hombach J (2016) Status of vaccine research and development of vaccines for dengue. *Vaccine* 34(26): 2934-2938.

19. Christofferson RC & Mores CN (2015) A role for vector control in dengue vaccine programs. *Vaccine* 33(50): 7069-7074.

20. Gubler DJ (2011) Dengue, urbanization and globalization: The unholy trinity of the 21(st) century. *Trop Med Health* 39(4 Suppl): 3-11.

21. Corbel V & N'Guessan R (2013) Distribution, mechanisms, impact and management of insecticide resistance in malaria vectors: A pragmatic review. *Anopheles Mosquitoes-New Insights into Malaria Vectors* 633

22. Gatton ML, *et al* (2013) The importance of mosquito behavioural adaptations to malaria control in africa. *Evolution* 67(4): 1218-1230.

23. Russell TL, *et al* (2011) Increased proportions of outdoor feeding among residual malaria vector populations following increased use of insecticide-treated nets in rural tanzania. *Malaria Journal* 10(1): 1.

24. Achee NL, *et al* (2012) Spatial repellents: From discovery and development to evidence-based validation. *Malar J* 11(1): 164.

25. Fanello C, *et al* (2003) Comparative evaluation of carbosulfan-and permethrin-impregnated curtains for preventing house-entry by the malaria vector anopheles gambiae in burkina faso. *Med Vet Entomol* 17(3): 333-338.

26. Lindsay S, Adiamah J & Armstrong J (1992) The effect of permethrin-impregnated bednets on house entry by mosquitoes (diptera: Culicidae) in the gambia. *Bull Entomol Res* 82(01): 49-55.

27. Pleass R, Armstrong J, Curtis C, Jawara M & Lindsay S (1993) Comparison of permethrin treatments for bednets in the gambia. *Bull Entomol Res* 83(01): 133-139.

APPENDIX A:

4-INFECTION MODEL EQUATIONS

System of differential equations for the 4-infection model. The parameters are equivalent to the 2-infection case. The subscripts (0000) denote the history of infection, where a zero denotes naivety to the i^{th} serotype and a one denotes a current or prior infection. I≥2i denotes all individuals with a secondary, tertiary or quaternary infection currently infectious with serotype i. This system of equations is adapted from (1).

$$\frac{dS}{dt} = \mu - \beta S(I_{1_{all}} + aI_{\geq 2_{all}} + \delta) - \mu S$$

$$\frac{dI_{1000}}{dt} = \beta S(I_{1000} + aI_{\geq 2_1} + \delta) - \gamma I_{1000} \mu I_{1000}$$

$$\frac{dI_{0100}}{dt} = \beta S(I_{0100} + aI_{\geq 2_2} + \delta) - \gamma I_{0100} \mu I_{0100}$$

$$\frac{dI_{0010}}{dt} = \beta S(I_{0010} + aI_{\geq 2_1} + \delta) - \gamma I_{0010} \mu I_{0010}$$

$$\frac{dI_{0001}}{dt} = \beta S(I_{0001} + aI_{\geq 2_1} + \delta) - \gamma I_{0001} \mu I_{0001}$$

$$\frac{dC_{1000}}{dt} = \gamma I_{1000} - \rho I_{1000} - \mu I_{1000}$$

$$\frac{dC_{0100}}{dt} = \gamma I_{0100} - \rho I_{0100} - \mu I_{0100}$$

$$\frac{dC_{0010}}{dt} = \gamma I_{0010} - \rho I_{0010} - \mu I_{0010}$$

$$\frac{dC_{0001}}{dt} = \gamma I_{0001} - \rho I_{0001} - \mu I_{0001}$$

$$\frac{dP_{1000}}{dt} = \rho I_{1000} - \alpha\beta P_{1000}(I_{1_{i\neq 1}} + aI_{\geq 2_{i\neq 1}} + \delta) - \mu P_{1000}$$

$$\frac{dP_{0100}}{dt} = \rho I_{0100} - \alpha\beta P_{0100}(I_{1_{i\neq 2}} + aI_{\geq 2_{i\neq 2}} + \delta) - \mu P_{0100}$$

$$\frac{dP_{0010}}{dt} = \rho I_{0010} - \alpha\beta P_{0010}(I_{1_{i\neq 3}} + aI_{\geq 2_{i\neq 3}} + \delta) - \mu P_{0010}$$

$$\frac{dP_{0001}}{dt} = \rho I_{0001} - \alpha\beta P_{0001}(I_{1_{i\neq 4}} + aI_{\geq 2_{i\neq 4}} + \delta) - \mu P_{0001}$$

$$\frac{dI_{1100}}{dt}=\alpha\beta P_{1000}(I_{0100}+aI_{\geq 2_2}+\delta)-\gamma I_{1100}-\mu I_{1100}$$
$$\frac{dI_{1010}}{dt}=\alpha\beta P_{1010}(I_{0010}+aI_{\geq 2_3}+\delta)-\gamma I_{1010}-\mu I_{1010}$$
$$\frac{dI_{1001}}{dt}=\alpha\beta P_{1001}(I_{0001}+aI_{\geq 2_4}+\delta)-\gamma I_{1001}-\mu I_{1001}$$
$$\frac{dI_{1100}}{dt}=\alpha\beta P_{1100}(I_{1000}+aI_{\geq 2_1}+\delta)-\gamma I_{1100}-\mu I_{1100}$$
$$\frac{dI_{0110}}{dt}=\alpha\beta P_{0110}(I_{0010}+aI_{\geq 2_3}+\delta)-\gamma I_{0110}-\mu I_{0110}$$
$$\frac{dI_{0101}}{dt}=\alpha\beta P_{0101}(I_{0001}+aI_{\geq 2_4}+\delta)-\gamma I_{0101}-\mu I_{0101}$$
$$\frac{dI_{1100}}{dt}=\alpha\beta P_{1000}(I_{0100}+aI_{\geq 2_2}+\delta)-\gamma I_{1100}-\mu I_{1100}$$
$$\frac{dC_{1100}}{dt}=I_{1100}-\rho C_{1100}-\mu C_{1100}$$
$$\frac{dC_{1010}}{dt}=I_{1010}-\rho C_{1010}-\mu C_{1010}$$
$$\frac{dC_{1001}}{dt}=I_{1001}-\rho C_{1001}-\mu C_{1001}$$
$$\frac{dC_{0110}}{dt}=I_{0110}-\rho C_{0110}-\mu C_{0110}$$
$$\frac{dC_{0101}}{dt}=I_{0101}-\rho C_{0101}-\mu C_{0101}$$
$$\frac{dC_{0011}}{dt}=I_{0011}-\rho C_{0011}-\mu C_{0011}$$
$$\frac{dP_{1100}}{dt}=\rho C_{1100}-\alpha\beta P_{1100}(I_{0010}+I_{0001}+a(I_{\geq 2_{i=3}}+I_{\geq 2_{i=4}})+\delta)-\mu P_{1100}$$
$$\frac{dP_{1010}}{dt}=\rho C_{1010}-\alpha\beta P_{1010}(I_{0100}+I_{0001}+a(I_{\geq 2_{i=2}}+I_{\geq 2_{i=4}})+\delta)-\mu P_{1010}$$
$$\frac{dP_{1001}}{dt}=\rho C_{1001}-\alpha\beta P_{1001}(I_{0010}+I_{0010}+a(I_{\geq 2_{i=2}}+I_{\geq 2_{i=3}})+\delta)-\mu P_{1001}$$
$$\frac{dP_{0110}}{dt}=\rho C_{0110}-\alpha\beta P_{0110}(I_{1000}+I_{0001}+a(I_{\geq 2_{i=1}}+I_{\geq 2_{i=4}})+\delta)-\mu P_{0110}$$
$$\frac{dP_{0101}}{dt}=\rho C_{0101}-\alpha\beta P_{0101}(I_{1000}+I_{0010}+a(I_{\geq 2_{i=1}}+I_{\geq 2_{i=3}})+\delta)-\mu P_{0101}$$
$$\frac{dP_{0011}}{dt}=\rho C_{0011}-\alpha\beta P_{0011}(I_{1000}+I_{0100}+a(I_{\geq 2_{i=1}}+I_{\geq 2_{i=2}})+\delta)-\mu P_{0011}$$

$$\frac{dI_{1110}}{dt} = \alpha\beta P_{1100}(I_{0010} + aI_{\geq 2_3} + \delta) - \gamma I_{1110} - \mu I_{1110}$$

$$\frac{dI_{1101}}{dt} = \alpha\beta P_{1100}(I_{0001} + aI_{\geq 2_4} + \delta) - \gamma I_{1101} - \mu I_{1101}$$

$$\frac{dI_{1110}}{dt} = \alpha\beta P_{1010}(I_{0100} + aI_{\geq 2_2} + \delta) - \gamma I_{1110} - \mu I_{1110}$$

$$\frac{dI_{1011}}{dt} = \alpha\beta P_{1010}(I_{0001} + aI_{\geq 2_4} + \delta) - \gamma I_{1011} - \mu I_{1011}$$

$$\frac{dI_{1101}}{dt} = \alpha\beta P_{1001}(I_{0100} + aI_{\geq 2_2} + \delta) - \gamma I_{1101} - \mu I_{1101}$$

$$\frac{dI_{1011}}{dt} = \alpha\beta P_{1001}(I_{0010} + aI_{\geq 2_3} + \delta) - \gamma I_{1011} - \mu I_{1011}$$

$$\frac{dI_{1110}}{dt} = \alpha\beta P_{0110}(I_{1000} + aI_{\geq 2_1} + \delta) - \gamma I_{1110} - \mu I_{1110}$$

$$\frac{dI_{0111}}{dt} = \alpha\beta P_{0110}(I_{0001} + aI_{\geq 2_4} + \delta) - \gamma I_{0111} - \mu I_{0111}$$

$$\frac{dI_{1101}}{dt} = \alpha\beta P_{0101}(I_{1000} + aI_{\geq 2_1} + \delta) - \gamma I_{1101} - \mu I_{1101}$$

$$\frac{dI_{0111}}{dt} = \alpha\beta P_{0101}(I_{0010} + aI_{\geq 2_3} + \delta) - \gamma I_{0111} - \mu I_{0111}$$

$$\frac{dI_{1011}}{dt} = \alpha\beta P_{0011}(I_{1000} + aI_{\geq 2_1} + \delta) - \gamma I_{1011} - \mu I_{1011}$$

$$\frac{dI_{0111}}{dt} = \alpha\beta P_{0011}(I_{0100} + aI_{\geq 2_2} + \delta) - \gamma I_{0111} - \mu I_{0111}$$

$$\frac{dC_{1110}}{dt} = \gamma I_{1110} - \rho C_{1110} - \mu C_{1110}$$

$$\frac{dC_{1101}}{dt} = \gamma I_{1101} - \rho C_{1101} - \mu C_{1101}$$

$$\frac{dC_{1011}}{dt} = \gamma I_{1011} - \rho C_{1011} - \mu C_{1011}$$

$$\frac{dC_{0111}}{dt} = \gamma I_{0111} - \rho C_{0111} - \mu C_{0111}$$

$$\frac{dP_{1110}}{dt} = \rho C_{1110} - \alpha\beta P_{1110}(I_{0001} + aI_{\geq 2_{i=4}} + \delta) - \mu P_{1110}$$
$$\frac{dP_{1101}}{dt} = \rho C_{1101} - \alpha\beta P_{1101}(I_{0010} + aI_{\geq 2_{i=3}} + \delta) - \mu P_{1101}$$
$$\frac{dP_{1011}}{dt} = \rho C_{1011} - \alpha\beta P_{1011}(I_{0100} + aI_{\geq 2_{i=2}} + \delta) - \mu P_{1011}$$
$$\frac{dP_{0111}}{dt} = \rho C_{0111} - \alpha\beta P_{0111}(I_{1000} + aI_{\geq 2_{i=1}} + \delta) - \mu P_{0111}$$
$$\frac{dI_{1111}}{dt} = \alpha\beta P_{1110}(I_{0001} + aI_{\geq 2_4} + \delta) - \gamma I_{1111} - \mu I_{1111}$$
$$\frac{dI_{1111}}{dt} = \alpha\beta P_{1101}(I_{0010} + aI_{\geq 2_3} + \delta) - \gamma I_{1111} - \mu I_{1111}$$
$$\frac{dI_{1111}}{dt} = \alpha\beta P_{1011}(I_{0100} + aI_{\geq 2_2} + \delta) - \gamma I_{1111} - \mu I_{1111}$$
$$\frac{dI_{1111}}{dt} = \alpha\beta P_{0111}(I_{1000} + aI_{\geq 2_1} + \delta) - \gamma I_{1111} - \mu I_{1111}$$
$$\frac{dR}{dt} = \gamma I_{1111} - \mu R$$

A.1 References

1. Alfaro-Murillo JA, Towers S & Feng Z (2013) A deterministic model for influenza infection with multiple strains and antigenic drift. *Journal of Biological Dynamics* 7(1): 199-211.

APPENDIX B:

PROOF R_0

We use the next generation matrix to compute the basic reproduction number (R_0) associated with the disease-free equilibrium (1-3). To obtain the disease-free equilibrium, we assume all parameters are constant over time and thus ignore the effect of seasonal forcing. The disease-free equilibrium for the system $(S, I_{i=1-n}, C_{i=1-n}, P_{i=1-n}, I_{\substack{i=1-n \\ j=1-n\neq i}}, R)$, where n is the number of serotypes equals $E_0 = (1,0,0,0,0,0)$. For simplicity, we show the derivation for n=2 serotypes, which gives the same result as larger serotype systems (4). From the infection terms $(I_{i=1-n}, I_{\substack{i=1-n \\ j=1-n\neq i}})$, with n=2:

$$\frac{dI_1}{dt} = \beta_t S(I_1 + aI_{21} + \delta) - \gamma I_1 - \mu I_1$$
$$\frac{dI_2}{dt} = \beta_t S(I_2 + aI_{12} + \delta) - \gamma I_2 - \mu I_2$$
$$\frac{dI_{12}}{dt} = \alpha\beta_t P_1(I_2 + aI_{12} + \delta) - \gamma I_{12} - \mu I_{12}$$
$$\frac{dI_{21}}{dt} = \alpha\beta_t P_2(I_1 + aI_{21} + \delta) - \gamma I_{21} - \mu I_{21}.$$

We can derive the non-negative matrix, F, which represents the rate of appearance of new infections at each infectious stage and, at the disease-fee equilibrium, is denoted as:

$$F = \begin{pmatrix} \beta & 0 & 0 & \beta a \\ 0 & \beta & \beta a & 0 \\ 0 & 0 & 0 & 0 \\ 0 & 0 & 0 & 0 \end{pmatrix}.$$

And the rate of change by all other means, at the disease-free equilibrium is defined as:

$$V = \begin{pmatrix} \gamma + \mu & 0 & 0 & 0 \\ 0 & \gamma + \mu & 0 & 0 \\ 0 & 0 & \gamma + \mu & 0 \\ 0 & 0 & 0 & \gamma + \mu \end{pmatrix},$$

with its inverse being:

$$V^{-1} = \begin{pmatrix} \frac{1}{\gamma + \mu} & 0 & 0 & 0 \\ 0 & \frac{1}{\gamma + \mu} & 0 & 0 \\ 0 & 0 & \frac{1}{\gamma + \mu} & 0 \\ 0 & 0 & 0 & \frac{1}{\gamma + \mu} \end{pmatrix}.$$

The basic reproduction number is defined as the largest eigenvalue of the matrix FV^{-1}, thus

$$0 = \det(FV^{-1} - \lambda I) = \det\begin{pmatrix} \frac{\beta}{\gamma - \mu} - \lambda & 0 & 0 & \frac{\beta a}{\gamma - \mu} - \lambda \\ 0 & \frac{\beta}{\gamma - \mu} - \lambda & \frac{\beta a}{\gamma - \mu} - \lambda & 0 \\ 0 & 0 & -\lambda & 0 \\ 0 & 0 & 0 & -\lambda \end{pmatrix},$$

where I is the identity matrix. Solving the determinant of this matrix leads to the basic reproduction number being

$$R_0 = \frac{\beta}{\gamma + \mu},$$

where the disease-free equilibrium is stable for values of $R_0<1$ and unstable for values of $R_0>1$. Mark that the stability of the disease-free equilibrium is not dependent on the ADE or cross-immunity. Because symmetry between the strains is assumed (α,a,β_0, β_1, γ and τ are equal for all strains), R_0 is equal for all strains.

B.1 References

1. Diekmann O, Heesterbeek J & Metz J (1990) On the definition and the computation of the basic reproduction ratio R 0 in models for infectious diseases in heterogeneous populations. *J Math Biol* 28(4): 365-382.

2. Van den Driessche P & Watmough J (2002) Reproduction numbers and sub-threshold endemic equilibria for compartmental models of disease transmission. *Math Biosci* 180(1): 29-48.

3. Diekmann O & Heesterbeek JAP (2000) *Mathematical epidemiology of infectious diseases: model building, analysis and interpretation,* (Wiley, West Sussex), pp 320.

4. Billings L*, et al* (2007) Instabilities in multiserotype disease models with antibody-dependent enhancement. *J Theor Biol* 246(1): 18-27.